Investigations into the role of pulmonary innate immunity during fibrotic lung disease

Author: Sarah Jayne Allden

Imperial College London

National Heart and Lung Institute

Thesis submitted in fulfilment of the requirements for the degree of Doctorate of Philosophy

Date: 18th April 2018

Supervisors:

Professor Clare Lloyd

Professor Toby Maher

Dr Adam Byrne

Statement of Originality

All experimental work submitted in this thesis is entirely the result of the candidates investigation with the following exceptions; clinical sample collection and patient differential counts were carried out by members of staff at the Royal Brompton Hospital, flow cytometry cell separations were carried out by members of Imperial College London's flow cytometry facility including Jane Srivastava, Jessica Rowley and Catherine Simpson (now UCB) and the extracellular matrix deposition (ECM) assay was carried out by Marianne Bergin (UCB) at UCB, with advice from Katrina Gore (statistician at UCB) on the statistics for the ECM assay. All other experiments were carried out at the NHLI, Imperial College London.

Copy Declaration

The copyright of this thesis rests with the author and is made available under a Creative Commons Attribution-Non Commercial-No Derivatives licence. Researchers are free to copy, distribute or transmit the thesis on the condition that they attribute it, that they do not use it for commercial purposes and that they do not alter, transform or build upon it. For any reuse or distribution, researchers must make clear to others the licence terms of this work.

Acknowledgements

Firstly I would like to acknowledge my supervisors Professor Clare Lloyd, Professor Toby Maher and Dr Adam Byrne for their support and advice throughout the project, and to UCB for funding and supporting the project. This generosity has enabled me to carry out patient focused research in the Interstitial lung disease (ILD) area, developing my skills and confidence as a Research Scientist whilst remaining an employee.

A special thank you goes to Dr Richard Toshner, who I have worked alongside throughout my PhD, not only for providing the clinical support but also for the morale boosting and always entertaining company in the lab. I also wish to thank the whole ILD team at the Royal Brompton hospital, including all the doctors, nurses and all support staff for their help in recruiting and taking care of the patients, without which none of this research would have been possible.

Many thanks to all members of the Lloyd lab for their help, advice and expertise, in particular Dr Cecilia Andersson and Dr Jua Iwasaki for all the fun and scientific advice.

Outside of the Lloyd lab I wish to thank members of the flow facility at imperial including Jane Srivastava, Dr Jessica Rowley and Catherine Simpson (now UCB) for their help with sorting cells and general flow cytometry expertise, and Marianne Bergin and Katrina Gore at UCB for their support with the ECM assay.

I wish to thank all my friends and family for their continual support, especially my sister Hannah Allden for agreeing to read through this thesis, a task I think she under estimated.

I especially wish to thank my husband, Martin Stanyon, who I married during my first year of PhD. Without his continuing support I would not be where I am today. I have appreciated all the extra burdens he has taken on, enabling me to focus on my PhD and for lifting my spirits when they needed it the most. I cannot thank him enough.

Finally, I wish to thank the patients and healthy controls for their kind sample donations enabling much-needed research in the ILD field. I sincerely hope their sample donations contribute to our understanding of ILD and eventually to the development of improved therapeutics.

Abstract

Interstitial lung diseases (ILD) incorporate a broad range of lung pathologies characterised by abnormalities in the pulmonary interstitium. The most common ILD is idiopathic pulmonary fibrosis (IPF), a progressive fibrotic lung disease with poor patient prognosis [1]. The pathological mechanisms and mediators driving IPF remain to be elucidated. The lung microbiome of IPF patients has been reported as altered compared to healthy controls [2, 3], with increased bacterial burden correlating with poor patient prognosis [2]. Our understanding as to why there are differences, and whether bacteria are contributing toward the pathology, has not yet been investigated. This project investigated the hypothesis that changes in specific bacterial genera in IPF may occur as a result of defective response by innate immune cells. This defective clearance of bacteria may lead to a pro-fibrotic response driven by repeat bacterial stimulation. To examine differences in immune composition, inflammatory profiles of the bronchial alveolar lavage (BAL) from healthy, IPF and other ILDs were compared with focus on the function and phenotype of airway macrophages (AMs). Furthermore, pro-inflammatory/pro-fibrotic responses by primary bronchial epithelial cells (BECs) and fibroblasts from IPF and healthy controls were examined post bacterial and TLR stimulation.

Characterisation of the inflammatory and leukocyte profiles of the BAL showed significant increases in monocytes, AMs, and mediators CCL2 and M-CSF in IPF, which inversely correlated with forced vital capacity (FVC). Phenotypic analysis of AMs revealed two distinct phenotypes based on CD71+/- expression. The CD71+/- AMs exhibited significantly different surface marker and gene expression, transferrin uptake, phagocytosis and nitric oxide (NO) production. Interestingly, CD71- AMs were increased in IPF, correlating inversely with FVC decline, but were

virtually absent from healthy control BAL. Supernatants from isolated and cultured IPF CD71- and CD71+ AMs differentially increased collagen IV secretion, with CD71- cells increasing collagen IV compared to CD71+. Supernatants from LPS stimulated CD71-/+ cells increased collagen IV deposition further. No differences were found comparing healthy and IPF AM ability to phagocytose bacteria, however, NO production appeared significantly higher in healthy compared to IPF.

Stimulation of primary healthy and IPF BECs with various TLR ligands revealed significant increases in pro-inflammatory and pro-fibrotic gene expression post viral ligand Poly: IC stimulation. Moreover, epithelial cell supernatants collected after Poly: IC stimulation increased the release of pro-inflammatory mediators by fibroblasts. However, direct bacterial stimulation, or after the TLR4 ligand, LPS, induced limited or no changes in BECs or fibroblasts, indicating viral infection, rather than bacterial, may influence disease pathogenesis.

Collectively, this body of data suggests that viral stimulation contributes toward fibrosis by activating BECs, inducing an upregulation of pro-fibrotic mediators including CCL2, IL-6, IL-8 and TGFβ1. CD71- AMs may enhance fibrotic progression in IPF patients increasing the deposition of collagen by epithelial cells and fibroblasts. Specific targeting of CD71- AM may represent a novel therapeutic strategy to alleviate fibrotic progression in patients.

Contents

Statement of Originality i

Copy Declaration ii

Acknowledgements iii

Abstract v

Contents vii

List of Abbreviations xvi

List of Figures xxiii

List of Tables xxxi

1. Introduction 1

1.1. Interstitial lung disease 1

1.1.1. Clinical examination and diagnosis of ILD 2

1.1.2. ILD aetiology and pathogenesis 3

1.2. Idiopathic Pulmonary Fibrosis 8

1.2.1. Incidence and Epidemiology 8

1.2.2. In vitro and in vivo models of pulmonary fibrosis 9

1.2.3. IPF Pathogenesis 12

1.2.3.1. Genetic polymorphisms 13

1.2.3.2. Cellular senescence 15

1.2.4. The roles of stromal cells in IPF pathogenesis 15
1.2.4.1. Epithelial cells in health and IPF 15
1.2.4.2. Fibroblasts in health and IPF 19
1.2.4.1. Leukocytes in fibrosis 20
1.2.4.1.1. The role of airway macrophages in health and disease 22
1.2.4.1.1.1. Macrophage phenotypes 23
1.2.4.1.1.2. Airway macrophage role in host defence 26
1.2.4.1.2. The role of airway macrophages in tissue remodelling and IPF pathology 27
1.2.1. Analysis of cellular mediators in the BAL 28
1.2.1.1. Possible environmental factors exacerbating IPF 33
1.2.1.2. Infectious mediators influencing fibrotic progression 33
1.2.1.2.1. Bacteria 34
1.2.1.2.2. Viral exacerbation 36
1.2.1.2.1. Detection of pathogens in IPF 37
1.2.2. Summary of IPF pathogenesis 38
1.2.3. IPF Therapeutics 40
1.2.3.1. Pirfenidone 40
1.2.3.2. Nintedanib 41
1.3. Other interstitial lung diseases 42

1.3.1. Undifferentiated connective tissue disease 42

1.3.2. Hypersensitivity pneumonitis and chronic hypersensitivity pneumonitis 44

1.4. Summary 46

1.5. Hypothesis 47

1.6. Aims 47

2. Materials and Methods 48

2.1. Collection of BAL samples 48

2.2. BAL Processing 48

2.3. Cytospins and staining of cells 49

2.4. General leukocyte FACS staining for extracellular surface markers 50

2.5. Macrophage FACS staining for extracellular surface markers 54

2.6. Intracellular stimulation and staining 54

2.7. Macrophage FACS Staining for phagocytosis, nitric oxide and transferrin. 59

2.8. Immunofluorescent staining and imaging 62

2.9. Total protein quantification 63

2.10. Multiplex measurement of cytokines, chemokines and growth factors 63

2.11. ELISA 64

2.12. Measurement of M-CSF using Quantikine® ELISA kit 65

2.13. Sorting and separating cells 66

2.13.1. FACS separation 66

2.13.2. MACS separation 68

2.14. Macrophage stimulation 69

2.15. Analysis of mediators in stimulated macrophage supernatant 69

2.16. RNA extraction from cells 70

2.17. Reverse Transcription of RNA to cDNA for qPCR using TaqMan primers 71

2.18. Gene expression analysis using TaqMan primers 71

2.19. Gene expression analysis 73

2.20. Reverse Transcription for fibrotic PCR array macrophage analysis 76

2.21. PCR fibrotic array real time quantitative PCR reaction and analysis 76

2.22. Culturing Bronchial epithelial cells for co-culture 77

2.22.1. Collagen coating flasks and plates 77

2.22.2. BEC isolation 77

2.22.3. Splitting cells 78

2.22.4. Freezing cells 78

2.23. Co-culture macrophages with BEC 78

2.24. Extracellular matrix deposition assay 80

2.25. BEC culture and stimulation 82

2.26. Bacterial challenge 83

2.26.1. Haemophilus influenzae b 84

2.26.2. Streptococcus pneumoniae 84

2.27. Fibroblast cultures 86

2.28. Freezing cells 87

2.29. Fibroblast stimulation 87

2.30. Stimulation of fibroblasts with conditioned BEC supernatant 89

2.31. Fibroblast proliferation assay 90

2.32. Statistical Analysis 91

3. Analysis of Leukocytes and mediators in the Bronchoalveolar lavage of patients with ILD. 92

3.1. Introduction 92

3.2. Hypothesis 94

3.3. Aims 94

3.4. Results 95

3.4.1. Cellular differential analysis reveal significantly different leukocyte proportions and cell numbers in ILD compared to healthy controls 95

3.4.2. Confirmation of cell morphology using flow cytometry to isolate specific populations 100

3.4.3. Analysis of key myeloid populations in the BAL reveal significant increases in monocytes and macrophages in IPF compared to healthy controls. 103

3.4.4. Analysis of lymphoid cells in the BAL reveal increased NK cells numbers in IPF patients compared to healthy controls. 109

3.4.1. Total protein in the BAL does not differ significantly between groups. 114

3.4.2. Quantification of inflammatory cytokine levels in ILD BAL supernatant 115

3.4.3. Quantification of chemokines in the BAL supernatant reveals distinct profiles in ILD correlating with increases in specific cell populations 117

3.4.4. Quantification of growth factors in the BAL supernatant 121

3.4.5. Increases in myeloid cells and associated mediators correlate inversely with predicted FVC 124

3.5. Discussion 126

3.5.1. Summary of cells and mediators in healthy and IPF airways 132

4. Examination of Airway Macrophages in ILD. 133

4.1. Introduction 133

4.1.1. Macrophage phenotypes in ILD 133

4.1. Hypothesis 135

4.2. Aims 135

4.3. Materials and Methods 136

4.3.1. Analysis of mediators in BAL supernatant 136

4.3.1.1. Transferrin 136

4.3.1.2. Ferritin 136

4.3.1.3. Iron 137

4.4. Results 138

4.4.1. Patient demographics 138

4.4.2. No clear M1/M2 phenotype observed in IPF or other ILDs..... 139

4.4.3. CD71- macrophage numbers are significantly increased and correlate with clinical progression in ILD patients 141

4.4.4. CD71- and CD71+ cells exhibit similar macrophage morphology but marker expression significantly differs 143

4.4.5. CD71- and CD71+ cells exhibit significantly different expression levels of genes involved in iron homeostasis 147

4.4.6. Examination of TLR expression in CD71- and CD71+ cells reveal significant differences. 151

4.4.7. Comparison of CD71- and CD71+ cell defence revealed significant differences in NO production and bacterial phagocytosis. 153

4.4.8. Examination of the production of pro-inflammatory mediators in CD71- and CD71+ cells post TLR stimulation 156

4.4.9. Examination of genes associated with fibrosis in CD71- and CD71+ cells..... 158

4.4.10. Examination of growth factors produced by CD71- and CD71+ cells 162

4.4.11. Co-culturing CD71- and CD71+ cells with BEC down regulates BEC genes involved in extracellular matrix production 164

4.4.12. Stimulation of epithelial cell and fibroblast co-culture with CD71- cell supernatants results in increased collagen IV deposition 167

4.5. Discussion 170

4.5.1. Summary of CD71- and CD71+ functional phenotypes 184

5. Investigation into the effects of TLR stimulation on IPF and healthy bronchial epithelial cells and fibroblasts 185

5.1. Introduction 185

5.2. Hypothesis 187

5.3. Aims 187

5.4. Results 188

5.4.1. BEC stimulation pro-inflammatory gene analysis 188

5.4.1. BEC stimulation pro-fibrotic gene analysis 193

5.4.2. BEC stimulation chemokine and cytokine analysis 197

5.4.3. BEC stimulation growth factor analysis 200

5.4.4. Fibroblast stimulation pro-inflammatory gene analysis 204

5.4.5. Fibroblast stimulation pro-fibrotic gene analysis 208

5.4.1. Fibroblast stimulation chemokine and cytokine analysis 213

5.4.2. Fibroblast stimulation growth factor analysis 216

5.4.3. Proinflammatory response of fibroblasts stimulated with conditioned BEC media..... 220

5.4.4. Pro-fibrotic gene expression analysis in fibroblasts stimulated with conditioned BEC media..... 226

5.4.5. Fibroblast proliferation assay 231

5.5. Discussion 236

6. Discussion 245

6.1. Innate immune responses to bacterial and TLR stimulation 246

6.2. Identification of distinct macrophage populations and functional role in IPF 250

6.3. Summary and future work 251

7. References 256

8. Appendix 279

8.1. Supplementary data for results chapter 2. 279

8.2. Supplementary data for results chapter 3. 282

8.3. Supplementary data for results chapter 4. 284

8.4. List of external oral and poster presentations 296

8.4.1. Conference oral presentations 296

8.4.2. Poster presentations 296

List of Abbreviations

ACE	Angiotensin converting enzyme
ACO1	Aconitase 1 (Iron regulatory protein 1)
ACTA2	Alpha smooth muscle actin 2
AE	Acute exacerbation
AF	Alexa fluor
AIP	Acute interstitial pneumonitis
AKT1	V-akt murine thymoma viral oncogene homolog 1
αSMA	Alpha smooth muscle actin
AM	Airway macrophages
ANGII	Angiotensin II
APC	Allophycocyanin
AT- 1/2	Alveolar type -1/2
Cy	Cyanine
BAL	Bronchoalveolar lavage
BCA	Bicinchoninic acid assay
BCL2	B-cell lymphoma 2
BEBM	Bronchial epithelial cell basal media
BEC	Bronchial epithelial cell
BEGM	Bronchial epithelial cell growth media
BSA	Bovine serum albumin
BV	Brilliant violet
CCL	C-C motif ligand
CCR	C-C motif receptor
CD	Cluster differential
cDNA	complementary DNA
CEBPB	CCAAT/enhancer binding protein (C/EBP), beta
cHP	Chronic hypersensitivity pneumonitis

COL1A1	Collagen Type I Alpha 1 Chain
COL3A1	Collagen Type III Alpha 1 Chain
COP	Cryptogenic organizing pneumonia
CTD	Connective Tissue Disease
CTGF	Connective tissue growth factor
CXCL	C-X-C motif ligand
CXCR	C-X-C motif receptor
DAD	Diffuse alveolar damage
DAF-FM Diacetate	4-Amino-5-Methylamino-2',7'-Difluorofluorescein Diacetate
DAMP	Damage associated molecular pattern
DIP	Desquamative interstitial pneumonitis
DMEM	Dulbecco's modified Eagle's medium
DMSO	Dimethyl sulfoxide
DNA	Deoxyribonucleic acid
dNTP	deoxyribose Nucleoside triphosphate
ds RNA	double stranded RNA
DSP	Desmoplankin
EBV	Epstein-Barr virus
ECM	Extra cellular matrix
EDTA	Ethylenediaminetetraacetic acid
ef450	excitation filter (450)
ELISA	Enzyme-linked immunosorbent assay
ELMO1	Engulfment and cell motility 1
ENA-78	Epithelial-derived neutrophil-activating peptide 78
ENG	Endoglin
EP	Eosinophilic pneumonia
FACS	Fluorescence-activated cell sorting
Fc	Fragment crystallizable

FCGR1A	Fcγ Receptor 1A
FcεR1	Fragment crystallizable epsiolon receptor 1
FCS	Fetal calf serum
FGFb	Fibroblast growth factor basic
FITC	Fluorescein isothiocyanate
FMO	Fluorescence minus one
FN1	Fibronectin
FVC	Forced vital capacity
GAPDH	Glyceraldehyde 3-phosphate dehydrogenase
G-CSF	granulocyte-colony stimulating factor
gDNA	genomic DNA
GM-CSF	Granulocyte macrophage-colony stimulating factor
GROα	Growth-regulated oncogene-alpha
HAMP	Hepcidin
HEPES	4-(2-hydroxyethyl)-1-piperazineethanesulfonic acid
HGF	Hepatocyte growth factor
HKG	House-keeping gene
HKHIB	Heat killed *Haemophilus influenza b*
HKSP	Heat killed *Streptococcus pneumonia*
HLA-DR	Human leukocyte antigen - D related
HMOX	Heme oxygenase (decycling) 1
HP	Hypersensitivity pneumonitis
HRCT	High-resolution computed tomography
HRP	Horse radish peroxidase
HV	herpes virus
IF	Immunofluorescence
IFN	Interferon
IGF-1	Insulin-like growth factor 1
IHC	Immunohistochemistry

IL	Interleukin
ILD	Interstitial lung disease
ILK	Integrin-linked kinase
IP-10	IFNγ inducible protein of 10 kDa
IPF	Idiopathic pulmonary fibrosis
IRAK1	Interleukin-1 receptor-associated kinase 1
IREB2 (IRP2)	Iron regulatory protein 2
IRF3	Interferon regulatory transcription factor 3
IRP	Iron regulatory protein
I-TAC	Interferon-inducible T-cell alpha chemoattractant
ITGA	Integrin alpha
ITGB	Integrin beta
JUN	Jun proto-oncogene
LAP	Latency associated peptide
LPS	Lipopolysaccharide
MACS	Magnetic-activated cellular sorting
MAPK	Mitogen-activated protein kinase
MCP-1	Monocyte chemoattractant protein-1
M-CSF	Macrophage-colony-stimulating factor
MHC	Major histocompatibility complex
MIG	Monokine induced by gamma interferon
MIP	Macrophage inflammatory protein
MMP	Matrix metalloproteinases
MOI	Multiplicity of infection
mRNA	messenger RNA
MUC5B	Mucin 5B
MYC	V-myc myelocytomatosis viral oncogene homolog (avian)
NFκβ1	Nuclear factor of kappa light polypeptide gene enhancer in B-cells 1
NK	Natural killer cell

NO	Nitric oxide
NOS2	Nitric oxide synthase 2
NSAIDs	Non-steroidal anti-inflammatory drugs
NSIP	Nonspecific interstitial pneumonitis
OB	Obliterative Bronchiolitis
PBS	Phosphate buffered saline
PCR	Polymerase chain reaction
PDGF	Platelet derived growth factor
PE	Phycoerythrin
PLAU	Plasminogen activator, urokinase (u-PA)
Poly: IC	Polyinosinic-polycytidylic acid
PRR	Pattern recognition receptor
qPCR	quantitative polymerase chain reaction
RANTES	Regulated on activation, normal T cell expressed and secreted
RIG-1	Retinoic acid-inducible gene I
RGS2	Regulator of G-protein Signalling 2
RNA	Ribonucleic acid
ROS	Reactive oxygen species
RPMI	Roswell Park Memorial Institute media
rRNA	ribosomal ribonucleic acid
RT	Reverse Transcription
RT-PCR	Real time - PCR
Sarcoid	Sarcoidosis
SCF	Stem cell factor
SERPIN	Serpin peptidase inhibitor
SFTP	Surfactant protein
Siglec 8	Sialic acid-binding Ig-like lectin 8
SLC11A2	Divalent metal transporter 1 (DMT1), Natural resistance associated macrophage protein 2

SLC40A1	Ferritin transporter; Ferriportin
SLC48A1	Heme transporter; Heregulin1 (HRG 1)
SNP	Single nucleotide polymorphism
SMAD	SMAD is derived from the *Caenorhabditis elegans* protein SMA (from gene sma for small body size) and the Drosophila protein, mothers against decapentaplegic (MAD). SMAD is a homologue of these proteins.
SP1	Sp1 transcription factor
SSc-ILD	Systemic sclerosis
STAT	Signal transducer and activator of transcription
TARC	Thymus and activation-regulated chemokine
TERC	Telomerase RNA component
TERT	Telomerase reverse transcriptase
TFRC	Transferrin receptor; CD71
TGFBR	Transforming growth factor, beta receptor
TGFα	Transforming growth factor alpha
TGFβ	Transforming growth factor beta
TGIF1	TGFB-induced factor homeobox 1
Th	T helper cell
THBS1 (TSP-1)	Thrombospondin 1
TIE	Tyrosine kinase with immunoglobulin-like and EGF-like domains
TIMP	Tissue inhibitors of metalloproteinases
TLCO	Transfer factor for carbon monoxide
TLR	Toll like receptor
TMB	Tetramethylbenzidine
TNFα	Tumor necrosis factor alpha
TOLLIP	Toll-interacting protein
UCTD	Undifferentiated connective tissue disease
UIP	Usual interstitial pneumonia
UK	United Kingdom

UNG	Uracil-N-glycosylase
USA	United States of America
VEGF	Vascular endothelial growth factor
Wnt	Wingless-type MMTV (mouse mammary tumor virus) integration site

List of Figures

Figure 1.1: Bronchiole and alveoli in health and in IPF. 18

Figure 1.2: M1/M2 Macrophage Phenotypes. 25

Figure 1.3: Hypothesised progression of IPF pathogenesis. 39

Figure 2.1: Example BAL cytospin for differential counts. 50

Figure 2.2: General leukocyte FACS gating strategy. 53

Figure 2.3: FACs gating strategy for CD11c+ macrophages. 57

Figure 2.4: FACs gating strategy for CD71+/- macrophages extracellular surface markers. 58

Figure 2.5: FACs gating strategy for CD71+/- macrophages NO, bacteria and transferrin stain. 61

Figure 2.6: Illustration of BEC and CD71-/+ macrophage co-culture conditions. 79

Figure 2.7: Illustration of BEC stimulation methods and sample collection. 85

Figure 2.8: Illustration of methods used to stimulate fibroblasts with conditioned BEC media. 89

Figure 3.1: Cellular differential leukocyte proportions. 97

Figure 3.2: Absolute leukocyte number per mL of BAL calculated from differential counts. 98

Figure 3.3: Summary of differential counts. 99

Figure 3.4: Images of cells separated using flow cytometry. 102

Figure 3.5: Myeloid cell proportion analysis in ILD. 105

Figure 3.6: Analysis of number of myeloid cells ($x10^4$) per mL of BAL. 106

Figure 3.7: Analysis of FcεR1 and CD1c expressing cells in ILD. 107

Figure 3.8: Summary of myeloid cells in the airways of healthy and ILD patients. 108

Figure 3.9: Lymphoid cell proportion analysis in ILD. 110

Figure 3.10: Analysis of number of lymphoid cells ($x10^4$) per mL of BAL. 111

Figure 3.11: Summary of lymphoid cells in the airways of healthy and ILD patients. 112

Figure 3.12: Heat map summary of cell numbers shows an increase in myeloid cells in IPF and lymphoid cells in cHP compared to healthy controls. 113

Figure 3.13: Total protein in the BAL supernatant. 114

Figure 3.14: Pro-inflammatory mediators in the BAL. 116

Figure 3.15: IL-6 in BAL supernatant. 116

Figure 3.16: Increased levels of CCL2 and CXCL10 significantly correlate with increased proportions of monocytes and lymphocytes respectively. 118

Figure 3.17: Heat map summary of median measurement of pro-inflammatory mediators in the BAL reveals different chemokine profiles in ILD. 120

Figure 3.18: M-CSF levels in the BAL supernatant. 123

Figure 3.19: Inverse correlations examining cells and mediators with % predicted FVC. 125

Figure 3.20: Illustration of cells and mediators in healthy and IPF airways. 132

Figure 4.1: Examination of M1 and M2 markers reveal no clear M1/M2 phenotype in airway macrophages from patients with ILD. 140

Figure 4.2: The proportion and number of CD71- cells are increased in IPF patients compared to healthy controls. 142

Figure 4.3: Imaging of separated CD11c+, CD11c+CD71- and CD11c+CD71+ cells. 145

Figure 4.4: Examination of the expression of surface markers reveals distinct phenotypes in CD71- compared to CD71+ cells. 146

Figure 4.5: Analysis of iron regulatory genes in CD71- and CD71+ cells. 148

Figure 4.6: Analysis of transferrin uptake by macrophages and transferrin levels in the BAL. . 149

Figure 4.7: Further analysis of genes involved in iron regulation. 150

Figure 4.8: Ferritin concentration in the BAL..... 150

Figure 4.9: Examination of CD71- and CD71+ cell TLR gene and protein expression. 152

Figure 4.10: Examination of pathogen defence in CD71- and CD71+ cells. 154

Figure 4.11: Examination of pathogen defence in CD71- and CD71+ cells in health and disease. 155

Figure 4.12: Production of inflammatory cytokines are similar comparing CD71- to CD71+ cells. 157

Figure 4.13: CD71-/+ cells express significantly different genes related to fibrosis. 159

Figure 4.14: Production of growth factors comparing CD71- to CD71+ cells..... 163

Figure 4.15: Gene expression fold change analysis of BEC after co-culture with CD71- and CD71+ cells for 6 hours..... 165

Figure 4.16: Measurement of IL-6 and IL-8 in the supernatant of BEC alone, CD71- and CD71+ alone in BEC and CD71- or CD71+ in co-culture. 166

Figure 4.17: Example of fluorescent staining of extracellular matrix produced by primary small airway epithelial cells (SAEpC) and IPF fibroblasts (IPF134)..... 168

Figure 4.18: Collagen IV deposition is increased by CD71- cell supernatants compared to CD71+ cell supernatants..... 169

Figure 4.19: Summary of CD71+ cells role in transferrin bound iron uptake..... 174

Figure 4.20: Summary of CD11c+ CD71+/CD71- Macrophage phenotypic and functional differences. 184

Figure 5.1: BEC stimulation: Pro-inflammatory gene expression analysis. 190

Figure 5.2: BEC stimulation: TLR gene expression analysis. 191

Figure 5.3: BEC stimulation: TLR mediator gene expression analysis. 192

Figure 5.4: BEC stimulation: TGFβ gene expression analysis..... 194

Figure 5.5: BEC stimulation: ECM gene expression analysis..... 195

Figure 5.6: BEC stimulation: Chemokine production analysis. 198

Figure 5.7: BEC stimulation: Pro-inflammatory cytokine and chemokine production analysis. 199

Figure 5.8: BEC stimulation: Growth factor analysis. 201

Figure 5.9: TGFβ1 levels post BEC stimulation. 202

Figure 5.10: Summary of gene changes and mediator production by healthy and IPF BECs in response to stimulations. 203

Figure 5.11: Fibroblast stimulation: Pro-inflammatory gene expression analysis. 205

Figure 5.12: Fibroblast stimulation: TLR gene expression analysis. 206

Figure 5.13: Fibroblast stimulation: TLR mediator gene expression analysis. 207

Figure 5.14: ACTA2 gene expression analysis. 209

Figure 5.15: Fibroblast stimulation: TGFβ superfamily gene expression analysis..... 210

Figure 5.16: Fibroblast stimulation: ECM gene expression analysis..... 211

Figure 5.17: Fibroblast stimulation: Chemokine production analysis. 214

Figure 5.18: Fibroblast stimulation: Pro-inflammatory cytokine and chemokine production analysis. 215

Figure 5.19: Fibroblast stimulation: Growth factor analysis. 217

Figure 5.20: TGFβ1 levels post fibroblast stimulation. 218

Figure 5.21: Summary of gene changes and mediator production by healthy and IPF BECs in response to stimulations. 219

Figure 5.22: Fibroblast BEC conditioned media stimulation control: pro-inflammatory gene expression analysis. 221

Figure 5.23: Fibroblast stimulation with conditioned healthy and IPF BEC supernatant: pro-inflammatory gene expression analysis. 222

Figure 5.24: Fibroblast pro-inflammatory cytokine and chemokine production analysis post stimulation with conditioned BEC Media. 225

Figure 5.25: Fibroblast stimulated controls for conditioned BEC supernatant pro-fibrotic gene expression analysis. 227

Figure 5.26: Pro-fibrotic gene expression analysis in fibroblasts stimulated with conditioned BEC media. 228

Figure 5.27: Summary of gene expression change and mediator production by fibroblasts stimulated with conditioned BEC media. 230

Figure 5.28: Fibroblast growth curve stimulation analysis. 233

Figure 5.29: Fibroblast growth curve stimulation comparison. 234

Figure 5.30: Percentage growth area under the curve of fibroblasts stimulated with conditioned BEC media. 235

Figure 5.31: Summary of IPF airway response to Poly: IC (dsRNA) stimulation. 244

Figure 6.1: Proposed model of viral stimulation and cellular interactions driving IPF pathology. 255

Figure 8.1.1: Bland-Altman comparison of methods reveals no significant difference comparing FACs analysis and differential analysis of cell number. 280
Figure 8.1.2: Increased numbers of FcεR1+ cells inversely correlate with percentage predicted forced vital capacity (FVC). 281
Figure 8.2.1: Co-culture of primary IPF fibroblasts (IPF134) and primary small airway epithelial cells (SAEpC) results in extracellular matrix (ECM) deposition..... 282
Figure 8.2.2: Examination of cell viability reveals no differences comparing co-culture control to CD71-/+ control unstimulated or LPS to CD71-/+ LPS stimulated..... 283
Figure 8.3.1: BEC stimulation: pro-inflammatory relative gene expression analysis. 284
Figure 8.3.2: BEC stimulation: TLR and TLR signalling relative gene expression analysis. 285
Figure 8.3.3: BEC stimulation: Pro-fibrotic relative gene expression analysis. 286
Figure 8.3.4: Fibroblast stimulation: pro-inflammatory relative gene expression analysis. 287
Figure 8.3.5: Fibroblast stimulation: TLR and TLR signalling relative gene expression analysis. 288
Figure 8.3.6: Fibroblast stimulation: ACTA2 (αSMA) relative gene expression analysis. 289
Figure 8.3.7: Fibroblast stimulation: TGFβ and TGFβ receptor relative gene expression analysis. 290
Figure 8.3.8: Fibroblast stimulation: ECM relative gene expression analysis. 291
Figure 8.3.9: Fibroblast BEC conditioned media stimulation control pro-inflammatory relative gene expression analysis..... 292
Figure 8.3.10: Fibroblast stimulation with conditioned healthy and IPF BEC supernatant pro-inflammatory relative gene expression analysis. 293

Figure 8.3.11: Fibroblast stimulated controls for conditioned BEC supernatant pro-fibrotic relative gene expression analysis. 294
Figure 8.3.12: Relative pro-fibrotic gene expression analysis in fibroblasts stimulated with conditioned BEC media. 295

List of Tables

Table 1.1: Summary of ILD pathologies and treatments. 7

Table 1.2: Summary of chemokines in IPF. 30

Table 1.3: Summary of literature examining growth factors in IPF. 32

Table 2.1: Antibodies used including dilutions with appropriate flow cytometer laser and filters for FACS staining and analysis. 52

Table 2.2: FACS panels for analysis of cell surface markers. 55

Table 2.3: FACS panels for analysis of TLRs. 56

Table 2.4: FACS panels for analysis of phagocytosis, nitric oxide production and transferrin uptake. 60

Table 2.5: FACS panels CD71-/CD71+ cell separation. 67

Table 2.6: TaqMan primers used for qPCR analysis. 74

Table 2.7: Primers used for qPCR of fibroblast and BEC stimulations. 75

Table 2.8: Reagent list for extracellular matrix deposition assay. 82

Table 2.9: BEC donor and analysis information. 85

Table 2.10: Fibroblast donor and analysis information. 88

Table 3.1: Patient and healthy control demographics for cellular differential analysis. 96

Table 3.2: Patient and healthy control demographics for general leukocyte analysis. 101

Table 3.3: Measurement of soluble chemokines in the BAL reveals different concentrations of chemokines comparing healthy to ILDs. 119

Table 3.4: Growth factors in BAL. 122

Table 4.1: Patient demographics for flow cytometry staining of airway macrophage populations. 138

Table 4.2: Patient demographics with clinical parameters for all samples that were separated for CD71- and CD71+ cell analysis. 144

Table 4.3: Summary of Genes expressed in both CD71- and CD71+ airway macrophages from fibrosis gene array..... 161

Table 5.1: Summary of BEC stimulation median gene fold change compared to unstimulated control cells. 196

Table 5.2: Summary of Fibroblast stimulation median gene fold change compared to unstimulated cells. 212

Table 5.3: Summary of Gene fold change with three different primary healthy fibroblasts 26789, 27065 and 27913, stimulated with the one healthy (26993) and one IPF (191015-1) primary BEC conditioned media. 229

Table 8.1.1: Cellular differential raw data. 279

1. Introduction

1.1. Interstitial lung disease

Interstitial lung diseases (ILDs) encompass a broad range of lung pathologies demonstrating pathological abnormalities in the pulmonary interstitium and connective tissues, which maintain normal lung morphology supporting the alveolar network. The ILDs consist of a heterogeneous group of diseases differing in cause, clinical manifestations, pathology and treatment (**Table 1.1**). Owing to the heterogenic nature of ILD accurate diagnosis often requires a combination of physical examination, information on patient environmental exposures, family history, examination of high-resolution computed tomography (HRCT) of the thorax, bronchoalveolar lavage (BAL) differential counts and, if required, lung tissue biopsy with histological analysis [4]. ILD pathologies may involve inflammation in response to environmental or infectious agents, genetic polymorphisms, autoimmunity, or develop from currently undetermined mechanisms. Specific ILDs may exhibit fibrosis in the parenchyma, which is characterised by significant interstitium thickening, due to enhanced extracellular matrix (ECM) deposition. This ECM consists primarily of collagen I and III, elastin and microfibrils [5] with alterations resulting in impaired gas exchange and a concomitant reduction in lung function. Our understanding of different factors influencing the development of specific ILDs is improving, however, further research is necessary to fully elucidate mechanisms involved in pathology. Essential to the treatment of different ILDs is the stratification and appropriate diagnosis of specific ILDs, often requiring input from multiple diagnostic procedures which will be discussed in more detail.

1.1.1. Clinical examination and diagnosis of ILD

Clinical measurements examining the presence of and progression of ILD include lung function readouts such as forced vital capacity (FVC) and transfer factor/diffusing capacity of the lung for carbon monoxide (CO) (TLCO or DLCO) [6]. The FVC provides an approximate estimate of the lung air capacity and ability of the individual to expel air from the lung. In restrictive lung diseases, such as ILD, the FVC is decreased, which differs from obstructive lung diseases where the FVC may be unchanged, but there is a decrease in forced expiratory volume in 1 s (FEV_1) [6]. A decrease in FVC provides an indication of progression of disease in a patient with ILD. Similarly, a reduction in TLCO/DLCO suggest progression of pathology in ILD. TLCO provides an estimate of the diffusing capacity of gas exchange, calculated from the conduction of CO through the alveolocapillary membrane, and blood conduction, calculated from the reaction rate of carboxyhaemoglobin and the volume of alveolar-capillary blood [6].

HRCT thoracic imaging and tissue biopsy examination differentiates histopathological abnormalities in patients with ILD including the presence of usual interstitial pneumonia (UIP) or non-specific interstitial pneumonia (NSIP) patterns which are indicative of specific ILDs. For example, ILDs such as Idiopathic pulmonary fibrosis (IPF) frequently exhibit areas of honeycombing, reticular lines and traction bronchiectasis. Alternatively, presence of nodules may indicate ILDs such as hypersensitivity pneumonitis (HP) or sarcoidosis [4].

Analysis of cellular composition of the airspace by the collection of BAL fluid, and subsequent differential counts of the cells present, is a low risk procedure allowing the analysis of a compartment relevant to the pathology, aiding the diagnosis of specific ILDs. Composition of

leukocyte populations in the BAL using cellular differential analysis aids the diagnosis of patients with known increases in specific populations. For example, increased lymphocytes are hallmark feature of pathologies including sarcoidosis, hypersensitivity pneumonitis (HP) and chronic hypersensitivity pneumonitis (cHP) [7], similarly increased eosinophils are a key diagnostic feature of eosinophilic pneumonia [8]. Determining the differential proportion and cell number of multiple leukocytes through morphological analysis of BAL cytospins has been used as part of the diagnosis of patients with ILD since the mid-1980s [9], however, the technique relies on the examination of the morphology of nucleated cells stained on a BAL cytospin by a trained individual counting >300 cells. Despite the usefulness of this analysis the technique remains subjective and relies on the analysis of a relatively small number of cells. With the advent of multi-parameter flow cytometry and multiplex analysis of proteins within the BAL our understanding of leukocyte populations and mediators which may affect disease progression is improving but combined analysis of cellular populations and mediators is still lacking.

The multi-disciplinary analysis of diagnostic observations, combined with assessment of family history and environmental exposure, provides invaluable information to determine diagnosis of defined ILDs enabling the prescription of the most efficacious therapeutics in the treatment of specific ILDs, which differ in causation and progression.

1.1.2. ILD aetiology and pathogenesis

ILDs may develop from a range of different environmental insults, genetic polymorphisms and autoimmune or inflammatory factors. For example repeat exposure to environmental antigens, such as bird or animal dander, may lead to hypersensitivity pneumonitis (HP), with hallmark

features including increased inflammatory lymphocyte infiltration into the airways leading to pulmonary pathology [10]. If HP is left untreated it may progress into a chronic form, cHP, with presence of both increased lymphocyte infiltrate into the airways and fibrosis in the lung parenchyma [10]. ILDs with an inflammatory stimulus, such as environmental antigen driven HP often respond well to removal of antigen stimulus, or if not possible, treatment with immunosuppressive therapies [4]. There are known specific environmental exposures that can lead to ILD, for example repeat exposure to specific substances such as asbestos can manifest in asbestosis-ILD, which currently has no known effective therapeutics [11]. Alongside specific environmental insults, pollution, smoking, metal and wood dusts are also believed to be contributing factors to ILDs [12-14]. Other risk factors include adverse reactions to specific drugs leading to ILD, for example bleomycin use in chemotherapy can trigger the development of ILD [15]. Drug induced ILD can result in inflammatory ILDs with or without the presence of fibrosis [16]. Bacterial, viral or fungal infections may result in ILD with a predominant cryptogenic organizing pneumonia (COP) pattern on the HRCT image [17]. However, in some patients where there is presence of clinical features resembling infectious pneumonia with inflammatory infiltrate, treatments with antibiotics are ineffective, and cultures are negative [18]. Infections may lead to acute exacerbations of existing conditions or acute interstitial pneumonitis characterized by inflammation and diffuse alveolar damage [19]. Further to environmental risk factors leading to ILD numerous genetic polymorphisms have been associated with increased risk of developing specific ILDs resulting in some cases in familial interstitial pneumonia [20]. Assessment of family history can therefore highlight the possible presence of genetic pre-disposition to developing familial forms of ILD. Finally, many ILDs are autoimmune related with

the presence of auto-immune antibodies in specific connective tissue diseases (CTDs), such as rheumatoid arthritis, or non-specific auto-immune related with the presence of auto-antibodies, which does not fit any known CTD criteria, classified as undifferentiated connective tissue disease (UCTD) ILD [31].

The most frequently diagnosed ILD is idiopathic pulmonary fibrosis (IPF), which is characterised by chronic and progressive dysregulated deposition of ECM. Currently the cause of IPF pathology is unknown with limited therapeutic interventions [21], therefore it is critical to develop our knowledge on factors driving pathology in order to better tailor future therapeutics.

ILD	Abbr.	Cause	Pathological Features	Treatment
Idiopathic pulmonary fibrosis	IPF	Unknown.	Chronic and progressive pulmonary fibrosis with areas of UIP including honeycombing.	Pirfenidone [22], Nintedanib [23]
Hypersensitivity pneumonitis and chronic HP	HP/ cHP	Continual exposure to irritants.	Acute, sub-acute, or chronic. Fibrotic development in chronic conditions.	Remove irritant if possible. Systemic corticosteroids [10].
Non-specific interstitial pneumonitis	NSIP	Unknown. Can be collagen vascular disease, HP or drug related.	Characterised by uniform interstitial inflammation with varying stages of fibrosis [24].	In cellular NSIP corticosteroids can be effective [25].
Cryptogenic organizing pneumonia	COP	Unknown, bacteria, virus, fungi, drug related.	All other ILDs must be excluded. Patients demonstrate a prominent pattern of organizing pneumonia [17].	Corticosteroid therapy [26].
Acute interstitial pneumonitis	AIP	Unknown, infection, acute exacerbation.	Severe and sudden respiratory failure, bilateral lung infiltrates and DAD.	Corticosteroid therapy, ventilation and supportive care [19].
Desquamative Interstitial Pneumonitis	DIP	Smoking related, inhaled toxins, infection.	Increased number of macrophages in the alveoli that are stained with yellow/black pigments.	Corticosteroid therapy [27].
Sarcoidosis	Sarcoid	Granulomatous reaction.	Increase in inflammatory cells (granulomas) that can form as nodules in multiple organs but are mainly in the lung.	NSAIDs and in more severe cases corticosteroids [28].
Systemic sclerosis	SSc-ILD	Autoimmune disease. ILD occurs in 75% of patients with SSc.	Areas of NSIP or UIP in lungs.	Cyclophosphamide [29].
Asbestosis		Asbestosis fiber inhalation.	Presence of asbestosis fibres, NSIP, UIP, pleural fibrosis.	No effective treatments [11].

ILD	Abbr.	Cause	Pathological Features	Treatment
Undifferentiated Connective Tissue Disease/ Connective Tissue Disease	UCTD/ CTD-ILD	Autoimmune related.	NSIP, presence of autoantibodies in CTD related to autoimmune diseases such as SLE, Sjögren's syndrome, and RA. If patients have autoantibodies but does not fit CTD criteria they can be diagnosed with UCTD [30].	Treatment related to underlying condition e.g. immuno-suppressants such as corticosteroids.
Eosinophilic Pneumonia	EP	Allergy, infection, drug related, irradiation.	Three forms; chronic, acute and allergic eosinophilia. Can be associated with diffuse lung diseases and CTD. Characterised by pulmonary eosinophilia.	Corticosteroid, allergy avoidance [31].
Obliterative Bronchiolitis	OB	Autoimmunity, exposure to inhaled toxins.	Pulmonary sub-epithelial inflammation and fibrotic bronchioles.	Corticosteroid [32].

Table 1.1: Summary of ILD pathologies and treatments.
Definition of abbreviations; usual interstitial pneumonia (UIP), diffuse alveolar damage (DAD), non-steroidal anti-inflammatory drugs (NSAIDs), systemic lupus erythematosus (SLE), rheumatoid arthritis (RA).

1.2. Idiopathic Pulmonary Fibrosis

1.2.1. Incidence and Epidemiology

IPF is the most frequently diagnosed ILD and is increasing in prevalence both in Europe and the United States of America (USA) [1]. IPF is characterised by the presence of usual interstitial pneumonia (UIP) including presence of honey combing on HRCT images [33]. Other diagnostic features include breathlessness upon exertion, presence of a dry cough, clubbing of finger tips and crepitations audible on auscultation of the lung [33]. In the USA the incidence of IPF was reported at 5.8 cases per 100,000 in 2010 [34] and in 2008 the incidence rate in the United Kingdom (UK) was reported to be 7.44 per 100,000, with over 5000 new cases diagnosed yearly [35]. Typically IPF is more common in elderly males aged over 65 years [34, 35] with a median survival between 2-5 years post diagnosis [1, 34, 35]. In the UK the survival rate inversely correlated with the increased age group of the patients with median survival rates of 6.8, 4.5, 3.2, 2.6, 2.0 and 1.6 years in individuals under the age of 65, 65–69, 70–74, 75–79, 80–84 years and 85 years and over respectively [35]. Although research comparing ethnicity and IPF are limited, Swigris and colleagues in 2012 examining IPF related deaths in the USA, reporting Hispanics were more likely, and African-American were less likely, to die of, and therefore likely to be diagnosed with IPF than Caucasians [36]. Whether this is related to genetic polymorphisms remains to be determined. With rising numbers of individuals diagnosed with IPF worldwide development of our understanding of causes of onset and progression is ever more critical.

1.2.2. *In vitro* and *in vivo* models of pulmonary fibrosis

In order to dissect the mechanisms involved in pulmonary fibrosis both *in vitro* and *in vivo* models have been utilised to understand contributing factors and pathways involved in pathology. One of the most widely studied cells in *in vitro* assays is the fibroblast. A hallmark pathological feature of the IPF lung is the presence of fibrotic foci, regions which are characterised by excessive numbers of apoptotic resistant localised fibroblasts [37]. Fibroblasts have been shown to differentiate into pro-fibrotic, alpha smooth muscle actin (αSMA) expressing, myofibroblasts, which lay down increased ECM, are highly proliferative, and are resistant to apoptosis [38]. To recapitulate this pathology and further interrogate fibroblasts *in vitro*, both healthy and IPF fibroblasts have been examined in the presence of possible pro-fibrotic mediators and anti-fibrotic mediators. Read outs from these assays often examine key features of fibroblasts in fibrosis including; fibroblast proliferation, differentiation, and the production of fibrotic mediators and ECM (Reviewed in [39]). Insights from *in vitro* fibroblast assays have identified numerous pro-fibrotic mediators, such as TGFβ, and have enabled the identification and dissection of pathways driving pathology, such as the PI3K/AKT signalling pathway [40-43]. Further investigation into *in vitro* assays using fibroblasts cultured on differing ECM has shown the ECM itself is able to activate fibroblasts, acting as a positive feedback loop in IPF [44]. This highlights the importance of considering the impact of culturing conditions in *in vitro* investigation. Complimentary to the study of fibroblasts, investigations into the role of epithelial cells in IPF have been examined. Several important features have been highlighted involving epithelial cells in the pathology of IPF including; epithelial to mesenchymal transition (EMT) [45-47], a process by which epithelial cells are thought to differentiate into fibroblasts, epithelial cell

death [48-50] as a key feature of fibrosis, and the production of profibrotic mediators [51] contributing to the ECM deposition in the lungs. Furthermore, investigators have examined leukocytes from the bronchoalveolar lavage (BAL) of IPF and healthy individuals. BAL is typically extracted by the administration of pre-warmed sterile saline into the right middle lobe of the lung using a bronchoscope, administering and aspirating aliquots, which can then be pooled for further examination and/or used for clinical diagnosis [52-54]. This has led to the identification of numerous different mediators in IPF BAL fluid supernatant [55, 56] and has enabled the examination of BAL cellular mediator production and how mediators produced by BAL leukocytes may impact disease pathogenesis [57]. Investigating differences in how primary cells from healthy and IPF donors respond to stimuli provides an important insight into how altered responses in cells from diseased individuals influence pathogenesis. Complimentary to the study of cells in *in vitro* assays, histological examination of the fibrotic lung tissues provides a snap-shot of fibrotic regions, identifying cell phenotypes and morphology with traditional staining, such as haematoxylin and eosin staining, and more detailed analysis of cells in the fibrotic tissue, by the binding of labelled antibodies to specific proteins, identifying key cell types present and what they may be producing in fibrotic areas by immunohistochemistry (IHC) or immunofluorescent (IF) staining [58-61].

In vitro systems provide an important platform to build upon in understanding what may contribute to disease pathogenesis in man, however, the simplicity of *in vitro* analysis does not address the multiple interactions in the airways and tissues, including cellular recruitment, complex cellular communication, mechanical stresses and combined interactions with multiple extracellular mediators. Advances in co-culture systems and computational co-culture modelling

[62] have enabled the dissection of fibrotic mechanisms improving the recapitulation of an *in vivo* setting, however, studies investigating fibrosis utilising co-culture systems are limited. Developments of these systems are technically very challenging and do not recapitulate an *in vivo* system. To address this numerous *in vivo* models have been established to examine lung fibrosis these include irradiation-induced lung fibrosis models [63], administration of silica in silicosis induced models [64] and administration of FITC into murine airways [65], all of which result in fibrotic lesions in the murine lungs [66]. The most widely used *in vivo* model of pulmonary fibrosis is the murine bleomycin model of pulmonary fibrosis.

Bleomycin was originally used as an antibiotic and was found to be effective against tumours [67], however, dose dependent side effects result in pulmonary toxicity and eventually pulmonary fibrosis in humans [15]. Typically, the bleomycin model of pulmonary fibrosis is initiated by the administration of bleomycin into the mouse airways via the intratracheal [68] or oropharyngeal routes [69], which results in an early inflammatory stage, and a later fibrotic phase, in the lung. The resulting pathology in the mouse includes acute lung injury involving damage to the alveolar epithelium with necrosis of type I epithelial cells and metaplasia in type II epithelial cells, with subsequent leakage of fluid and plasma proteins into the alveolar space. Inflammatory infiltrates occur in response to this damage, with an influx of lymphocytes [70], neutrophils [71] and monocytes [72] into the airways. The fibrotic phase follows with the accumulation of ECM proteins, such as collagen, leading to fibrosis in subpleural regions [68, 73]. The inflammatory stage occurs up to day 14 when the fibrotic phase develops with maximum fibrosis day 21-28 [73]. However, there are a number of disadvantages in the translatability of this system to man, notably the initiation of the disease using bleomycin, which does not drive

the development of human IPF, and the resolution of fibrosis in the model [74], which does not occur in man. Despite the limitations to either *in vitro* and/or *in vivo* systems the continuing development of human *in vitro* assays and development of translatable *in vivo* models have assisted in our understanding of factors initiating and driving pulmonary fibrosis leading to the development of novel therapeutics.

1.2.3. IPF Pathogenesis

IPF is a progressive and chronic disease characterised by periods of acute exacerbation (AE), which is defined by a sharp decline in lung function [33]. The cause and progression of IPF during stable periods or during periods of AE is currently unknown, nevertheless, research into the field is providing a valuable insight into our current understanding of disease pathogenesis resulting in the development of therapeutics. IPF was initially thought to be driven by ongoing inflammatory insults, however, anti-inflammatory therapeutics have been shown to be ineffective and in some cases detrimental [75]. Increasing evidence indicates that abnormal wound healing in response to repeat epithelial damage is driving IPF pathology [76], despite this the cause of the insult is yet to be determined. A 'multiple hit' model has been proposed comprising a combination of environmental factors, cellular interactions and genetic polymorphisms exacerbating repeat injury to the epithelial layer resulting in abnormal wound repair [77]. These ongoing insults led to the release of pro-inflammatory and pro-fibrotic mediators including, connective tissue growth factor (CTGF), TGFβ and activation of the coagulation pathway [78]. Pro-fibrotic mediators such as TGFβ have been shown to promote the activation of mesenchymal cells resulting in the differentiation and proliferation of myofibroblasts, which excessively produce collagen and other components of the ECM [79].

Other potential triggers for the activation of fibroblasts include the ECM itself with increased 'stiffness' reported to induce an activated myofibroblast phenotype [44]. A number of cellular sources have been proposed as contributing to the increased number of fibroblasts in the IPF lung including; proliferation of resident fibroblasts, recruitment of fibrocytes from circulation and EMT, whereby the epithelial cells lose their phenotype and transition into a pro-fibrotic fibroblast. It is possible that one or combinations of the described sources are contributing toward the increased numbers of fibroblasts seen in the IPF lungs. The initial triggers and cause of AE and ongoing progression remain to be determined, with numerous contributing factors including genetic polymorphisms, cellular influence and senescence, soluble mediators and environmental exposures which will be discussed in further detail.

1.2.3.1. Genetic polymorphisms

Numerous genetic polymorphisms have been reported in IPF with a number of genes found to be associated with epithelial alveolar type 2 (AT2) function including surfactant protein C/A (SFTPC/SFTPA) encoding surfactant proteins [80], which function to aid gas exchange, maintaining stability in the alveoli, and are involved in host defence [81]. The impaired surfactant production may lead to cellular toxicity resulting in alveolar epithelial cell death [82]. Taken together disruption of normal production of surfactants acts not only to impair normal gas exchange, but also disrupts alveolar morphology, adding additional stress to the alveolar type 1 (AT1) and AT2 cells further progressing IPF. Mucin 5B (MUC5B) polymorphisms result in the increase in the production of mucins by the bronchial epithelial cells (BEC) [83-85]. Mucins are known to be involved in host defence and clearance of debris from the airways, an increase in the mucins may disrupt the normal function of these proteins in the clearance of debris [86].

However, the MUC5B polymorphism is associated with an improved prognosis in IPF patients when compared to IPF patients who do not exhibit this polymorphism [87] further adding to the complex nature of IPF initiation and progression. Desmoplankin (DSP) polymorphisms, the gene which encodes desmoplankin, have also been reported in some cases of IPF [88, 89]. DSP is an important component in epithelial barrier formation suggesting the epithelial barrier may be altered in IPF individuals with this polymorphism [88], however analysis of expression revealed an increase in DSP suggesting a possible increase as a result of persistent epithelial injury [88]. Alongside these epithelial associated gene polymorphisms a number of polymorphisms have been identified that may involve multiple cell types including Telomerase Reverse Transcriptase (TERT) and Telomerase RNA component (TERC) polymorphisms [89, 90], which have been associated with increased risk and poor prognosis [90]. TERT/TERC encodes components of telomerase, which is involved in maintaining telomere length and is therefore involved in the aging/senescence and cell exhaustion [90] and may cause exhaustion of epithelial stem cell resources preventing the cells from undergoing normal renewal and repair after injury [91, 92]. Toll-interacting protein (TOLLIP) single nucleotide polymorphisms (SNPs) are also associated with some cases of IPF [83]. TOLLIP is a negative regulator of the toll like receptor (TLR) signalling pathway suggesting this SNP may result in aberrant activation of the TLR signalling [93]. These genetic predispositions can manifest as familial pulmonary fibrosis, where multiple relatives develop pulmonary fibrosis, or they may contribute indirectly toward IPF pathogenesis when combined with additional environmental or pathogen insults.

1.2.3.2. Cellular senescence

As previously discussed IPF incidence is increased in elderly populations, this could be because of increased exposure to unknown environmental insults accumulating in elderly populations and/or as a result of cellular senescence [94]. Investigations into senescence in IPF have shown an increase in the abundance of senescent phenotypes in IPF patients compared to healthy aged matched controls, with an increased senescent phenotype reported in (myo)fibroblasts [95] and BECs [96]. Senescent IPF myofibroblasts have been shown to be highly resistance to oxidative-stress-induced cell death. This finding suggests a potential mechanism for myofibroblast accumulation in the IPF airways [95]. Furthermore, BECs could be induced into a senescent phenotype with TGFβ, a key pro-fibrotic cytokine. The senescent IPF BECs were shown to produce increased levels of Interleukin-1 beta (IL-1β), and the increased IL-1β levels were able to induce fibroblast differentiation in pro-fibrotic myofibroblasts [96]. Taken together the data highlights the pathological role senescence can play on influencing profibrotic phenotypes in multiple cell types.

1.2.4. The roles of stromal cells in IPF pathogenesis

1.2.4.1. Epithelial cells in health and IPF

Airway epithelial cells play an integral role in maintaining a physical barrier from the external environment, impeding entry of foreign particles, defending against invading pathogens and aiding the principle role of the lung in facilitating gas exchange. Lung epithelial cells lining the airways are composed of a heterogeneous population of cells which differ in composition dependent on anatomical location. Epithelial cells lining the trachea consist of club, basal, goblet,

neuroendocrine and ciliated basal cells, in a complex pseudo-stratified layer [97]. Each cell type plays key roles within the airways. Club cells produce proteins that protect the trachea and bronchioles, and aid the conjugation of the secretory portion of IgA antibodies [98]. Goblet cells secrete mucins, proteins which comprise the main proportion of airway mucus [99]. Neuroendocrine cells are able to integrate the nervous and endocrine system [100] and ciliated basal cells, which produce mucins, remove debris through muco-ciliary clearance [101]. The epithelial cells bind together maintaining tight junctions with one another to prevent the entry of foreign particles [100]. The bronchioles consist of simple columnar club and ciliated cells with occasional basal cells [100]. Club cell numbers decrease and ciliated cells increase toward the alveoli [100, 102]. The alveoli consist of AT1 and AT2 pneumocytes. Over 90% of the lower airways consist of AT1 cells forming a fine cellular lattice, maximising surface area enabling optimal gas exchange between the alveoli and blood capillaries. AT2 cells play key roles in the production of surfactant, lowering surface tension within the alveoli and facilitating the exchange of gases. AT2 cells are also thought to be able to proliferate and differentiate into AT1 cells after injury [100, 102].

It is widely believed that IPF results from repeated injury to the alveolar epithelium, resulting in AT1 cell apoptosis and activation of aberrant wound healing (**Figure 1.1**). Observations of lung tissue morphology in IPF patients have highlighted severely altered epithelial phenotypes; with an increase in AT1 apoptosis in the airways, increased AT2 cells in the airways and surrounding fibrotic foci, and increased BECs lining areas of honey comb cysts [100, 102]. A number of factors may influence the progression of this cascade including repeat injury, aforementioned genetic polymorphisms, release of fibrotic mediators, activation of TGFβ1 by epithelial cells, and

epithelial-mesenchymal cross-talk resulting in excessive proliferation of fibroblasts and ECM production. Epithelial cells release a variety of pro-inflammatory cytokines and chemokines in response to infectious challenge, for example viral infection, which result in the expression of chemokines known to be associated with IPF such as CCL2 and IL-8 [103]. In response to damage associated molecular patterns (DAMPs) epithelial cells are able to release pro-fibrotic wound healing factors such as connective tissue growth factor (CTGF) [104, 105], vascular endothelial growth factor (VEGF) [106], platelet derived growth factor (PDGF) [107] and TGFβ1 [108]. Complimentary to this, ECs are also known to express integrins, such αVβ6, which activate TGFβ from its latent to active form [109]. Integrins are also able to influence the activation and differentiation of fibroblasts via epithelial-mesenchymal cross-talk [110]. The release of the aforementioned pro-fibrotic factors by epithelial cells can lead to the proliferation and differentiation of ECM producing myofibroblasts [111]. The complex interplay between the epithelial cells and fibroblasts is critical in potentiating the progression of fibroblast mediated fibrosis.

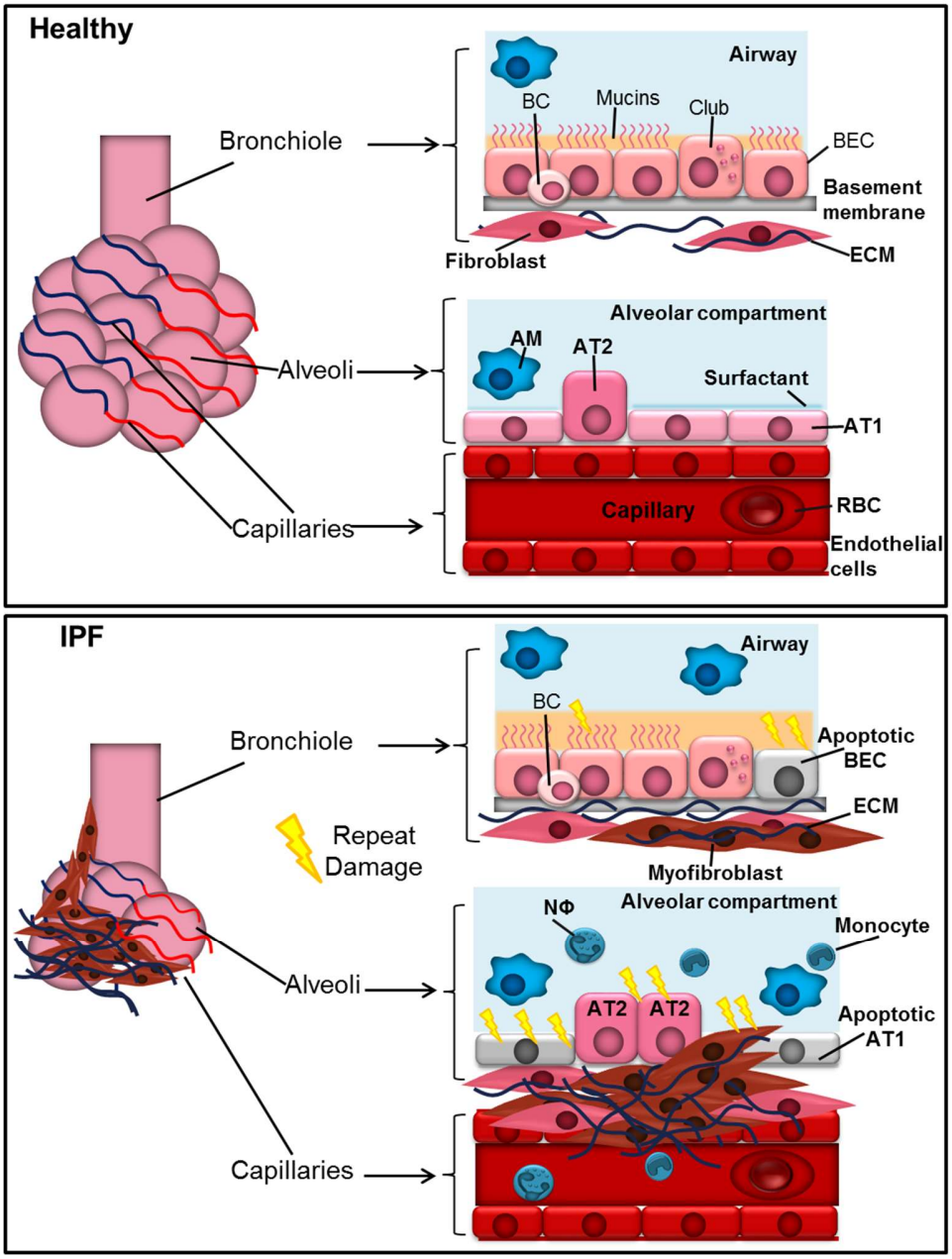


Figure 1.1: Bronchiole and alveoli in health and in IPF.
Repeat damage to the alveolar epithelial cells leads to the destruction of the alveoli characterised by alveolar type 1 (AT1) cell apoptosis and proliferation of AT2 cells. The destruction of the AT1 leads to the release of pro-fibrotic mediators such as TGFβ1 and chemokines resulting in the proliferation and differentiation of fibroblasts into ECM producing myofibroblasts and recruitment of leukocytes from the blood. Definition of abbreviations; basal cell (BC), bronchial epithelial cell (BEC), extracellular matrix (ECM), alveolar type 1 and 2 (AT1/2), red blood cell (RBC), neutrophil (NΦ).

1.2.4.2. Fibroblasts in health and IPF

Fibroblasts are critical in preserving lung tissue architecture, maintaining ECM and assisting wound healing when required. Fibroblasts are able to release a variety of soluble pro-angiogenic chemokines and growth factors important in both wound healing and fibrosis, including IL-8 (CXCL8) [112], VEGF [113], and activate TGFβ via expression of integrin αVβ5 [109]. Release of these mediators and activation of TGFβ are critical to both wound healing and fibrosis leading to the production of ECM. Myofibroblasts are the main source of ECM deposition, which is comprised of a highly dynamic complex of fibrous proteins including collagens I, III, IV and fibronectin [114, 115]. Activation of fibroblasts can occur in response to stimuli from mediators produced by the endothelium, leukocytes and the epithelium. The epithelium produces a variety of growth factors in response to injury that stimulate the differentiation and activation of myofibroblasts, which are characterised by an upregulation of α-smooth muscle actin (αSMA) [116]. This excessive proliferation of (myo)fibroblasts results in a characteristic histopathological feature of the IPF lung; the presence of fibrotic foci [117]. Interestingly AT2 cells are often found surrounding the fibrotic foci, and are thought to play a role in maintaining (myo)fibroblasts through EMT [118, 119]. The source of ECM producing myofibroblast and fibrotic foci remains controversial. There are currently three possible sources, or a combination thereof, for myofibroblasts in the IPF lung. Firstly, fibroblasts already present in the tissue may become activated, proliferate and differentiate into myofibroblasts via previously highlighted mechanisms, for example activation via TGFβ1 signalling, with experimental evidence suggesting the ECM stiffness potentiates the activation of myofibroblasts [120]. Secondly, the increases in fibroblasts may result from the recruitment and differentiation of CXCR4-positive fibrocytes into

the lung via CCL2 and CXCL12 from circulation [121-123]. This is further supported by reported increases of fibrocytes in IPF lung [123]. Finally, the increases in fibroblasts are thought, at least in part, to result from EMT whereby the epithelial cells are believed to reduce the expression of E-Cadherin and upregulate the expression of αSMA and fibronectin as a result of TGFβ signalling [124] and Wnt/β-catenin signalling cascade [125], however, the influence of EMT in the IPF lung remains controversial.

1.2.4.1. Leukocytes in fibrosis

Numerous studies have examined the content of leukocytes using cellular differentials in both healthy individuals and in individuals with ILD. A typical healthy BAL profile consists of myeloid cells such as airway macrophages comprising the majority of the leukocytes at approximately 80-100%, neutrophils between approximately 0-2%, and eosinophils less than 1% [126]. Lymphoid populations are typically the second largest cellular population of between 5-15% of total leukocytes [126]. Studies examining healthy BAL has revealed an increase in the proportion of CD4+ T cells and a decrease in CD8+ T cells in older individuals [127]. As ILDs are more common in individuals over 60 years old, multiple studies have examined CD4+ and CD8+ T cell ratios. CD8+ T cells have been reported as increased in IPF BAL [128], with comparisons showing that the lung and BAL ratios correlate [129]. Similarly studies examining other ILDs such as HP and cHP have shown differences in the CD4+ and CD8+ ratio suggesting that CD8+ T cells are increased in HP, and CD4+ T cells are increased in cHP [130, 131], however, a recent study examining a large cohort of individuals with HP and cHP suggest there is no clear relationship with stages of HP and CD4/CD8 ratios [132]. IPF is believed to be T helper type 2 (Th2) CD4+ lymphocyte skewed, with evidence showing an increased Th2 profile in the BAL of IPF patients [133]. Evidence to support

this has shown that IPF fibroblasts are hyper-responsive to Th2 cytokine IL-13 inducing an upregulation of TGFβ receptor [134] and Th2 cytokine IL-4 polymorphisms correlate with progressive disease [135, 136]. However, measurements of HRCT score from patients with IL-4 polymorphisms showed patients progression was more stable [137] and anti-IL-13 therapeutics have failed to show efficacy in IPF [138]. Examination of other lymphocytes such as B cells in the bleomycin model of lung fibrosis revealed B cells produced fibrogenic cytokines, such as IL-6, upon stimulation with ligand (hyaluronan) [139], alongside this evidence has shown increased plasma levels of B-lymphocyte stimulator, which correlates with poor prognosis in IPF patients [140]. Examination of innate lymphocytes, including the natural killer (NK) cells, have shown differences comparing IPF to other interstitial pneumonia patients with increased percentage and number of NK cells in the peripheral blood and BAL of IPF patients [128, 141] and HP [142]. Studies investigating function and composition of other lymphocytes including regulatory T cells, showed impaired ability to suppress inflammation in IPF [143] and analysis of γδ T cells show no difference compared to healthy controls [144].

Although lymphocytes have been examined in the BAL extensively there is still limited information on innate immune cells, particularly in combination with study of lymphocytes. Early studies examining BAL by Immunohistochemistry (IHC) revealed an increase in a cell with a monocyte-like appearance [145-147] and a recent study examining myeloid populations in blood, lung and BAL showed differences in IPF patients myeloid cells in lung and blood samples, however, this study included a small number of healthy BAL samples with no disease comparison [148]. Myeloid cells, such as mast cells have been implicated in the pathogenesis of IPF. Mast cells have been reported as increased in IPF lung tissue [149, 150], and are able to stimulate

fibroblast proliferation by release of tryptase, which stimulated proliferation in a PAR-2/PKC-α/Raf-1/p44/42-dependent manner, potentiating PAR-2 dependent ECM production [150]. Fibroblast in turn were able to enhance mast cell survival and proliferation through stem cell growth factor receptor, CD117, signalling [150]. Neutrophils are also reportedly increased in IPF, with increased numbers correlating with a worse prognosis [151]. Evidence *in vitro* suggests neutrophil elastase promotes myofibroblast differentiation and proliferation [152] and in an *in vivo* bleomycin acute exacerbation (AE)-IPF model, increased neutrophils corresponded with an induced AE [153]. Eosinophils have also been reported as increased in IPF BAL [154], correlating with worse prognosis [155], however this remains controversial with other groups finding no correlation with disease prognosis [151].

The most widely reported leukocyte to play a role in IPF pathogenesis is the macrophage, it's role in the lung in homeostasis and in fibrosis will be discussed in detail.

1.2.4.1.1. The role of airway macrophages in health and disease

Macrophages play fundamental roles in maintaining tissue homeostasis in organs throughout the body. Under normal homeostatic conditions macrophages in the lung are thought to be long lived and embryonically derived [156, 157], however bone marrow derived monocytes have been shown to be able to differentiate into airway macrophages after entering the lung environment in mouse [158], with increasing evidence suggesting monocytes can recapitulate the airway or alveolar macrophages (AMs) niche in man, especially after injury [159]. There are two main types of macrophage in the lung, the interstitial macrophage, which resides in the lung tissue, and the airway or alveolar macrophage which resides in the airspace [160]. Environmental signals

including growth factors, such as macrophage-colony stimulating factor (M-CSF) and granulocyte macrophage-colony stimulating factor (GM-CSF), alongside cytokines, such as tumour necrosis factor (TNF), IL-4 and IL-13, are known to be able to influence the differentiation of macrophages [161-171]. Differing signals can alter the macrophages to carry out specific roles in the airways such as host defence from invading pathogens or tissue repair [172, 173]. Macrophage phenotypes and their roles in health and disease will be further described.

1.2.4.1.1.1. Macrophage phenotypes

Investigations into macrophage phenotypes have led to the sub classification of macrophages into two major phenotypes, the M1 'classical' inflammatory macrophage and the M2 'alternatively activated' wound healing/immunoregulatory macrophage [161, 162]. Numerous reports in the late 1980s and early 1990s described a changed phenotype in human blood derived monocytes, and mouse derived macrophages in response to Th1 cytokines; IFNγ and IL-2, compared to the Th2 cytokine IL-4. Examination of macrophages post stimulation revealed that macrophages increased their production of pro-inflammatory mediators in response to Th1 cytokines, and decreased inflammatory mediator production in response to Th2 cytokines [163-166]. The term 'alternative activated' macrophage was first introduced after the observation that macrophages isolated from mouse peritoneum increased the expression of mannose receptor and decreased production of inflammatory cytokines in response to the Th2 cytokine IL-4 [167]. This led to the classification of macrophages into the two broad categories the 'classically activated' M1 macrophage and 'alternatively activated' M2 macrophage. Supporting this work early observations that macrophages derived from the predominantly Th1 skewed, C57BL6 mouse strain, compared to macrophages derived from the Th2 skewed, Balb/c mouse strain,

showed a polarised M1 phenotype in C57BL6 mice compared to an M2 phenotype in Balb/c mice [168-171]. Later, the observed differences reported in M1 phenotypes in C57BL6 mice were attributed to distinct metabolic profiles, characterised by reduced arginine metabolism in the M1 macrophage [174]. Subsequently however, it was shown that the C57BL6 strain have a deletion in a cationic amino acid transporter, impairing arginine transport. This deletion is likely to result in the previously described 'M1' metabolic profile [175]. Additional confusion in the use of the M1/M2 nomenclature has arisen from discrepancies in marker expression on macrophages in mouse compared to man. In order to highlight phenotypic differences specific to human macrophages, human blood derived monocytes were differentiated into M1 or M2 macrophages and detailed analysis of marker expression using FACS, and gene expression using RNA-seq, has provided a comprehensive overview of differential expression of specific human markers [162]. Owing to the complexity and variation in protocol used in the differentiation of macrophages from monocyte into the M2 phenotype, the M2 phenotype was further sub classified into M2a (alternative), M2b (Type II) and M2c (deactivated) [176]. **Figure 1.2** illustrates the M1 and M2a-c macrophage phenotypes, their cytokine production and role in inflammation or wound healing.

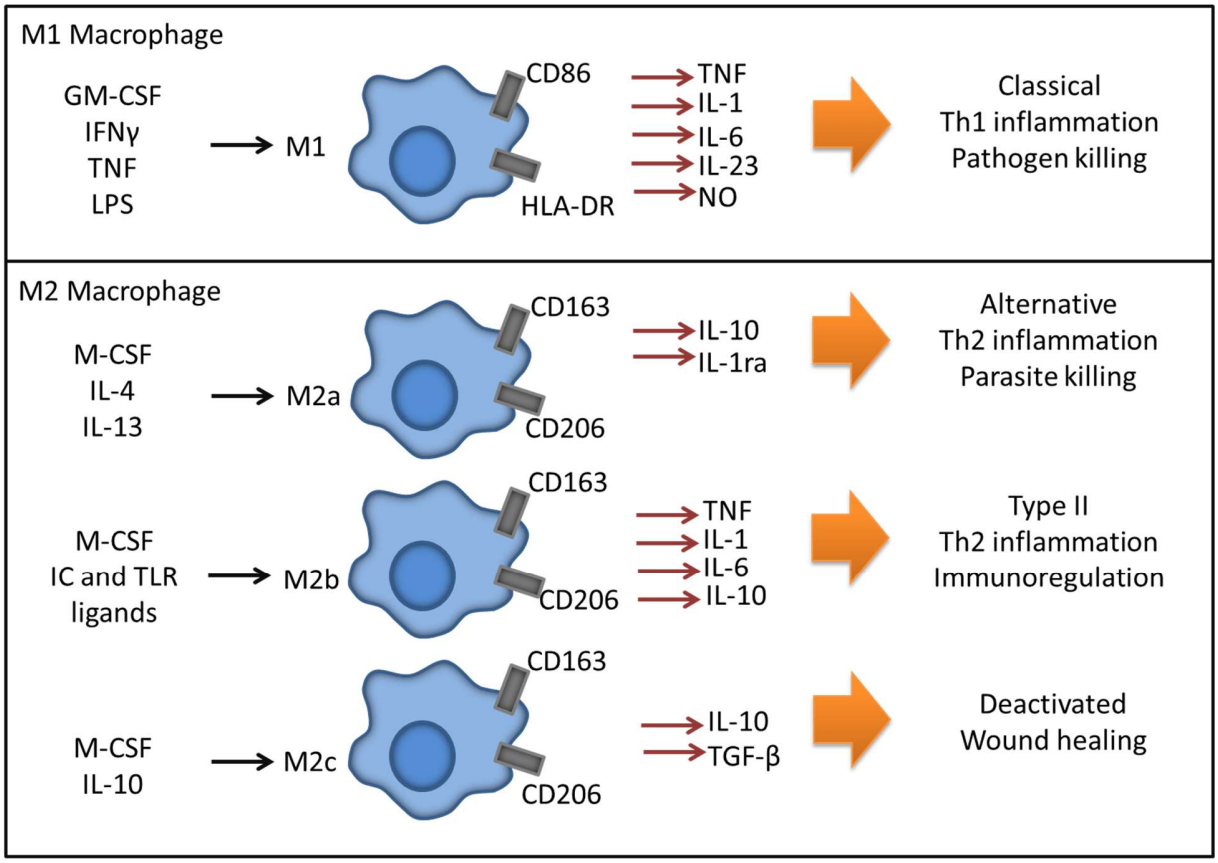


Figure 1.2: M1/M2 Macrophage Phenotypes.
The two main macrophage populations defined in literature M1 and M2 with subclasses of M2 macrophages described. M1 inflammatory macrophages can be differentiated from human peripheral blood mononuclear cells (PBMCs) with granulocyte macrophage colony-stimulating factor (GM-CSF) and cytokines such as Interferon gamma (IFNγ) and tumour necrosis factor (TNF) or lipopolysaccharide (LPS) and show increased expression of CD86 and HLA-DR [177]. Alternative M2 macrophages can be differentiated with macrophage colony-stimulating factor (M-CSF) in combination with cytokines and other factors including IL-4 and IL-13 (M2a), immune complex (IC) and Toll like receptor (TLR) and IL-1R ligands (M2b) and IL-10 (M2c) [176]. Expression of mannose receptor, CD206, and scavenger receptor, CD163, are reportedly increased on M2 macrophages [161, 178]. M2 macrophages are thought to be involved in Th2 inflammatory responses such as in allergy and parasite killing. The subclass of the M2 phenotype, the M2c macrophages, play a key role in wound healing as they release mediators that effect extracellular matrix deposition and remodelling [176, 179].

Taken together the work identifying M1 and M2 macrophages has largely involved the differentiation of monocytes using different methods (**Figure 1.2**) and from work examining tissue macrophages (typically peritoneal) isolated from the mouse. Recently a collective of researchers studying macrophages have called the M1/M2 classification nomenclature into question. The confusion that arises from the multiple methods used to generate macrophages and the lack of distinct markers, led the consortium to suggest defining macrophages in relation to how they have been generated and activated e.g. using IL-4 to activate your macrophage would result in the classification of an M(IL-4) macrophage [180]. Emphasis was placed on understanding the activation status of the macrophage as opposed to characterising by M1/M2 phenotype [180]. The simplistic M1/M2 phenotypic analysis is further limited by observations that macrophages in situ exhibit clear and distinct patterns depending on the influencing tissue microenvironment [172, 173], which suggests skewing of blood derived monocytes into M1 or M2 phenotypes does not recapitulate tissue residing macrophages. It is therefore important to focus on the resident macrophages in the tissue of interest when trying to understand the role of resident macrophages in both homeostasis and disease.

1.2.4.1.1.2. Airway macrophage role in host defence

AMs play a critical role in the elimination of pathogens, employing a number of different mechanisms to destroy invading bacteria. These include; presentation of bacterial antigen to T helper cells via the HLA-DR (MHC class II) receptor, opsonic and non-opsonic phagocytosis, the production of pro-inflammatory cytokines and chemokines, and the production of reactive oxygen species (ROS) and nitric oxide (NO) [146]. AMs use pattern recognition receptors (PRRs), such as Toll like receptors (TLRs), to detect the presence of pathogens [147]. To date 13 TLRs have

been identified in humans capable of detecting different ligands from bacteria, viruses and fungi [148]. Defects have been reported in the activation of TLR2 and TLR4 in AMs in patients with COPD resulting in abnormal TLR signalling [149]. With polymorphisms reported in TLR3 [150] and TOLLIP [83] in IPF patients it is likely similar abnormalities may be occurring in IPF AM TLR signalling. A number of other functional defects in IPF AM have been described, including defective autophagy [151], efferocytosis [152], and impaired ability to eliminate facultative intracellular bacteria [153]. However, investigation into the efficiency of IPF AM bacterial mediated elimination is very limited with only one early study investigating IPF AM function [153]. Further research in this area is crucial as bacteria and other invading pathogens may contribute to epithelial cell damage observed in the IPF lung.

1.2.4.1.2. The role of airway macrophages in tissue remodelling and IPF pathology

AMs have been shown to influence matrix remodelling directly through the phagocytosis of collagen, observed in mouse models of emphysema [181], and indirectly through the production of pro-fibrotic mediators. Numerous *in vivo* studies, in mouse and rat, modelling pulmonary fibrosis, have investigated the role of AM in the progression of the pathology. Investigations into the mechanisms have highlighted the importance of AMs in driving fibrosis via their production of the pro-wound healing, pro-fibrotic mediators including TGFβ1 [182-186]. Alongside this anti-fibrotic effects have been demonstrated after the depletion of macrophages in the bleomycin model of lung fibrosis [187]. Studies examining samples from IPF patients have shown that AMs produce a number of mediators that are involved in the progression of fibrosis including angiotensin II (ANGII) and ANG converting enzyme (ACE) [188], insulin-like growth factor 1 (IGF-

1), platelet-derived growth factor (PDGF), and the aforementioned TGFβ1 [189]. AMs from IPF patients exhibit an increase in the production of ECM modifying enzymes the matrix metalloproteinases (MMPs) [190-192], suggesting a role in mediating the breakdown of ECM. Observations in human IPF AMs have shown evidence of increased mitophagy, which enhanced apoptosis resistance. The authors demonstrated that the enhanced Akt1-mediated mitophagy resulted in an increased production of TGFβ1 by the AMs in mouse, leading to increased fibrosis [193]. They speculated a similar mechanism is likely to be occurring in IPF AMs [193]. Combined evidence from mechanistic studies in mouse alongside the examination of AMs from IPF patients suggests that AMs play an integral role in the progression of IPF pathology.

1.2.1. Analysis of cellular mediators in the BAL

Complimentary to cellular analysis, examination of mediators in the BAL provides an additional readout as to the inflammatory status of the lung environment. Willems et al (2013) used proteomic analysis of BAL to examine multiple extracellular mediators in patients with IPF and HP compared to healthy volunteers [194]. They highlighted key differences in matrix metalloproteinases, growth factors and chemokines, however, in this study they did not combine this analysis with the cellular content of the BAL [194]. Numerous independent studies have revealed significant increases in chemokines in IPF BAL compared to healthy controls, for example CCL2 and CXCL8 (IL-8), often correlating significantly with poor patient prognosis [195-200]. Differences in chemokine levels suggest recruitment of specific cell populations into the airways which may play a role in the progression of the disease. Chemokines have multiple functions in the airways, alongside their roles in cellular recruitment they have also been shown to influence angiogenesis. Although evidence implicating angiogenesis in the exacerbation of ILD

is controversial [201], numerous studies have reported an increase in pro-angiogenic chemokines such as CXCL8, CXCL5 and CXCL12 in IPF, with evidence showing pro-fibrotic effects in the bleomycin model [112, 202-205]. Conversely anti-angiogenic chemokines such as CXCL9, CXCL10 and CXCL11 are reported to be decreased and exert anti-fibrotic effects in the bleomycin model [47, 112, 206, 207]. This further highlights the complexity of the roles of mediators within the BAL at steady state and within a disease setting. A summary of literature investigating chemokines in the BAL of IPF patients is highlighted in **Table 1.2**.

Name	AKA	Receptor	Pro - Fibrotic	Increased/ decreased compared to healthy controls
CCL2	MCP-1	CCR2	Pro [208-212] [57, 134]	Increased [208-212] [57]
CCL3	MIP-1α	CCR4, 5	Pro [195, 213]	Increased [205, 213, 214]
CCL4	MIP-1β	CCR1, 5	Unknown	Unknown
CCL5	RANTES	CCR1, 3, 4, 5	Unknown	Increased [215] No difference [194]
CCL11	Eotaxin	CCR3, 5	Unknown	No difference [194]
CCL17	TARC	CCR4	Pro [195, 216]	Increased [57, 198]
CCL20	MIP-3α	CCR6	Unknown	Unknown
CXCL1	GROα	CXCR1, 2	Unknown	Increased [57](BAL Cell production)
CXCL5	ENA-78	CXCR2	Pro [202]	Increased [202]
CXCL8	IL-8	IL-8RA/B	Pro	Increased [112, 204, 205]
CXCL9	MIG	CXCR3	Anti [47]	No difference [197]
CXCL10	IP-10	CXCR3	Anti [207]	Decreased [112] No difference [197]
CXCL11	I-TAC	CXCR3	Anti [206]	Decreased [206]
CXCL2	MIP-2	CXCR2	Pro [217]	Unknown
CXCL12	SDF-1	CXCR4	Pro [203]	Unknown
CCL22	MDC	CCR4	Pro [195, 198]	Increased [57]

Table 1.2: Summary of chemokines in IPF.
Definition of abbreviations: CC motif ligand (CCL), CXC motif ligand (CXCL), monocyte chemoattractant protein (MCP), macrophage inflammatory protein (MIP), regulated on activation, normal T cell expressed and secreted (RANTES), thymus and activation-regulated chemokine (TARC), growth-regulated oncogene-alpha (GROα), epithelial-derived neutrophil-activating peptide 78 (ENA-78), monokine induced by gamma interferon (MIG), IFNγ inducible protein of 10 kDa (IP-10), interferon-inducible T-cell alpha chemoattractant (I-TAC), Stromal cell-derived factor 1 (SDF-1), macrophage derived chemokine (MDC).

Alongside chemokines influencing pathogenesis, cytokines and growth factors are thought to play roles, not only in the maturation, activation and differentiation of leukocytes in the airways, but also eliciting pro-fibrotic effects in the lung. TGFβ1 is widely regarded as a key pro-fibrotic

cytokine in the pathology of IPF through its actions differentiating fibroblasts into myofibroblasts, leading to the increased deposition of ECM [218]. Pro-inflammatory cytokines including TNFα and IL-6 are also believed to influence disease progression. TNFα has been shown to induce the production of cytokines TGFβ and growth factors such as platelet derived growth factor (PDGF) [219], which contribute toward disease pathogenesis. However, more recently TNFα has been shown to play a protective role in the bleomycin lung fibrosis mouse model [220]. Similarly IL-6 has been shown to exert pro-fibrotic effects inducing proliferation of fibroblasts and enhancing matrix deposition [221], however, macrophages producing IL-1β, TNFα and IL-6 are classified as inflammatory anti-fibrotic macrophages, further complicating the roles of these cytokines in pathology [193].

The hallmark feature of fibrosis is excessive and dysregulated production of ECM by myofibroblasts, this involves the interplay between multiple cell types and mediators released by cells influencing the remodelling of the lung. Key factors involved in remodelling of the airways, and in turn fibrosis, include vascular endothelial growth factor (VEGF) which plays a critical role in angiogenesis [222], and is increased in IPF plasma [223], and PDGF, which potently induces fibroblast proliferation and matrix deposition [224]. Alongside growth factors thought to influence stromal cells, there are also multiple growth factors such as granulocyte-colony stimulating factor (G-CSF) involved in the differentiation and maturation of granulocytes such as neutrophils [225] and macrophage colony stimulating factor (M-CSF) which is involved in the maturation of macrophages [226]. Interestingly both are reported increased in IPF and may play a role in the pathogenesis of fibrosis through their effects on leukocytes in the airways [227, 228]. **Table 1.3** summarises literature examining the role of multiple growth factors in IPF.

Growth Factor	Receptor	Function	Role in IPF
Angio-poietin-1	TIE-1 TIE-2 [229]	Vascular growth and lung vascular permeability [230].	Decreased in BAL compared to healthy [231]. No clinical correlation (serum) [230].
FGFb (FGF-2)	FGF-R [232]	Fibroblast growth [233]. Required for epithelial growth [234].	Protective in bleo [234].
G-CSF	G-CSF-R [225]	Primarily promotes the survival, proliferation, differentiation and function of neutrophils [225].	Increased in IPF BAL [227].
GM-CSF	CD116 [235]	Maturation and activation of macrophages and other granulocytes [236].	No difference in concentration in IPF BAL [237]. Protective in bleo [238].
HGF	HGFR [239]	Secreted by mesenchymal cells and acts mainly on epithelial cells. Stimulates cell motility, tissue regeneration and angiogenesis [240].	Decreased production by IPF fibroblasts [241]. Significantly higher in serum [242].
M-CSF	CD115 [226]	Promotes the differentiation of macrophages [226]	Increased in IPF BAL [228]. M-CSF$^{-/-}$ mice protected in bleo [228].
PDGF-AA	PDGFRα PDGFRβ [224]	Potent mitogen of mesenchymal cells such as fibroblasts and endothelial cells. Fibroblast chemoattractant [224].	Upregulated PDGF-AA in AM IPF [243]. IPF fibroblasts do not respond effectively to PDGF-AA [244]. Inhibitors protective in radiation-induced fibrosis [245].
PDGF-BB	PDGFRα PDGFRβ [224]	Potent mitogen of mesenchymal cells such as fibroblasts and endothelial cells [224].	IPF and normal lung mRNA similar, however, localised accumulation is observed [246]. Upregulated PDGF-BB in AM IPF [243]. Stimulated increased proliferation of normal lung fibroblasts compared to UIP fibroblasts [247]
SCF	c-KIT [248]	Cytokine that binds to the c-KIT receptor (CD177 on mast cells and others). Important in hematopoiesis [248].	Similar levels in IPF and healthy plasma [223]. Transmembrane SCF (not soluble SCF) elevated in fibroblasts and IPF lung tissue [150]. Transmembrane SCF promote mast cell survival in IPF [150].
TGF-α	EGFR [249]	TGF-α is a ligand for the EGFR, inducing cell proliferation and differentiation. [250]	Significantly higher in BAL [251]. Increased staining, particularly vascular endothelial cells [252].
VEGF	VEGFR2 [222]	Stimulates cell migration, survival, angiogenesis and vasculogenesis [222].	Increase in IPF plasma [223]. No difference in serum [253]. Significantly decreased in BAL [253]. TLCO values positively correlate with VEGF [199].

Table 1.3: Summary of literature examining growth factors in IPF.
Definition of abbreviations; Tyrosine kinase with immunoglobulin-like and EGF-like domains (TIE), bronchoalveolar lavage (BAL), fibroblast growth factor (FGF), bleomycin model of fibrosis (bleo), granulocyte-colony stimulating factor (G-CSF), granulocyte macrophage-colony stimulating factor (GM-CSF), hepatocyte growth factor (HGF), macrophage-colony-stimulating factor (M-CSF), platelet derived growth factor (PDGF), stem cell factor (SCF), transforming growth factor (TGF), vascular endothelial growth factor (VEGF).

1.2.1.1. Possible environmental factors exacerbating IPF

Multiple environmental insults have been associated with the development of IPF including increased risk associated with a smoking history [12]. Investigations have identified occupational exposure to metal dusts [13], wood dusts and farming exposure, such as exposure to pesticides and animal feeds [14] are also associated with increased risk. Repeat exposure to and close contact with animals including birds and cats have also been reported as an increased risk factor [14]. Recent studies have now highlighted air pollution as a possible influencing factor in acute exacerbation in IPF, with emphasis on increased ozone and nitrogen dioxide exposure associating with increased risk of AE-IPF [254]. These multiple and complex environmental triggers may act independently or in concert in potentiating IPF disease pathogenesis. Further work examining the mechanisms involved in environmental impact will help elucidate the contributing pathways that may play a role in potentiating fibrotic pathogenesis.

1.2.1.2. Infectious mediators influencing fibrotic progression

Apoptosis of the alveolar epithelial cells is a hallmark feature of IPF and is likely to be critical in the initiation of fibrosis. Alongside genetic susceptibilities to cell apoptosis, and environmental triggers resulting in cell death, apoptosis may also be triggered by bacterial or viral infection. Recent research has highlighted a differing lung microbiome comparing IPF to healthy, with increased burden of bacteria correlating with disease progression [26]. Whether these bacteria are increased as a result of the altered lung architecture, or as result of impaired clearance by leukocytes, or whether the bacteria contribute toward fibrotic pathology still remains to be determined. Alongside bacterial infection viral exacerbation with specific viruses has been reported associated with IPF disease model progression [255], making resistant mouse strains

susceptible to bleomycin mediated fibrosis [256], combined with evidence in IPF patients showing an increased presence of specific virus including herpes virus (HV) [257-259] and Epstein-Barr virus (EBV) [260]. The potential roles of bacterial and viral infection in IPF pathogenesis will be discussed in detail.

1.2.1.2.1. Bacteria

The advent of improved sequencing technology has enabled the accurate determination of the microbiome from lung BAL fluid samples. Sequencing of bacterial species specific ribosomal subunit, the 16S rRNA, has enabled scientists to detect and quantify relative abundance of specific species of bacteria by relative PCR [261]. Numerous studies have investigated the lung microbiome identifying changes comparing healthy controls to those with asthma [262], cystic fibrosis [263], COPD [264] and IPF [2, 3]. The bacterial phylum reported in healthy individuals consists predominantly of *Bacteroides*, *Proteobacteria* and *Firmicutes*, with predominant genera comprising of *Veillonella, Prevotella*, *Streptococcus* and *Pseudomonas* [265]. Interestingly differences in the constituents of the IPF microbiome have highlighted an increase in the relative abundance of *Streptococcus*, *Haemophilus, Neisseria* and *Veillonella* [26]. The increased bacterial burden in the IPF lung correlated with poor patient prognosis, which suggests a possible role for bacteria in the lung in the progression of fibrosis [266, 267]. Recently investigations into the changes in the microbiome during stable and AE-IPF has highlighted increased bacterial burden in AE-IPF compared to stable [268]. Furthermore, analysis of microbiome composition with paired gene expression profiles revealed a host defence response which correlated with increased bacterial burden [269]. Gene expression analysis identified increased expression of genes encoding antimicrobial peptides, SLPI and CAMP, and genes involved in host defence, but

also fibrosis, including the gene encoding the enzyme matrix metalloproteinase-9 (MMP-9), which can activate TGFβ, and therefore may also be playing a role in fibrotic progression [269]. Many of these genes remained elevated in longitudinal follow up suggesting persistent stimulation by bacteria in the airways [269]. Examination of the respiratory microbiome influence on host innate immune cells has highlighted distinct changes in the innate immune cells depending on the pulmonary microbiotic landscape [270]. Investigation into specific bacterial genera including proinflammatory *Staphylococcus* and *Pseudomonas* and low stimulatory *Prevotella* and *Streptococcus* bacteria, resulted in 'inflammatory' and 'remodelling' profiles respectively [270]. These profiles could in part be attributed to the influence the bacteria exerted on airway macrophages resulting in the induction of inflammatory or remodelling macrophage profiles [270]. Under normal homeostatic microbiome conditions the macrophages phenotypes were not skewed [270]. A detailed investigation into the host innate immune response and the microbiome with progression free survival of IPF patients revealed a down-regulation of immune response pathways, including Retinoic acid-inducible gene I (RIG1)-like, nucleotide-binding oligomerization domain and TLR pathways were associated with worse survival rates [271], suggesting an impaired ability to defend against pathogens, which may contribute to disease progression. Despite these advances investigations have not resolved why the microbiome may differ in IPF; is it as a consequence of the environment i.e. the altered lung architecture, or dysfunction in the immune cells regulating microbes in these patients? And is the microbiome contributing toward the pathology? Addressing these key questions is essential in order to develop our understanding of the progression of this debilitating disease.

1.2.1.2.2. Viral exacerbation

Examination of the presence of specific virus in the IPF lung has shown an increase in the detection of herpes virus (HV) [257-259] and Epstein-Barr virus (EBV)[260]. Investigations into the role of virally induced exacerbation of the bleomycin model of fibrosis have shown that resistant BALB/c mouse strains are able to develop pulmonary fibrosis with a viral challenge [256]. Furthermore viral challenge of mice in the bleomycin model with murine gamma herpes virus (γHV-68) but not gram negative bacteria *Pseudomonas aeruginosa* nor H1N1 viral challenge, resulted in increased apoptosis of alveolar epithelial cells, which showed increased TGFβ receptor 1 expression and SMAD3 phosphorylation [255]. Models of pulmonary fibrosis can be induced in a Th2 skewed IFNγR knockout mouse with γHV-68 infection resulting in increased TGFβ and matrix metalloproteinase-7 (MMP-7) expression, myofibroblast differentiation, hyperplasia of type II cells and production of Th2 cytokines [272]. Further investigation into factors driving this model showed a recruitment of arginase I expressing alternatively activated airway macrophages to areas of fibrosis, which showed high levels of expression of insulin-like growth factor-1 and fibronectin, a component of the extracellular matrix [273]. Similarly, IPF lung tissue showed increased expression of arginase I in epithelial cells, fibroblast foci, and alveolar macrophages compared with normal lung, suggesting arginase I could be upregulated by viral stimulation and may play a role in lung fibrosis [273]. Complimentary to the *in vivo* models *in vitro* experiments investigating the role of the EBV in the progression of fibrosis has shown that the human lung epithelial cell line, the A549 cell line, co-treated with low levels of TGFβ1 and latent membrane protein-1, expressed by EPV, resulted in a synergistic induction of EMT [274]. Furthermore, a study investigating the impact of EBV stimulation on A549 and primary human AT2 cells showed

an increase in expression of TGFβ1 post stimulation [275]. Collectively evidence from *in vitro* experiments combined with evidence from *in vivo* models suggests a role for viruses in IPF pathology.

1.2.1.2.1. Detection of pathogens in IPF

As previously discussed epithelial cells are able to play key roles in airway defence, not only by acting as a physical barrier, but also by orchestrating the innate and adaptive immune responses. Alongside macrophages, epithelial cells and fibroblasts are able to detect and respond to a variety of pathogens through pathogen recognition receptors (PRRs) such as the toll like receptors (TLRs), releasing both pro-inflammatory chemokines and cytokines in response to infection. A number of differences in expression of TLRs have been found to be associated with IPF. For example expression of TLR2, which detects bacterial, fungal, viral and endogenous substances, has been found to be increased in the lungs of IPF patients [276]. TLR2 has also been shown to promote collagen and fibronectin deposition in the bleomycin model of fibrosis [277]. Polymorphisms associated with TLR3, which detects viral double stranded (ds) RNA, have been discovered in some individuals with IPF and associated with a greater risk of mortality [278]. IPF derived fibroblasts carrying this polymorphism have been found to produce abnormal cytokine production in response to stimulation [278], suggesting the polymorphism may impair normal anti-inflammatory responses. Data from the bleomycin model of fibrosis has demonstrated TLR3-deficent mice have increased collagen deposition in the lungs [278]. Other TLRs including TLR9, which detects bacterial and viral DNA, has been found to be overexpressed in rapidly progressing IPF patients fibroblasts, which were more responsive to TLR9 ligand CpG DNA [279], suggesting differences in the detection and response to pathogens in IPF patients. In addition to the

polymorphisms associated directly with TLRs, single nucleotide polymorphisms (SNPs) have been found associated with TOLLIP [83-85], which is a negative regulator of TLR signalling [280], suggesting possible dysregulation in TLR signalling pathways. Taken together evidence showing an increased bacterial burden, potential viral exacerbation, genetic polymorphisms and alterations in TLR expression and signalling, suggest IPF patient cells may have an altered ability in the defence against invading pathogens.

1.2.2. Summary of IPF pathogenesis

IPF is multifaceted disease with numerous influencing factors acting in concert to drive pathogenesis. A graphical summary of IPF pathogenesis is illustrated in **Table 1.3** highlighting the complex nature of the disease progression.

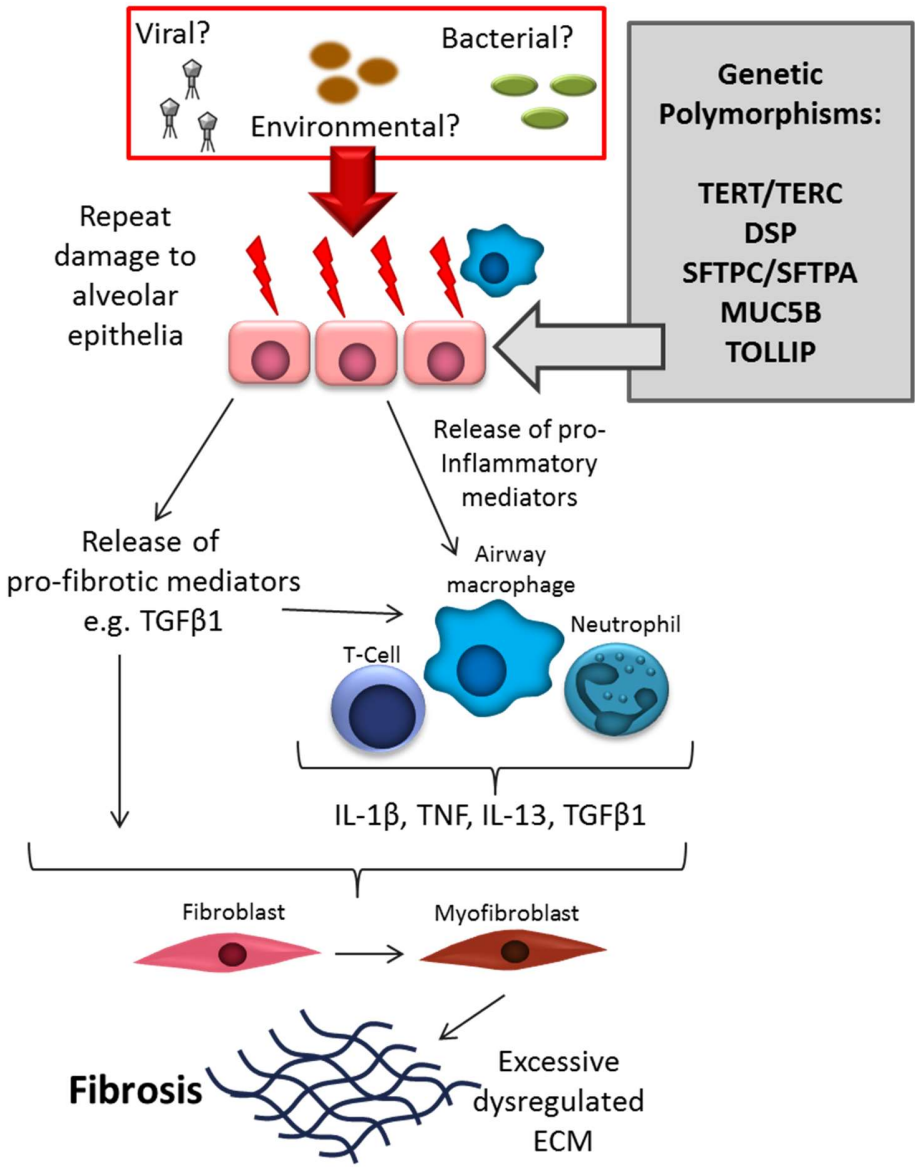


Figure 1.3: Hypothesised progression of IPF pathogenesis.
Several polymorphisms have been associated with IPF including; telomerase TERT/TERC, desmoplankin (DSP), surfactant protein (SFTP)-C and SFTPA, mucin5B encoding gene MUC5B, and toll like receptor regulator TOLLIP polymorphisms [100]. Individually or combined gene polymorphisms lead to increased susceptibility to environmental and/or infectious mediated disruption and apoptosis. In turn this leads to the release of pro-fibrotic and pro-inflammatory mediators by epithelial cells and leukocytes, leading to fibroblast proliferation and differentiation into extracellular matrix (ECM) producing myofibroblasts in the airways [281].

1.2.3. IPF Therapeutics

Owing to the heterogenous nature of IPF, the development of therapeutics is particularly challenging. Currently there are only two licenced therapeutics available for the treatment of IPF in the UK; pirfenidone and nintedanib. Pirfenidone and nintedanib are able to slow the progression of the disease; however, they do not reverse the pathology. Complete understanding of all aspects of the mechanism of action of these drugs remains to be fully elucidated, however, extensive research has provided an understanding into the complexity of the multiple pathways the drugs target to exert therapeutic efficacy as well as providing an insight into the complexity of factors driving fibrosis.

1.2.3.1. Pirfenidone

Pirfenidone is believed to exert therapeutic effects by inhibiting multiple pathways and mediators, acting as an anti-oxidative [282], anti-inflammatory and anti-fibrotic [283]. Through examination in *in vivo* models of fibrosis, such as the murine bleomycin model, pirfenidone has been shown to modulate pro-fibrotic growth factors, including transforming growth factor beta-1 (TGFβ1) and basic fibroblast growth factor (FGFb) [283] and reduce the recruitment of fibrocytes into the lungs [284]. Alongside this pirfenidone is able to inhibit pro-inflammatory cytokines and chemokines including, IFNγ, IL-6, IL-18 and CCL2 [283]. Pirfenidone was shown to alter the deposition of ECM by fibroblasts, down-regulating collagen V production, with both nintedanib and pirfenidone treatment resulting in fewer and thinner collagen fibrils compared to untreated controls, and a delayed fibril formation of collagen I resulted in the observed reduction of, and altered appearance of, collagen fibril bundles in a dose dependent manor [285]. Examination of fibroblasts post-treatment using GeneChip microarray and confirmation of genes

with real time polymerase chain reaction (PCR) and quantification of protein by western blot analysis revealed increased expression of regulator of G-protein Signalling 2 (RGS2), which inhibits the profibrotic effects of thrombin [286]. Clinically pirfenidone reduces FVC decline, improving patient survival [287, 288]. The multiple and complex mechanisms of action pirfenidone utilises to exert an efficacious response is likely to result in the reported side-effects including dizziness, vomiting, anorexia, rash and photosensitivity [26]. This highlights the need to improve upon existing therapeutics, identifiying the most critical pathogenic pathways or mediators inhibiting these specifically.

1.2.3.2. Nintedanib

Nintedanib targets multiple tyrosine kinases inhibiting the receptor kinases upstream of growth factors including platelet derived growth factor (PDGF), vascular endothelial growth factor (VEGF) and fibroblast growth factor (FGF) [289-291]. Furthermore, Nintedinib has been shown to inhibit TGFβ receptor signalling, inhibiting the activation of SMAD3 and phosphorlaytion of p38 mitogen-activated protein kinase (MAPK), resulting in the inhibition of TGFβ-mediated fibroblast to myofibroblast differentiation [292]. Independent of TGFβ signalling, nintedinib has been shown to reduce the production of collagen and fibronectin [292] and induce noncanonical autophagy in IPF fibroblast [292]. Like pirfenidone, adverse effects are reported, in particular gastrointestinal disorders [293].

With limited, non-reversible, therapeutic intervention it is vital we develop our understanding of disease pathogenesis in order to better tailor future therapeutic intervention.

1.3. Other interstitial lung diseases

Understanding and investigating the pathology of other ILDs facilitates the identification of similarities and differences comparing pathologies and therefore helps us understand potential new mechanisms driving disease. Other commonly diagnosed ILDs, with different mechanisms driving pathology, include undifferentiated connective tissue disease (UCTD), hypersensitivity pneumonitis (HP) and chronic HP (cHP). The mechanisms driving these pathologies will be discussed in more detail.

1.3.1. Undifferentiated connective tissue disease

Undifferentiated connective tissue disease (UCTD) is an umbrella classification of patients with connective tissue diseases (CTDs), for example rheumatoid arthritis or systemic sclerosis, but do not fulfil any existing classification criteria. Patients with UCTD represent an unclassifiable systemic autoimmune disease with the presence of auto-antibodies which may develop into a systemic autoimmune disease (SAID) [294, 295]. Typically UCTD is more common in females and patients are usually younger than IPF patients, the duration of disease is longer, however the prevalence of those developing ILD is low [296]. Examination of HRCT images reveal UCTD-ILD is more likely to have ground-glass opacity and less likely to have honeycombing [297]. Analysis of biopsies revealed NSIP patterns were also more likely, and UIP patterns were less likely to be visible in UCTD [297]. Contrary to these finding UIP has been reported to be more common in UCTD, which showed a poorer prognosis than those with UCTD-NSIP patterns [298]. Comparisons to IPF patients in the same study revealed an improved prognosis comparing the UCTD-UIP to IPF-UIP [298]. Studies examining the risk factors associated with decline in FVC, specifically in CTD-ILD, showed that the presence of a ‘highly specific’ CTD manifestation (e.g. Raynaud’s

phenomenon, dry eyes or arthritis) were more common in younger men, and were associated smaller decline in FVC compared to those without highly specific CTD [299]. Comparisons between ILD populations have revealed a number of differences comparing UCTD to other ILDs. Analysis of the progression of UCTD compared to IPF revealed a significant improvement in FVC after 8 months in UCTD patients compared with IPF patients [300] indicating a less severe disease progression in UCTD compared to IPF. Examinations of blood antibody tests between UCTD-ILD, CTD-ILD and IPF revealed patients with CTD-ILD had more abnormal antibody tests than those of UCTD-ILD and IPF [301] suggesting an increased autoimmune phenotype in CTD-ILD compared to UCTD-ILD. The exact mechanisms driving the pathology still remains to be elucidated but work has highlighted alterations to peripheral blood lymphocyte populations with an increase in the numbers of activated T cells with a Th1 IFNγ producing phenotype and natural killer T cells (NK) T cells in peripheral blood [302], with further work showing that inflammatory Th17 (IL-17 producing) T cells are increased, and anti-inflammatory regulatory T cells decreased (Treg) in patients with UCTD that progressed into a SAID [295]. Furthermore analysis of BAL T cell phenotypes revealed significantly higher percentages of lymphocytes with a lower CD4/CD8 ratio in UCTD compared to non-UCTD-NSIP [303]. Studies examining alveolar macrophages (AMs) in UCTD BAL have revealed similarities comparing UCTD to healthy controls with low levels of Ki-67 (a marker of proliferation) staining, with an increased percentage of patients with systemic sclerosis showing Ki67 AM staining [304]. Studies examining the BAL are limited in UCTD, further work into the investigation of leukocytes present in the BAL of UCTD may provide clues as to what may be driving this poorly understood pathology.

1.3.2. Hypersensitivity pneumonitis and chronic hypersensitivity pneumonitis

Hypersensitivity pneumonitis (HP), previously referred to as extrinsic allergic alveolitis, is an inflammatory ILD with a reported incidence in the UK of approximately 1 per 100,000 [305]. HP develops from repeat environmental antigen exposure leading to increased inflammatory infiltrate resulting in lung pathology [306] and can be further categorised into acute or subacute HP. Acute HP resembles an acute respiratory infection, which may occur as a result of exposure to high levels of environmental antigen [10]. Subacute HP may result from repeated low-level exposure to inhaled antigens and is a progressive pathology characterised by fatigue, dyspnoea and persistent cough [10]. If left untreated HP can progress into chronic (cHP) with presence of fibrosis in the lung parenchyma [10].

Environmental antigens thought able to initiate HP include bacteria, fungi, animal proteins and chemicals [306], with the most common antigen sources derived from avian and microbial antigens [307]. Identification of specific environmental antigens can be used to further sub-classify disease into farmer's lung or bird fancier's lung for example, however, regardless of antigen the immunopathogenesis is likely to be similar [306].

Genetic predisposition to developing disease is believed to play a part in the 'two hit' model of HP development, with the first hit being either a genetic susceptibility or environmental exposure followed by a second hit of environmental antigen exposure [10]. Genetic polymorphisms reported to be associated with an increased risk of developing HP include genes associated with the class II major histocompatibility complex (MHC) [308, 309], which is expressed on specialised immune antigen presenting cells and involved in antigen presentation and priming of the

adaptive immune system. Similarly polymorphisms associated with PSMB8, an immunoproteasome catalytic subunit β type 8, which aids the degradation of proteins that would be presented by the MHC class I receptors, and transporters associated with antigen processing (TAP) have been reported to be significantly increased in HP [310, 311]. Taken together these polymorphisms suggest abnormalities in MHC processing and antigen presentation in patients with these polymorphisms in HP.

Additionally to environmental antigen insult and genetic susceptibility viruses have been reportedly increased in patients with HP [312], with animal models showing an exacerbated and persistent inflammatory response after viral infection [313], indicating an additional potential risk factor in HP pathogenesis. Multiple immune cells have been implicated in HP pathogenesis with evidence suggesting a role for lymphocytes in HP initiation and progression [306]. Regulatory T cells (Tregs), which supress inflammatory T cells, and have been shown to play a protective role in animal models of HP [314]. Furthermore, Tregs have been isolated from the BAL and blood of patients with HP and show an impaired ability to supress T cell proliferation compared to those isolated from healthy controls [315]. Gene expression profile analysis of HP compared to IPF lung tissue revealed an increase in genes functionally associated T-cell activation, inflammation and IL-17 driven immune responses in HP tissue differing from the profile of IPF tissue which was characterized by the expression of epithelial, tissue remodelling, and myofibroblast genes [316]. Supporting IL-17 driven inflammation, studies examining mechanisms driving pathogenesis in mouse models of HP have shown that IL-17 producing Th17 cells play a critical role in the progression of disease pathogenesis [317]. Alongside the role of IL-17 producing Th17 cells in driving pathology, IL-4 and IL-13 producing Th2 cells have been

reported increased in HP patients [130] with murine models supporting the pathological role of Th2 cells in disease models [318]. Contrary to the pathological role of Th2/Th17 cells, γδ T cells subsets have been shown to be decreased in patients with HP [130], and play a protective role in disease pathogenesis by producing IL-22, a cytokine which mediated protective effects by inhibiting pro-fibrotic αβ T cells [319]. Taken together this research has highlighting possible mechanisms underpinning the pathology of HP, and how this pathology may differ from other ILDs. Further interrogation of this disease will aid our existing understanding of disease progression possibly identifying new mechanisms in disease pathogenesis.

1.4. Summary

The pathogenesis of ILDs like IPF involves multiple complex pathways, genetic predispositions, cellular interactions and external sources of ongoing epithelial insult. However, our understanding of factors driving the pathology of IPF is still lacking. Analysing disease relevant compartments such as cells and mediators from the BAL, from IPF patients in combination with other ILDs and healthy controls may highlight novel differences related to pathogenesis. Furthermore investigations into why there are reported differences in possible drivers of pathology, such as the reported increase in bacteria in IPF [2, 3], and the roles they may play in disease progression remain to be determined. It is possible that the bacteria themselves are playing a role in injuring the epithelial layer and they may be increased as a result of defective immune responses. Investigations into immune function and the possible impact of specific bacteria in IPF are therefore required to elucidate the role of bacteria in IPF disease progression.

1.5. Hypothesis

An increased bacterial burden has been reported in IPF airways correlating with clinical decline. IPF innate immune cells, including airway macrophages, epithelial cells and fibroblasts, will exhibit defective host defence responses, with decreased release of pro-inflammatory mediators after stimulation with bacterial or bacterial mimetic TLR ligands compared to healthy control cells. Furthermore, IPF innate immune cells stimulated with bacterial or bacterial mimetic TLR ligands will induce an exacerbated fibrotic response, quantified by increased release of extracellular pro-fibrotic mediators, upregulation of ECM gene expression and fibroblast proliferation post stimulation, indicating a role for bacteria in driving disease pathology.

1.6. Aims

- To examine and compare the inflammatory profiles of the BAL from healthy controls, IPF and other ILD patients, leukocyte composition will be analysed by flow cytometry, and extracellular pro-inflammatory and pro-fibrotic mediators will be quantified by multiplex analysis and ELISAs. Cellular and extracellular readouts will be correlated with clinical lung function parameters.
- To examine and compare airway macrophage phenotypes and functions in host defence and fibrosis using flow cytometry, gene expression analysis and *in vitro* stimulation, of airway macrophages from IPF patients, other ILD patients, and healthy controls.
- To examine and compare IPF patient and healthy control primary epithelial cell and fibroblast pro-inflammatory and pro-fibrotic changes post heat killed bacteria and TLR ligand stimulation, analysing inflammatory and fibrotic gene expression, protein secretion and fibroblast proliferation.

2. Materials and Methods

2.1. Collection of BAL samples

All patients and control subjects provided written, informed consent to participate in the study, which was approved by a Royal Brompton Hospital ethics committee (10/HO720/12). The flexible bronchoscopies were performed under a light sedation with midazolam in combination with local anaesthesia with lidocaine. Four 60 mL aliquots of warmed sterile saline were instilled in to the right middle lung lobe, in most circumstances, and aspirated by syringe. Approximately 50% of the instilled volume was collected. Lavage aliquots collected after each instillation were pooled for each patient and 40 mL of the total volume per patient was taken for clinical diagnostic analysis including cellular differential counts and routine clinical culture. The remaining yield was used for experimental investigation.

2.2. BAL Processing

BAL samples were processed and stained on the day of sample collection. Volume and BAL appearance was recorded for all samples. 6 mL of whole BAL was collected and immediately stored at -80°C. Whole BAL was then strained through a 70 µM sterile strainer into a 50 mL falcon tube to remove any mucus and spun at 400 x g, 4°C, for 5 minutes, break 9 (Hettich Centrifuge, Rotina 420R). BAL supernatant was collected, aliquoted and stored at -80°C for analysis of mediators in the BAL. BAL pellets were lysed for red blood cells (RBC), using RBC lysis buffer (155 mM NH_4Cl, 10 mM $KHCO_3$, 0.1 mM EDTA, pH 7.3) for 10 minutes before spinning again as previously described. The supernatant was discarded and the pellet resuspended in approximately 3 mL PBS (137 mM NaCl, 10 mM Phosphate, 2.7 mM KCl, and a pH 7.2-7.4). 10 µL

of resuspended cells were added to 90 µL of Tryphan blue (Sigma, cat# 93595) counting live unstained cells or using white blood cell counting fluid (PBS containing 4% acetic acid, 2% crystal violet in methanol) counting live stained cells. 10 µL of resuspended cells in counting fluid was added to haemocytometer and three 4 x 4 squares on the haemocytometer grid were counted to ascertain total cell number per mL using the following formula:

Average cell count (average of 3 counted 4 x 4 squares) x sample dilution (i.e. 10 as a 1:10 dilution of sample to stain) x 10^4 = cells/mL

2.3. Cytospins and staining of cells

Cells were resuspended in a 100 µL PBS containing between 4 x 10^3 to 2 x 10^4 cells, and added to the bottom of the cytospin chamber and spun using a Shandon Cytospin III centrifuge at 18 x g for 4 minutes. Cells on the slides were then fixed in methanol for 5 minutes and air dried overnight. Cytospins were then rehydrated for 30 minutes in A + B solution (1:1, A:B, then 1:10 of A+B in demineralised (d)H_2O (e.g. 50 mL of A + 50 mL of B + 900 mL dH_20) pH 7.2- 7.4, A = 9.47 g/L NaH_2PO_4; B = 13.609g/L KH_2PO_4) stained for 20 minutes in Wright-Giemsa stain (Sigma, cat# WG16), then placed back in A + B solution for 20 minutes, washed with H_2O and cover slipped. For differential (diff) counts healthy control samples were stained as above and leukocyte cell type was determined based on morphology counting >300 cells per cytospin. An example of cell morphology is illustrated in **Figure 2.1**.

Patient sample diff counts were stained and determined by qualified personnel at the Royal Brompton Hospital. Cell numbers were calculated from total cell counts, assuming all cells are leukocytes, using the following formulae:

Cell 'Y' number(/mL BAL)= (Cell 'Y' percentage/100) x total cell number/mL BAL

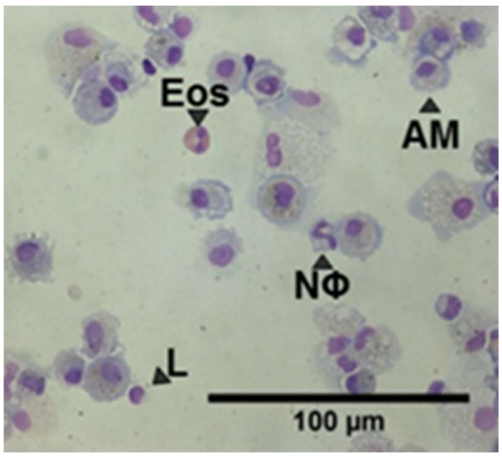


Figure 2.1: Example BAL cytospin for differential counts.
Wright-Giesma stained BAL cytospin at 20X magnification. Eos= Eosinophils, NΦ= neutrophils, L=Lymphocytes and AM= airway macrophages.

2.4. General leukocyte FACS staining for extracellular surface markers

Cells were plated at 2.5 x 10^5 or 1 x 10^5 per well in a 96 well round bottom plate in approximately 100 µL PBS. The plate was spun at 500 x g, 4°C, for 3 minutes, break 9 (Hettich Centrifuge, Rotina 420R). Supernatant was removed and cells were resuspended in 50 µL of 1:1000 live/dead stain (Zombie UV, Biolegend, cat# 423107) and kept in the dark at 4°C for 20 minutes. Cells were spun as previously described, supernatant removed and cells were resuspended in 50 µL FACs buffer (PBS containing 1% BSA or FBS, 25 mM HEPES and 1 mM EDTA) containing antibody stain and Fc Block (1:100, Biolegend, cat# 422301) at concentrations described in **Table 2.1** for 20 minutes at 4°C in the dark. The cells were spun as previously described, supernatant removed and washed in 200 µL FACs buffer. Cells were fixed in 100 µL IC fix (ebioscience, cat# 00-8222-49) for 10 minutes, 4°C, in the dark, spun and resuspended in 200 µL FACs buffer. Stained samples were stored in the dark overnight at 4°C and examined using 5 laser BD LSRFortessa™ the following

day and analysed using FlowJo7. In order to determine accurate gating, fluorescence minus one (FMO) controls were examined for all Abs, where a sample was stained with the whole stain omitting each test Ab individually. Gating strategy with example FMOs are included in **Figure 2.2**. Samples were sorted using BD FACSAria™ II on the same day as stain using the gating strategy described in **Figure 2.2**.

Cell number per mL of BAL fluid was determined for FACS analysis using the following equations:

Firstly determining the number of live CD45+ leukocytes per mL of BAL:

1. Number of live $CD45^+$ leukocytes ($x10^6$) per mL BAL= (% live $CD45^+$ cells/ 100) x total cell number/mL BAL ($x10^6$)

Cell proportions are determined based on the % of live CD45+ cells, therefore, the below equation is used to determine the approximate number of each cell type per mL of BAL:

e.g. Determining the number of CD206+ macrophages

2. Number of $CD206^+$ ($x10^6$/mL BAL) = (% of $CD206^+$ cells/ 100) x number of live $CD45^+$ cells (10^6/mL BAL)

Marker	Conjugate	Dilution	Clone	Source	Laser	Filter
CD3	ef450	1:100	OKT3	eBiosciences	Violet (405nm)	450/50
CD19	BV605	1:100	HIB19	Biolegend	Violet (405nm)	610/20
CD14	BV711	1:100	M5E2	Biolegend	Violet (405nm)	710/50
CD177	FITC	1:100	MEM-166	Biolegend	Blue (488nm)	530/30
FcεR1	PE	1:100	AER-37 (CRA-1)	Biolegend	Yellow-Green (561nm)	585/15
CD56	PE Dazzle	1:100	HCD56	Biolegend	Yellow-Green (561nm)	610/20
CD45	PE Cy5	1:50	HI30	Biolegend	Yellow-Green (561nm)	670/30
Siglec 8	APC	1:50	7C9	Biolegend	Red (640nm)	670/14
CD1c	AF700	1:50	L161	Biolegend	Red (640nm)	730/45
CD206	APC Cy7	1:1000	15-2	Biolegend	Red (640nm)	780/60
Live/dead	Zombie UV	1:1000	Dye (cat# 423107)	Biolegend	UV (355nm)	450/50

Table 2.1: Antibodies used including dilutions with appropriate flow cytometer laser and filters for FACS staining and analysis.

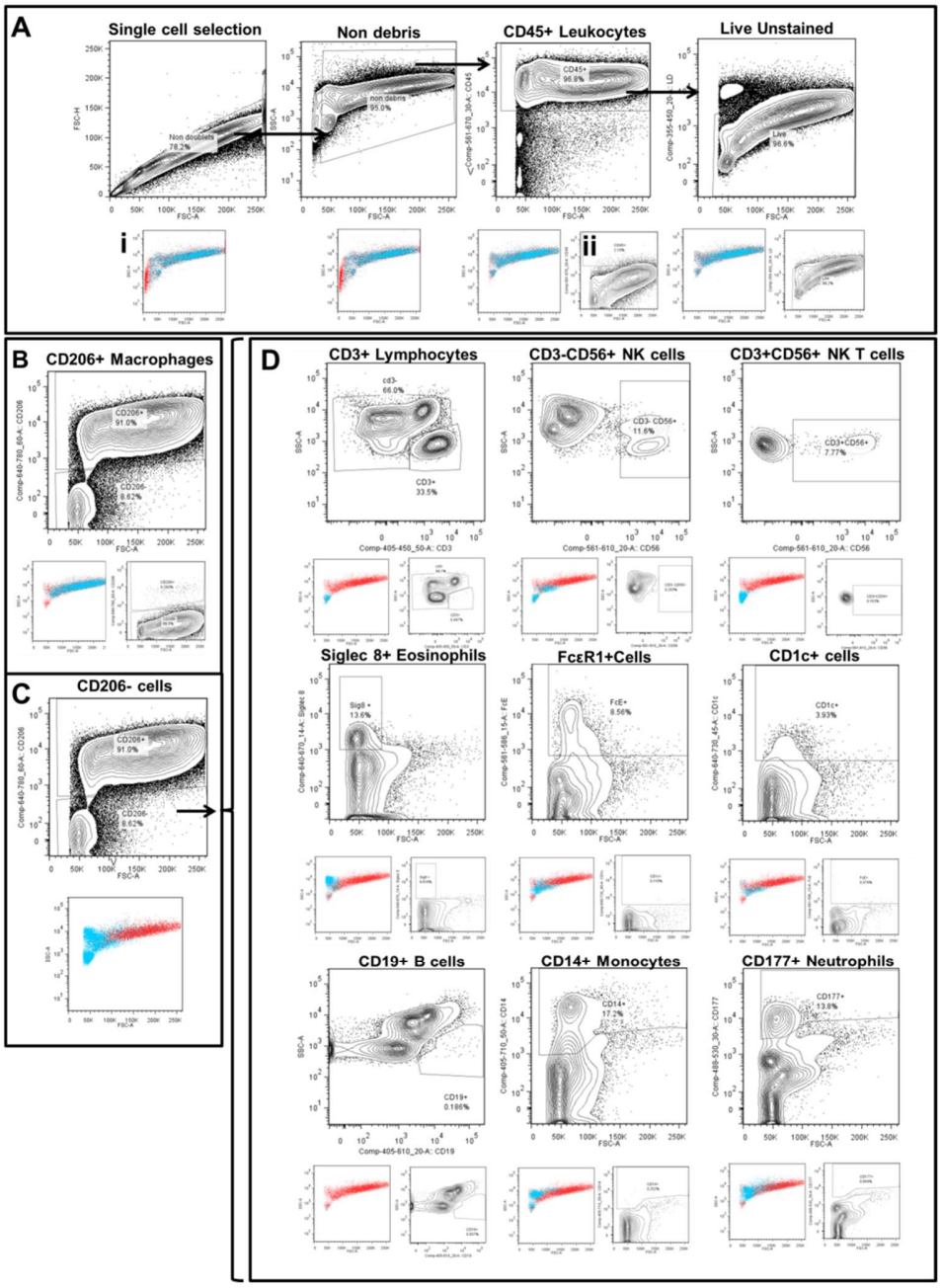


Figure 2.2: General leukocyte FACS gating strategy.
Panel A shows the basic gating strategy from left to right gating; single cell selection, non-debris, CD45+ leukocytes, live unstained cells. Directly below main example contour plots show populations back-gated in blue (i) and, where relevant, the fluorescence minus one (FMO) control (ii) in all panels. Panel B shows CD206+ macrophage gating. Panel C shows CD206- gating. CD206- cells are then examined for other leukocyte populations illustrated in panel D.

2.5. Macrophage FACS staining for extracellular surface markers

Cells were stained as previously described (see **2.4**). FACS stains are outlined in **Table 2.2** and **Table 2.3**. If staining required the addition of a secondary antibody (e.g. biotin-streptavidin staining of TLR1 and TLR6 outlined in **Table 2.3**), secondary antibodies were added at concentrations described (**Table 2.3**) for 30 minutes in FACS buffer. Samples were then washed resuspended in IC fix, as previously described (**2.4**), and resuspended in FACS buffer. Stained samples were stored in the dark overnight at 4°C and analysed using 5 laser BD LSRFortessa™ the following day. Data was analysed using FlowJo7. Analysis followed gating strategies outlined in **Figure 2.3** for CD11c+ total macrophages and **Figure 2.4** for CD11c+ CD71+/- cells.

2.6. Intracellular stimulation and staining

Cells were stained the following day after fixation for intracellular marker TLR3. Cells were washed with 100 µL permeabilisation (perm) buffer (1:10 dilution in dH2O, ebioscience, cat#00-8333) spun and resuspended in 50 µL intracellular stain (antibodies diluted in 1x perm buffer) for 40 minutes at dilutions shown in **Table 2.3**. Cells were then spun and washed in 1 x perm buffer twice before resuspending in a final volume of 200 µL FACs buffer. Samples were analysed within 24 hours.

Marker	Conjugate/ Dye	Dilution	Clone/ Dye	Source	Laser	Filter
Live/ Dead	Zombie UV	1:1000	Dye (cat# 423107)	Biolegend	UV (355nm)	450/50
CD45	PE-Cy5	1:50	HI30	Biolegend	Yellow-Green (561nm)	670/30
CD11c	Pe-Cy7	1:50	3.9	Biolegend	Yellow-Green (561nm)	780/60
CD71	PE	1:1000	CY1G4	Biolegend	Yellow-Green (561nm)	585/15
CD206	AF488 (FITC)	1:100	15-2	Biolegend	Blue (488nm)	530/30
CD163	AF647 (APC)	1:100	GHI/61	Biolegend	Red (640nm)	670/14
CD86	PE/Dazzle™ 594	1:100	IT2.2	Biolegend	Yellow-Green (561nm)	610/20
HLA-DR	BV421	1:100	L243	Biolegend	Violet (405nm)	450/50
CD14	BV711	1:50	M5E2	Biolegend	Violet (405nm)	710/50
Panel 2; as Panel 1 with below conjugate substitutes:						
CD71	APC	1:1000	CY1G4	Biolegend	Red (640nm)	670/14
CD163	APC-Cy7	1:100	GHI/61	Biolegend	Red (640nm)	780/60
Panel 3; as Panel 1 with below conjugate substitutes:						
CD11c	AF700	1:50	Bu15	Biolegend	Red (640nm)	730/45
CD206	APC-Cy7	1:100	15-2	Biolegend	Red (640nm)	780/60
CD163	PE-Cy7	1:100	GHI/61	Biolegend	Yellow-Green (561nm)	780/60
CD86	BV605	1:100	IT2.2	Biolegend	Violet (405nm)	610/20

Table 2.2: FACS panels for analysis of cell surface markers.
Table shows surface marker, conjugate or dye, dilution concentration in PBS or FACs buffer, antibody clone or dye information, and laser with filters used for analysis.

Marker	Conjugate/ Dye	Dilution	Clone	Supplier	Laser	Filter
Live/Dead	Zombie UV	1:1000	Dye (cat# 423107)	Biolegend	UV (355nm)	450/50
CD45	PE Cy5	1:50	HI30	Biolegend	Yellow-Green (561nm)	670/30
CD11c	PE/Cy7	1:50	3.9	Biolegend	Yellow-Green (561nm)	780/60
TLR2	AF647	1:50	T2.5	Biolegend	Red (640nm)	670/14
TLR4	BV421	1:50	HTA125	Biolegend	Violet (405nm)	450/50
AND						
CD71	PE	1:1000	CY1G4	Biolegend	Yellow-Green (561nm)	585/15
OR						
TLR3	PE	1:50	TLR-104	Biolegend	Yellow-Green (561nm)	585/15
OR						
TLR1	Biotin	1:50	TLR1.136	Biolegend	N/A	585/15
Streptavidin	PE	1:100	N/A	Biolegend	Yellow-Green (561nm)	585/15
OR						
TLR6	Biotin	1:50	TLR6.127	Biolegend	N/A	585/15
Streptavidin	PE	1:100	N/A	Biolegend	Yellow-Green (561nm)	585/15

Table 2.3: FACS panels for analysis of TLRs.
Table shows surface marker, conjugate or dye, dilution concentration in PBS or FACs buffer, antibody clone or dye information, and laser with filters used for analysis.

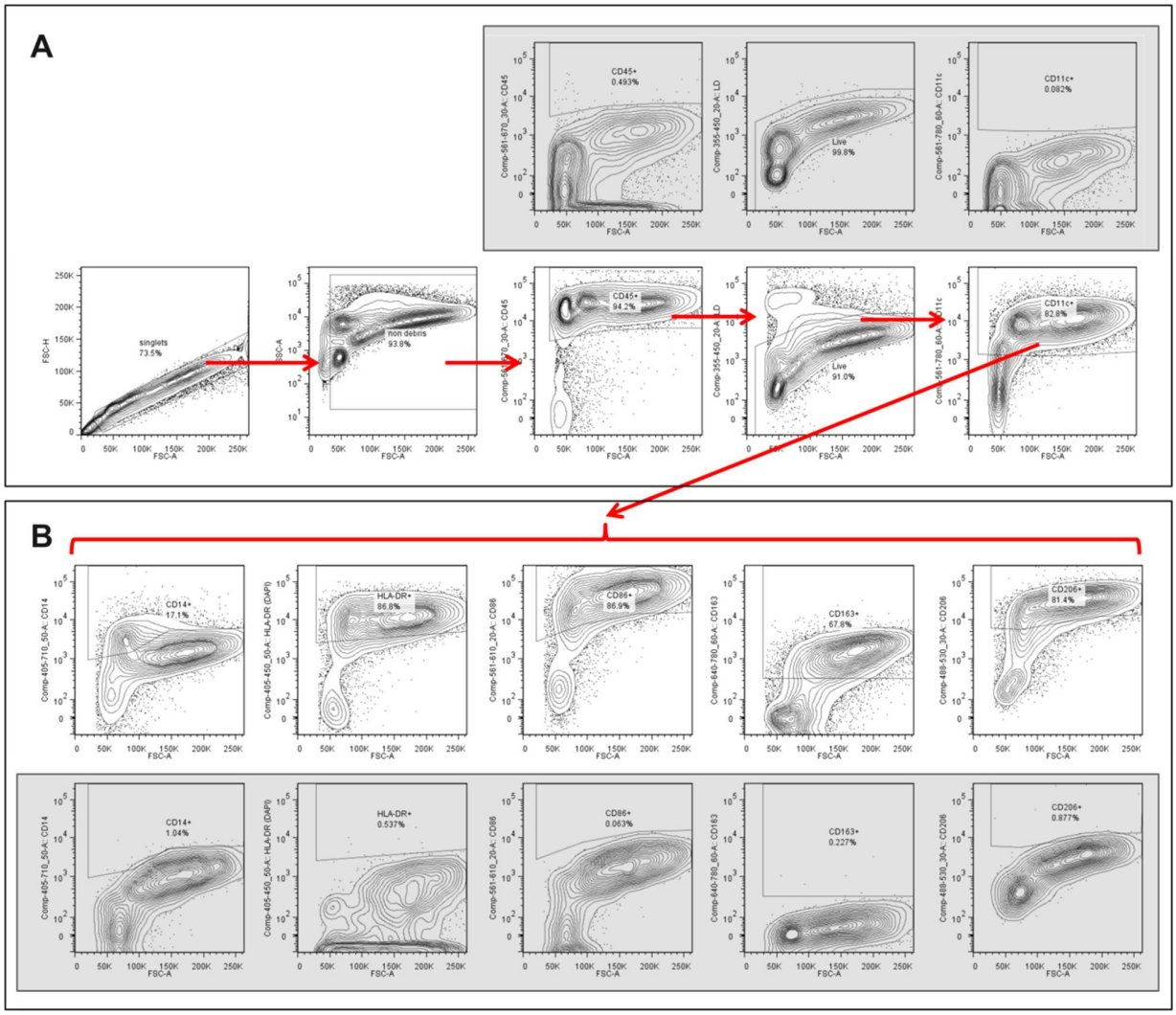


Figure 2.3: FACs gating strategy for CD11c+ macrophages.
The basic gating strategy for CD11c+ cells is outlined above. Panel A from left to right shows the gating of single cells, non debris, CD45+ leukocytes, Live unstained cells, CD11c+ macrophages, with FMO control highlighted in grey above, for CD45, live/dead and CD11c stain. Panel B shows the gating for markers macrophage/monocyte marker CD14+, M1 markers HLA-DR+ and CD86, M2 markers CD163 and CD206, with FMO control highlighted in grey below.

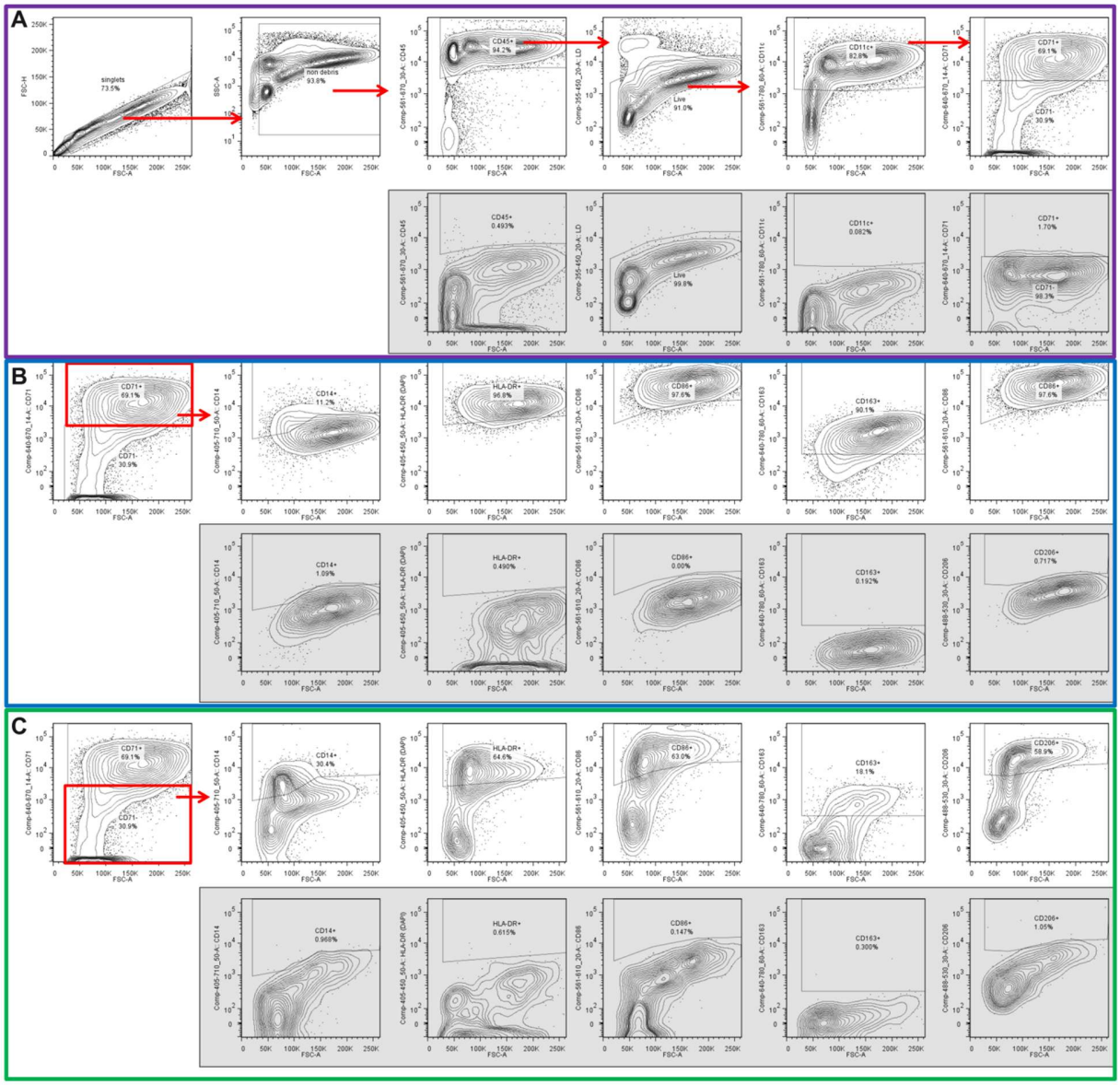


Figure 2.4: FACs gating strategy for CD71+/- macrophages extracellular surface markers.
The basic gating strategy for CD71+/- cells is outlined in panel A. Panel A from left to right shows the gating of single cells, non debris, CD45+ leukocytes, Live unstained cells, CD11c+ macrophages and CD71+ and CD71- gates. FMO controls are highlighted in grey below. Panel B shows the gating for CD71+ cells and panel C shows the gating for CD71- cells. From left to right Panels B and C show CD14+, HLA-DR+, CD86, CD163 and CD206, with FMO control highlighted in grey below.

2.7. Macrophage FACS Staining for phagocytosis, nitric oxide and transferrin.

Cells were plated at 1 x 10^5 per well in a 96 well round bottom plate in approximately 100 µL PBS. Cells were spun at 500 x g, 4°C, for 3 minutes, break 9 (Hettich Centrifuge, Rotina 420R) and resuspended in 200 µL PBS containing either 5 µM transferrin (life technologies, cat# P35376) or 0.1 µM nitric oxide stain (DAF-FM Diacetate, Life technologies, cat# D23842) or control condition containing PBS alone (control) for 30 minutes at 37°C, 5% CO_2. Cells were then stained as previously described (see **2.4**) with live/dead dye and antibodies outlined in **Table 2.4**. For phagocytosis assay 2.5 x 10^5 cells were added per well in a 96 well round bottom plate spun as previously described, resuspended in 200 µL complete RPMI (RPMI 1620, life technologies, cat# 21870-076, 10% FBS, 1000 U/mL Penicillin and 1 mg/mL Streptomycin) alone as a control or containing 0.125 mg/mL S. aureus Bioparticles, (Life Technologies, cat# P35367) for 2 hours. Cells were then washed with PBS and stained as previously described (see **2.4**) using antibodies outlined in **Table 2.4**. Samples were stained on the day of collection and stained samples were fixed and stored in the dark overnight at 4°C and examined using 5 laser BD LSRFortessa™ the following day. Data was analysed using FlowJo7. Analysis followed gating strategies outlined in **Figure 2.5**.

Marker	Conjugate / Dye	Dilution/ Concent-ration	Clone/ Dye	Source	Laser	Filter
Live/ Dead	Zombie UV	1:1000	Dye (cat# 423107)	Biolegend	UV (355nm)	450/50
CD45	PE Cy5	1:50	HI30	Biolegend	Yellow-Green (561nm)	670/30
CD11c	AF700	1:50	Bu15	Biolegend	Red (640nm)	730/45
CD71	APC	1:1000	CY1G4	Biolegend	Red (640nm)	670/14
CD206	APC Cy7	1:100	15-2	Biolegend	Red (640nm)	780/60
With one of the below:						
Bacteria	AF488	0.125 mg/mL	*S. aureus* Bioparticles, cat# P35367	Life Technologies	Blue (488nm)	530/30
OR						
Nitric Oxide	AF488	0.1µM	DAF-FM Diacetate, cat# D23842	Life Technologies	Blue (488nm)	530/30
OR						
Transferrin	PE	5µM	pHrodo® Red Transferrin Conjugate, P35376	Life Technologies	Yellow-Green (561nm)	585/15

Table 2.4: FACS panels for analysis of phagocytosis, nitric oxide production and transferrin uptake.
Table shows surface marker, conjugate or dye, dilution concentration in PBS or FACs buffer, antibody clone or dye info, and laser with filters used for analysis.

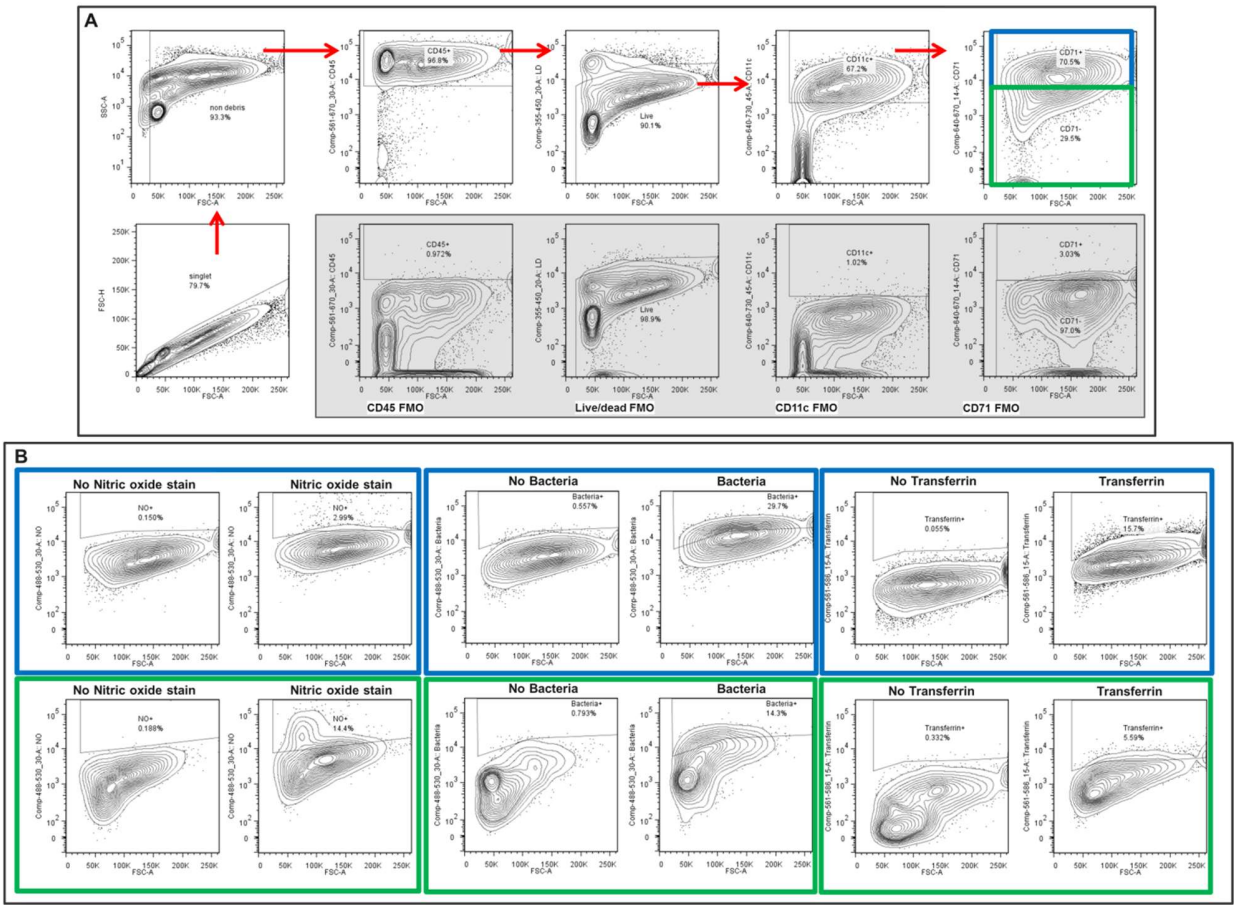


Figure 2.5: FACs gating strategy for CD71+/- macrophages NO, bacteria and transferrin stain. The basic gating strategy for CD71+/- cells is outlined in panel A showing the gating of single cells, non debris, CD45+ leukocytes, Live unstained cells, CD11c+ macrophages and CD71+ (blue) and CD71- (green) gates. FMO controls are highlighted in directly below each stain. Panel B shows the gating for CD71+ cells in blue boxes and CD71- cells in green boxes. From left to right panel B shows cells without and with nitric oxide staining, without and with bacteria staining, without and with transferrin staining.

2.8. Immunofluorescent staining and imaging

Cell cytospins of whole BAL and separated CD71- and CD71+ cells were collected as previously described and Wright-Giemsa stained using methods (**2.3**). Cytospins were also collected for immunofluorescent analysis. Immunofluorescent staining was carried out on cytospins that were fixed in methanol for 5 minutes, left to air dry and stored at 4°C until staining. Cells were washed 3 times for 5 minutes in PBS with 0.05% tween. Primary transferrin receptor Ab (Sigma-Aldrich, cat# PA5-27739) or negative control Ab (Rabbit Immunoglobulin fraction, Dako, cat# X0936) were added at 1 µg/mL in PBS 1% BSA containing 0.05% tween for at least 2 hours at 4°C, samples slides were washed as above and secondary goat anti-rabbit alexa- fluor 488 Ab (life technologies, cat# A-11008) was added at 1:200 in PBS 1% BSA containing 0.05% tween. Slides were washed as before and a drop of DAPI (life technologies, cat# P36941) was added to each cytospin and cover slipped for imaging. For bacteria phagocytosis 1 x 10^5 whole BAL cells were placed in a 8 well chamber slide (VWR, cat# 734-2050) in live cell imaging solution containing 1% BSA (life technologies, cat# A14291DJ). The whole BAL image of bacteria phagocytosis was captured 2 hours after addition of 100 µL of 0.25 mg/mL pHrodo™ Green S. aureus BioParticles® (Life Technologies, cat# P35382). Cells were incubated with bioparticles for 2hrs at 37°C, 5% CO_2. Wells were washed x3 with 500 µL of PBS and aspirated, chambers were carefully removed and a drop of Hoechst 33342 nuclear stain (Life Technologies, cat# R37605) was added to each section and the slide was cover slipped for imaging on Leica DM2500 and analysed using ImageJ- win32 software.

2.9. Total protein quantification

A bicinchoninic acid assay (BCA) assay (ThermoScientific, cat #23225) was carried out according to manufacturer's protocol. Briefly BCA Reagent A, (containing sodium carbonate, sodium bicarbonate, bicinchoninic acid and sodium tartrate in 0.1M sodium) and BCA Reagent B (containing 4% cupric sulphate) were combined in a 50:1 (A:B) dilution, 200 µL of this solution was added to 25 µL of standards (containing bovine serum albumin (BSA) at 2 mg/mL in 0.9% saline and 0.05% sodium azide in serial dilution) or 25 µL of sample in a 96 well plate (Corning, cat #3590). The plate was mixed on a plate shaker for 2 minutes at 600 rpm (approx. 2 x g, Camlab Choice MX-M Microplate Shaker) and placed in an incubator at 37°C for 30 minutes. Optical density (OD) was determined at 562 nm wavelength using Sunrise remote Tecan reader (F039300) analysis on Magellan V5.0 software. Data interpolation was carried out using a line of best fit from the standard curve on GraphPad Prism V6.

2.10. Multiplex measurement of cytokines, chemokines and growth factors

For measurement of mediators using multiplex analysis 25 µL of sample was assayed following manufacturers protocol (LEGENDplex™ Human Proinflammatory Chemokine Panel, Biolegend, Cat # 740003 or Human Inflammation panel, Biolegend, Cat # 740118 or Human Growth Factor Panel, Biolegend, Cat # 740180). Briefly 25 µL of sample or standard was added to equal volumes of assay buffer, mixed beads and detection antibodies and added to wells in a polypropylene V bottom 96 well plate. The plate was sealed then light protected with aluminium foil and placed on plate shaker at 600 rpm (approx. 2 x g, Camlab Choice MX-M Microplate Shaker) for 2hrs at room temperature. 25 µL SA-PE was then added to each well, the plate was re-covered with aluminium foil and incubated on the plate shaker as previously described for 30 minutes at room

temperature. The plate was then spun at 1000 x g for 5 minutes, supernatant removed by pipetting, and samples with beads were washed with 200 µL of 1X wash buffer, centrifuged as described previously, supernatant removed and resuspended in 150 µL of 1X wash buffer. The samples were then examined using a BD LSRFortessa™ and analysed using Legendplex 7.0 software according to manufactures guidelines.

2.11. ELISA

Duoset ELISAs were carried out in accordance to R&D manufacturing protocol. Briefly, high binding 96 well plates (Corning, cat #3590) were coated with 100 µL capture antibodies in PBS overnight at room temperature according to manufactures guidelines, plates were washed three times with 300 µL using wash buffer out lined in protocol, typically PBS containing with 0.05% tween 20, plates were blocked for non-specific binding using 300 µL block buffer (typically PBS containing 1% BSA). Plates were washed as before and 50 µL volume of standards (which were diluted in reagent diluent, typically PBS containing 1% BSA) or samples were added to wells for 2 hours at room temperature. Plates were washed as previously described and 100 µL of detection antibody in reagent diluent was added to each well for 2 hours at room temperature. Plates were washed again and 100 µL of diluted streptavidin HRP (horse radish peroxidase) was added to each well for 20 minutes at room temperature. Plates were washed and 100 µL of 3,3',5,5'-Tetramethylbenzidine (TMB) substrate solution (ThermoFischer, cat # N301) for approximately 15-30 minutes until standards developed a graduated blue appearance. Finally, 50 µL of stop solution (2N sulphuric acid) was added to each well and plate optical density (OD) was determined at 450 nm with 540 nm as a reference wavelength using Sunrise remote Tecan reader (F039300) analysis on Magellan V5.0 software. Data interpolation was carried out using a second

order polynomial analysis calculated from the standard curve on GraphPad Prism V6. The following ELISAs were used; IL-6 (R&D, cat# DY206), IL-10 (R&D, cat# D1000B), TNF (R&D, cat# DTA00C), TGFβ1 (R&D, cat# DY240), GM-CSF (R&D, cat# DY215) and IL-22 (R&D, cat# DY782).

2.12. Measurement of M-CSF using Quantikine® ELISA kit

Samples were assayed following manufacturers guidelines (R&D M-CSF quantikine ELISA, cat# DMC00B). Briefly, 100 µL of Assay Diluent and 100 µL of standard, control, or sample was added per well, covered and incubated for 2 hours at room temperature. Wells were aspirated and washed four times with 400 µL of wash buffer. Human M-CSF Conjugate (200 µL) was then added to each well, covered and incubated for 1 hour at room temperature. Wells were washed as previously described and 200 µL of substrate solution was added to each well and the plate was covered. The plate was then protected from light and incubated for 20 minutes at room temperature. Finally, 50 µL of stop solution was added to each well and optical density of each well was determined at 450 nm with 540 nm as a reference wavelength using Sunrise remote Tecan reader (F039300) analysis on Magellan V5.0 software. Data interpolation was carried out using a second order polynomial analysis calculated from the standard curve on GraphPad Prism V6.

2.13. Sorting and separating cells

2.13.1. FACS separation

Between 8 – 20 x 10^6 cells, depending on patient total cell number, were stained for flow cytometry sorting using sterile buffers. No live/dead dye was added, antibody staining was carried out with Fc Block added (1:100) following protocol outlined in **2.4**. FMO controls were stained for each patient using 1 - 2.5 x 10^5 cells in a 96 round bottom well as previously described (see **2.4**). Approximately 1 mL of sterile FACs sorting buffer (Sterile PBS, pH 7.0, containing 1 mM EDTA, 25 mM Hepes and 1% fetal bovine serum (FBS, Heat inactivated)) containing antibodies outlined in **Table 2.5** were used to stain every 5 x 10^6 cells in a 15 mL, aluminium foil covered, conical bottom tube (Corning, cat# 430053). Tubes were stained and spun at the same speeds as described for plate staining of cells in **2.4**. Cells were not fixed as previously described but washed after staining in double antibody staining volume with sterile FACS sorting buffer (i.e. if 1 mL of antibody containing FACS buffer was used to stain the cells then the stained pellet would be washed in 2 mL of sterile FACS sorting buffer). Cells were then added to FACs tubes (BD, cat# 352054) at approximately 5 x 10^6 per mL of FACs buffer. In all but DAPI FMO, 25 μg/mL of DAPI (Biolegend, cat# 422801) was added to each tube and cells transported on ice to be sorted using a BD FACSAria III. Cells were sorted by a trained member of Imperial College London's flow facility following a gating strategy similar to that outlined in **Figure 2.4A**. Live (DAPI unstained), CD45+, CD11c+ cells were separated into those that were CD71- and CD71+ into 15 mL conical bottom tubes containing FACs buffer and used for further analysis.

Marker	Conjugate/ Dye	Dilution/ Concent-ration	Clone/ Dye	Source	Laser	Filter
Live/ Dead	DAPI	25 µg/mL	Dye (cat# 422801)	Biolegend	Violet (405nm)	450/50
CD45	PE Cy5	1:50	HI30	Biolegend	Yellow-Green (561nm)	670/30
CD11c	Pe-Cy7	1:50	3.9	Biolegend	Yellow-Green (561nm)	780/60
CD71	APC	1:1000	CY1G4	Biolegend	Red (640nm)	670/14

Table 2.5: FACS panels CD71-/CD71+ cell separation.
Table shows surface marker, conjugate or dye, dilution concentration in PBS or FACs buffer, antibody clone or dye info, and laser with filters used for analysis.

2.13.2. MACS separation

Magnetic-activated cell sorting (MACS) separation was used to sort CD11c+ cells from whole BAL cells. Cells were separated using anti-Cy7 binding microbeads (Miltenyi Biotec, cat# 130-091-652) following the standard protocol provided with the MACS separation kit. Briefly, whole BAL was preppared as previously described (**2.2**) and a known number of cells in sterile PBS were added to a 15 mL conical tube and spun at 300 x g, 4°C, for 10 minutes, break 9 (Hettich Centrifuge, Rotina 420R). Cells were resuspended in 1 mL cold (approx 4-8°C) MACS buffer (PBS, pH 7.2, 0.5% FBS, 2 mM EDTA) containing CD11c Pe-Cy7 antibody (1:50 dilution, Biolegend, cat# 301607) and Fc Block (1:100, Biolegend, cat# 422301) per 5 x 10^6 cells for 10 minutes, and stained at 4°C in the dark. Cells were then spun as previously described and washed by pipetting gently up and down with 2 mL of buffer per 10^7 cells, spun again and resusupended in 80 µL of buffer per 10^7 cells and 20 µL of vortexed anti-Cy7 binding microbeads (Miltenyi Biotec, cat# 130-091-652). Cells were mixed and left at 4°C for 15 minutes. Cells were washed with 2 mL of buffer per 10^7 cells, spun as previously described and up to 10^8 cells were resuspended in 500 µL MACS buffer. LS columns (Miltenyi Biotec, cat#, 130-042-401) were placed in a midiMACS magnetic separator (Miltenyi Biotec, cat#, 130-042-302) on a MACS MultiStand (130-042-303). The LS column was washed with at least 3 mL of MACS buffer and the 500 µL volume of cells were added to the column. At least 3 x 3 mL of MACS buffer was run through the column into a 15 mL conical bottomed tube, labelled negative fraction. Once the reservoir was empty a new tube labelled as positive fraction was placed under the column. The column was removed from the midiMACS magnetic separator and 5 mL of MACS buffer was added to the LS column. The 5 mL volume was

then immediately flushed through the column using the provided plunger. The positive fraction was then used for further analysis and purity examined using Flow cytometry.

2.14. Macrophage stimulation

Separated cells were added to a 96 round bottom well at 5 x 10^4 cells per well. Cells were left unstimulated in complete RPMI as a control or stimulated with either of the following; 100 ng/mL LPS (Invivogen, cat# tlrl-eklps), 10 µg/mL Poly: IC (HMW) (Invivogen, cat# tlrl-pic), 10 ng/mL recombinant human TGFβ1 (R&D, cat# 240-B-002) in complete RPMI for 24 hours. Cell supernatant was collected, aliquoted and immediately stored at -80°C for later analysis. Trizol (Ambion, cat# 15596018) was added (200 µL per well) and cells pipetted up and down. Trizol containing cells were then placed into an RNAse/ DNAse free eppendorf (ThermoFisher scientific, cat # AM12400) and immediately frozen and stored at -80°C.

2.15. Analysis of mediators in stimulated macrophage supernatant

Cell supernatant from stimulated cells was measured for the production of extracellular mediators by multiplex (LEGENDplex™ Human Inflammation panel, Biolegend, Cat# 740118 or Human Growth Factor Panel, Biolegend, Cat# 740180) following protocol outlined in **2.10**. LPS stimulated samples were diluted 1:10 in provided diluent buffer with resulting pg/mL readout multiplied by the dilution factor.

2.16. RNA extraction from cells

Cells were added to 300 µL Trizol and pipetted up and down in an RNAse/ DNAse free eppendorf and stored immediately at -80°C until extraction. RNA was extracted using RNeasy Plus Mini Kits (Qiagen, Cat# 74134) following manufacturers protocol. Trizol containing samples were thawed on ice and an equal volume of chloroform was added to the Trizol and thoroughly mixed. Samples were then spun at 8000 x g, 4°C, for 15 minutes. The chloroform containing RNA clear layer was removed from the top and added to a genomic DNA (gDNA) elimination column. The column was spun at 8000 x g for 30 seconds. The flow through was mixed in a 1:1 ratio with 70% RNA grade ethanol. The samples were then transferred to the RNeasy spin columns within the provided 2 ml collection tube. The samples were then centrifuged for 30 seconds at 8000 x g and flow through discarded. Seven hundred microliters of Buffer RW1 was then added to the column, centrifuged and flow through discarded as before, 500 µL of buffer RPE was added to the columns, centrifuged and flow through discarded, another 500 µL of buffer RPE was added to the column and spun for 2 minutes at 8000 x g. A new 2 mL collection tube was added to the bottom of the column and the column in the collection tube was spun for 1 minute on full speed. A new 1.5 mL collection tube was added to the bottom of the column and approximately 30 µL of RNase-free water was added carefully to the column membrane without touching the membrane. The column was then spun at 8000 x g for 1 minute to elute the RNA. The concentration of RNA was then measured using a NanoDrop 1000 Spectrophotometer with V3.7 software to analyse the data.

2.17. Reverse Transcription of RNA to cDNA for qPCR using TaqMan primers

RNA was reverse transcribed into complementary DNA (cDNA) for quantitative polymerase chain reaction (qPCR) using a High-Capacity cDNA Reverse Transcription (RT) Kit (ThermoFisher, Cat# 4368813) following manufacturers protocol. Briefly, for every reaction 2 µL of 10X RT buffer, 0.8 µL of 25x dNTP Mix (100 mM), 2 µL of 10X random primers, 1 µL of MultiScribe™ Reverse Transcriptase and 4.2 µL of nuclease free H_2O (total volume 10 µL) were added to 10 µL of RNA in PCR 0.2 mL tube on ice (ThermoFisher, A30588) and sealed. The quantity of RNA added was adjusted by dilution in nuclease free H_2O based on RNA concentration. The concentration of RNA added was the same for reactions comparing cells and the total final volume of RNA was equal to 10 µL. The final 20 µL volume for reaction was added to a PCR thermocycler (Veriti® 96-Well Fast Thermal Cycler, Applied Biosystems®) using the following protocol; Step 1, 10 minutes at 25°C; Step 2, 120 minutes at 37°C; Step 3, 5 minutes at 85°C; Step 4, held at 4°C until samples retrieved and stored short term (up to 24 hours before use at 2 - 6°C or for long term storage stored at -20°C.

2.18. Gene expression analysis using TaqMan primers

Gene expression was analysed using TaqMan probe-based assay for specific genes, using specific TaqMan primers. Assays were carried out in a 384 well plate with genes measured in duplicate. cDNA (reverse transcribed as described previously in **2.17**) was diluted in nuclease free water depending on RNA quantity, typically a 1:3 dilution, so final volume of total cDNA for reactions was 60 µL (i.e. 20 µL of cDNA from RT reaction + 40 µL of nuclease free water). For each reaction, in each well of 384 well plate (MicroAmp® Optical 384-Well Reaction Plate, ThermoFisher, Applied Biosystems, cat# 4309849), 2.4 µL cDNA was added followed by 3.6 µL of primer master

mix containing; 0.3 µL of nuclease free water, 0.3 µL of TaqMan primer of interest, and 3 µL of TaqMan® Fast Advanced Master Mix (Lifetechnologies, cat# 4368813) so the final volume per well was 6 µL. The plate was tightly sealed with optical adhesive film (MicroAmp® Optical Adhesive Film, ThermoFisher, Applied Biosystems cat# 4313663) and the plate centrifuged for 1 minute at 1000 x g, 4°C. The settings applied to the qPCR 384 well block (Applied Biosystems, Viia 7) were 1 hold cycle at 2 minutes 50°C and 20 seconds at 95°C to incubate the Uracil-N-glycosylase (UNG) and activate the polymerase respectively. The next stage immediately followed which consisted of 40 cycles of denaturing at 95°C for 1 second and annealing/extending at 60°C for 20 seconds. The fluorescence was measured and cycle threshold (CT) values generated from exponential phase of gene amplification (Applied Biosystems, Life Technologies, Viia 7 software v1.2). The CT values were used to analyse gene expression, using Microsoft excel 2010 software, inputting the following equations where GOI = gene of interest, HKG = housekeeping gene (GAPDH for analysis):

1) Calculation of delta CT (ΔCT):

   ΔCT= Average CT GOI – Average CT HKG

2) Calculation of relative expression

   Relative expression = 1000 x ($2^{-\Delta CT}$)

3) Calculation of delta delta CT (ΔΔCT):

   ΔΔCT= ΔCT (Group 1 e.g. stimulated cell or cell type B) - ΔCT (Group 2 (control group) e.g. unstimulated cell or cell type A)

4) Expression of gene fold change between examined groups/cells:

   Expression Fold change= $2^{-\Delta\Delta CT}$

2.19. Gene expression analysis

Gene expression was examined in unstimulated separated macrophages (between 2.5 x 10^5 – 5 x 10^5 cells), which were added to 300 µL Trizol and pipetted up and down in an RNAse/ DNAse free eppendorf and stored immediately at -80°C until extraction. RNA extraction followed protocol highlighted in **2.16**, reverse transcription of RNA to cDNA was carried out following protocol highlighted in **2.17** and gene expression analysis was preformed following protocol outlined in **2.18**. Genes examined for macrophages are highlighted in **Table 2.6** and primers used for BEC and fibroblasts stimulations are highlighted in **Table 2.7**.

Gene	Protein	Supplier	ID
House-keeping gene			
GAPDH	Glyceraldehyde 3-phosphate dehydrogenase	ThermoFisher	Hs02758991_g1
TGFB superfamily			
TGFB1	Transforming Growth Factor Beta 1	ThermoFisher	Hs00998133_m1
TGFBR1	Transforming Growth Factor Beta Receptor 1	ThermoFisher	Hs00610320_m1
TGFBR2	Transforming Growth Factor Beta Receptor 2	ThermoFisher	Hs00234253_m1
Extracellular matrix and mediators			
COL1A1	Collagen Type I Alpha 1 Chain	ThermoFisher	Hs00164004_m1
COL3A1	Collagen Type III Alpha 1 Chain	ThermoFisher	Hs00943809_m1
CTGF	Connective Tissue Growth Factor	ThermoFisher	Hs01026927_g1
FN1	Fibronectin	ThermoFisher	Hs01549976_m1
Cytokines and Chemokines			
IL6	Interleukin-6	ThermoFisher	Hs00985639_m1
IL8	Interleukin-8	ThermoFisher	Hs00174103_m1
CCL2	C-C motif chemokine 2, MCP-1	ThermoFisher	Hs00234140_m1
Toll like Receptor (TLR) and TLR signaling			
TLR1	Toll like receptor 1	ThermoFisher	Hs00413978_m1
TLR2	Toll like receptor 2	ThermoFisher	Hs02621280_s1
TLR3	Toll like receptor 3	ThermoFisher	Hs01551078_m1
TLR4	Toll like receptor 4	ThermoFisher	Hs00152939_m1
TLR6	Toll like receptor 6	ThermoFisher	Hs01039989_s1
TLR7	Toll like receptor 7	ThermoFisher	Hs01933259_s1
IRF3	Interferon regulatory transcription factor 3	ThermoFisher	Hs01547283_m1
Phagocytosis and Host defence			
FCGR1A	Fcγ Receptor 1A	ThermoFisher	Hs00174081_m1
ELMO1	Engulfment And Cell Motility 1	ThermoFisher	Hs00404992_m1
NOS2	Nitric Oxide Synthase 2	ThermoFisher	Hs01075529_m1
Iron Regulation			
TFRC	Transferrin receptor; CD71	ThermoFisher	Hs00951083_m1
ACO1	Iron regulatory protein 1	ThermoFisher	Hs00158095_m1
IREB2	Iron regulatory protein 2	ThermoFisher	Hs00386293_m1
SLC40A1	Ferritin transporter; Ferriportin	ThermoFisher	Hs00205888_m1
SLC48A1	Heme transporter; Heregulin1 (HRG 1)	ThermoFisher	Hs01060393_m1
SLC11A2	Divalent metal transporter 1 (DMT1), Natural resistance associated macrophage protein 2	ThermoFisher	Hs00167206_m1
HAMP	Hepcidin	ThermoFisher	Hs00221783_m1
HMOX	Heme oxygenase (decycling) 1	ThermoFisher	Hs01558390_m1

Table 2.6: TaqMan primers used for qPCR analysis.
The table illustrates the gene, the protein the gene encodes, the supplier and identification of primer (ID).

Gene	Protein	Supplier	ID
House-keeping gene			
GAPDH	Glyceraldehyde 3-phosphate dehydrogenase	ThermoFisher	Hs02758991_g1
TGFB superfamily			
TGFB1	Transforming Growth Factor Beta 1	ThermoFisher	Hs00998133_m1
TGFBR1	Transforming Growth Factor Beta Receptor 1	ThermoFisher	Hs00610320_m1
TGFBR2	Transforming Growth Factor Beta Receptor 2	ThermoFisher	Hs00234253_m1
Extracellular matrix and mediators			
COL1A1	Collagen Type I Alpha 1 Chain	ThermoFisher	Hs00164004_m1
COL3A1	Collagen Type III Alpha 1 Chain	ThermoFisher	Hs00943809_m1
CTGF	Connective Tissue Growth Factor	ThermoFisher	Hs01026927_g1
FN1	Fibronectin	ThermoFisher	Hs01549976_m1
Cytokines and Chemokines			
IL6	Interleukin-6	ThermoFisher	Hs00985639_m1
IL8	Interleukin-8	ThermoFisher	Hs00174103_m1
CCL2	C-C motif chemokine 2 (Monocyte chemoattractant protein-1 (MCP-1)	ThermoFisher	Hs00234140_m1
Toll like Receptor (TLR) and TLR signalling			
TLR2	Toll like receptor 2	ThermoFisher	Hs02621280_s1
TLR3	Toll like receptor 3	ThermoFisher	Hs01551078_m1
TLR4	Toll like receptor 4	ThermoFisher	Hs00152939_m1
TLR7	Toll like receptor 7	ThermoFisher	Hs01933259_s1
TOLLIP	Toll-interacting protein 1	ThermoFisher	Hs01553188_m1
IRAK1	Interleukin-1 receptor-associated kinase 1	ThermoFisher	Hs00155570_m1
IRF3	Interferon regulatory transcription factor 3	ThermoFisher	Hs01547283_m1
Myofibroblast differentiation			
ACTA2	Alpha smooth muscle actin 2	ThermoFisher	Hs00426835_g1

Table 2.7: Primers used for qPCR of fibroblast and BEC stimulations.
The table illustrates the gene, the protein the gene encodes, the supplier and identification of primer (ID).

2.20. Reverse Transcription for fibrotic PCR array macrophage analysis

Examination of genes using a human fibrosis RT^2 Profiler PCR Array (SABiosciences, PAHS-120Z) was conducted following manufacturers guidelines. Firstly, RNA concentration was determined as previously described (**2.16**) and 400 ng of RNA was used in the reverse transcription reaction. All components of RT reaction were contained in the RT^2 First Strand Kit (Qiagen, cat# 330401). Genomic DNA (gDNA) elimination mix was prepared adding 2 µL of buffer GE to RNA in RNase free water so the final volume equalled 10 µL. This was incubated at 42°C for 5 minutes before being place immediately on ice. For the reverse transcription reaction 4 µL of 5x buffer BC3, 1 µL of control P2, 2 µL of RE3 reverse transcriptase mix and 3 µL of RNase-free water was added to each reaction (i.e. added to each tube containing the 10 µL of RNA with gDNA elimination mix). This was then incubated for exactly 15 minutes at 42°C then stopped by incubating at 95°C for 5 minutes. RNAse free water (91 µL) was then added to each reaction and pipetted up and down several times. The reaction was then placed on ice and the real time PCR protocol performed.

2.21. PCR fibrotic array real time quantitative PCR reaction and analysis

To perform the real time quantitative PCR for the gene array plate 1350 µL of 2x RT2 SYBR Green Mastermix (Qiagen, cat# 330520), 102 µL of cDNA synthesis reaction (generated as previously described, **2.20**) and 1248 µL of RNase-free water were combined and mixed by pipetting up and down several times. Finally 25 µL of this PCR reaction mix was added to each of the 96 wells on the PCR array plate (SABiosciences, cat# PAHS-120Z). The plate was tightly sealed with provided optical adhesive film and the plate centrifuged for 1 minute at 1000 x g, room temperature. The array was placed on ice while the qPCR was set up. The settings applied to the qPCR 96 well fast-block (Applied Biosystems, Viia 7) were 1 cycle at 10 minutes 95°C to activate the HotStart DNA

Taq Polymerase, followed by 40 cycles of 15 seconds at 95°C and 1 minute at 60°C to collected the fluorescence data for gene analysis. All gene expression analysis was performed using RT^2 Profiler PCR Array Data Analysis version 3.5.

2.22. Culturing Bronchial epithelial cells for co-culture

2.22.1. Collagen coating flasks and plates

Flasks (T25 (Corning, cat# 431463), T75 (Corning, cat# 430641U)) or wells (12 well plate (Corning, Costar, cat# 3737)) were coated with approximately 5 µg/cm^2 of collagen ((Corning, Collagen I rat tail, cat# 354236) diluted to 50 µg/mL in 0.02N acetic acid) for 1 hour at room temperature. Collagen was then aspirated and plates/flasks are washed twice with sterile PBS or culture medium BEGM growth medium (Lonza, cat# CC-3170 with gentamycin removed from supplements and primocin (invivogen, cat# ant-pm-1) at 50 mg/ 500 mL media substituted) and stored at 2 - 8°C for up to 2 weeks in sterile conditions (e.g. wrapped in parafilm) or used immediately for bronchial epithelial cell (BEC) culture.

2.22.2. BEC isolation

All patients and control subjects provided written, informed consent to donate BECs, which was approved by a Royal Brompton Hospital ethics committee (10/HO720/12). BECs were harvested from brushings using a 3mm sheathed Bronchial cytology brushes (Olympus KeyMed Group of Companies, Olympus UK, cat# BC-202D-3010) of airways at time of bronchoscopy. The brush was immediately placed into a 50 mL falcon containing 5 mL of BEGM. Cells are spun at 300 x g for 10 minutes, resuspended in 5 mL BEGM and plated into a collagen coated T25 flask. Media is changed the following day then 3 x weekly.

2.22.3. Splitting cells

In order to split cells for passage sterile TrypLE (Invitrogen, cat# 12604-021), PBS and complete media were warmed at 37°C in water bath. Media was aspirated from confluent flask and cells were washed with PBS (e.g. 5 mL T25, 10 mL for T75) for 1-2 minutes and aspirated. TrypLE was added (1 mL T25, 3 mL T75) and tilted to cover all cells. Cells were then returned to the incubator for 7-10 minutes (no more than 12 minutes), flasks were tapped and cells checked for detachment (>80%). Once cells had lifted over twice the volume of media was added to the flask as TrypLE (e.g. 3 mL T25, 7 mL for T75) and pipetted up and down the flask 5 times. Cells were then added to a 50 mL falcon and spun in the centrifuge (300 x g, 10 minutes at room temperature). Media was aspirated and cells resuspended in approximately 2 mL of media for counting. Cells were then seeded at approximately 0.7 x 10^6/ T25 flask, 2 x 10^6/ T75 flask and 5 x 10^4/ 12 well plates or frozen.

2.22.4. Freezing cells

To freeze cells for later use, freeze mix (Complete medium (BEGM as described) with 10% FCS and 10% DMSO) was placed on ice for >15 minutes and cells are resuspended at 5 x 10^5/mL in freeze mix. 1 mL of cells in freeze mix was added to 1.8 mL cryovials and placed in liquid nitrogen insert for at least 2 hours before placing cells in liquid nitrogen for long term storage (1 x T75 at 100% confluence is approximately 6 vials).

2.23. Co-culture macrophages with BEC

BECs isolated from a healthy control (ILDCON1018) volunteer were grown in a 12 well plate as previously described at passage 3 and left until fully confluent. BECs were grown so they would

become confluent in the 12 well plate at day of separation of CD71- and CD71+ macrophages. BECs were starved in BEBM Basal medium (Lonza, CC-3171) containing no supplements for 3 hours and macrophages were added to the confluent BECs in BEBM at a 1:10 ratio (i.e. 1 macrophage to 10 epithelial cells) with a final volume per well of 1 mL. After 6 hours of co-culture cells were lifted using tryplee as previously described and cells were sorted into CD45+ and CD45- cells to separate the BEC from the macrophages for RNA analysis. Cells were then stored in Trizol for later RNA analysis. Cell supernatants were stored and analysed for extracellular mediator analysis at 6 hours. Cell culture conditions are illustrated in **Figure 2.6**.

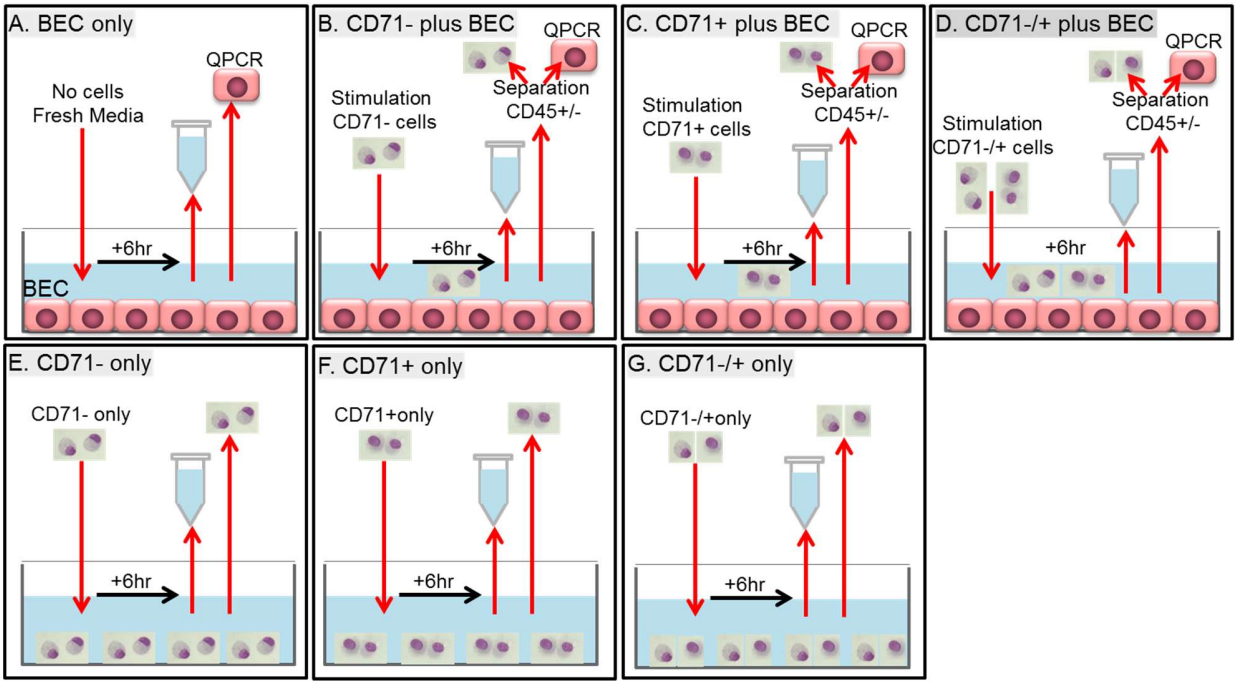


Figure 2.6: Illustration of BEC and CD71-/+ macrophage co-culture conditions.
BEC in culture alone (qPCR and supernatant control) (A), BEC + CD71- cells (B), BEC + CD71+ (C), BEC + CD71-/+ cells (D), CD71- cells alone (supernatant control) (E), CD71+ cells alone (supernatant control) (F), CD71-/+ cells alone (supernatant control) (G). Conditions, where possible, were carried out in triplicate.

2.24. Extracellular matrix deposition assay

CD71- and CD71+ cells were isolated from 5 patients (**Table 4.2**, Patient ID #16-20) and cultured at 5 x 10^4 cells per well in a 96 well round bottom plate in 200 µL of the medium required for the ECM accumulation assay (renal epithelial cell media; ATCC, PCS-400-030 with supplements PCS-400-040). Cells were either left unstimulated or stimulated with 100 ng/mL LPS (Invivogen, tlrl-eklps) for 48 hours. Supernatants were then collected, aliquoted and stored at -80°C until use in the ECM assay. Methods have been provided by Marianne Bergin (UCB) and/or directly quoted and adapted to fit specific methods used in this analysis from the publication by Holdsworth et al, 2017 [320]. Please refer to publication for full details. Briefly, human primary small airway epithelial cells (SAEpC, ATCC, PCS-301-010) and human primary lung fibroblasts (IPF134, ATCC, CCL-134) were maintained prior to assay in airway epithelial cell medium, comprising basal medium (ATCC PCS-300-030) and supplements (ATCC, PCS-301-040) or primary fibroblast medium (Lonza, FGM-2 Bulletkit, CC-3132) respectively. Cells were cultured in 100% humidity, 5% CO_2 at 37°C, and were used until passage 6. For the ECM accumulation assay cells were cultured in 384-well, darkwalled imaging plate (Greiner, 781090) at 2 × 10^3 cells per well at 37°C, 5% CO_2, 100% humidity. SAEpC and IPF134 were incubated as monocultures and in co-culture, each in the presence of medium alone for 6 days as controls to measure basal ECM accumulation. To assess the effect of the isolated CD71-/+ supernatants on matrix deposition the harvested supernatants were used to stimulate the SAEpC/IPF134 co-culture at a final dilution of 1/8 in assay medium. As a control for the LPS stimulation, the same concentration of LPS used to stimulated the CD71-/+ cells was used to stimulate the SAEpC/fibroblast co-culture. Stimulations for each condition were carried out in quadruplicate wells. After 6 days of culture cell viability

was assessed as a surrogate measure of cell proliferation, using PrestoBlue Cell Viability reagent (Thermo Fisher Scientific, A13261) following the instructions of the manufacturer. Briefly, 5 µL of Presto Blue was added per well for 10 minutes at 37°C and fluorescence was measured at excitation wavelength: 530/25 and emission wavelength 620/40. After PrestoBlue analysis supernatant was flicked off and plate blotted on tissue paper; cells were lysed with 25 µL of 0.25 M NH_4OH in 25 mM Tris for 15 minutes at 37°C. Plates were then washed three times with 50 µL PBS and ECM proteins were fixed with 50 µL 100% ice-cold methanol at -20°C for 30 minutes. Wells were then washed twice with 50 µL PBS and stored in blocking buffer (PBS containing 1% goat serum) at 4°C overnight. After discarding the blocking buffer the plate was stained with 25 µL collagen I, III and IV antibodies at a 1:100 dilution in PBS/1% goat serum (see **Table 2.8**). The plate was then incubated for 1 hour and 30 minutes at room temperature with agitation. The plate was then washed three times with 50 µL PBS. Secondary antibodies were added, 25 µL per well at a 1:500 dilution in PBS/1% goat serum (see **Table 2.8**). The plate was then incubated for 1 hour 30 minutes followed by washing as previously described. A directly labelled antibody to fibronectin was added, 25 µL per well at 1:400 dilution in PBS/1% goat serum for 1 hour 30 minutes then wells washed as previously described. To aid microscope focussing, 50 µL of AlignFlow Plus alignment beads were added per well at 1 drop beads per 5mL PBS (see **Table 2.8**). Matrix deposition was then measured by Cellomics Arrayscan HC reader (Life Technologies) analysis of labelled proteins.

Reagent	Supplier	Product number
Goat Serum	R&D Systems	DY005
AlignFlow Plus alignment beads	Invitrogen	A16505
Rabbit-anti-Col III	Millipore	AB747
Rabbit anti-Col I	Millipore	AB745
Anti-human Collagen type IV	ebioscience	14-9871-82
Anti-human fibronectin Alexa 488	ebioscience	53-9869-82
AlexaFluor 555 Goat-anti-mouse IgG (H+L)	Invitrogen	A21424
AlexaFluor 647 Goat-anti-rabbit IgG (H+L)	Invitrogen	A21244

Table 2.8: Reagent list for extracellular matrix deposition assay.

Images were acquired using a Cellomics Arrayscan HC reader (Life Technologies) using a 10x Objective, ORCA-ER or X1 camera with 2 × 2 binning (1104 × 1104 pixels/field). Stained ECM was detected using relevant excitation and emission filter sets for each fluorophore. Staining above a fixed threshold was analysed and total intensity measurements of Collagen I + III, fibronectin and collagen IV are reported. Images from four fields within each well (384-well plate) were tiled together before an adaptive segmentation threshold was applied to each individual pixel [320]. Mean fluorescence intensity was calculated for Collagen I + III, fibronectin and collagen IV to determine increased/decreased ECM deposition. The geomean of total mean fluorescence was calculated and CD71- vs CD71+ cell supernatant stimulations were compared. Further to this CD71-/+ media only unstimulated control was compared to ECM media only and CD71-/+ LPS stimulated was compared to LPS stimulation alone. The ECM assay was carried out by Marianne Bergin (UCB) at UCB, Slough and statistical analysis was carried out with statistician Katrina Gore (UCB) using analysis of variance (ANOVA with linear mixed model post-test).

2.25. BEC culture and stimulation

Bronchial epithelial cells were harvested at time of bronchoscopy from healthy or IPF donors who had provided written, informed consent, which was approved by a Royal Brompton Hospital ethics committee (10/HO720/12). Additional healthy BECs were also bought from Lonza.

Isolation and culture of BEC is described in **2.22**. All stimulations were carried out in triplicate wells in confluent 12 well plates at passage 3, after 3 hour starvation of cells in BEBM (bronchial epithelial cell basal media, Lonza, cat# CC-3171). Cells were left unstimulated in BEBM as a control or stimulated with either of the following; 100 ng/mL LPS (Invivogen, cat# tlrl-eklps), 10 µg/mL Poly: IC (HMW) (Invivogen, cat# tlrl-pic), 10 ng/mL recombinant human (rh)TGFβ1 (R&D, cat# 240-B-002), 10 MOI (multiplicity of infection, 10 bacteria per cell) HKSP (heat killed *Streptococcus pneumonia*), or 10 MOI HKHIB (Heat killed *Haemophilus influenza b*) in 1 mL BEBM for 6 and 24 hours. Cell supernatant was collected after 24 hours of stimulation for analysis of extracellular mediators, aliquoted and immediately stored at -80°C for later interrogation. Gene expression analysis was examined 6 hours post stimulation, after collection of the supernatant. To prepare cells for gene expression analysis 300 µL of Trizol (Ambion, cat# 15596018) was added per well, cells were scraped using a cell scraper (SLS, cat# TIS7040) and Trizol containing cells were then placed into an RNAse/ DNAse free eppendorf (ThermoFisher scientific, cat # AM12400) and immediately frozen and stored at -80°C. Graphical representation of stimulation is outlined in **Figure 2.7**. BECs used with donor information are included in **Table 2.9**.

2.26. Bacterial challenge

Bacteria were heat killed at 80°C in a water bath for 30 minutes. Heat killed bacteria were a kind gift from Dr R. Snelgrove (NHLI, Imperial College London), who had received the bacteria from Professor T. Hussell (Institute of Inflammation and Repair, The University of Manchester, UK). Dr R. Snelgrove provided the protocols below used for initial bacterial culture (**2.26.1** and **2.26.2**).

2.26.1. Haemophilus influenzae b

Hib Eagan strain were cultured at 37°C in 5% CO_2 in Brain Heart Infusion (BHI) broth (OXOID, Hampshire, UK) supplemented with 10 μg ml^{-1} of both Hemin (Roche, West Sussex, UK) and nictinamide adenine dinucleotide (Sigma-Aldrich, Dorset, UK) or on BHI agar (OXOID) supplemented with 4% Levinthals. Levinthals was made by adding 50% horse blood (TCS Biosciences, Buckingham, UK) to BHI broth and heating to 70°C for 45 min. On cooling to 50°C, 0.7 mg ml−1 nictinamide adenine dinucleotide was added and the supernatant was stored at −80°C. Bacteria were cultured to an optical density (OD) 600 nm of 0.3 (∼1 × 109 c.f.u. ml^{-1}) and stored at −80°C in 10% glycerol as single-use aliquots.

2.26.2. Streptococcus pneumoniae

S. pneumoniae (serotype 2) strain D39 (NCTC 7466, National Collection of Type Cultures, London, UK) was cultured at 37°C in 5% CO_2 on blood agar plates or in Todd-Hewitt broth (OXOID) supplemented with 0.5% yeast extract (OXOID) (THY broth) to an OD 600 nm of 0.4 (∼1 × 108 c.f.u. ml−1) and stored at −80°C in 10% glycerol as single-use aliquots.

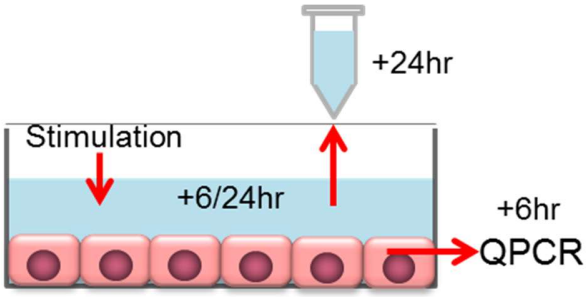


Figure 2.7: Illustration of BEC stimulation methods and sample collection.
Stimulation is added in BEBM media for 6 or 24 hours and collected with pipette. Cells are collected at 6hrs for qPCR.

ID	Disease	Source	Analysis	Age (years)	Gender	TLCO % of predicted (up to 6mth prior to bronch)	FVC % of predicted (up to 6mth prior to bronch)	Smoker
26993	Healthy	Lonza	S, GE	60	F	ND	ND	no
28265	Healthy	Lonza	S, GE	69	M	ND	ND	no
28910	Healthy	Lonza	S, GE	62	M	ND	ND	no
ILDCON1017	Healthy	Donor	S, GE	36	M	ND	86	no
ILDCON1018	Healthy	Donor	S, GE	65	M	ND	97	no
27501	Healthy	Lonza	GE	29	M	ND	ND	no
A	IPF	Donor	S, GE	76	M	ND	ND	no
B	IPF	Donor	GE	82	F	48.7	103.7	no
C	IPF	Donor	S, GE	75	F	48.1	94.7	ex
D	IPF	Donor	GE	70	M	42.8	51.6	ND
E	IPF	Donor	S, GE	68	M	51.2	72.1	no
F	IPF	Donor	S, GE	76	M	59.8	66.3	ex
G	IPF	Donor	S, GE	79	M	54	73.8	no

Table 2.9: BEC donor and analysis information.
Definition of abbreviations; transfer factor for carbon monoxide (TLCO), forced vital capacity (FVC), supernatant analysis (S), Gene expression analysis (GE), no data (ND), female (F), male (M), ex-smoker (ex).

2.27. Fibroblast cultures

Fibroblasts isolated from IPF patients lung tissue biopsies were donated from the Royal Brompton Hospital at passage 3-5. Additional healthy fibroblasts were bought from Lonza. Cells were thawed from liquid nitrogen in a water bath at 37°C and immediately pipetted into a 50 mL conical bottomed tube containing 5 mL of complete DMEM-Glutamax (Invitrogen, cat# 61965-059, 10% FBS, 1000 U/mL Penicillin and 1 mg/mL Streptomycin). Cells were centrifuged at 300 x g, 10 minutes, at room temperature, media was aspirated and cells resuspended by pipetting in 5 mL complete DMEM. Media containing cells were then placed in a T75 flask (Corning, 430641U)), media was aspirated and replaced with 15 mL pre-warmed complete DMEM 3 x per week until confluent. Cells were split when confluent using sterile TrypLE (Invitrogen, 12604-021), PBS and complete media were warmed to 37°C in water bath. Media was aspirated from confluent flask and cells are washed with PBS (10 mL for T75) for 1-2 minutes and aspirated. TrypLE was added (3 mL T75) and tilted to cover all cells. Cells were then returned to the incubator for 7- 12 minutes, flasks were tapped and cells checked for detachment (>80%). Once cells had lifted over twice the volume of complete DMEM (e.g. 7 mL for T75) was added and pipetted up and down the flask 5 times. Cells were then added to a 50 mL falcon and spun in the centrifuge (300 x g, 10 minutes at room temperature). Cells were then seeded into 4 x 12 well plates (Corning® Costar® TC-Treated Multiple Wells, Sigma-aldrich, cat# CLS3513-50EA) and left until confluent. Media was changed with 1 mL per well of complete DMEM 3 x per week.

2.28. Freezing cells

To freeze cells for later use, freeze mix (Complete medium (DMEM as described) with 10% FCS and 10% DMSO) was placed on ice for at least 15 minutes cell and cells are resuspended at 5 x 10^5/mL in freeze mix. One millilitre of cells in freeze mix was added to 1.8 mL cryovials and placed in liquid nitrogen insert for at least 2 hours before placing cells in liquid nitrogen for long term storage (1 x T75 at 100% confluence is approximately 6 vials).

2.29. Fibroblast stimulation

All stimulations were carried out in triplicate wells in confluent 12 well plates between passage 4-6, after overnight starvation of cells in incomplete DMEM ((Invitrogen, cat# 61965-059) containing 1000 U/mL Penicillin and 1 mg/mL Streptomycin). Cells were left unstimulated in incomplete DMEM as a control or stimulated with either of the following; 100 ng/mL LPS, 10 µg/mL Poly: IC (HMW), 10 ng/mL (rh)TGFβ1, 10 MOI HKSP or 10 MOI HKHib in 1 mL DMEM for 6 and 24 hours. Cell supernatant was collected for analysis of extracellular mediators at 24 hours and gene expression analysis was carried out at 6 hours. Cell supernatant was collected after 24 hours of stimulation by pipetting, aliquoted and immediately stored at -80°C for later analysis. For gene expression analysis, after collection of the supernatant, 300 µL of Trizol (Ambion, cat# 15596018) was added per well, cells were scraped using a cell scraper (SLS, cat# TIS7040) and Trizol containing cells were then placed into an RNAse/ DNAse free eppendorf (ThermoFisher scientific, cat # AM12400) and immediately frozen and stored at -80°C. Graphical representation of stimulation is outlined in **Figure 2.7**. Information on stimulated fibroblasts is outlined in **Table 2.10**.

ID	Disease	Source	Analysis	Age	Gender	Smoker
26789	Healthy	Lonza	S, GE, BC, P	66	M	N
27913	Healthy	Lonza	BC	48	M	N
27068	Healthy	Lonza	S, GE, P, BC	57	M	N
86509	Healthy	Lonza	S, GE	56	F	N
120188	Healthy	Lonza	S, GE	45	M	N
BILEL1	Healthy	Donated	S, GE	57	M	Y
ER29a	IPF	RBH	S, GE	69	M	ND
ER34	IPF	RBH	S, GE	69	M	ND
ER35	IPF	RBH	S	67	F	ND
ER55	IPF	RBH	S, GE	62	F	ND
ER62a	IPF	RBH	S, GE	64	M	ND
ER57a	IPF	RBH	GE	64	M	ND
ER56	IPF	RBH	GE	68	M	ND

Table 2.10: Fibroblast donor and analysis information.
Definition of abbreviations; supernatant analysis (S), Gene expression analysis (GE), BEC conditioned media stimulation (BC), proliferation (P), no data (ND), female (F), male (M), yes (Y) and no (N).

2.30. Stimulation of fibroblasts with conditioned BEC supernatant

Fibroblasts were grown until confluent in a 24 well plate (Corning® Costar® TC-Treated Multiple Well Plates, Sigma Aldrich, cat# CLS3527). At confluence fibroblasts were serum starved using incomplete DMEM overnight. Cells were then stimulated with 150 µL of conditioned BEC supernatant (i.e. BEBM with stimulation in contact with BECs for 24 hours) or 150 µL of stimulation only in BEBM at the same concentration used to stimulate BEC alone (e.g. LPS at concentrations described in **2.24**), for 6 hours only. An additional 150 µL of incomplete DMEM was added to all wells. An illustration of methods is provided in **Figure 2.8**.

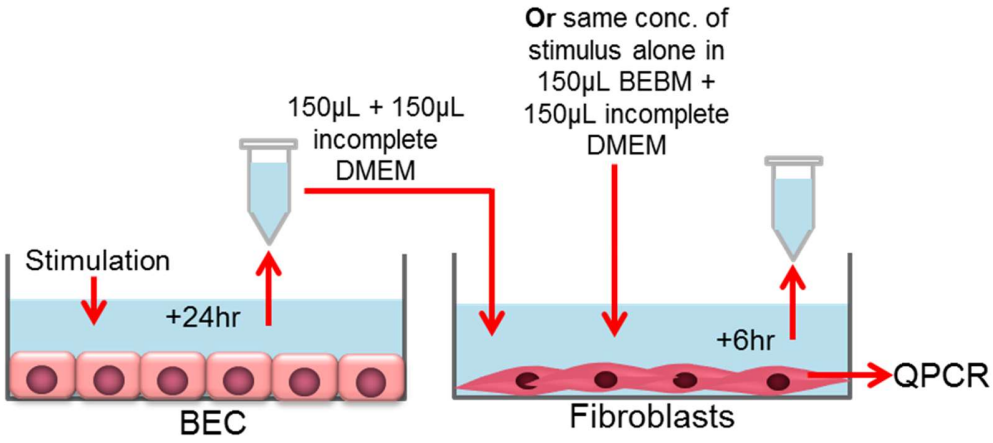


Figure 2.8: Illustration of methods used to stimulate fibroblasts with conditioned BEC media. BECs are stimulated for 24 hours at which time point the supernatants are collected. This BEC conditioned media is mixed in a 1:1 ration with incomplete DMEM and added to the fibroblasts for 6 hours. Supernatants are collected and cells harvested for QPCR analysis at 6 hours.

2.31. Fibroblast proliferation assay

Fibroblasts were seeded at 5000 cells per well in incomplete DMEM at 100µL volume in a 96 well plate (Corning® 96 Well TC-Treated Microplates, Sigma-Aldrich cat# CLS3596). Cells were left to adhere for at least 3 hours or until attached. Once attached stimulation media was added, either stimulus alone in 50 µL BEBM + 50 µL incomplete DMEM or conditioned BEC supernatant (as previously described **2.30**) using 50 µL of conditioned media + 50 µL of incomplete DMEM in 3 replicate wells. Confluence was determined using 4x magnification, auto-focus, measuring growth curves (i.e. the percentage of cells that cover the well image) in each well every 1.5 hours or every 1 hour for 72 hours, using the Automated Cell Imaging System - JuLI™ Stage (NanoEntek, Cambridge Bioscience, UK) and analysed using JuLI™ Stage software V1.5.

2.32. Statistical Analysis

Gaussian distribution was examined using the D'Agostino-Pearson omnibus normality test to examine whether or not the data was parametric. Statistical significance was determined for unpaired normally distributed (parametric) data, comparing one read out to another using unpaired T test, or paired T test for paired data (e.g. pre- and post- stimulation). For non-parametric analysis, comparing one read out to another, a Mann-Whitney U T test was performed, and for paired data, a Wilcoxon matched-pairs signed rank test was performed. For multiple comparisons of parametric data a One-Way ANOVA with Dunnett's post-test was carried out, for non-parametric data a Kruskal-Wallis test with Dunn's multiple comparison test was performed and for paired non-parametric data Friedman test with Dunn's multiple comparison test was performed. Correlations were carried out using Pearson correlation coefficients for parametric data or Spearman rank correlation for non-parametric data. Correlations with $p < 0.05$ were considered significant. Bland-Altman analysis was used to compare different methods of leukocyte analysis (FACS versus differential analysis), if the data was not normally distributed then the data was first log transformed, normality assessed using KS normality test and Bland-Altman carried out using log transformed data [321]. Statistical tests used are described in figure legends. Statistical differences required confidence level of 95%, a probability value (p value) of less than 0.05. Significant differences are denoted using asterisks; *p<0.05, **p<0.01, ***p<0.001, ****p<0.0001 and calculated using GraphPad Prism V6. All statistical analysis was carried out using GraphPad Prism 6 software.

3. Analysis of Leukocytes and mediators in the Bronchoalveolar lavage of patients with ILD.

3.1. Introduction

The pathogenesis of IPF is likely to result from a combination of multiple factors including environmental mediators, infectious agents, genetic components, but also influences from cells and their mediators both in the lung tissue and in the BAL. A combined in depth analysis of BAL cellular populations, with analysis of mediators in the BAL from healthy controls, and patients with IPF and other ILDs of known causes such as UCTD and cHP, will not only improve our understanding of the different disease pathologies but may also highlight key mediators and cell types contributing to IPF disease progression. As discussed in the introduction, there are numerous studies examining cellular differential analysis of the BAL in ILD highlighting possible increases in cell populations including eosinophils [154], neutrophils [151] and mast cells [149, 150] in IPF. However, these studies are often limited to subjective morphological differential analysis of only a few hundred cells. With the advent of multi-parameter flow cytometry, studies have examined the phenotype of lymphocytes in the IPF BAL as well as in other ILDs including HP, cHP and UCTD revealing differing CD4+/CD8+ ratios [127] [128] [129] [130, 131], Treg profiles [295] [315], NK T cells[128, 141, 142], B cells [140] and γδT cells. [130] However, owing to the restriction on the number of analysed parameters examination tends to focus on either lymphoid or myeloid cells with relatively few studies examining a broader profile of leukocytes in the diseased BAL.

Alongside cellular analysis studies have examined mediators in the BAL using traditional protein quantifications methods such as ELISA, identifying increases in chemokines including CCL2 [57, 208-212] and IL-8 in IPF [112, 204, 205]. With the advent of new technology, proteomic analysis has been performed quantifying multiple parameters in IPF BAL revealing key differences in matrix metalloproteinases, growth factors and chemokines [194]. These studies are valuable in identifying biomarkers in IPF but do not take into account the cellular profile from matched BAL combination.

Analysis of both cellular and extra cellular mediators has not been reported in IPF or other ILDs previously. Using a combined approach to analyse ILD BAL cellular and mediator contents, with focus on IPF, and in context with healthy BAL may reveal novel cellular and or mediator signatures specific to disease phenotype. Furthermore, analysis of chemoattractant factors with cells in disease provides an indication of factors recruiting and possible influencing and possible contributing toward pathology.

3.2. Hypothesis

Examination of BAL cellular and extracellular mediators combined with clinical readouts from IPF patients will reveal distinct profiles with increased presence of pro-fibrotic and anti-inflammatory mediators in the BAL comparing IPF patients to healthy controls or inflammatory ILDs. Increases in specific leukocyte populations reported to play a role in murine models of IPF, such as the macrophage, and pro-fibrotic mediators will correlate with clinical progression in patients, highlighting known and novel cells and mediators which may contribute to pathology in man.

3.3. Aims

- To develop and validate a multi parameter flow cytometry panel measuring cell surface receptors identifying specific leukocytes in the BAL from individuals with ILD and healthy controls, building a profile of leukocytes in the airways in health and disease.
- Analyse extracellular mediators including pro-inflammatory cytokines, chemokines and growth factors to provide information on the inflammatory environment in the airways. Extracellular mediators will be compared to paired cellular profiles to highlight trends in augmented cellular composition to chemotactic and inflammatory mediators.
- Investigate whether cellular and inflammatory profiles differ in ILD and whether changes correlate with clinical functional parameters.

3.4. Results

3.4.1. Cellular differential analysis reveal significantly different leukocyte proportions and cell numbers in ILD compared to healthy controls

Differential cell counts provide a basic overview of proportions of leukocytes that can be used to determine approximate number from total cell count per mL of BAL. Patient demographics for the differential counts are shown in **Table 3.1**. **Figure 3.1** illustrates the proportion of macrophages (**Figure 3.1A**), lymphocytes (**Figure 3.1B**), neutrophils (**Figure 3.1C**) and eosinophils (**Figure 3.1D**) in healthy controls, individuals with IPF, UCTD, HP, cHP and sarcoidosis. Healthy controls have a significantly higher proportion of macrophages compared to all ILDs (**Figure 3.1A**). Lymphocytes proportions are significantly increased in HP and cHP (**Figure 3.1B**) and neutrophil proportions are increased in all ILDs compared to healthy (**Figure 3.1C**). Eosinophil proportion is significantly higher in IPF, UCTD and cHP compared to healthy (**Figure 3.1D**). Conversely to macrophage percentage proportions, macrophages cell numbers are increased in IPF, UCTD and HP compared to healthy (**Figure 3.2A**). Lymphocyte number is increased in IPF, HP and cHP (**Figure 3.2B**) and neutrophil number is increased in all ILDs (**Figure 3.2C**). Eosinophil number is significantly increased in all ILDs except sarcoidosis (**Figure 3.2D**). This highlights the importance of considering increased cell numbers alongside analysis of proportion of leukocytes. The percentage of macrophages in the IPF BAL are decreased, however the cell numbers are increased, suggesting recruitment of, or proliferation of resident macrophages in the IPF airways. The leukocytes highlighted here as significantly increased may be contributing toward disease pathology. The data is summarised in **Figure 3.3**, which shows a clear increase in macrophage

cell number per mL of BAL fluid. A summary of all data including n numbers is detailed in Appendix 8.1 (**Table 8.1.1**).

	Healthy	IPF	UCTD	HP	cHP	Sarcoid
Number	7	120	20	15	29	9
Age years (min, max)	45 (22, 65)	70 (45, 84)	62 (42, 79)	63.5 (35, 82)	63 (31, 78)	52 (42, 71)
Gender (M, F)	6, 1	79, 41	12, 8	6, 9	19, 10	7, 2
Smoking status (current, ex, non, unknown)	0, 0, 2, 5	5, 52, 27, 36	1, 6, 9, 4	0, 4, 7, 4	1, 7, 11, 10	0, 2, 4, 3
Steroid (yes, no, unknown)	0, 7, 0	22, 57, 41	5, 11, 4	3, 9, 3	13, 8, 8	4, 1, 4
FVC % (min, max)	104.7 (86, 131)	77.6 (49, 127.1)	76.7 (33, 102.8)	77.1 (60.1, 120.1)	78.1 (50.1, 151)	84.4 (72, 98)
TLCO % (min, max)	ND	46.9 (24.1, 75.5)	47.7 (29, 67.3)	44.1 (27.7, 64)	43.5 (29.8, 73)	54.9 (28.9, 87.5)
Culture (unknown, negative, positive)	7, 0, 0	37, 77, 6	6, 12, 2	3, 11, 1	11, 17, 1	1, 6, 2

Table 3.1: Patient and healthy control demographics for cellular differential analysis.
Data given as mean value (min, max) for age, FVC % and TLCO % of predicted value. Definition of abbreviations; Idiopathic pulmonary fibrosis (IPF), undifferentiated connective tissue disease (UCTD), hypersensitivity pneumonitis (HP), chronic hypersensitivity pneumonitis (cHP), sarcoidosis (sarcoid), male (M), female (F), forced vital capacity (FVC) % of predicted, diffusing capacity for carbon monoxide (TLCO) % of predicted, and not determined (ND).

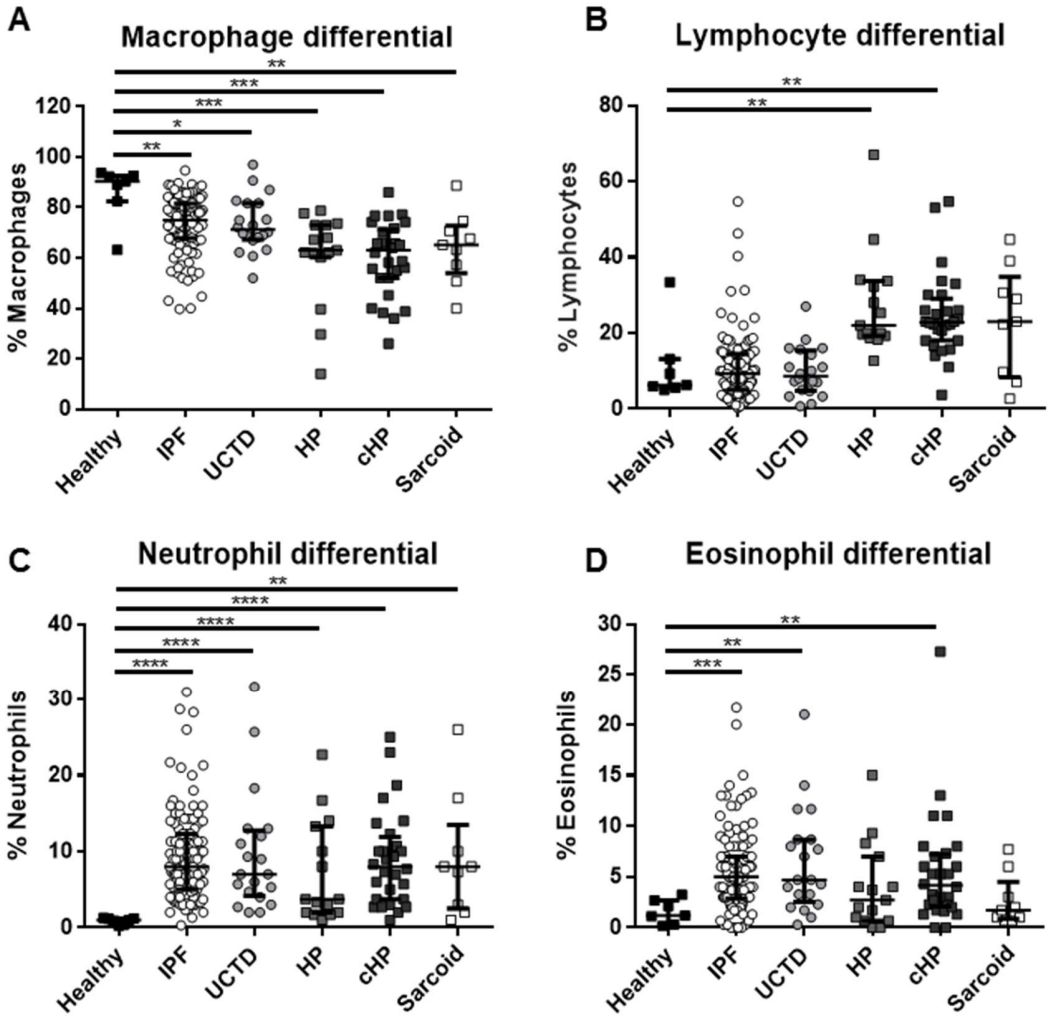


Figure 3.1: Cellular differential leukocyte proportions.
Macrophage, Lymphocyte, neutrophil and eosinophil proportions (%) (A-D respectively) in BAL from healthy controls compared to patients with ILD. Median value and interquartile range is shown for healthy controls (n=7), Idiopathic pulmonary fibrosis, IPF (n=120), undifferentiated connective tissue disease, UCTD (n=20), hypersensitive pneumonitis, HP (n=15), chronic hypersensitive pneumonitis, cHP (n=29) and sarcoidosis, sarcoid (n=9).Each ILD is compared to healthy control using Mann-Whitney U statistical analysis *p<0.05, **p<0.01, ***p<0.001, ****p<0.0001.

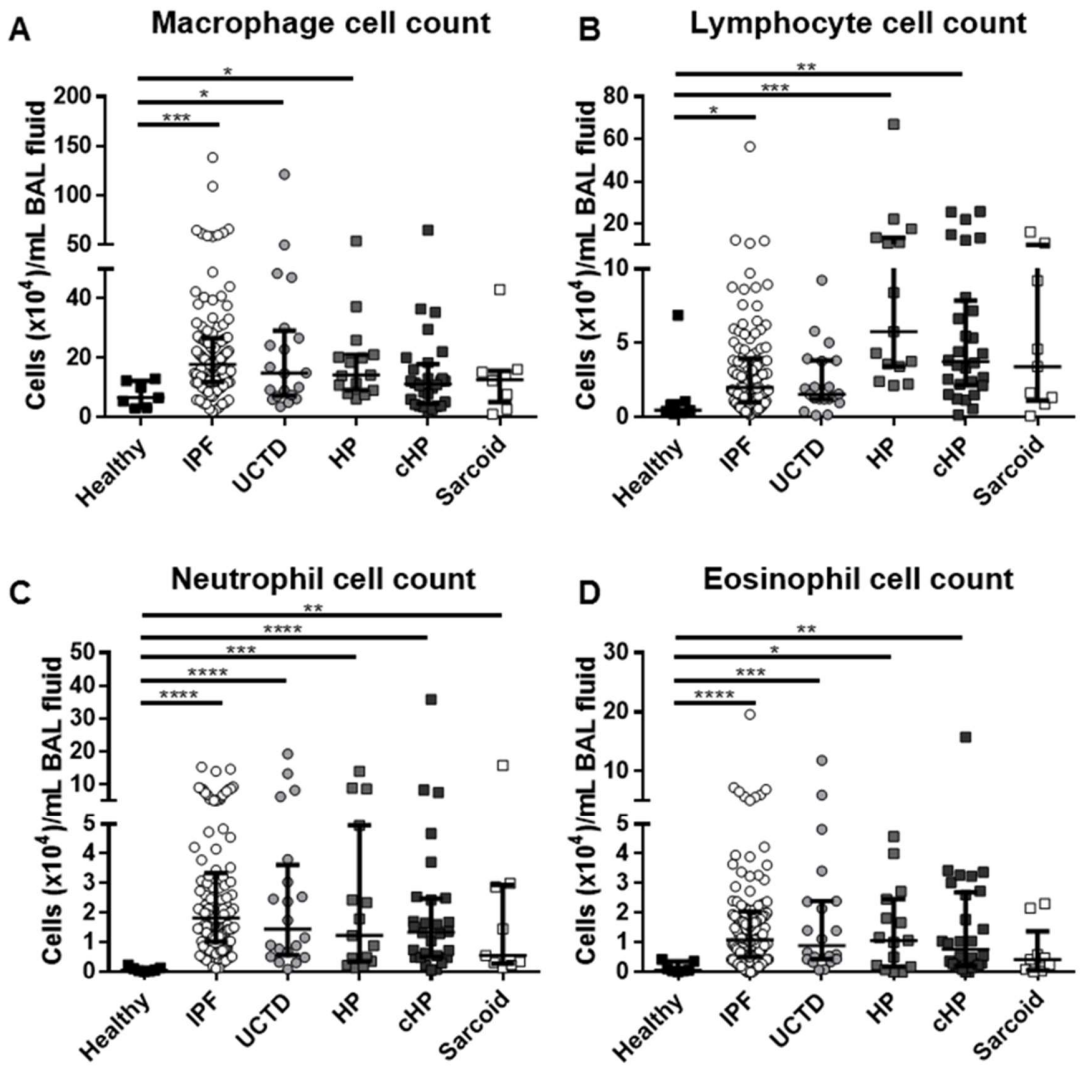


Figure 3.2: Absolute leukocyte number per mL of BAL calculated from differential counts. Macrophage, Lymphocyte, neutrophil and eosinophils (A-D) leukocyte numbers (x10^4) per mL of BAL from healthy controls compared to patients with ILD. Median value and interquartile range is shown for healthy controls (n=7), Idiopathic pulmonary fibrosis, IPF (n=120), undifferentiated connective tissue disease, UCTD (n=20), hypersensitive pneumonitis, HP (n=15), chronic hypersensitive pneumonitis, cHP (n=29) and sarcoidosis, sarcoid (n=9).. Each ILD is compared to healthy control using Mann-Whitney U statistical analysis *p<0.05, **p<0.01, ***p<0.001, ****p<0.0001.

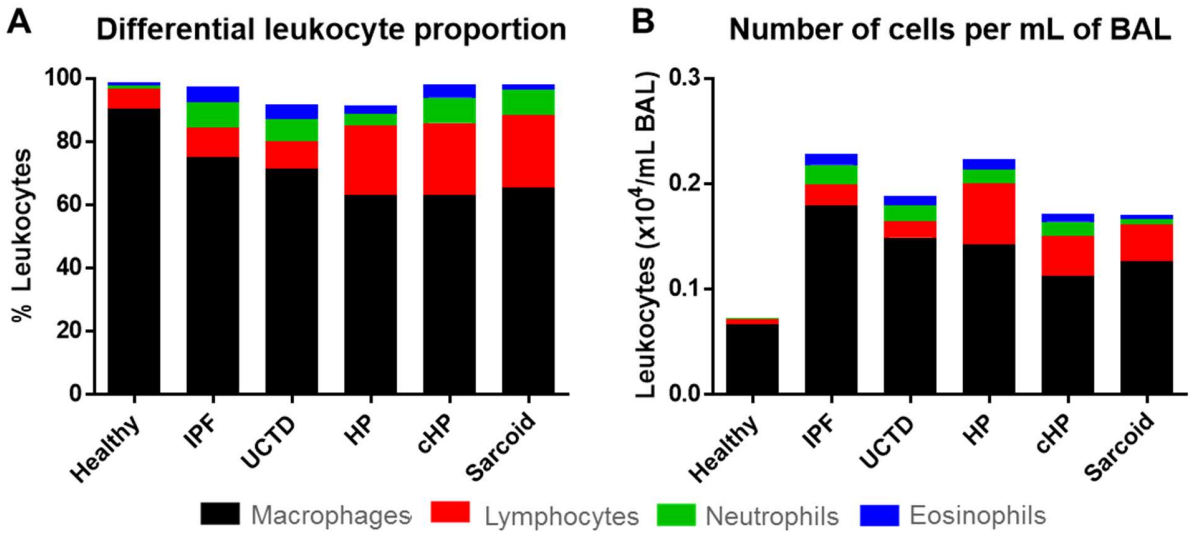


Figure 3.3: Summary of differential counts.
Summary of differential count analysis shows differential leukocyte proportion (A) and differential cell count number (x10^4 per mL of BAL) (B). Macrophages are illustrated in black, lymphocytes in red, neutrophils in green and eosinophils in blue. Median value for healthy controls (n=7), Idiopathic pulmonary fibrosis, IPF (n=120), undifferentiated connective tissue disease, UCTD (n=20), hypersensitive pneumonitis, HP (n=15), chronic hypersensitive pneumonitis, cHP (n=29) and sarcoidosis, sarcoid (n=9).

3.4.2. Confirmation of cell morphology using flow cytometry to isolate specific populations

Analysis using differential counts provide a relatively affordable and effective way to aid diagnosis of individuals with specific ILDs. Bland-Altman analysis was employed to compare differential analysis to FACs analysis of 42 paired samples revealing the number of macrophages, lymphocytes, neutrophils and eosinophils do not differ significantly comparing methods (Appendix 8.1;**Figure 8.1.1**) as over 95% of comparisons are within the upper and lower 95% limits of agreement (Appendix 8.1;**Figure 8.1.1A-D**). The comparable data examining two different methods to analyse cellular populations provides confidence in both the methods, however, differential analysis is very limited in terms of examination of multiple cell types as it relies upon interpretation of morphology alone. Nevertheless, morphology does provide confidence in flow gating strategies, confirming identification of specific and pure cell populations. In order to better to characterise leukocyte populations in ILD multi-parameter flow cytometry was employed. To confirm population purity, where possible, cells were isolated using flow cytometry and Wright-Giemsa stained to examine morphology. The demographics for patients and healthy controls for this flow cytometry are outlined in **Table 3.2** and flow cytometry gating strategy is highlighted in materials and methods **Figure 2.2**. **Figure 3.4** shows the morphology of separated cells confirming purity of cell populations using the FACs gating strategy previously described. Unfortunately insufficient numbers of Siglec 8+ eosinophils, CD56+ natural killer cells and CD19+ B cells prevented morphological examination, however, presence of these markers on these specific cells is well described in literature [142, 322, 323]. Examination of the morphology of the isolated cells; airway macrophages (CD206+, **Figure 3.4A**), monocytes (CD206-

CD14+, **Figure 3.4B**), neutrophils (CD206-CD177+, **Figure 3.4C**) and CD3+ lymphocytes (**Figure 3.4D**) confirms a pure population of each examined cell type.

	Healthy	IPF	UCTD	cHP
Number	7	22	6	7
Age years (min, max)	45 (22, 65)	70 (45, 82)	62 (42,76)	61 (52, 75)
Gender (M, F)	6, 1	16, 6	4, 2	5, 2
Smoking status (unknown, current, ex, never)	5, 0, 0, 2	6, 1, 10, 5	1, 0, 2, 3	2, 0, 1, 4
Steroid (yes, no, unknown)	0, 7, 0	2, 20, 0	0, 6, 0	3, 4, 0
FVC % (min, max)	104.7 (86, 131)	78.6 (49.9, 126.6)	75.6 (49, 99.4)	93.5 (59, 151)
TLCO % (min, max)	ND	44.3 (29.2, 64.9)	55.8 (44.3, 64.1)	48.1 (36.5, 73)
Culture (unknown, negative, positive)	7, 0, 0	0, 22, 0	0, 5, 1	0, 7, 0

Table 3.2: Patient and healthy control demographics for general leukocyte analysis.
Data given as mean value (min, max) for age, FVC % and TLCO % of predicted value. Definition of abbreviations; Idiopathic pulmonary fibrosis (IPF), undifferentiated connective tissue disease (UCTD), chronic hypersensitivity pneumonitis (cHP), male (M), female (F), forced vital capacity (FVC) % of predicted, diffusing capacity for carbon monoxide (TLCO) % of predicted, and not determined (ND).

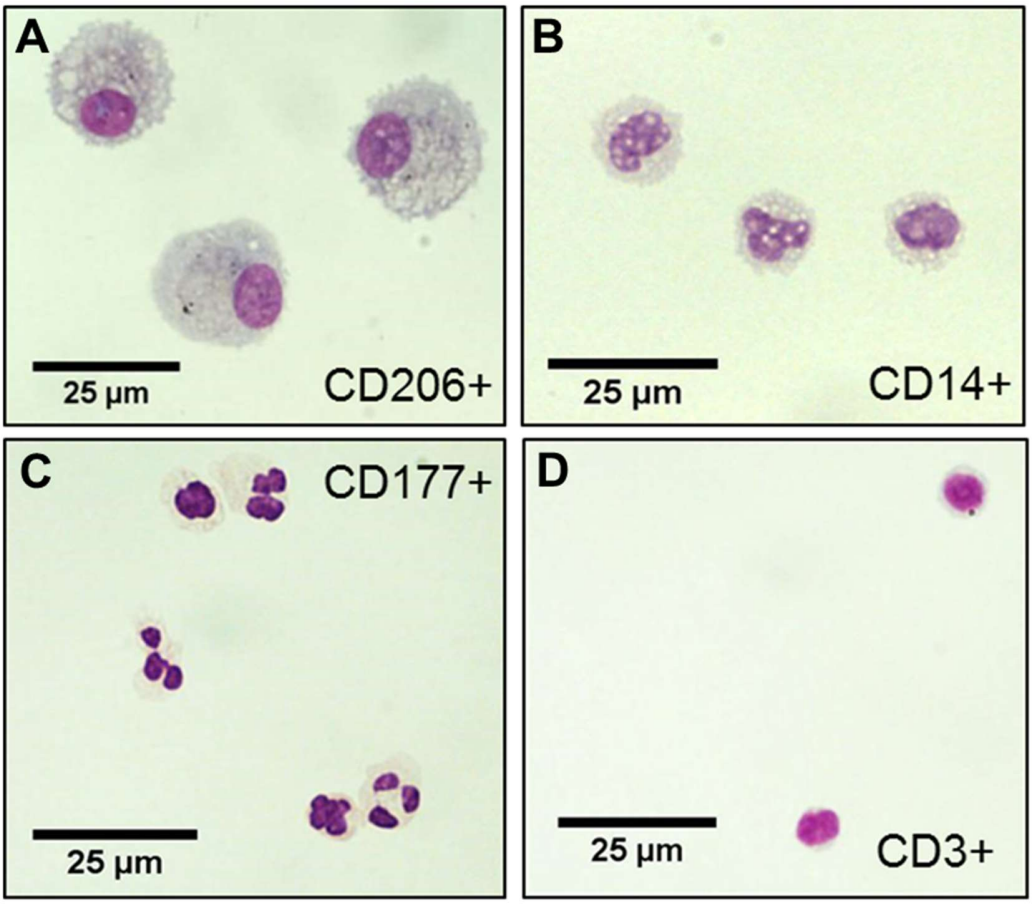


Figure 3.4: Images of cells separated using flow cytometry.
CD45+ leukocytes were separated and stained using Wright-Giemsa stain. Bright field images were taken at x20 magnification. Scale bars are present in the bottom right corner of each image. CD206+ (A), CD206- CD14+ (B), CD206- CD177+ (C) and CD206- CD3+ (D) were isolated and reveal the morphological appearance of airway macrophages, monocytes, neutrophils and lymphocytes respectively.

3.4.3. Analysis of key myeloid populations in the BAL reveal significant increases in monocytes and macrophages in IPF compared to healthy controls.

Analysis of myeloid populations by FACs show a significant decrease in the proportion of macrophages in cHP compared to healthy controls, with no differences comparing healthy to other ILDs (**Figure 3.5A**). There was a significant increase in proportions of CD14+ monocytes in IPF and UCTD (**Figure 3.5B**) compared to healthy controls, and no significant differences examining the proportion of neutrophils and eosinophils (**Figure 3.5C-D**, respectively). Increased numbers of both macrophages and monocytes were observed in IPF compared to healthy controls suggesting possible cell recruitment into the airways (**Figure 3.6A-B**, respectively). No significant increases in neutrophil number in IPF compared to healthy controls were observed, however, there appears to be an overall increase in neutrophil cell number (**Figure 3.6C**), indicative of low level inflammation. Surprisingly, there is a significant increase in Siglec 8+ eosinophils in IPF, which are commonly associated with T helper type 2 (Th2) response in allergic airways [324], compared to healthy controls which is illustrated in **Figure 3.6D**. FcεR1 and CD1c expression were also incorporated and analysed in this stain. FcεR1 is thought to be expressed on mast cells, basophils and to a lesser extent dendritic cells, some monocytes and eosinophils [325-327]. CD1c is reported to be expressed on dendritic cells [328]. Analysis of cell proportions, cell number and staining of isolated cells are shown in **Figure 3.7A-C** for CD206-FcεR1+ and **Figure 3.7D-F** CD206-CD1c+ respectively. There is an increase in both the proportion of and cell number of FcεR1+ cells in all ILDs compared to healthy controls (**Figure 3.7A-B**), however, examination of the morphology of FcεR1+ revealed mixed populations of myeloid cells, which is most likely a combination of granulocytes and dendritic cells, with no clear increase in a specific

morphologically recognisable population (**Figure 3.7C**). CD1c+ proportions do not differ compared to healthy controls (**Figure 3.7D**), however, the number of CD1c+ cells are significantly increased in IPF and UCTD (**Figure 3.7B**). Separation and staining of CD1c+ cells revealed cells exhibiting a very similar morphology but not recognisably dendritic cell-like in appearance (**Figure 3.7F**). It is interesting that these cell types are significantly increased in cell number in IPF, the inclusion of further markers is required to fully elucidate and define these populations. A summary of myeloid cell proportions and numbers are highlighted in **Figure 3.8**.

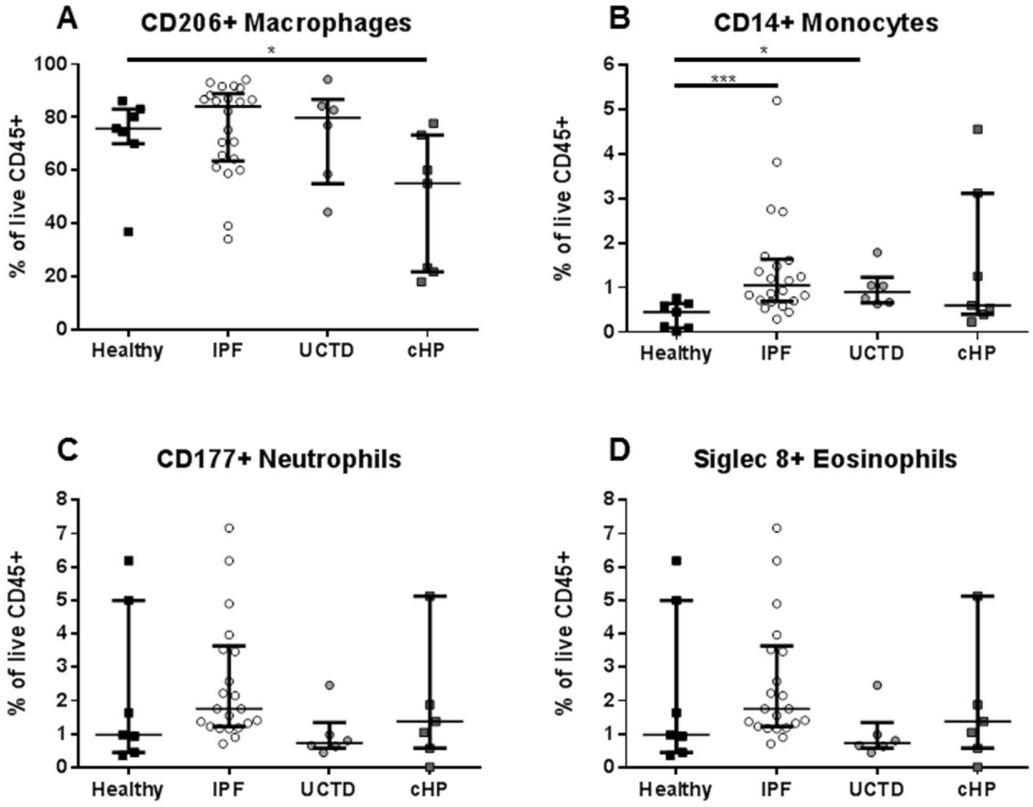


Figure 3.5: Myeloid cell proportion analysis in ILD.
The percentage of airway macrophages (A), monocytes (B), neutrophils (C) and eosinophils (D) were analysed using multi-parameter flow cytometry. Median and interquartile range is shown in healthy controls, Idiopathic pulmonary fibrosis (IPF), undifferentiated connective tissue disease (UCTD) and chronic hypersensitive pneumonitis (cHP) patients. Significant differences were calculated using Mann-Whitney U analysis comparing each ILD to healthy controls analysis *p<0.05, **p<0.01, ***p<0.001.

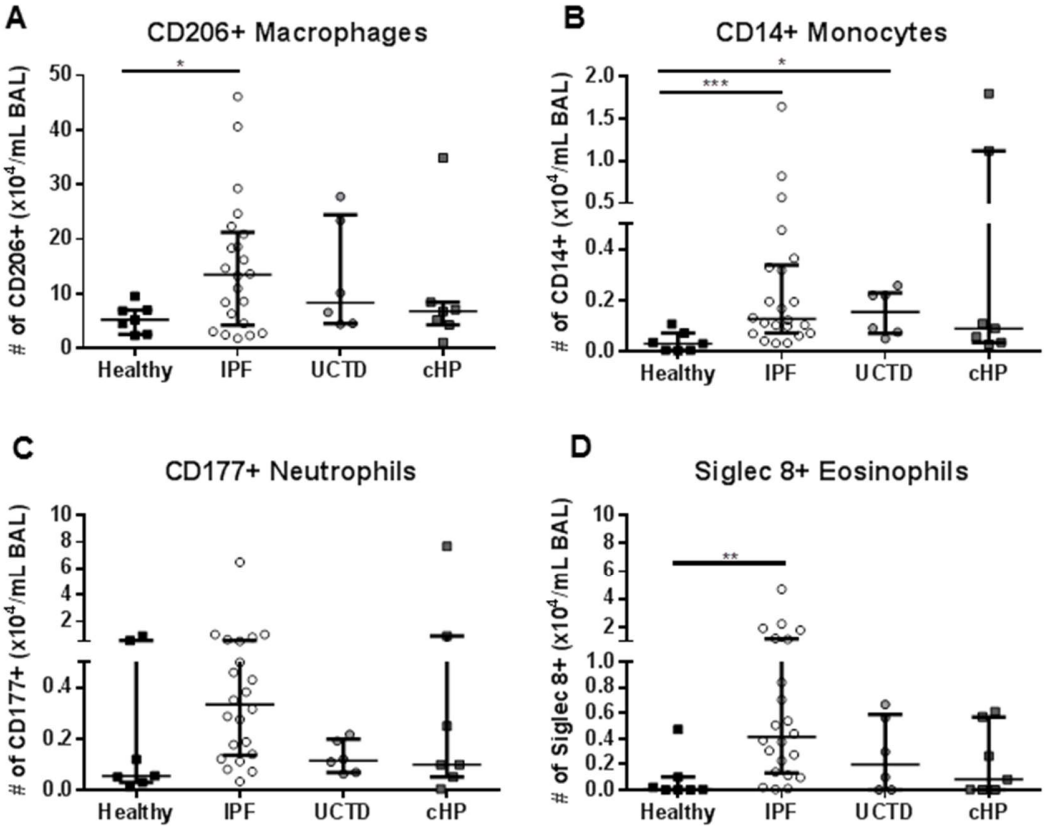


Figure 3.6: Analysis of number of myeloid cells (x10^4) per mL of BAL.
The number of myeloid cells (x10^4) per mL of BAL was determined. A-D show the cell number x10^4 per mL of BAL of airway macrophages, monocytes, neutrophils and eosinophils respectvely. Median and interquartile range is shown in healthy controls, Idiopathic pulmonary fibrosis (IPF), undifferentiated connective tissue disease (UCTD) and chronic hypersensitive pneumonitis (cHP) patients. Significant differences were calculated using Mann-Whitney U analysis comparing each ILD to healthy controls analysis *p<0.05, **p<0.01, ***p<0.001.

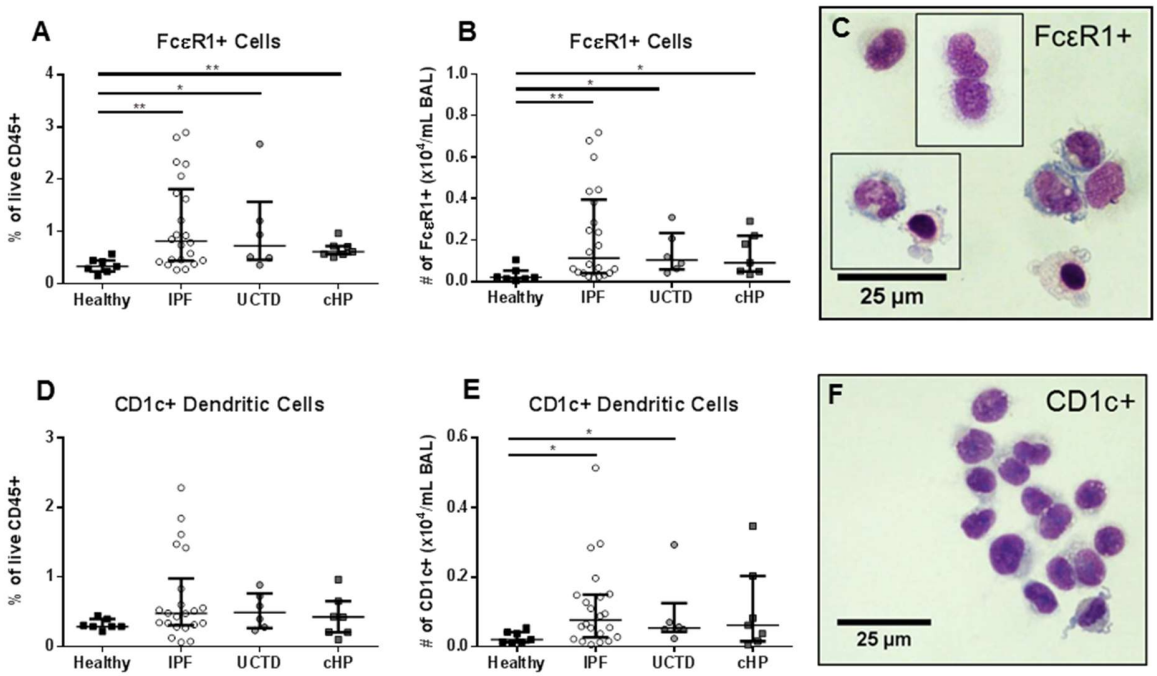


Figure 3.7: Analysis of FcεR1 and CD1c expressing cells in ILD.
CD206- FcεR1+ cell proportion and cell number (x10^4/mL BAL) are shown in A and B respectively. CD206- FcεR1+ isolated Wright-Giemsa stained cells are shown with additional examples of cells in inset boxes (C). All images were captured from the same cytospin, under the same magnification, settings and scale (C). CD1c+ cell proportion, cell number (x10^4/mL BAL) and isolated Wright-Giemsa stained cells are shown in D-F respectively. Median and interquartile range is shown in healthy controls, Idiopathic pulmonary fibrosis (IPF), undifferentiated connective tissue disease (UCTD) and chronic hypersensitive pneumonitis (cHP) patients. Significant differences were calculated using Mann-Whitney U analysis comparing each ILD to healthy controls analysis *p<0.05, **p<0.01.

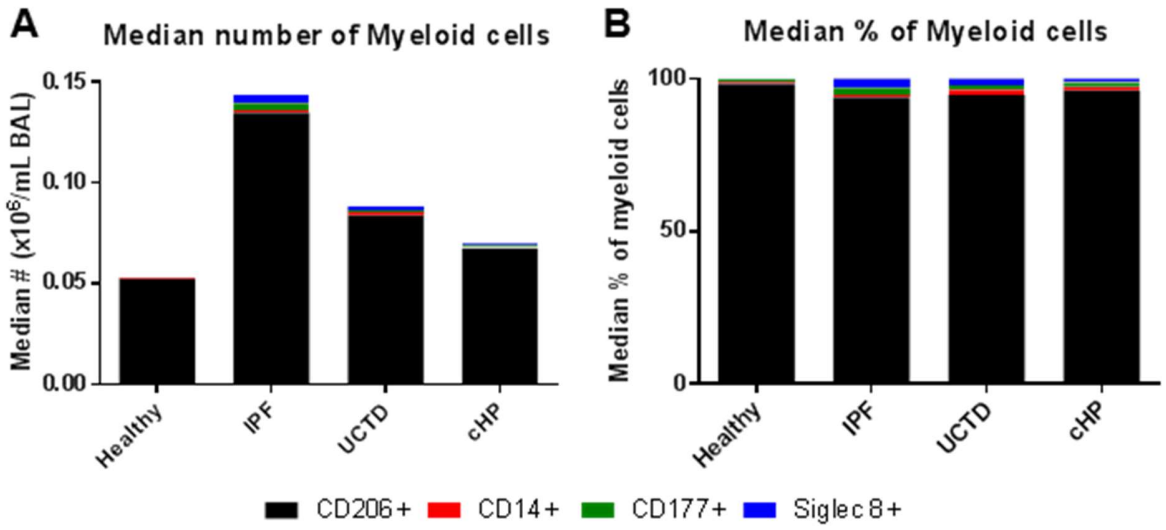


Figure 3.8: Summary of myeloid cells in the airways of healthy controls and ILD patients.
The median number (x10^6/mL BAL) (A) and proportions (B) of examined myeloid cell populations; CD206+ airway macrophages (black), CD14+ monocytes (red), CD177+ neutrophils (green) and Siglec 8+ eosinophils (blue) are illustrated for healthy controls, Idiopathic pulmonary fibrosis (IPF), undifferentiated connective tissue disease (UCTD) and chronic hypersensitive pneumonitis (cHP) patients in the grouped bar graphs.

3.4.4. Analysis of lymphoid cells in the BAL reveal increased NK cells numbers in IPF patients compared to healthy controls.

In general, the proportion of lymphoid cells did not differ comparing healthy controls to ILDs (**Figure 3.9**). The proportion of CD3+ lymphocytes appears significantly decreased in IPF patients compared to healthy controls and the proportion of CD3+ cells in cHP was increased, however this was not significant (**Figure 3.9A**). The number of CD3+ lymphocytes per mL of BAL was significantly increased in cHP compared to healthy (**Figure 3.9A**) and there was a general trend for an increase in lymphoid cells in cHP compared to healthy controls (**Figure 3.10**). There was a significant increase in the number of NK cells per mL of BAL in IPF compared to healthy controls (**Figure 3.10C**) with no differences in other lymphoid cell numbers. A summary of lymphoid cell proportions and numbers are highlighted in **Figure 3.11.**

Taken together there appears to be an increase in myeloid cells in IPF and UCTD, with an increase in lymphoid cells in cHP, which is summarised in a heat map shown in **Figure 3.12.** This suggests that myeloid cells and not lymphoid cells are playing a role in IPF and UCTD pathology, contrasting cHP where lymphocytes are involved in driving the pathology.

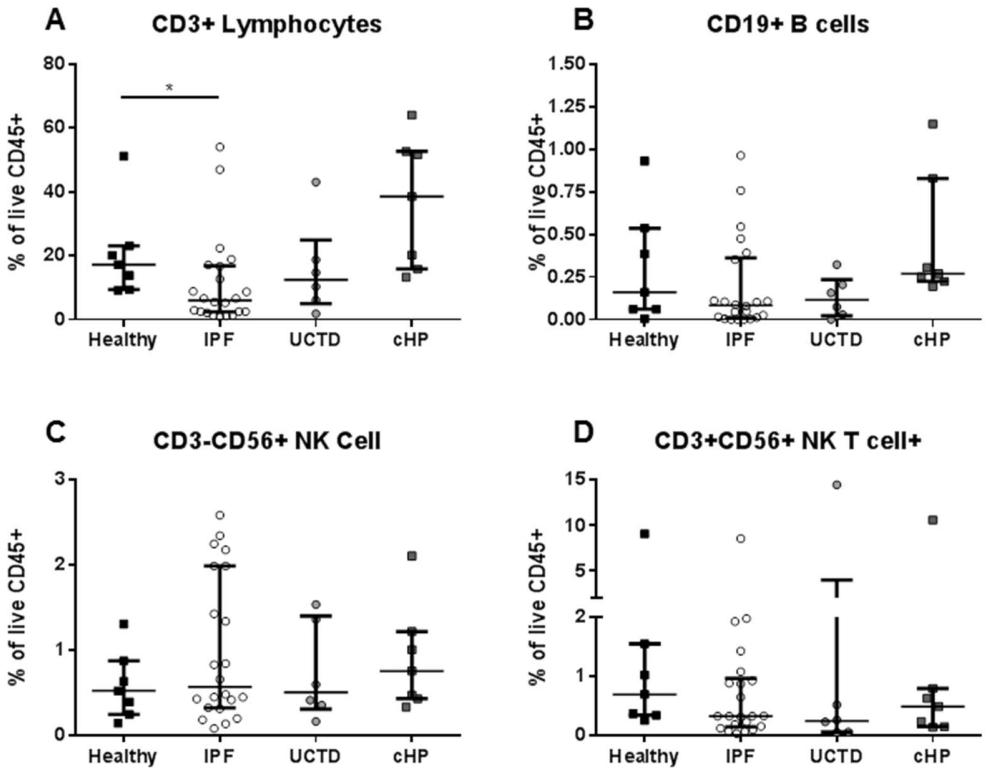


Figure 3.9: Lymphoid cell proportion analysis in ILD.
The percentage live CD45+ leukocytes that were CD3+ lymphocytes (A), CD19+ B cells (B), CD3-CD56+ NK cells (C) and CD3+CD56+ NK T cells (D) were analysed using multi-parameter flow cytometry. Median and interquartile range is shown for healthy controls, Idiopathic pulmonary fibrosis (IPF), undifferentiated connective tissue disease (UCTD) and chronic hypersensitive pneumonitis (cHP) patients. Significant differences were calculated suing Mann-Whitney U analysis comparing each ILD to healthy controls analysis *$p<0.05$.

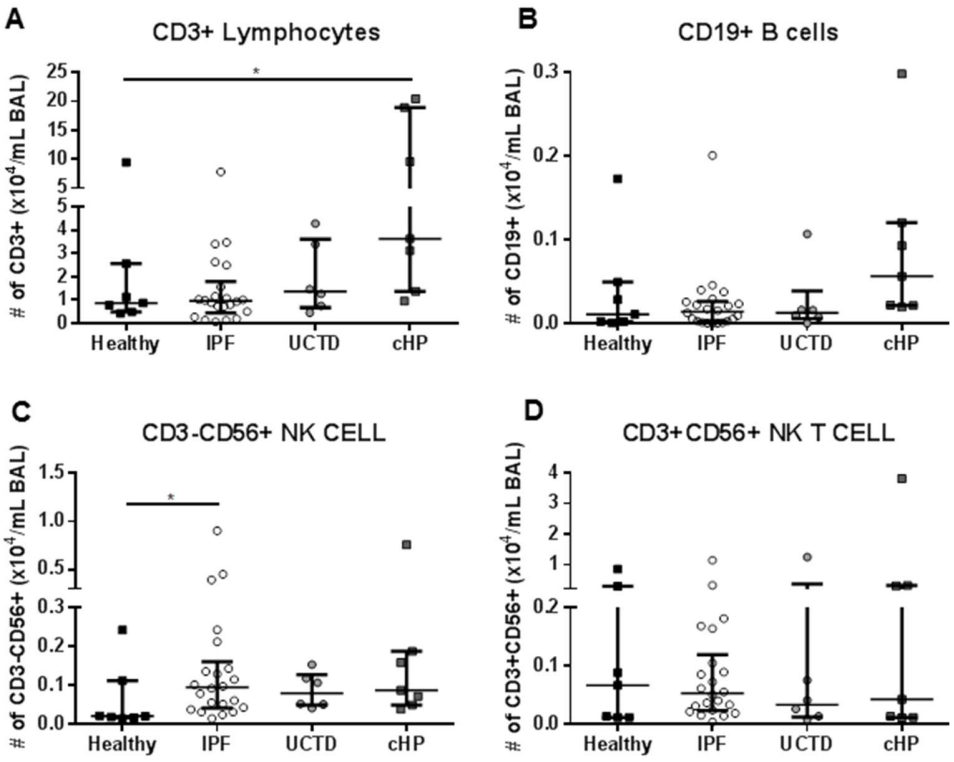


Figure 3.10: Analysis of number of lymphoid cells (x10^4) per mL of BAL.
The number of lymphoid cells (x10^4) per mL of BAL was determined in healthy controls, Idiopathic pulmonary fibrosis (IPF), undifferentiated connective tissue disease (UCTD) and chronic hypersensitive pneumonitis (cHP) patients. CD3+ lymphocytes , CD19+ B cells , CD3-CD56+ NK cells and CD3+CD56+ NK T cells are shown in A-D respectively. Median and interquartile range is illustrated. Significant differences were calculated using Mann-Whitney U analysis comparing each ILD to healthy controls analysis *$p<0.05$.

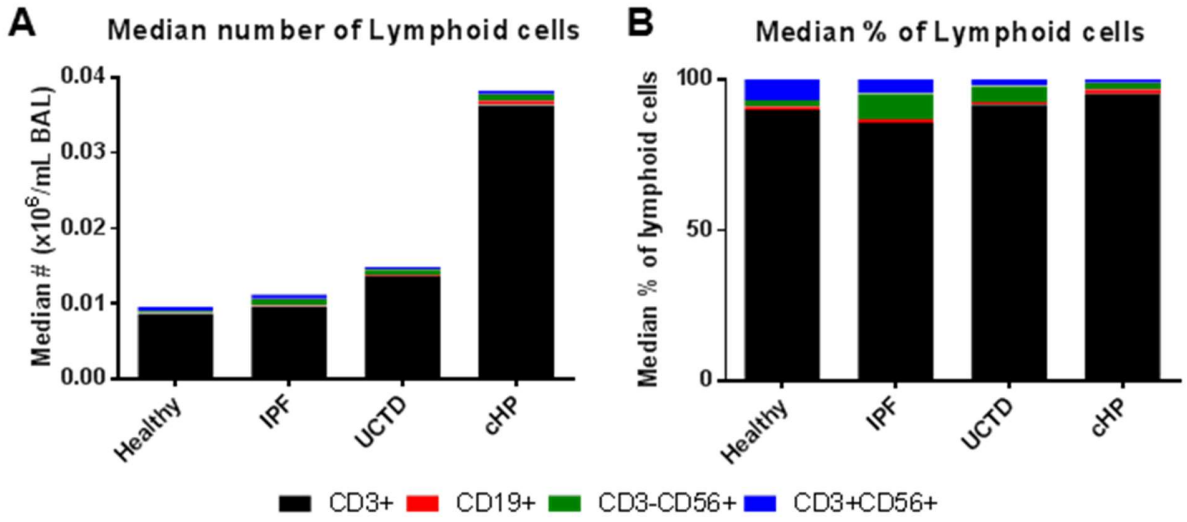


Figure 3.11: Summary of lymphoid cells in the airways of healthy controls and ILD patients.
The median number (x10^6/mL BAL) (A) and proportions (B) of examined lymphoid cell populations in healthy controls, Idiopathic pulmonary fibrosis (IPF), undifferentiated connective tissue disease (UCTD) and chronic hypersensitive pneumonitis (cHP) patients. CD3+ lymphocytes (black), CD19+ B cells (red), CD3-CD56+ NK cells (green) CD3+CD56+ NK T cells (blue) are illustrated in the grouped bar graphs.

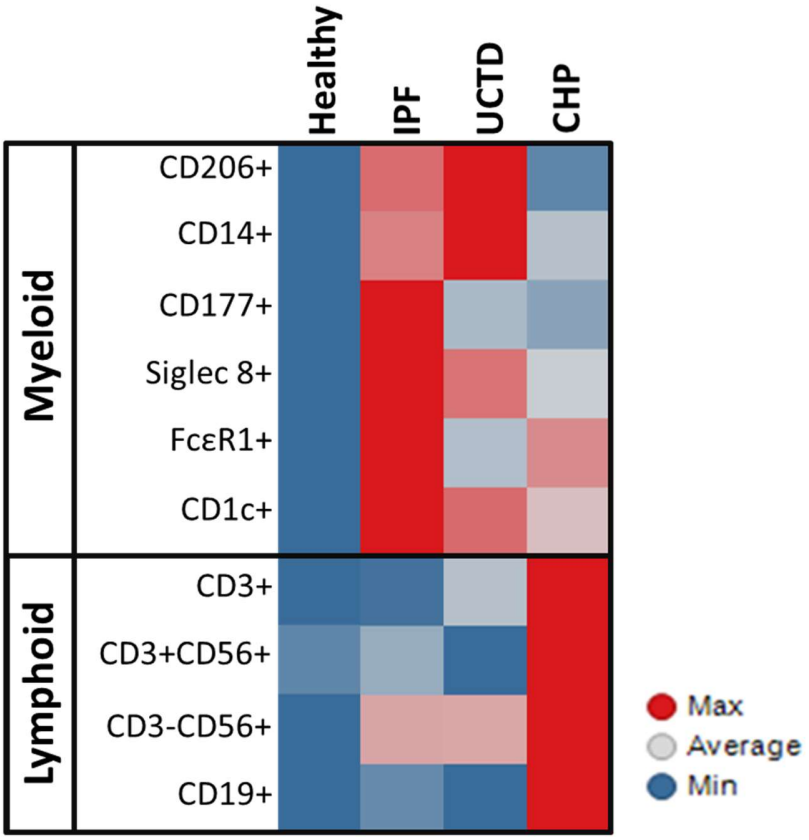


Figure 3.12: Heat map summary of cell numbers shows an increase in myeloid cells in IPF and lymphoid cells in cHP compared to healthy controls.

Heat map visualisation of the median cell number per millilitre of BAL fluid of myeloid cell populations (CD206+ macrophages, CD14+ monocytes, CD177+ neutrophils, Siglec 8+ eosinophils, FcεR1+ and CD1c+ expressing cells) and lymphoid cell populations (CD3+ T cells, CD3+CD56+ NK T cells, CD3-CD56+ NK cells and CD19+ B cells). Each cell population is compared across groups, healthy control median cell numbers are illustrated in the first column on the left with idiopathic pulmonary fibrosis (IPF), undifferentiated connective tissue disease (UCTD) and chronic hypersensitivity pneumonitis (cHP) patient median cell numbers illustrated in the second to forth column respectively. Red indicates increased cell number, with the darkest red indicating the greatest cell number, blue indicates lower cell numbers with the darkest blue indicating the lowest cell number for each cell population comparing the ILDs and healthy controls.

3.4.1. Total protein in the BAL does not differ significantly between groups.

The BAL procedure followed a standardised protocol outlined in the methods section (**2.1**). However, on occasion the total volume of saline administered may have to be altered based on individual requirements of patients, and equally, owing to technical aspects of the procedure, the amount of BAL aspirated is variable. Total protein was measured in the BAL supernatant from patients with ILD and healthy controls to examine differences in protein concentration of BAL which may result from variation in volumes administered and aspirated. There were no significant differences in total protein concentration in the BAL comparing disease to healthy controls suggesting the BAL protein concentrations are comparable for analysis of differences examining other specific proteins (**Figure 3.13**). There are slight increases in total protein in the BAL of ILD patients, which is likely a result of underlying damage to the cells as a consequence of the pathology.

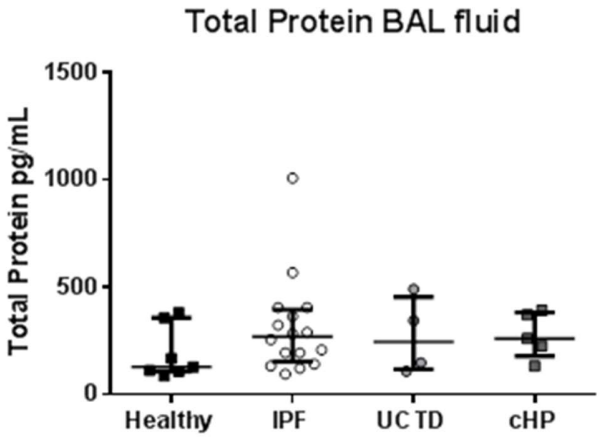


Figure 3.13: Total protein in the BAL supernatant.
BAL supernatant was assayed using BCA total protein assay. No significant differences were found examining total protein using Mann-Whitney U comparing each ILD to healthy control and each ILD to one another. Median and interquartile range is shown for total protein (pg/mL).

3.4.2. Quantification of inflammatory cytokine levels in ILD BAL supernatant

Cytokines play key roles in the activation and regulation of leukocytes. In order to examine the BAL environment, multiple inflammatory cytokines in the BAL of patients with ILD and healthy controls were measured. Owing to the quantity of saline solution administered into the airways to obtain BAL, mediators are very dilute. Firstly, to test whether cytokines could be quantified in the BAL an inflammatory mediator multiplex assay on 3 IPF and 3 cHP BAL supernatants was performed. This assay measured key interferons including IFNα, IFNβ and IFNγ, the alarmin IL-33, Th1 differentiation promoting cytokine IL-27, immunoregulatory cytokine IL-10 and pro-inflammatory cytokine IL-6. All these cytokines were at levels too low for detection (data not shown). In addition to the aforementioned cytokines the multiplex measured pro-inflammatory mediator IL-23, which is thought to play a role in Th17 mediated inflammation [329] and MMP9 upregulation [330], IL-12p70 plays a role in Th1 differentiation and NK cell activation [331], and pro-inflammatory cytokine TNFα, which were detectable in the BAL in some samples but at very low levels (**Figure 3.14A-C**). Similarly IL-18, which plays a role in inducing IFNɣ production [332] was detectable but at low levels (**Figure 3.14D**). The assay did indicate that the chemokines IL-8 and CCL2 were detectable and at higher levels than cytokines in the BAL, suggesting other chemokines would be quantifiable and are discussed in the next results section. In addition to the multiplex analysis TNFα, IL-10, IL-22 and IL-6 ELISAs of multiple samples from the BAL were performed. TNFα, IL-10 and IL-22 were below the limits of detection (data not shown). Some BAL supernatants did show detectable levels of IL-6, albeit at very low levels, no significant differences were found comparing healthy to ILD BAL (**Figure 3.15**). It is likely the BAL supernatants are too dilute resulting in cytokine levels below the limit of detection.

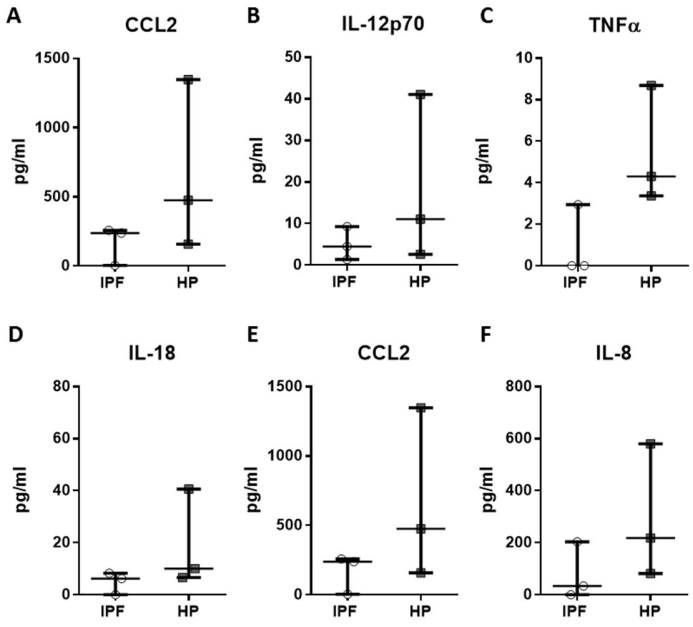


Figure 3.14: Pro-inflammatory mediators in the BAL.
Cytokines were quantified using Legendplex™, multiplex assay. Detectable cytokines and chemokines IL-23, IL-12p70, TNFα, IL-18, CCL2 and IL-8 (A-F respectively) were measured in the supernatant from 3 individuals with idiopathic pulmonary fibrosis (IPF) and 3 individuals with hypersensitivity pneumonitis (HP). Median and interquartile range is shown.

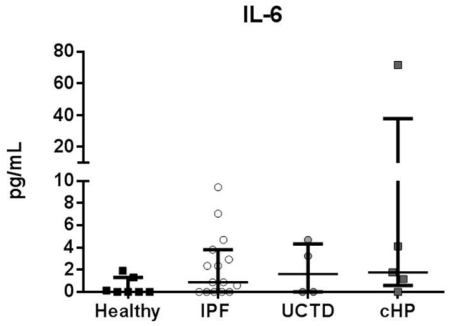


Figure 3.15: IL-6 in BAL supernatant.
IL-6 levels were quantified by ELISA in healthy (n=7), idiopathic pulmonary fibrosis, IPF (n=15), undifferentiated connective tissue disease, UCTD (n=4) and chronic hypersensitivity pneumonitis cHP (n=5) BAL supernatants. Median and interquartile range is shown. No significant differences were found examining total protein using Mann-Whitney U comparing each ILD to healthy control.

3.4.3. Quantification of chemokines in the BAL supernatant reveals distinct profiles in ILD correlating with increases in specific cell populations

Understanding what factors may be recruiting specific cell populations into the airways is critical to enable the dissection of observed cellular changes and to highlight targets for therapeutic intervention. Therefore, the concentrations of a key set of pro-inflammatory chemokines were examined in BAL fluid supernatant from samples where analysis of cellular populations had been carried out using flow cytometry. This was carried out in order to elucidate possible chemokines that may be attracting cells into the airways. Analysis of chemokine levels revealed a significant increase in CCL2 (MCP-1) in IPF and UCTD (**Figure 3.16A**) and elevated CXCL10 in cHP (**Figure 3.16B**) which correlated with expanded monocytes and lymphocytes (**Figure 3.16C** and **D** respectively)**. Table 3.3** shows the median and 25/75% percentiles of the measured chemokines. CCL17 and CXCL11 were very low or undetectable in the BAL supernatant. CXCL5, CCL11, CCL5, CCL3 and CCL4 were similar across groups. CXCL9 and CXCL10 were elevated in cHP. CXCL10 was also enhanced in UCTD compared to healthy controls. CXCL1, CCL2 and IL-8 were increased in all ILDs compared to healthy controls. A heat map summary of chemokines in the BAL is shown in **Figure 3.17**. Taken together the data shows a characteristic chemokine profile in ILD BAL which correlates with distinct leukocyte signatures.

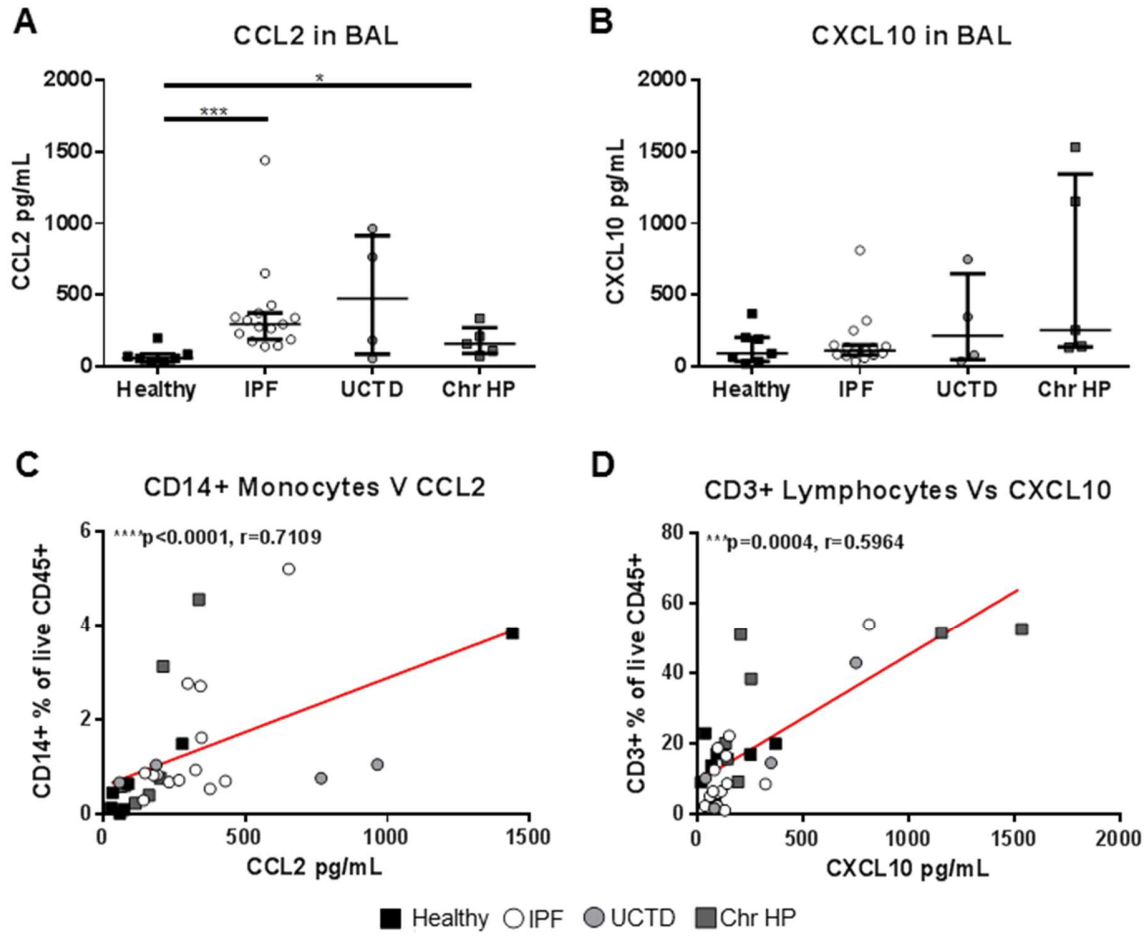


Figure 3.16: Increased levels of CCL2 and CXCL10 significantly correlate with increased proportions of monocytes and lymphocytes respectively.

CCL2 and CXCL10 levels (pg/mL) were measured in the BAL of healthy individuals and those with ILD and shown in A and B respectively. Median and interquartile range is shown. Significant differences were calculated using Mann-Whitney U analysis comparing each ILD; Idiopathic pulmonary fibrosis (IPF), undifferentiated connective tissue disease (UCTD), chronic hypersensitivity pneumonitis (Chr HP) to healthy controls analysis *p<0.05, **p<0.01, ***p<0.001. Levels of chemokines were correlated to increased proportions of leukocytes revealing a significant correlation examining levels of CCL2 with proportions of monocytes (C) and CXCL10 with proportions of lymphocytes in the BAL (D). Correlations were carried out using Spearman's rank correlation with r values and p values written on the top left of graphs. Linear regression is highlighted in red.

Chemo-kine		Healthy controls n=7 (pg/mL)			IPF n=15 (pg/mL)			UCTD n=4 (pg/mL)			cHP n=5 (pg/mL)		
Name	AKA	**Median**	25%	75%	**Median**	25%	75%	**Median**	25%	75%	**Median**	25%	75%
CXCL9	MIG	**5.965**	0	12.59	**6.41**	0	15.9	**5.145**	0	22.1	**15.15**	7.085	92.8
CXCL10	IP-10	**92.97**	35.69	204.8	**113.1**	80.31	151.1	**214.2**	48.73	649.5	**254.4**	137.2	1343
CXCL5	ENA-78	**42.78**	37.67	48.28	**59.47**	49.77	118.5	**47.62**	13.98	382.9	**62.64**	31.25	128.1
CXCL1	GROα	**543.6**	328.4	2197	**1060**	395	1558	**1034**	135.3	1702	**1002**	199.3	1270
CXCL8	IL-8	**35.04**	32.18	70.07	**86.14**	53.54	194.4	**131.8**	12.03	1104	**73.46**	57.14	817.6
CCL2	MCP-1	**59.08**	31.28	86.19	**296.3**	188.7	374.6	**475.5**	87.5	914.8	**159.5**	92.47	272.8
CCL11	Eotaxin	**12.8**	8.96	16.62	**7.64**	3.6	23.38	**15.13**	9.03	33.96	**9.06**	7.73	21.65
CCL5	RANTES	**39.2**	27.49	46.89	**48.18**	0	55.88	**40.45**	4.165	85.31	**27.63**	0	65.79
CCL3	MIP-1A	**28.38**	13.65	30.39	**27.3**	0	39.33	**21.43**	4.77	24.66	**25.04**	10.07	29.3
CCL4	MIP-1B	**42.11**	32.21	51.26	**35.7**	26.75	43.82	**53.48**	32.91	62.86	**34.44**	33.81	48.79
CCL20	MIP-3A	**6.175**	0	25.14	**7.11**	0	12.09	**6.125**	1.005	9.498	**3.81**	0	12.96
CCL17	TARC	**0**	0	0	**0**	0	36.48	**20**	0	42.56	**0**	0	37.84
CXCL11	I-TAC	**0**	0	0	**0**	0	0	**0**	0	9.938	**0**	0	20.7

Table 3.3: Measurement of soluble chemokines in the BAL reveals different concentrations of chemokines comparing healthy to ILDs.

The table shows the median value with 25 and 75 percentiles for 13 pro-inflammatory chemokines. Definition of abbreviations: Idiopathic pulmonary fibrosis (IPF), undifferentiated connective tissue disease (UCTD), chronic hypersensitivity pneumonitis (cHP), CC motif ligand (CCL), CXC motif ligand (CXCL), monocyte chemoattractant protein (MCP), macrophage inflammatory protein (MIP), regulated on activation, normal T cell expressed and secreted (RANTES), thymus and activation-regulated chemokine (TARC), growth-regulated oncogene-alpha (GROα), epithelial-derived neutrophil-activating peptide 78 (ENA-78), monokine induced by gamma interferon (MIG), IFNγ inducible protein of 10 kDa (IP-10), interferon-inducible T-cell alpha chemoattractant (I-TAC).

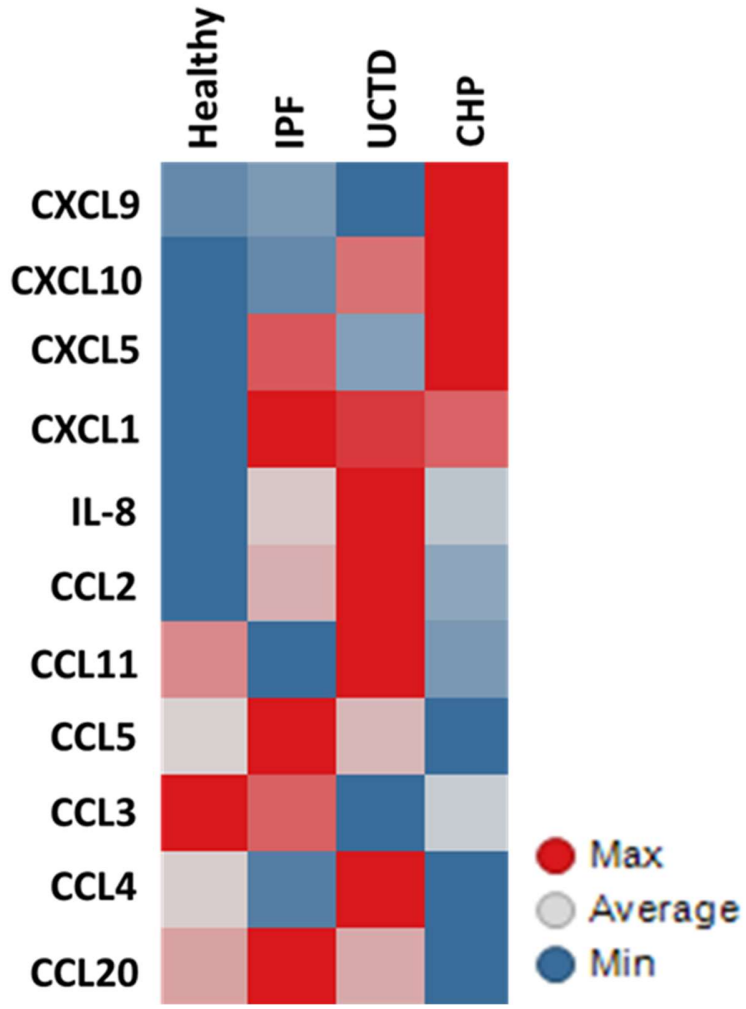


Figure 3.17: Heat map summary of median measurement of pro-inflammatory mediators in the BAL reveals different chemokine profiles in ILD.
Heat map illustrates the median pg/mL of pro-inflammatory mediators measured in the BAL. Each chemokine is compared across groups, healthy control median chemokine concentration (pg/mL) are illustrated in the first column on the left with idiopathic pulmonary fibrosis (IPF), undifferentiated connective tissue disease (UCTD) and chronic hypersensitivity pneumonitis (cHP) illustrated in the second to forth column respectively. Red indicates increased concentration (pg/ml), with the darkest red indicating the highest concentration, blue indicates lower concentrations with the darkest blue indicating the lowest concentration and grey represents average concentration for each individual chemokine comparing the ILDs and healthy controls.

3.4.4. Quantification of growth factors in the BAL supernatant

A key feature of fibrosis is excessive and dysregulated production of ECM by myofibroblasts, which involves multiple factors influencing the remodelling of the lung. **Table 3.4** shows the median and interquartile range (25%, 75% percentiles) concentration of growth factors (pg/mL) in the BAL supernatant from healthy controls (n=7), IPF (n=9), UCTD (n=6) and cHP patients (n=6). GM-CSF, Angiopoietin-2, hepatocyte growth factor (HGF), basic fibroblast growth factor (FGFb), PDGF-AA, were below levels of detection for most samples. PDGF-BB, G-CSF, VEGF, Erythropoietin (EPO), stem cell factor (SCF) and Epidermal growth factor (EGF) levels were low and similar in all groups, TGFα concentration was higher in healthy compared to ILD groups but this was not significant. TGFβ1 and GM-CSF were measured in BAL and were not detectable (data not shown). M-CSF was detectable and showed significantly higher levels in the BAL of IPF and UCTD compared to healthy (**Figure 3.18**), this suggests M-CSF may be involved in macrophage maturation in the IPF lung with limited GM-CSF involvement.

Growth factor	Healthy (n=7)	IPF (n=9)	UCTD (n=6)	cHP (n=6)
G-CSF	0 (0, 19.57)	12.07 (0, 23.3)	0 (0, 14)	33.05 (8.25, 55.5)
GM-CSF	0 (0, 15.51)	0 (0, 3.17)	2.435 (0, 6)	0 (0, 0)
Angio-2	0 (0, 0)	0 (0, 0)	4 (0, 10.98)	0 (0,0)
HGF	0 (0, 185.6)	0 (0, 58.02)	0 (0, 80.58)	0 (0, 79.11)
SCF	4.46 (0, 8.64)	3.84 (0, 8.73)	0 (0, 7.6)	3.19 (0, 8.06)
FGF basic	0 (0, 0)	0 (0, 0)	0 (0, 14.19)	0 (0, 3.63)
PDGF-AA	0 (0, 0)	0 (0, 0)	0 (0, 0)	0 (0, 0)
PDGF-BB	17.1 (0, 18.75)	24.33 (0, 28.39)	0 (0, 3.45)	22.7 (0, 28.14)
EPO	10.99 (0, 15.19)	0 (0, 12.37)	12.88 (12.22, 15.83)	5.57 (0, 12.22)
EGF	1.31 (0.81, 2.96)	1.45 (1.15, 1.77)	0.89 (0.65, 1.64)	1.3 (0.99, 1.60)
TGFα	55.62 (0, 85.56)	11.54 (0, 50.4)	26.7 (12.56, 33.18)	7.965 (0, 22.23)
VEGF	23.92 (0, 49.02)	24.43 (16.41, 41.39)	29.83 (0, 51.22)	29.61 (13.67, 35.38)

Table 3.4: Growth factors in BAL.

Multiplex analysis was used to quantify the amount of growth factors present in the BAL. The table summarises the findings showing pg per mL BAL median value (25%, 75% percentiles) for healthy and ILD. Definition of abbreviations; Idiopathic pulmonary fibrosis (IPF), undifferentiated connective tissue disease (UCTD), chronic hypersensitivity pneumonitis (cHP), granulocyte-colony stimulating factor (G-CSF), granulocyte macrophage-colony stimulating factor (GM-CSF), Angiopoietin-2 (Angio-2), hepatocyte growth factor (HGF), stem cell factor (SCF), fibroblast growth factor (FGF), platelet derived growth factor (PDGF), erythropoietin (EPO), epidermal growth factor (EGF), transforming growth factor (TGF), vascular endothelial growth factor (VEGF).

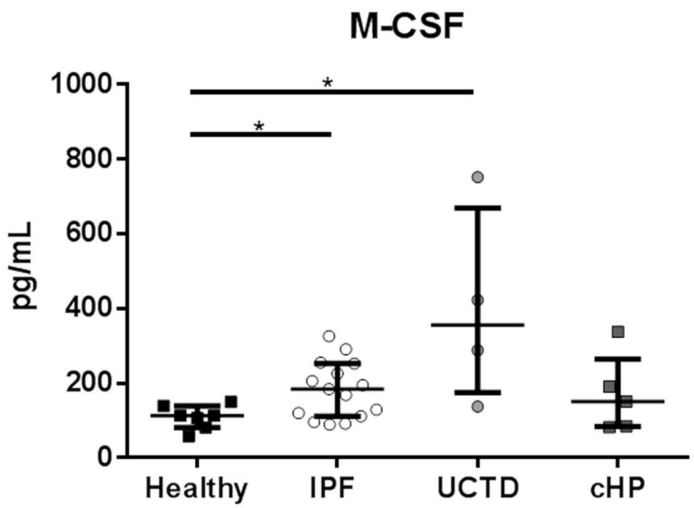


Figure 3.18: M-CSF levels in the BAL supernatant.
M-CSF was quantified using ELISA in the BAL supernatant of healthy controls (n=7), and idiopathic pulmonary fibrosis, IPF (n=15), undifferentiated connective tissue disease, UCTD (n=4) and chronic hypersensitivity pneumonitis, cHP (n=5) patients. Median and interquartile range is shown. Significant differences were calculated using Mann-Whitney U analysis comparing each ILD to healthy controls analysis *$p<0.05$.

3.4.5. Increases in myeloid cells and associated mediators correlate inversely with predicted FVC

Examination of the aforementioned BAL cellular and mediator content in the context of clinical parameters provides a valuable insight into which specific cells or mediators may contribute to the underlying pathology. Examination of both monocyte and macrophage cell number per mL of BAL, reveal an inverse correlation when compared to predicted % FVC (**Figure 3.19A** and **B** respectively). Similarly, an associated increase in both the monocyte chemoattractant CCL2 and growth factor M-CSF correlate with a decline in the predicted FVC % (**Figure 3.19C** and **D** respectively). These key findings suggest that macrophages and mediators related to monocyte recruitment and macrophage survival and differentiation are potentially playing a role in disease pathogenesis.

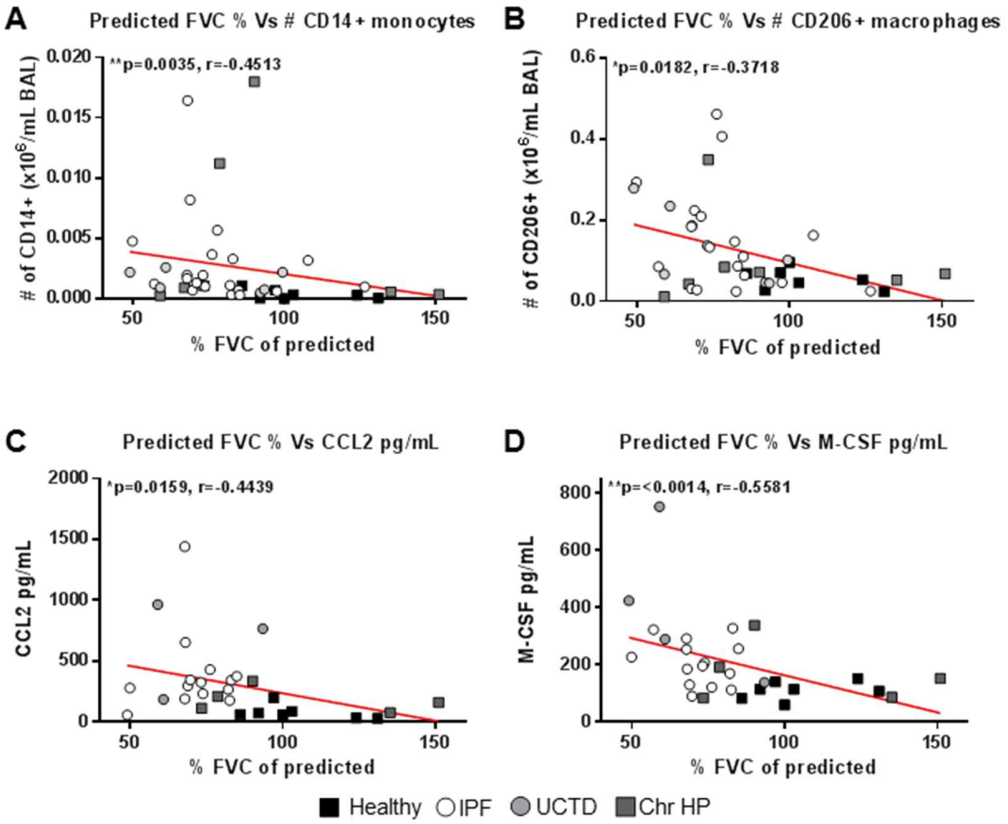


Figure 3.19: Inverse correlations examining cells and mediators with % predicted FVC.
Monocyte and macrophage number (x10^6/mL BAL) in the BAL of healthy controls, and idiopathic pulmonary fibrosis (IPF), undifferentiated connective tissue disease (UCTD) and chronic hypersensitivity pneumonitis (cHP) patients inversely correlated with percentage predicted FVC (A and B respectively). CCL2 and M-CSF (pg/mL BAL supernatant) inversely correlated with percentage predicted FVC. Correlations were carried out using Spearman's rank correlation with r values and p values written on the top left of graphs. Linear regression is highlighted in red.

3.5. Discussion

Cellular differentials have been used to aid the diagnosis of specific ILDs for over 30 years, however, the information it provides is very limited and does not clearly distinguish distinct ILD phenotypes. Multi-parameter flow cytometry was used in order to distinguish multiple cell populations and phenotypes, in combination with multiplex analysis of mediators in the BAL, to gain a comprehensive profile of distinct BAL signatures in ILD. Here the data clearly demonstrates differences in cellular composition of healthy control BAL to that from IPF, UCTD and cHP patients. This work has highlighted for the first time, using flow cytometry, a significant increase in monocytes in IPF airways. This increase in monocytes correlated with the enhanced CCL2 levels indicating CCL2 may be attracting monocytes into IPF airways. Furthermore, the research has highlighted an increase in monocytes, macrophages, CCL2, and the macrophage growth factor M-CSF, correlate with decreased percentage predicted FVC, suggesting these cells are indicative of poor lung function. Comparing ILDs, there are increased numbers of myeloid derived cells in IPF and UCTD with limited change in lymphoid numbers. Contrary to this the lymphoid cell numbers were increased in cHP as expected [306]. Similar patterns of leukocytes are observed in UCTD and IPF. UCTD is diagnosed when auto-immune antibodies are present in patient serum, and believed to result from an underlying autoimmune disease. Unlike UCTD, cHP is thought to arise from the repeat exposure to an environmental irritant, progressing from inflammatory HP to fibrotic cHP. The similar profile of UCTD to IPF suggests the underlying pathological disease mechanisms involved in the progression of fibrosis may be more similar in these ILDs, with less involvement of lymphocytes.

Although the overall cellular changes appear to involve an increase predominantly in myeloid cells in IPF it is interesting that there is a significant increase in the number of NK cells in the BAL of patients with IPF. This may point to a possible viral infection of IPF patients, which could contribute to the damage observed in IPF epithelial cells. Previous work has linked viral infection with the pathogenesis in the bleomycin animal model, demonstrating murine gamma herpes virus infections activate lung epithelial cells leading to epithelial cell production of profibrotic factors [255, 256]. Data from the murine model of IPF compliments reports of the presence of herpes viral infection in IPF patients, suggesting a possible similar role for viral infection in the initiation or progression of fibrosis [333]. To better understand the increase in NK cells, examination of the presence of virus in the whole BAL from these samples may provide a link between NK cell increases and the presence of a viral infection. It would also be interesting to tie these observations with reported exacerbations in patients.

Contrasting the cellular differential data, flow cytometric analysis revealed no significant increases in CD177+ neutrophils in the airways of patients with IPF and cHP compared to healthy. Examination of neutrophil populations using flow cytometry compared to differential counts in paired BAL samples revealed no differences comparing the methods using Bland-Altman analysis (Appendix 8.1; **Figure 8.1.1**). However, the differential analysis examining neutrophil cell numbers per mL of BAL in healthy controls show minimal presence of neutrophils in all samples, contrary to these findings two healthy samples in flow cytometry show increased numbers of neutrophils in BAL. This highlights that the use of flow cytometry may provide a more accurate measure of cell counts, particularly in rarer cell populations. The number of cells analysed per sample is greatly increased in flow cytometry providing greater confidence in population analysis.

Increased patient numbers and repetition of data across multiple sites provides greater confidence for data analysis interpretation when examining cellular populations and would be required to verify these findings. The neutrophil differential analysis is supported by previous research showing increases in neutrophils in IPF [151, 334], which may be exerting pathological effects by the production of mediators known to influence fibrosis [152].

Analysis of other cells types, such as eosinophils, using both cellular differential analysis and FACs staining, revealed an increase in eosinophils in IPF compared to healthy controls. Eosinophils, and mediators, including IL-5 and GM-CSF, involved in the stimulation and activation of eosinophils, have been reported as increased in the BAL of IPF patients [154, 237]. Increased numbers of eosinophils in the IPF BAL was shown to correlate with a decline in functional clinical parameters [155]. Eosinophils are associated with type 2 mediated inflammation, being able to respond to and produce IL-13. Evidence has shown T helper type 2 (Th2) cytokines, such as IL-13, are increased in IPF [335] with inhibition of IL-13 ameliorating fibrosis induced in severe combined immunodeficiency (SCID) murine model using engraftment of IPF fibroblasts to induce fibrosis [335, 336]. However, anti-IL-13, Tralokinumab did not met efficacy end points in recent Phase II clinical trials [138], suggesting Th2 cytokines, such as IL-13, in IPF may not play a pivotal role in driving disease progression. Other mechanisms by which eosinophils potentiate fibrosis include a profibrotic role mediated through direct cellular interactions with fibroblasts. Eosinophils isolated from the bleomycin model of fibrosis have been shown to increase collagen and aSMA expression on fibroblasts when co-cultured *in vitro* with fibroblasts [337]. It is possible the eosinophils, shown increased here in IPF, may be acting in the IPF lung in a similar manner. Isolation and co-culture of eosinophils from human IPF BAL with human fibroblasts may help to

elucidate whether this reported observation in mouse translates to man, highlighting a role for human eosinophils in the progression of IPF. Further work would be required to understand the mechanisms involved in these cellular interactions.

The isolation and analysis of morphology of the FcεR1+ cells did not show a pure mast cell or basophil population on the cytospin. Previous reports have shown an increase in the number of mast cells in the lung tissue of patients with IPF [149]. Mast cells are known to be able to release TGFβ [149], a key pro-fibrotic mediator, and interact with fibroblasts [150]. It is possible that an increase in FcεR1+ cells may represent, at least in part, an increase in mast cells entering the airways in patients with IPF. FcεR1 expressing cells are increased in all ILDs, and an increase in FcεR1+ cells inversely correlated with predicted % FVC (Appendix 8.1, **Figure 8.1.2**). This suggests they may contribute to fibrotic pathology or represent a biomarker of pathology regardless of ILD. Further phenotypic analysis may help to better characterise these cells and elucidate the role they may play in pathology.

Analysis of recruited myeloid cells such as monocytes show a significant increase in IPF compared to healthy controls. Monocytes share a similar morphology to activated lymphocytes and other cell types in the BAL. It is therefore unsurprising this phenotype is not counted when carrying out differential analysis and highlights the need to improve quantification of this cell type. Previous reports examining BAL cells using IHC have identified an increase in a monocyte-like-cell in IPF supporting these observations [145, 147]. Furthermore the data demonstrates an increase in CCL2 levels in IPF BAL, which has been reported increased previously [195, 200, 338], correlating with disease progression [195, 228, 338, 339]. An elevation in the levels of the chemokine CCL2

correlates with an increase in monocytes and macrophages, suggesting CCL2 is acting to recruit monocytes via the CCR2 receptor expressed on monocytes [339]. An increase in monocyte number and the chemokine CCL2 correlate inversely with clinical parameter predicted % FVC, which may indicate a role for these cells in the progression of the pathology in patients, or increased monocytes may represent a marker of poor patient prognosis. Monocytes and CCL2 are known to play a critical role in the progression of the bleomycin model of IPF as blockade of CCL2 signalling ameliorates disease [208-212]. It is possible that monocytes are maturing into macrophages in the airways resulting in the observed significant increase in macrophage number. Although the origins of the airway macrophages in normal homeostatic conditions is reported to be embryonically derived in mice [156, 157] recent studies have shown bone marrow derived monocytes are able to differentiate into airway macrophages [158]. Furthermore, increased macrophage number and increased M-CSF concentration correlated significantly with a decline in predicted % FVC. This highlights a potential role for macrophages in the pathology, with M-CSF, in combination with specific IL-4, IL-10 or TGF-β1, reported to mature monocytes into macrophages and altering their phenotype to a pro-fibrotic 'M2' macrophage [340]. Taken together macrophages and monocytes have been reported to play critical roles in driving the pathology of both the bleomycin model [341] and IPF, producing pro-fibrotic mediators such as TGFβ [193]. Dissecting the cause of cell number increases and examining the phenotype of these cells, identifying specific markers and/or pro-fibrotic mediators produced may provide an important insight into developing future therapeutics targeting these specific cells/mediators.

Unfortunately, multiplex analysis of BAL lavage revealed multiple cytokines and growth factors were below the limit of detection. The collection of BAL fluid involves the administration of, and

aspiration of, large volumes of pre-warmed saline, which is likely to result in a very dilute sample, leading to many mediators being below the limit of detection. This could be overcome using alternative methods including bronchosorption, whereby a synthetic absorptive matrix is placed on top of bronchial mucosa during bronchoscopy [342]. However, this technique collects samples from a specific area, excluding the lower airways, such as the alveoli. Alternatively using more sensitive techniques, such as mass spectrometry, to analyse multiple proteins in the BAL could provide a more comprehensive measure of environmental proteins which may play a role in disease pathology.

In conclusion these data highlight key BAL signatures in different ILDs. Collectively this data helps provide a framework to build upon to better understand the pathology of ILD. As the data is predominantly correlative future work investigating the pathological role of specifically increased cell types and mediators is critical in order to understand their potential pathological role human disease. As monocytes and macrophages were shown to be significantly increased, and that their increase correlated with decreased predicted FVC, further analysis of the macrophage, its phenotype and function will be examined and discussed in the next results chapter. A summary of findings is highlighted in **Figure 3.20**.

3.5.1. Summary of cells and mediators in healthy and IPF airways

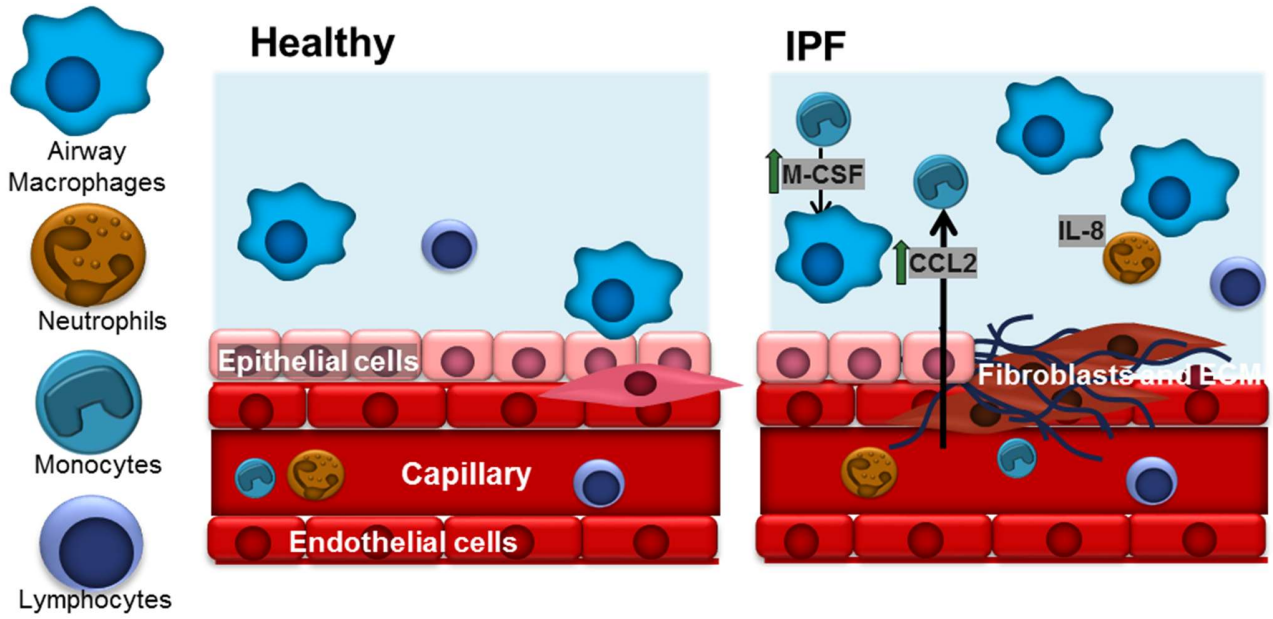


Figure 3.20: Illustration of cells and mediators in healthy and IPF airways.
IPF airways show increased numbers of monocytes and macrophages. Increased M-CSF in IPF suggests differentiation of monocytes into M2 like macrophages, increased CCL2 may attract monocytes into the airways.

4. Examination of Airway Macrophages in ILD.

4.1. Introduction

Airway Macrophages (AMs) play fundamental roles in the maintenance of normal homeostasis of the airway. They are essential in host defence, aid the repair of damaged tissue, maintain normal protein and surfactant levels and are thought to influence other leukocytes through the production of pro- or anti-inflammatory mediators [343]. Results from the previous chapter indicate an increase in both monocytes and macrophages in IPF. Therefore, further study of this cell type is essential in order to understand the direct or indirect affects these cells may have on disease pathogenesis. The role of the macrophage in health, fibrosis and host defence have been discussed in the introduction. Macrophage phenotypes in ILDs and IPF models will be discussed here in more detail.

4.1.1. Macrophage phenotypes in ILD

Macrophages are thought to play a critical role in tissue remodelling both in lung development [344] and in pathology [181]. Specifically, alternatively activated TGFβ1 producing M2 macrophages are reported to be increased in the murine bleomycin model of IPF, driving the pathology of this model [345-347], however, there is limited evidence of an M2 phenotype in man. Specific markers are associated with M1 and M2 phenotypes including M1 markers such as HLA-DR, an MHC-class II receptor and CD86, a T cell co-stimulator [177], and M2 markers CD163, a haemoglobin scavenger receptor [348] and mannose receptor CD206 [161, 178]. Studies examining the expression of M1 marker CD40 and M2 marker CD163 using immunohistochemistry on BAL samples revealed an increase in the M1 marker in sarcoidosis

compared to other ILDs including HP, non-specific interstitial pneumonia (NSIP) and IPF [349]. However, this study grouped together fibrotic ILDs, and no healthy controls were examined [349]. IPF macrophages have been shown to express significantly increased levels of M2 marker CD204 compared to healthy controls [48], and production of M2 cytokines in the supernatant of cells from whole BAL in stable IPF and IPF with acute exacerbation (AE) revealed an increase in M2 markers in patients with AE [57]. Further to these studies, examination of scavenger receptor CD163, as a marker of M2 macrophages, and the production of reportedly M2 mediators, CCL2 and IL1Rα, were shown to be increased in progressive IPF patients compared to controls [350]. Airway macrophages in the BAL can be isolated for further analysis by flow cytometry as cells positive for pan leukocyte marker CD45 with high expression of CD11c. Expression of the integrin CD11c has been reported increased on airway macrophages in mouse [351-353] and man [148, 354-356] and is not associated with either an 'M1' or 'M2' phenotype. As the macrophage classification of phenotypes is changing other studies have focused on examining activation status of airway macrophages. Taylor *et al* showed an upregulation of adhesion, signal transduction and inflammation markers on IPF macrophages compared to healthy controls, with 4 IPF patient BAL samples [357]. An examination of myeloid cells in the blood, lung tissue and BAL of patients with ILD and healthy controls revealed some differences in macrophage population marker expression in the lung and blood of IPF patients, however, there was no IPF BAL group [148].

If IPF AM show an increased M2 pro-fibrotic anti-inflammatory cell phenotype, it is possible the reduced M1 inflammatory phenotype may result in an impaired ability of IPF AM to carry out roles in host defence, which in turn may lead to the increased bacterial burden observed in IPF

[2]. It is therefore critical to explore IPF AM phenotype and function in fibrosis and host defence further.

4.1. Hypothesis

Airway macrophages isolated from IPF patients will exhibit a distinct anti-inflammatory, pro-fibrotic M2-like phenotype resulting in an impaired inflammatory host defence response to bacterial stimulus compared to healthy airway macrophages. Furthermore IPF airway macrophages will directly or indirectly drive the progression of fibrosis increasing ECM deposition by stromal cells by juxtracrine or paracrine signalling compared to healthy airway macrophages.

4.2. Aims

- Characterise the M1/M2 airway macrophage phenotype in IPF, other ILDs and healthy controls examining the presence of M1 or M2 related markers by FACs.
- Examine airway macrophage function in host defence assessing phagocytosis and production of pro-inflammatory mediators by IPF airway macrophages compared to other ILD and healthy controls.
- Investigate whether airway macrophages isolated from IPF patients demonstrate a fibrotic phenotype, examining expression of genes and proteins known to drive fibrosis, and evaluate whether isolated IPF airway macrophages are able to induce the production of extracellular matrix by stromal cells.

4.3. Materials and Methods

4.3.1. Analysis of mediators in BAL supernatant

4.3.1.1. Transferrin

Transferrin was measured following manufacturers guidelines (Abcam, ab187391). Briefly, 50 µL of 1:500 diluted (diluted in PBS) BAL supernatant or serially diluted standard was added to the pre-coated microplate wells. To this 50 µL of the Antibody Cocktail was added to each well, sealed and incubated for 1 hour at room temperature on a plate shaker (400 rpm). Wells were then aspirated and washed with 350 µL of 1 x wash buffer three times. After the last wash the plate was inverted and blotted on clean paper towels to remove excess liquid. TMB Substrate (100 µL) was added to each well, sealed and covered with aluminium foil. The plate was then incubated for 15 minutes in the dark on a plate shaker (400 rpm). Finally 100 µL of stop solution was added to each well and the plate was tapped until thoroughly mixed. The optical density (OD) was read at 450 nm using Sunrise remote Tecan reader (F039300) analysis on Magellan V5.0 software. Data interpolation was carried out using a four parameter algorithm curve analysis and data interpolated from the standard curve on GraphPad Prism V6. Sample values were multiplied by the dilution factor.

4.3.1.2. Ferritin

Ferritin was measured following manufacturers guidelines (Abcam, ab108837). Briefly, 50 µL of ferritin standard or 1:50 diluted (in PBS) BAL supernatant was added to each well, samples were sealed and incubated at room temperature for 2 hours. Wells were then aspirated and washed five times with 200 µL of 1X Wash Buffer. After the last wash the plate was inverted and blotted

on clean paper towels to remove excess liquid. Fifty microlitres of 1X Biotinylated Ferritin antibody was added to each well and incubated at room temperature for one hour. The plate was washed as previously described and 50 µL of 1X SP Conjugate was added to each well and incubated for 30 minutes. The plate was washed as previously described and 50 µL of chromogen substrate was added to each well and incubated for approximately 15 minutes. Stop solution (50 µL) was then added to each well and plate was tapped until thoroughly mixed. The OD was read at 450 nm, subtracting 570 nm, using Sunrise remote Tecan reader (F039300) analysis on Magellan V5.0 software. Data interpolation was carried out using four-parameter logistic curve-fit and data interpolated from the standard curve on GraphPad Prism V6. Sample values were multiplied by the dilution factor.

4.3.1.3. Iron

Iron in the BAL supernatant was measured following manufacturers guidleines (Abcam, ab83366). Briefly, 100 µL of standard or undiluted BAL supernatant were added to each well and 5 µL iron reducer was added to all wells to measure total iron. Samples were mixed on a plate shaker (400 rpm) at room temperature for 30 minutes. After 30 minutes 100 µL of Iron Probe was added to each well. Samples were mixed on a plate shaker (400 rpm) at room temperature for 60 minutes protected from light. The OD was read at 593 nm, using Sunrise remote Tecan reader (F039300) analysis on Magellan V5.0 software. Data interpolation was carried out using a linear standard curve and data interpolated from the standard curve on GraphPad Prism V6.

4.4. Results

4.4.1. Patient demographics

Patient demographics for FACs staining are outlined in **Table 4.1**. The average age of healthy controls was lower than IPF, HP and cHP patients and Forced vital capacity (FVC) percentage of predicted was significantly higher in the healthy controls compare to all ILDs ($p<0.05$, Mann-Whitney U T –test).

	Healthy	IPF	UCTD	HP	cHP	Sarcoid
Number	7	96	20	9	20	6
Age (mean) years (min, max)	45 (22, 65)	71 (45, 84)	63 (42, 80)	64 (35, 82)	66 (52, 85)	54 (43, 71)
Gender (M, F)	6, 1	63, 33	9, 11	7, 2	11, 9	5, 1
Smoking status (Current, ex, non, unknown)	0, 0, 7, 0	3, 45, 24, 24	1, 9, 7, 3	0, 3, 5, 1	1, 3, 10, 6	0, 0, 3, 3
Steriods (yes, no, unknown)	0, 7, 0,	19, 48, 29	4, 12, 4	3, 5, 1	5, 10, 5	3, 1, 2
FVC % (min, max)	104.7 (86, 131)	77.5 (49.9, 126.6)	77.8 (33, 102.8)	80.9 (62.1, 120.1)	91.2 (50.1, 151)	83.0 (77.9, 95.6)
TLCO % (min, max)	ND	45.7 (24, 75.5)	47.8 (24.8, 84)	43.2 (27.7, 64)	48.3 (29.8, 78.6)	52.8 (28.9, 87.5)
Culture (unknown, negative, positive)	7, 0, 0	23, 70, 3	4, 15, 1	1, 7, 1	6, 13, 1	1, 5, 0

Table 4.1: Patient demographics for flow cytometry staining of airway macrophage populations.
Definition of Abbreviations; Idiopathic Pulmonary Fibrosis (IPF), Undifferentiated connective tissue disease (UCTD), hypersensitivity pneumonitis (HP), chronic hypersensitivity pneumonitis (cHP), sarcoidosis (sarcoid), male (M), female (F), minimum (min), maximum (max), ex-smoker (ex), no data (ND), forced vital capacity (FVC) % of predicted function, carbon monoxide transfer factor (TLCO) % of predicted function, standard deviation (Std dev).

4.4.2. No clear M1/M2 phenotype observed in IPF or other ILDs

Firstly, purity of AMs was determined by separating and staining CD11c+ cells from whole BAL to examine morphology. This revealed a pure AM population, with no neutrophils, eosinophils or lymphocytes present (illustrated in **Figure 4.3A**). Macrophage markers, which have been reported as increased on specific phenotypes of macrophages, were examined on CD11c+ cells to examine M1/M2 phenotypes. **Figure 4.1** shows the proportion of macrophages expressing M1 markers HLA-DR (**Figure 4.1A**) and CD86 (**Figure 4.1B**) and M2 markers CD206 (**Figure 4.1C**) and CD163 (**Figure 4.1D**). No significant differences were observed comparing ILD to healthy controls suggesting no clear M2 phenotype in ILD.

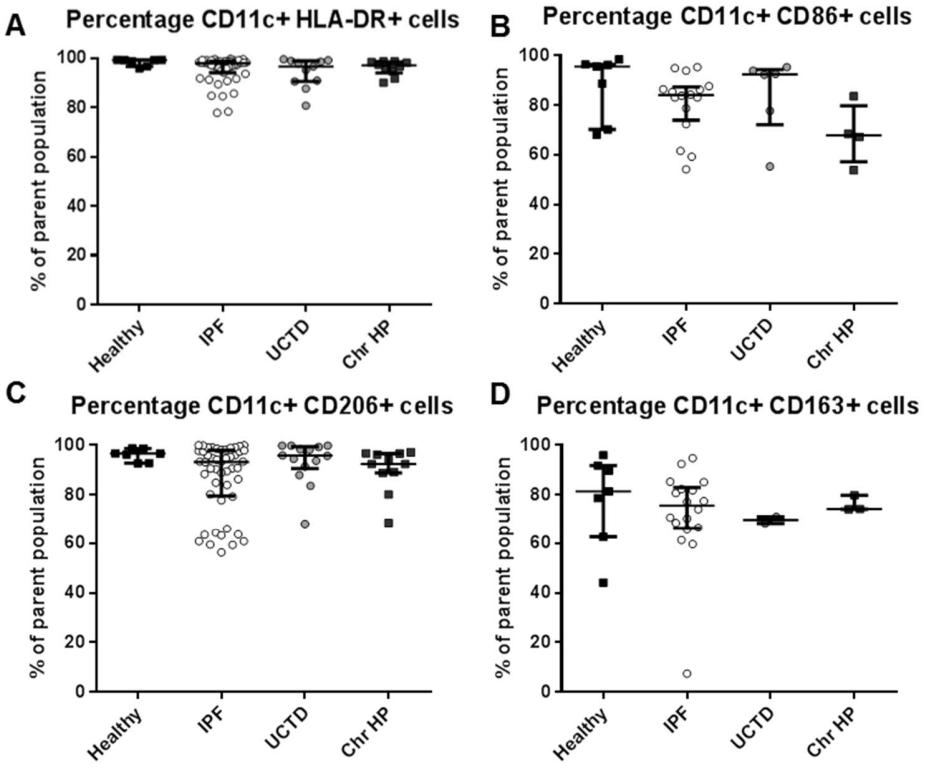


Figure 4.1: Examination of M1 and M2 markers reveal no clear M1/M2 phenotype in airway macrophages from patients with ILD.

The percentage of CD11c+ macrophages expressing M1 markers HLA-DR and CD86 (A and B respectively) and M2 markers CD206 and CD163 (C and D respectively) are shown. Median value with interquartile range is illustrated for healthy controls, and idiopathic pulmonary fibrosis (IPF), undifferentiated connective tissue disease (UCTD), chronic hypersensitivity pneumonitis (cHP) patients. No significant differences were found comparing healthy to patients with different ILD. Statistical analysis using Mann-Whitney U comparing each ILD to healthy control *$p<0.05$.

4.4.3. CD71- macrophage numbers are significantly increased and correlate with clinical progression in ILD patients

Macrophages were examined for other markers alongside M1/M2 markers, such as CD71, a transferrin receptor, as a marker of mature macrophages [358, 359], which has previously been described increased in ILD [357] and in the bleomycin mouse model of IPF [360]. Airway macrophage number per mL of BAL, based on CD11c expression, is significantly increased in IPF patients (**Figure 4.2A**) which corroborates findings reported in the previous chapter looking at CD206+ cells. The majority of CD11c+ macrophages (>70%) express CD71 (**Figure 4.2B**), however, the proportions of CD11c+ CD71+ cells are significantly decreased in IPF, UCTD and cHP compared to healthy controls, therefore the proportion of CD11c+CD71- is significantly increased in IPF, UCTD and cHP. The number of CD11c+CD71+ cells are significantly increased in IPF and UCTD compared to healthy controls (**Figure 4.2C**) and the number of CD11c+ CD71- cells are significantly increased in IPF and HP BAL compared to healthy controls. Interestingly the number of CD11c+CD71- cells per mL of BAL correlates with the FVC decline as determined by absolute and relative differences examining FVC data from all ILDs (**Figure 4.2E** and **F** respectively).

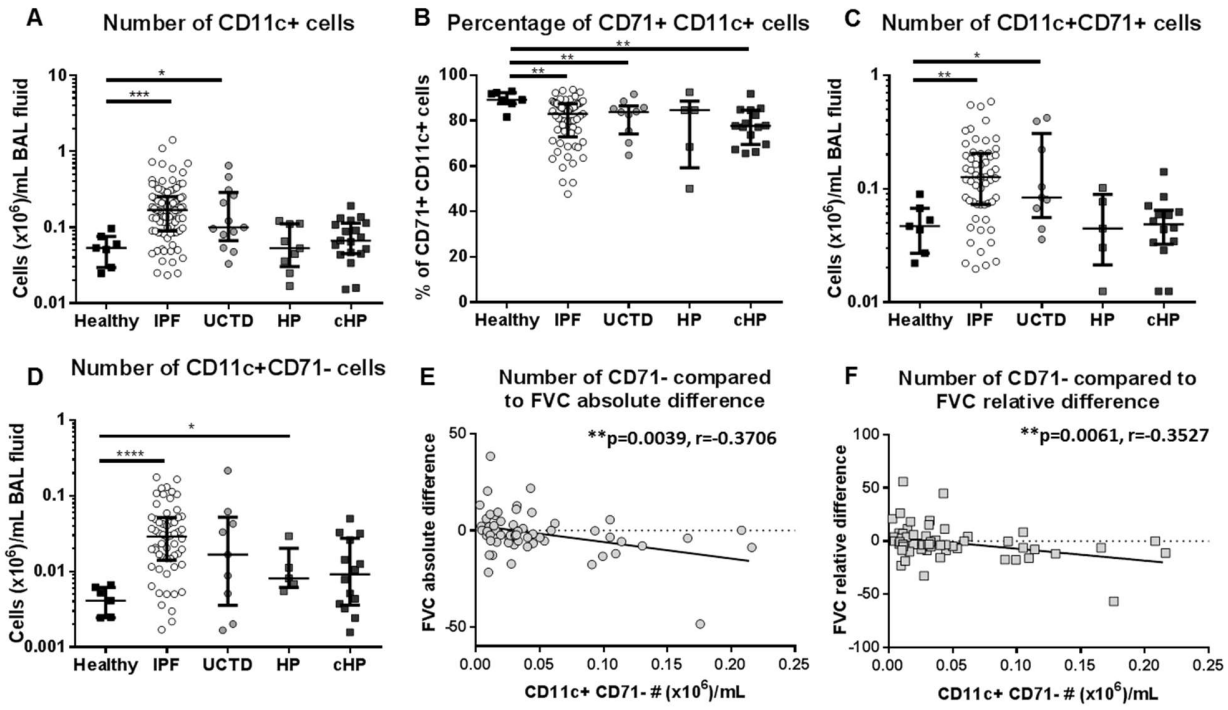


Figure 4.2: The proportion and number of CD71- cells are increased in IPF patients compared to healthy controls.

Increases in CD71- cell number correlate significantly with FVC decline. CD11c+ macrophage numbers are significantly increased in IPF and UCTD compared to healthy (A). The percentage of CD11c+ cells expressing CD71 is significantly higher in healthy compared to IPF, UCTD and cHP (B). The number of CD71+ and CD71- cells are significantly increased in IPF (C and D respectively) and the increased number of CD71- cells correlates with a decline in absolute and relative FVC difference (G and H). Median with interquartile range shown for healthy controls, and idiopathic pulmonary fibrosis (IPF), undifferentiated connective tissue disease (UCTD), hypersensitivity pneumonitis (HP) and chronic hypersensitivity pneumonitis (cHP) patients. Statistical analysis using Mann-Whitney U comparing each ILD to healthy control *p<0.05, **p<0.01, ***p<0.001, ****p<0.0001. Correlation analysis using Pearson correlation.

4.4.4. CD71- and CD71+ cells exhibit similar macrophage morphology but marker expression significantly differs

As CD71 has been shown to be marker of mature macrophages [358, 359], with the expression of CD71 reported as increased in the bleomycin model of fibrosis [360], next the (CD11c+) CD71- and CD71+ cells were isolated to verify if they represented distinct populations, which may play divergent roles in fibrosis. CD71- and CD71+ cells were separated by FACS sorting. Patient demographics from separated CD71-/+ samples are outlined in **Table 4.2**. **Figure 4.3** shows Wright-Giemsa stained magnetic-activated cellular sorting (MACS) separated CD11c+ cells (**Figure 4.3A**), and FACS separated CD71- cells (**Figure 4.3B**) and CD71+ cells (**Figure 4.3C**). CD11c expression purifies AM from the BAL (**Figure 4.3A**), and CD71- and CD71+ cells exhibit macrophage morphology (**Figure 4.3B** and **C** respectively). **Figure 4.3D-F** show immunostaining of CD71 on the separated populations. Isotype control antibody was examined on CD71+ cells and shows limited staining (**Figure 4.3D**). Staining was less visible or absent on the CD71- population (**Figure 4.3E**) compared to the CD71+ population where staining (in red) was visible (**Figure 4.3F**) as expected.

The previously described M1 and M2 markers and a monocyte/macrophage marker CD14, which is a co-receptor for several Toll-like Receptors (TLRs) [361] were examined revealing significantly increased expression of HLA-DR (**Figure 4.4A**), CD86 (**Figure 4.4B**), CD163 (**Figure 4.4C**) and CD206 (**Figure 4.4D**) on CD71+ cells compared to CD71-. Conversely the monocyte marker CD14, which is reported by some on macrophages, but previously shown to isolate monocytes in the BAL in the absence of CD206 expression in **Figure 3.3**, is significantly increased on CD71- cells (**Figure 4.4E**).

Sample	Diagnosis	Sample use	Fibrotic	Age (years)	Gender	Smoker (Ex, Current, Never)	Steroids at time of Bronchoscopy	TLCO (up to 6 mths pre bronch) %	TLCO (9-18 mths post bronch) %	FVC (up to 6 mths pre bronch) %	FVC (9-18 mths post bronch) %
1	IPF	GE	Y	73	F	Never	Non	ND	ND	ND	ND
2	IPF	GE	Y	72	F	ND	Non	56.3	ND	108.9	ND
3	UCTD	S	Y	73	M	Ex	Non	38.2	ND	82.3	ND
4	IPF	S	Y	79	M	Never	Non	27.6	ND	67	ND
5	IPF	S	Y	74	F	Ex	Non	36.1	ND	92.1	ND
6	IPF	GE, S	Y	58	M	Current	Non	40.9	40.6	59.8	56.7
7	UCTD	GE	Y	76	M	Ex	Non	59.8	ND	66.3	ND
8	UCTD	GE, S	Y	49	M	Never	Non	46.1	ND	77.1	ND
9	HP	GE	N	49	F	Never	Non	46.8	51	79.9	83.1
10	IPF	GE, GA	Y	55	M	Current	Non	62.9	ND	76.2	ND
11	PPFE	GE	Y	56	F	ND	ND	ND	ND	ND	ND
12	IPF	GE, GA	Y	67	M	Ex	Non	51.1	ND	77.9	ND
13	IPF	GE, GA	Y	61	M	ND	ND	43.9	ND	68.9	ND
14	IPF	CC	Y	76	M	Current	Non	ND	ND	ND	ND
15	IPF	GE, CC,S	Y	80	M	Never	Non	57.9	ND	79.1	ND
16	IPF	GE, CC,S	Y	63	M	Ex	Non	53	ND	58	ND
17	IPF	GE, CC	Y	64	M	ND	Non	ND	ND	ND	ND
18	IPF	GE, CC	Y	55	M	Ex	Non	ND	ND	ND	ND
19	IPF	GE, S	Y	76	M	Ex	Non	ND	ND	ND	ND
20	IPF	GE, S	Y	72	F	Never	Non	ND	ND	ND	ND

Table 4.2: Patient demographics with clinical parameters for all samples that were separated for CD71- and CD71+ cell analysis.

Table illustrates sample ID, diagnosis, sample use, presence of fibrosis in lung (Fibrotic); yes (Y), no (N), age, gender; male (M), female (F), smoking status, steroid use, carbon monoxide transfer factor (TLCO) percentage of predicted up to 6 months prior to bronchoscopy and 9-18 month post bronchoscopy (bronch), Forced vital capacity (FVC) percentage of predicted up to 6 months prior to bronchoscopy and 9-18 month post bronchoscopy. Definition of all other abbreviations: Idiopathic pulmonary Fibrosis (IPF), undifferentiated connective tissue disease (UCTD), hypersensitivity pneumonitis (HP), Pleuroparenchymal Fibroelastosis (PPFE), gene expression (GE) analysis, stimulation (S), gene array (GA), co-culture (CC) with bronchial epithelial cells, no data (ND).

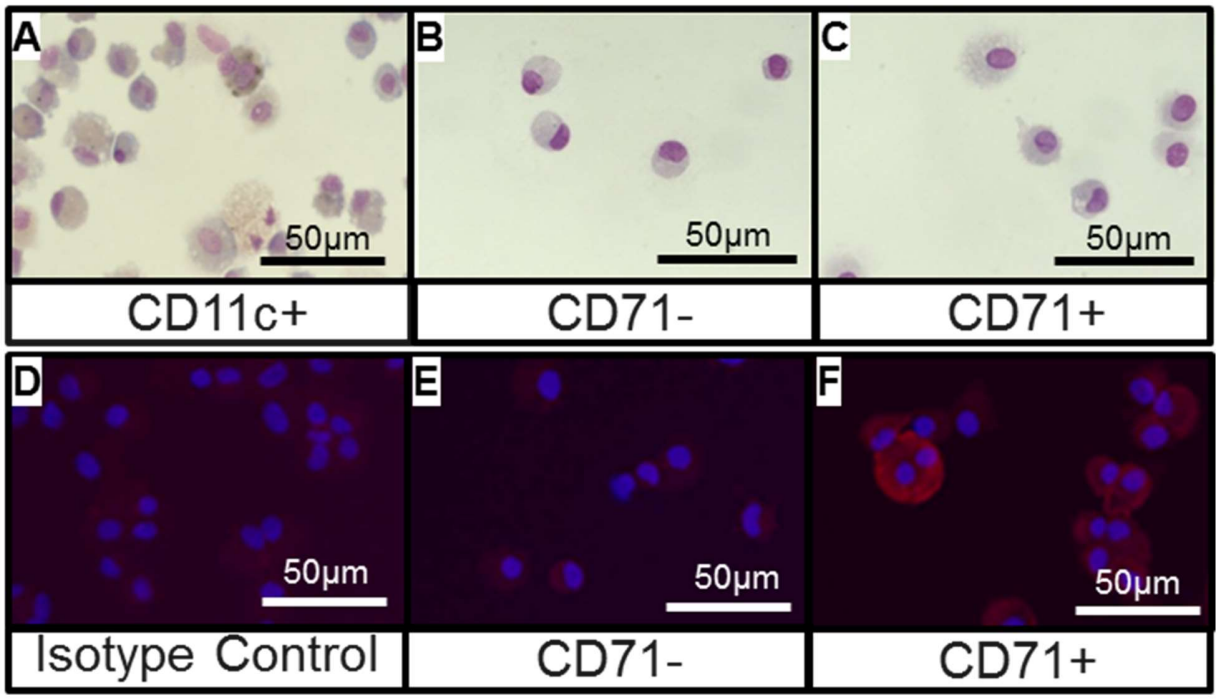


Figure 4.3: Imaging of separated CD11c+, CD11c+CD71- and CD11c+CD71+ cells.
MACS separated CD11c+ cells and FACS separated CD71- and CD71+ that have been cytospun and Wright-Giemsa stained with representative image shown in A-C respectively. FACS separated CD71+ cells, used for isotype control for CD71 immunostaining (D), and CD71 immunostaining of CD71- (E) and CD71+ cells (F). CD71 immunostaining in red with DAPI nuclear stain in blue.

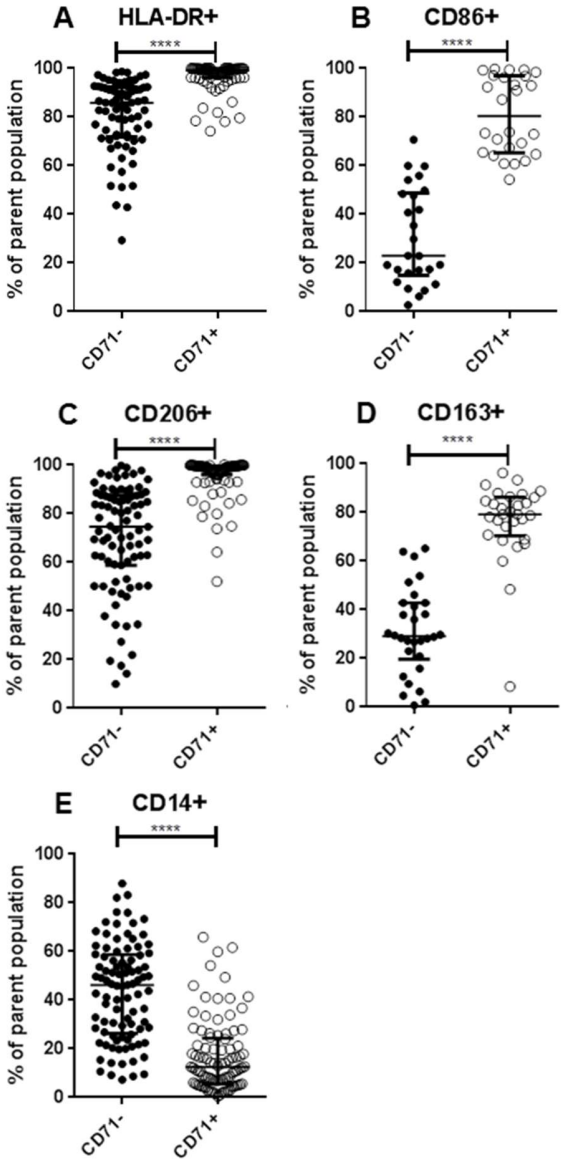


Figure 4.4: Examination of the expression of surface markers reveals distinct phenotypes in CD71- compared to CD71+ cells.

Percentage of parent populations ((CD11c+) CD71- or (CD11c+) CD71+) expressing M1 markers HLA-DR, CD86, (A and B respectively) and M2 markers CD206 and CD163 (C and D respectively) are significantly increased on CD71+ macrophages compared to CD71-. Conversely monocyte marker CD14 is significantly increased on CD71- macrophages compared to CD71+ (E). Median and interquartile range is shown. Statistical analysis using Mann-Whitney U T test, ****$p<0.0001$.

4.4.5. CD71- and CD71+ cells exhibit significantly different expression levels of genes involved in iron homeostasis

As CD71 is a transferrin receptor the expression of genes involved in iron homeostasis were next examined (**Figure 4.5**). Complementary to this analysis, the ability of the cells to uptake transferrin and levels of transferrin in the airways were also assessed (**Figure 4.6**). Firstly, the gene encoding CD71 (TFRC) expression was measured. As expected the CD71+ cells exhibit increased expression of the gene encoding transferrin receptor CD71 (**Figure 4.5A**). In order to understand what may be controlling the upregulation of CD71 receptor, genes encoding iron regulatory proteins (IRP) 1 and IRP2 were examined. IRP1 expression was significantly increased in the CD71+ cells (**Figure 4.5B**), whereas IRP2 showed similar expression levels between both cells (**Figure 4.5C**). The gene encoding ferriportin, an iron exporter, was examined showing significantly decreased expression in CD71+ cells (**Figure 4.5D**). Next examination of the ability of the cells to uptake transferrin was assessed by flow cytometry revealing a significant increase in transferrin uptake in the CD71+ cells (**Figure 4.6A**). Transferrin was measured in the BAL in healthy volunteers and in patients with ILD showing significantly higher levels of transferrin in IPF, HP and cHP (**Figure 4.6B**). Finally, there was an inverse correlation in levels of transferrin in the airways compared to the proportion of CD11c+ cells expressing CD71 (**Figure 4.6C**). Additional genes involved in iron uptake and homeostasis were examined including HMOX1, SLC11A2 (NRAMP2), HAMP and SLC48A1 (HRG1) revealing no significant differences in expression comparing the cells (**Figure 4.7A-D** respectively). Analysis of ferritin in the airways showed a significant increase in ferritin in cHP compared to healthy but no significant difference comparing

healthy controls to IPF patients (**Figure 4.8**). Iron levels were examined, however free iron was not detected in BAL supernatant (data not shown).

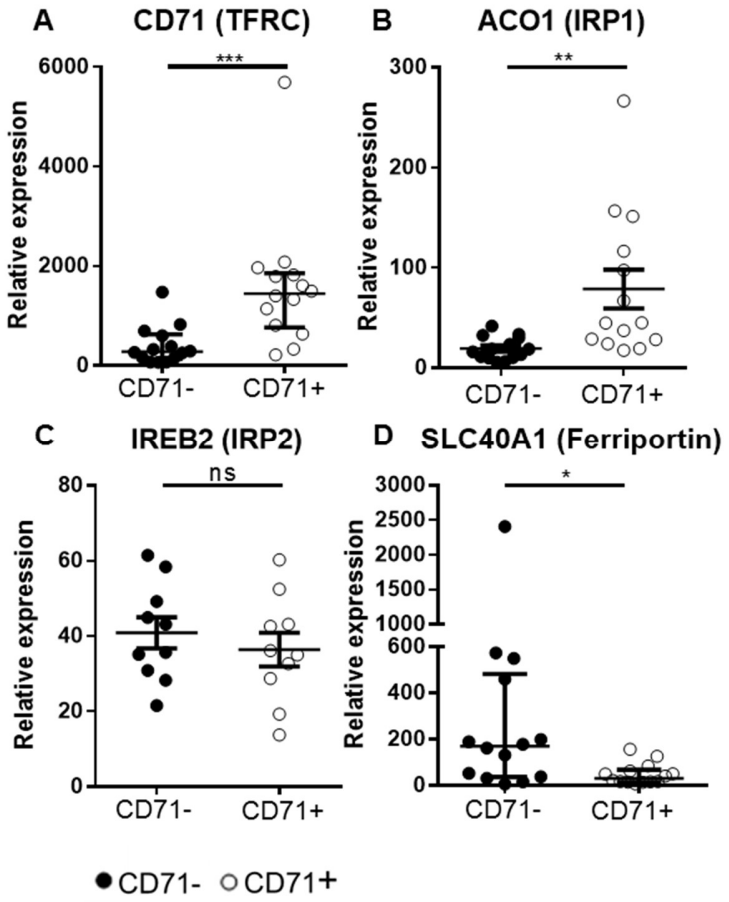


Figure 4.5: Analysis of iron regulatory genes in CD71- and CD71+ cells.
CD71- or CD71+ cell gene expression analysis relative to housekeeping gene GAPDH are shown for TFRC, ACO1 (IRP1), IREB2 (IRP2) and SLC40A1 in A-D respectively. Median and interquartile range is shown. Statistical analysis was performed using Mann-Whitney U *p<0.05, **p<0.01, ***p<0.001, ****p<0.0001 comparing CD71- gene expression to CD71+ gene expression (A-D).

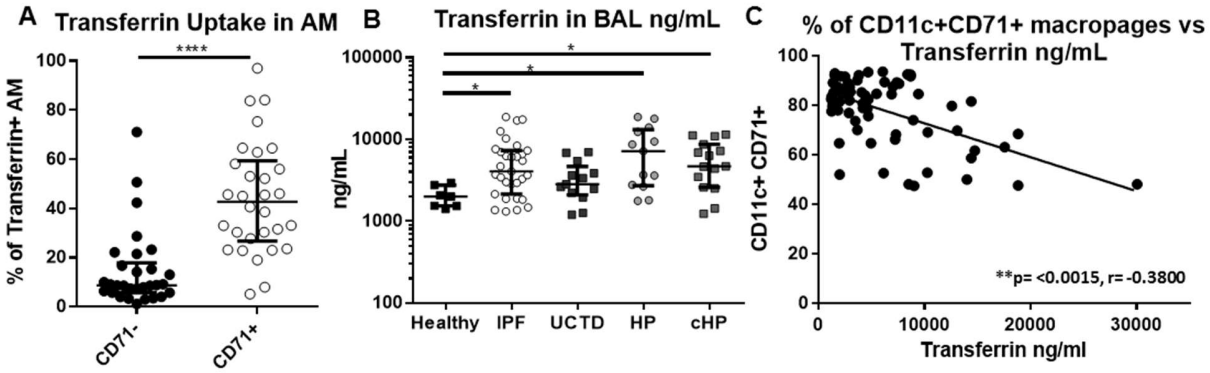


Figure 4.6: Analysis of transferrin uptake by macrophages and transferrin levels in the BAL. Transferrin uptake as a percentage of total CD71- and CD71+ populations are shown in A. B shows the levels of transferrin in the BAL (ng/mL) for healthy controls, and idiopathic pulmonary fibrosis (IPF), undifferentiated connective tissue disease (UCTD), hypersensitivity pneumonitis (HP) and chronic hypersensitivity pneumonitis (cHP) patients. C shows Pearson's correlation analysis comparing the % of CD11c cells expressing CD71 to the levels of transferrin the airways. Median and interquartile range are shown on graphs. Statistical analysis was performed using Mann-Whitney U *p<0.05, **p<0.01, ***p<0.001, ****p<0.0001 comparing CD71- to CD71+ (A) or each ILD to healthy (B).

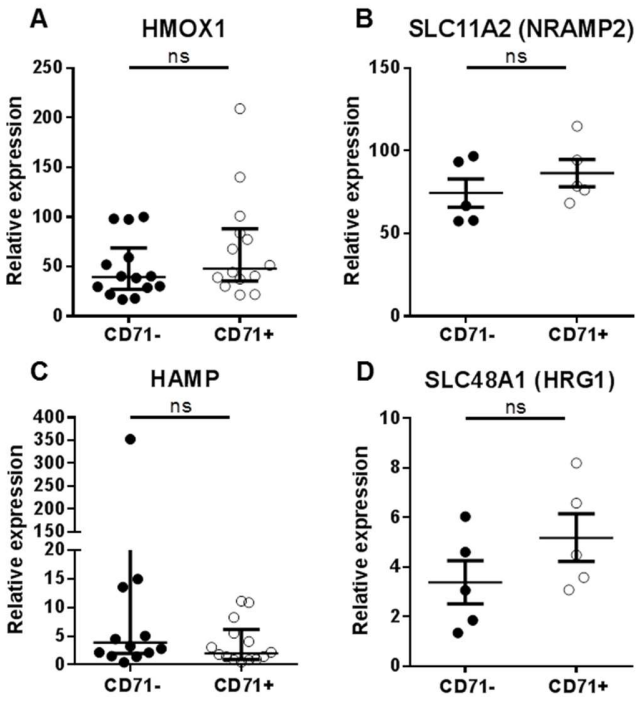


Figure 4.7: Further analysis of genes involved in iron regulation.
Expression of HMOX, SLC11A2, HAMP and SLC48A1 relative to housekeeping control gene, GAPDH, in CD71- and CD71+ cells do not significantly differ (A-D respectively).

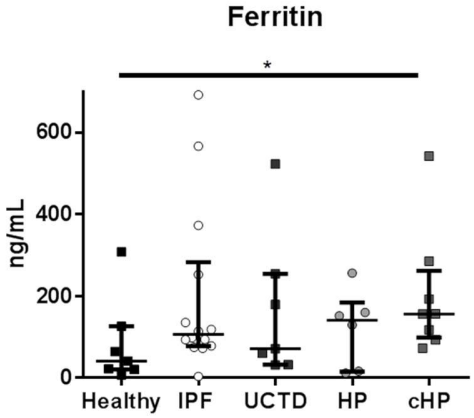


Figure 4.8: Ferritin concentration in the BAL.
Ferritin (ng/mL) was measured in the BAL supernatant from healthy controls and individuals with ILD; idiopathic pulmonary fibrosis (IPF), undifferentiated connective tissue disease (UCTD), hypersensitivity pneumonitis (HP) and chronic hypersensitivity pneumonitis (cHP). Median and interquartile range shown. Statistical analysis using Mann-Whitney U *p<0.05.

4.4.6. Examination of TLR expression in CD71- and CD71+ cells reveal significant differences.

One of the key roles of airway macrophages in maintaining homeostasis is host defence, which requires detection and elimination of pathogens in the airways. Toll like receptors (TLRs) are critical in the detection of pathogen associated molecular patterns (PAMPs) and damage associated molecular patterns (DAMPs). The expression of TLR genes was examined in the CD71- and CD71+ cells. TLR2, which detects gram positive bacteria, TLR3, which detects viral (double-stranded) dsRNA, TLR4, which detects gram negative bacteria, TLR1, which interacts with TLR2 and detects gram positive bacteria, TLR6, which interacts with TLR2 in detecting bacterial lipoproteins and TLR7, which detects viral (single-stranded) ssRNA were examined **Figure 4.9A-F** respectively. Expression of TLR2 (**Figure 4.9A**) and TLR3 (**Figure 4.9B**) were significantly increased in CD71- cells compared to CD71+. Protein expression was quantified by FACs examining geomean mean fluorescence intensity (MFI) on macrophages as a whole (**Figure 4.9G**) and specifically in CD71- and CD71+ cells for TLR2 and TLR4 (**Figure 4.9H** and **I** respectively). Similar to the gene expression data, expression of TLR2 protein appears higher in CD71- cells compared to CD71+ (**Figure 4.9H**) whereas expression of TLR4 protein appears the same in both cells.

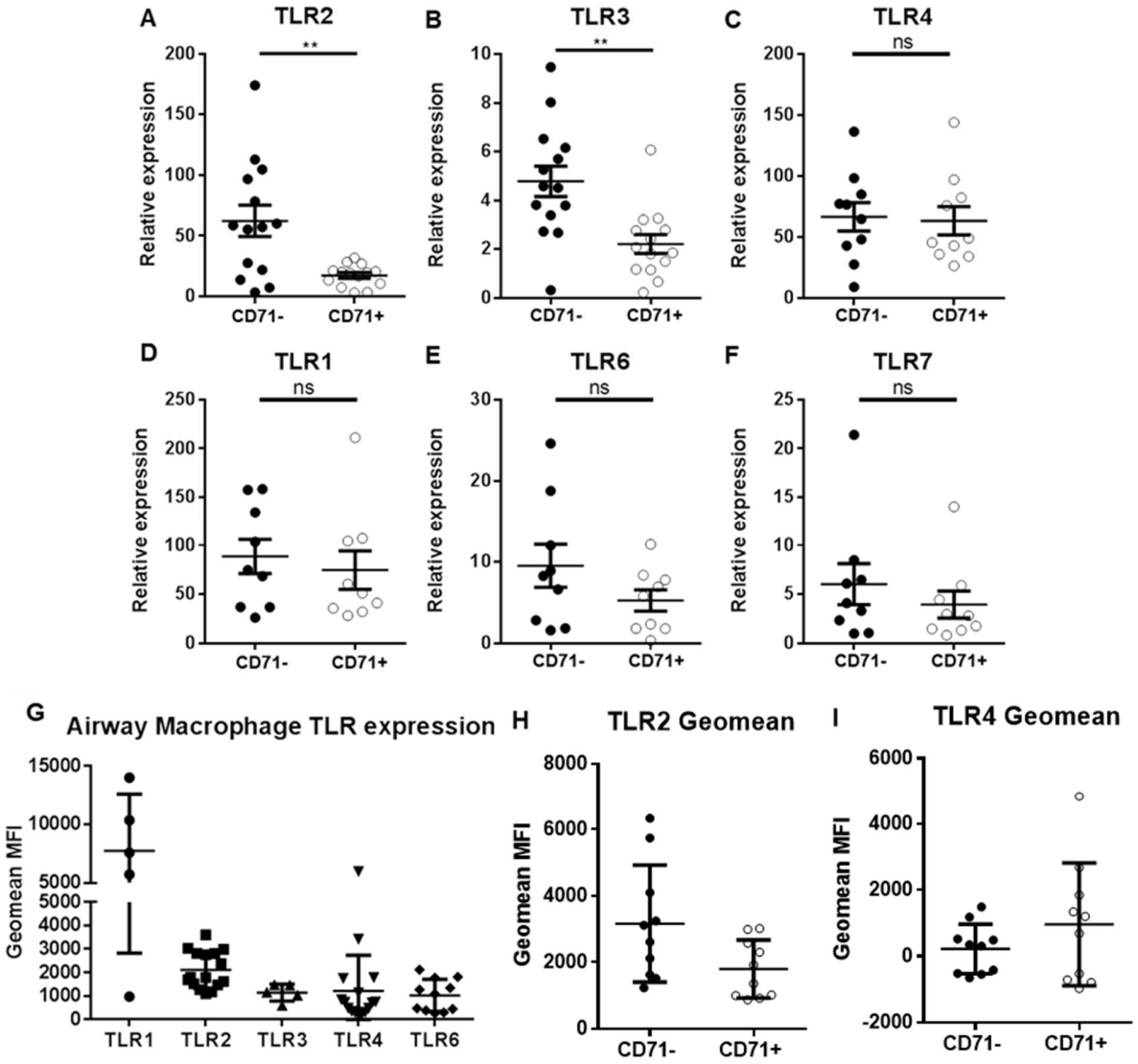


Figure 4.9: Examination of CD71- and CD71+ cell TLR gene and protein expression.
Gene expression, relative to housekeeping gene GAPDH, of TLR2 and TLR3 are significantly lower in CD71+ cells (A and B respectively). Expression of TLR4, TLR1, TLR6 and TLR7 are not significantly different (C-F). Overall protein expression of TLR1, TLR2, TLR3, TLR4 and TLR6 were measured using FACs. The geomean of mean fluorescence intensity minus the FMO is shown (G). TLR2 expression, as measured by geomean MFI, appears higher in the CD71- cells (H) and TLR4 appears the same (I). Median and interquartile range shown. Statistical analysis using Mann-Whitney U T test, *p<0.05, **p<0.01.

4.4.7. Comparison of CD71- and CD71+ cell defence revealed significant differences in NO production and bacterial phagocytosis.

As the expression of specific TLRs significantly differed comparing CD71- and CD71+ cells, next host defence function was examined. Nitric oxide production was measured at baseline in unstimulated cells revealing a significant increase in the presence of nitric oxide in CD71- cells compared to CD71+ (**Figure 4.10A**). Additionally, the CD71- and CD71+ cells ability to phagocytose bacteria was assessed in a separate assay revealing the percentage of cells which had phagocytosed bacteria was significantly increased in the CD71+ cells compared to the CD71- (**Figure 4.10B**). To elucidate why there were observed differences in nitric oxide production expression of NOS2, which is involved in nitric oxide synthesis, was examined, however, the gene was not detected in either CD71- or CD71+ cells (data not shown). Expression analysis of genes involved in phagocytosis was also quantified. ELMO, which is involved in phagocytosis and cell motility and FCGR1B, which is involved in antibody mediated phagocytosis, do not differ significantly in expression comparing CD71- to CD71+ cells (**Figure 4.10D-E** respectively). Nitric oxide appeared significantly increased in CD71- and CD71+ cells in healthy individuals compared to IPF (**Figure 4.11A** and **B** respectively), whereas phagocytosis looked similar across all groups in CD71- and CD71+ cells (**Figure 4.11C** and **D** respectively).

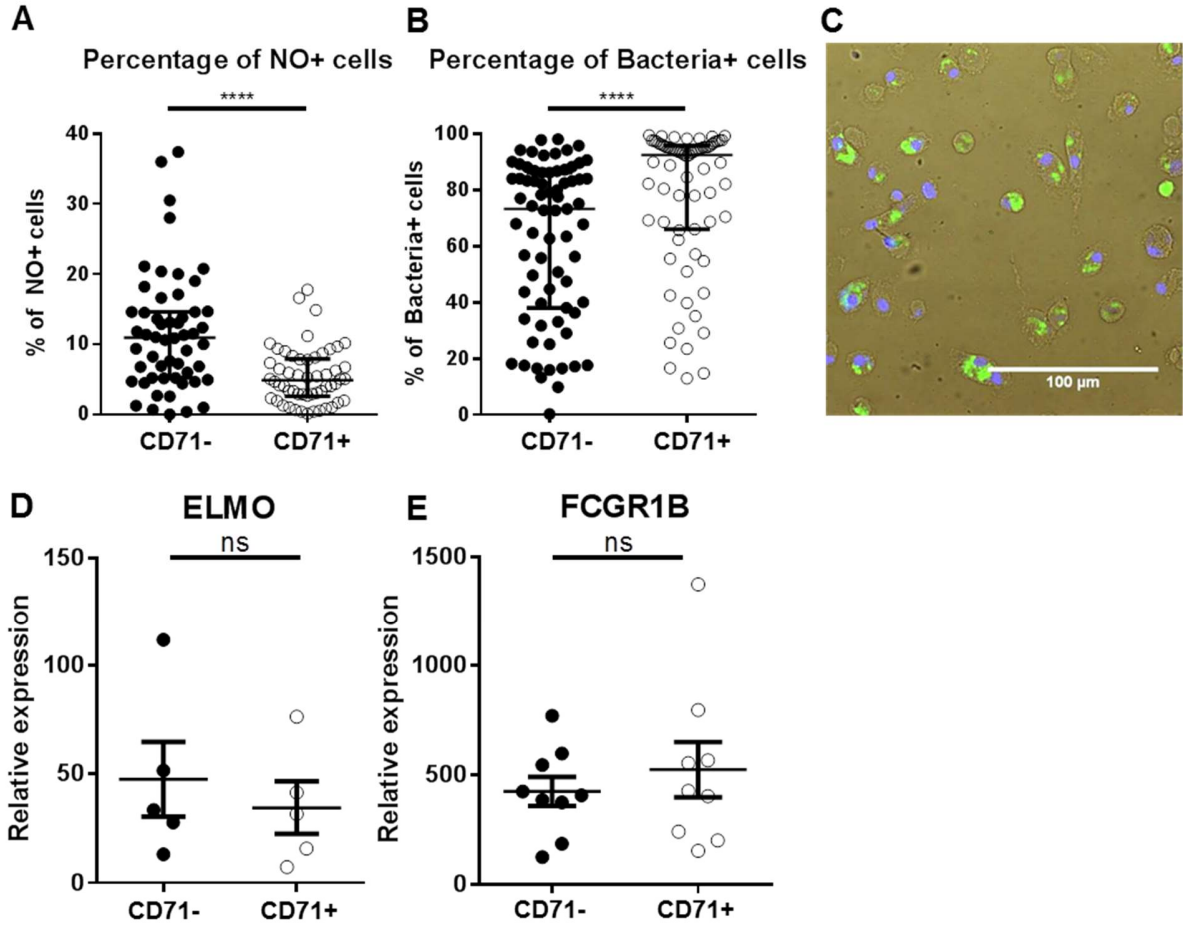


Figure 4.10: Examination of pathogen defence in CD71- and CD71+ cells.
The percentage of nitric oxide (NO)+ cells were increased significantly in the CD71- cells compared to CD71+ (A). In a separate experiment examining phagocytosis the percentage of cells positive for bacteria are significantly increased in the CD71+ cells (B). C shows an image of cells having phagocytosed bacteria, bacteria in green and DAPI nuclear stain in blue, overlayed on white field image. ELMO (D) involved in phagocytosis and cell motility and FCGR1B (E) involved in antibody mediated phagocytosis do not differ significantly in expression relative to housekeeping gene GAPDH. Median and interquartile ranges shown. Statistical analysis using Mann-Whitney U T test, ****p<0.0001.

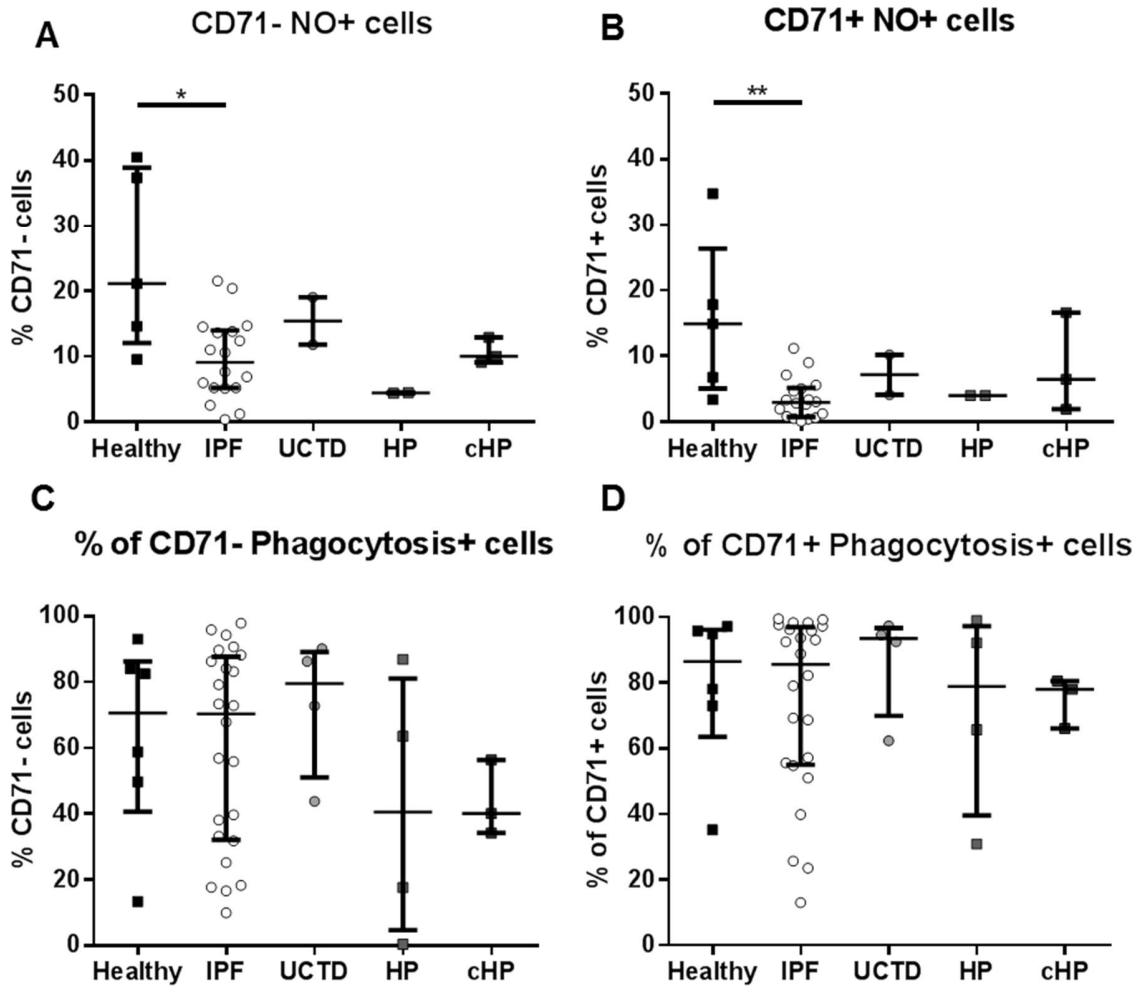


Figure 4.11: Examination of pathogen defence in CD71- and CD71+ cells in health and disease. The percentage of nitric oxide (NO)+ cells were increased significantly in the CD71- (A) and CD71+ cells (B) in healthy controls compared to IPF. There were no observed differences in the percentage of CD71- (C) or CD71+ (D) phagocytosing cells across disease group. Median and interquartile ranges shown for healthy controls and individuals with ILD; idiopathic pulmonary fibrosis (IPF), undifferentiated connective tissue disease (UCTD), hypersensitivity pneumonitis (HP) and chronic hypersensitivity pneumonitis (cHP). Statistical analysis using Mann-Whitney U T test, *p<0.05, **p<0.01.

4.4.8. Examination of the production of pro-inflammatory mediators in CD71- and CD71+ cells post TLR stimulation

As differences both in TLR expression and in defence mechanisms were observed comparing the CD71- and CD71+ cells, analysis of the production of pro-inflammatory mediators in response to TLR stimulation were next examined. A pro-inflammatory multiplex was used to quantify mediators in the supernatant produced by separated cells, which were unstimulated or stimulated with LPS, a TLR4 ligand, and Poly: IC, a TLR3 ligand, for 24 hours. Pro-inflammatory chemokines IL-8 (CXCL8) and CCL2, and cytokines TNFα, IL-1β, immunoregulatory IL-10, and pro-inflammatory IFNγ, IL-23 and IL-18 were measured (**Figure 4.12A-I** respectively). No significant differences were observed comparing CD71- to CD71+ cell cytokine production. It is interesting that stimulation with Poly: IC appeared to induce an increase in IL-8 and CCL2 production (**Figure 4.12A-B**), and a slight increase in IFNγ and IL-23 (**Figure 4.12G-H**) but no other cytokines. LPS stimulation induced an increase in all cytokines except IL-18 (**Figure 4.12A-I**).

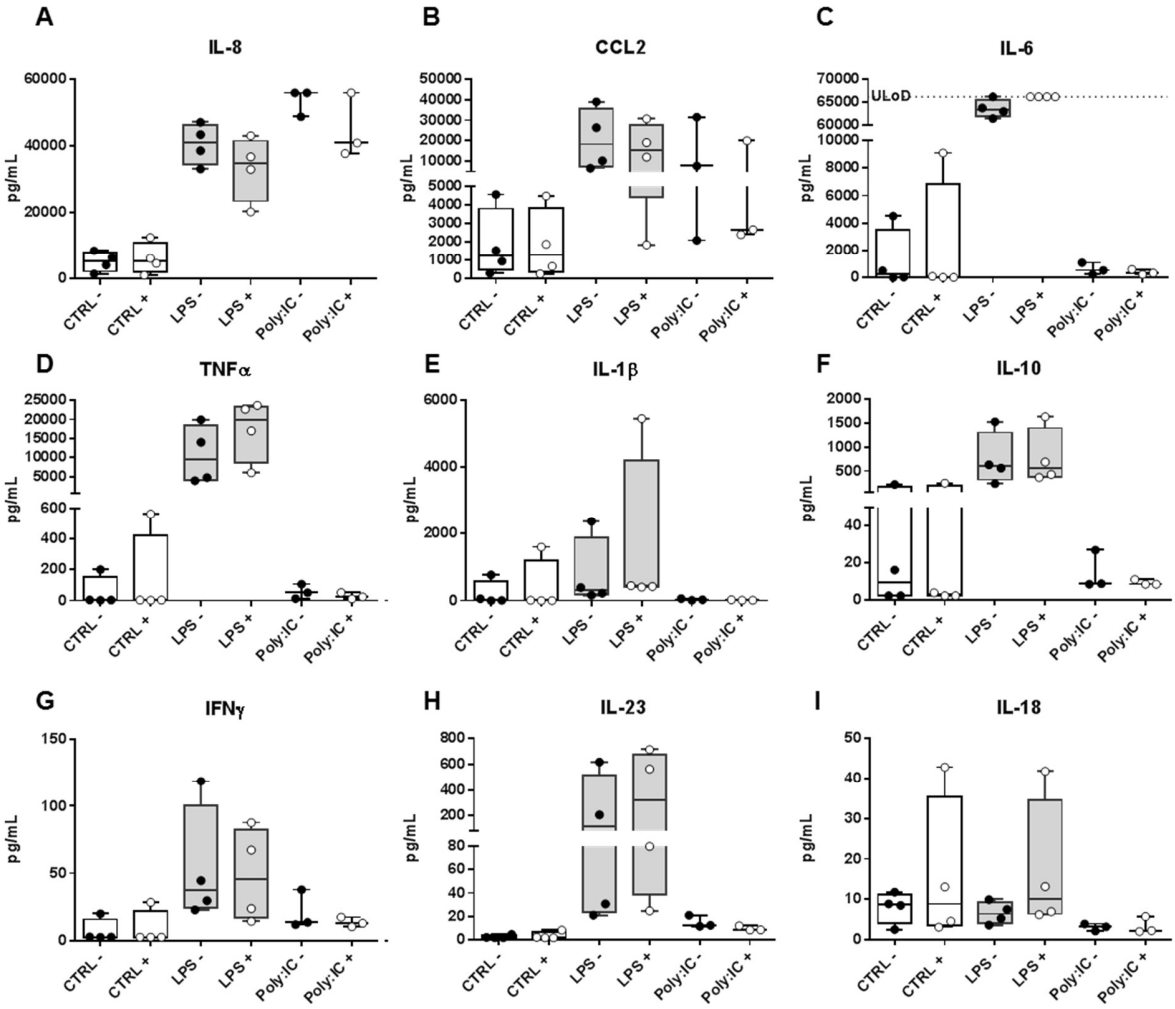


Figure 4.12: Production of inflammatory cytokines are similar comparing CD71- to CD71+ cells. Pro-inflammatory cytokines and chemokines were measured in the supernatant of seperated and stimulated CD71- (•) and CD71+ (o) cells. Cells were left unstimulated (ctrl), or stimulated with LPS (10 ng/mL) or Poly:IC (10 μg/mL) in complete RPMI for 24 hours. Cell supernatant was analysed to examine the production of IL-6, IL-8, CCL2, TNFα, IL-1β, IL-10, IFNγ, IL-23 and IL-18 (pg/mL), which is shown in A-I respectively. Median and interquartile range shown. Wilcoxon's ranked paired test was used to compare unstimulated to paired stimulated cells and Mann-Whitney U T test was used to compare same stimulus CD71- to CD71+. No significant differences were found.

4.4.9. Examination of genes associated with fibrosis in CD71- and CD71+ cells

CD71- cells appear increased in IPF, and the increase in CD71- cells correlates with FVC decline (see **4.4.3**), however, the role the CD71- cells may play in fibrosis remains to be determined. To further examine this the CD71- and CD71+ cells were separated from 3 patients with IPF and the expression of multiple genes thought to be involved in fibrosis were examined to try to elucidate roles in the pathology. **Figure 4.13** shows a heat map clustergram of genes expressed in CD71- and CD71+ cells from a fibrotic gene array, and a scatter plot of genes increased in CD71- cells (along the x axis) and CD71+ cells (along the y axis). Clustergram analysis clustered the CD71- and CD71+ cells together, suggesting different gene signatures in the cells (**Figure 4.13A**). Significantly differentially expressed genes are highlighted with red stars showing CCL2, CCL3, IL-10 and CCR2 were significantly increased in CD71- cells, whereas CEBPB, IL1A, TIMP2 and ITGB5 and ITGB8 were increased in the CD71+ cells (*$p<0.05$,**$p<0.01$, **Figure 4.13A**). Scatter plot analysis shows genes which were over 4 fold increased in CD71+ cells (up the y axis, highlighted in red and labelled) and those which were over 4 fold increased in the CD71- cells (along the x axis, highlighted in green and labelled) (**Figure 4.13B**). A summary of the genes expressed in CD71- and CD71+ cells is highlighted in **Table 4.3**, with expression of genes increased, decreased or the same in CD71- cells compared to CD71+ cells.

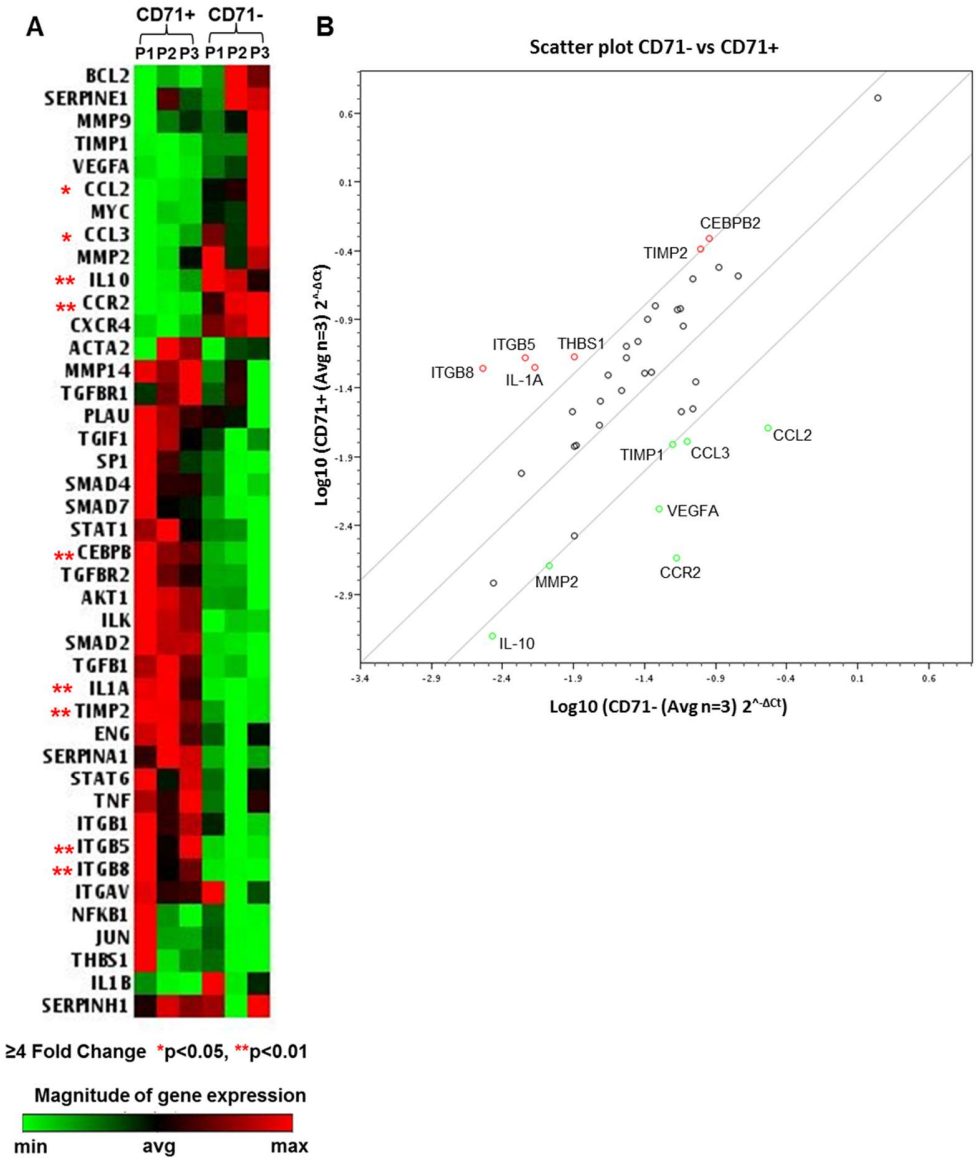


Figure 4.13: CD71-/+ cells express significantly different genes related to fibrosis.
Clustergram analysis (A) with CD71+ cells clustering from 3 individuals with IPF on the left and CD71- cells clustering to the right from the same 3 individuals. Expression levels are shown in the form of a heat map where high expression is red, low expression is green and black is average. B shows a scatter plot. Genes that show similar expression between the two cell types are close to the central diagonal line. The two lines either side of the central diagonal line highlight genes where expression is over 4 fold increased in either the CD71+ population (y axis highlighted in red and labelled) or the CD71- population (x axis highlighted in green and labelled). Overall gene expression increases from left to right (along x axis) in the CD71- cells, and from the bottom (along y axis) to the top in the CD71+ cells.

Gene	Protein	CD71-expression	General Role
CCL2	Chemokine (C-C motif) ligand 2 (MCP-1)	↑	Cytokine/chemokine, receptor
CCL3	Chemokine (C-C motif) ligand 3 (MIP-1α)	↑	Cytokine/chemokine, receptor
IL-10	Interleukin 10	↑	Cytokine/chemokine, receptor
CCR2	Chemokine (C-C motif) receptor 2 (MCP-1R), CD192	↑	Cytokine/chemokine, receptor
CXCR4	Chemokine (C-X-C motif) receptor 4, CD184	↑	Cytokine/chemokine, receptor
IL1A	Interleukin 1, alpha	↓	Cytokine/chemokine, receptor
TNF	Tumor necrosis factor (TNFα)	↓	Cytokine/chemokine, receptor
IL1B	Interleukin 1, beta	↑	Cytokine/chemokine, receptor
ILK	Integrin-linked kinase (P59)	↔	Integrins and integrin signalling
ITGB1	Integrin, beta 1 (fibronectin receptor, CD29)	↓	Integrins and integrin signalling
ITGB5	Integrin, beta 5	↓	Integrins and integrin signalling
ITGB8	Integrin, beta 8	↓	Integrins and integrin signalling
ITGAV	Integrin, alpha V (vitronectin receptor, CD51)	↓	Integrins and integrin signalling
SERPINE1	Serpin peptidase inhibitor, clade E (plasminogen activator inhibitor-1), member 1	↑	Remodelling
MMP9	Matrix metallopeptidase 9 (gelatinase B, type IV collagenase)	↑	Remodelling
TIMP1	TIMP metallopeptidase inhibitor 1	↑	Remodelling
VEGFA	Vascular endothelial growth factor A	↑	Remodelling
MMP2	Matrix metallopeptidase 2 (gelatinase A, type IV collagenase)	↑	Remodelling
MMP14	Matrix metallopeptidase 14 (membrane-inserted)	↔	Remodelling
PLAU	Plasminogen activator, urokinase (u-PA)	↔	Remodelling
TIMP2	TIMP metallopeptidase inhibitor 2	↓	Remodelling
SERPINA1	Serpin peptidase inhibitor, clade A (antitrypsin), member 1	↓	Remodelling
SERPINH1	Serpin peptidase inhibitor, clade H (heat shock protein 47), member 1	↔	Remodelling
TGFBR1	Transforming growth factor, beta receptor 1 (ALK5)	↔	TGFβ superfamily
TGIF1	TGFB-induced factor homeobox 1	↔	TGFβ superfamily
SMAD4	SMAD family member 4	↓	TGFβ superfamily
SMAD7	SMAD family member 7	↓	TGFβ superfamily
TGFBR2	Transforming growth factor, beta receptor II	↓	TGFβ superfamily

SMAD2	SMAD family member 2	↓	TGFβ superfamily
TGFB1	Transforming growth factor, beta 1	↓	TGFβ superfamily
ENG	Endoglin (END)	↔	TGFβ superfamily
THBS1	Thrombospondin 1	↓	TGFβ superfamily
MYC	V-myc myelocytomatosis viral oncogene homolog (avian)	↑	Transcription factor
SP1	Sp1 transcription factor	↓	Transcription factor
STAT1	Signal transducer and activator of transcription 1, 91kDa	↓	Transcription factor
CEBPB	CCAAT/enhancer binding protein (C/EBP), beta	↓	Transcription factor
STAT6	Signal transducer and activator of transcription 6, interleukin-4 induced	↓	Transcription factor
NFKB1	Nuclear factor of kappa light polypeptide gene enhancer in B-cells 1	↔	Transcription factor
JUN	Jun proto-oncogene	↓	Transcription factor
AKT1	V-akt murine thymoma viral oncogene homolog 1	↓	Serine-threonine kinase
BCL2	B-cell lymphoma 2	↑	Regulate apoptosis (anti – apoptotic)

Table 4.3: Summary of Genes expressed in both CD71- and CD71+ airway macrophages from fibrosis gene array.

Fold change Increase/decrease in expression showing CD71- cells genes compared to CD71+ cells relative to housekeeping control GAPDH.

4.4.10. Examination of growth factors produced by CD71- and CD71+ cells

Growth factors play key roles in the differentiation and maturation of leukocytes, and in the remodelling of the airways, a hallmark feature of fibrosis. In order to examine any differences in growth factor production by CD71- and CD71+ cells growth factors were measured using multiplex analysis in the supernatant (pg/mL) of separated cells which had been stimulated with TLR ligands (TLR4-LPS or TLR3-Poly: IC) or the pro-fibrotic cytokine TGFβ1 for 24 hours (**Figure 4.14**). LPS stimulation increased the production of growth factors involved in the maturation and differentiation of myeloid cells G-CSF, GM-CSF and M-CSF (**Figure 4.14A-C**) and in VEGF in CD71+ cells (**Figure 4.14D**). G-CSF and GM-CSF production appears increased in the supernatant of LPS stimulated CD71+ cells compared to LPS stimulated CD71- cells (**Figure 4.14A-B**). Poly: IC increased the production of M-CSF only (**Figure 4.14C**). TGFβ1 stimulation induced an increase in the production of TGFα only in both CD71- and CD71+ cells (**Figure 4.14F**). No differences were observed in the production of Angiopoeitin-1, EGF, SCF and HGF (**Figure 4.14G-J**) either with stimulation or comparing production of growth factors by CD71- and CD71+ cells.

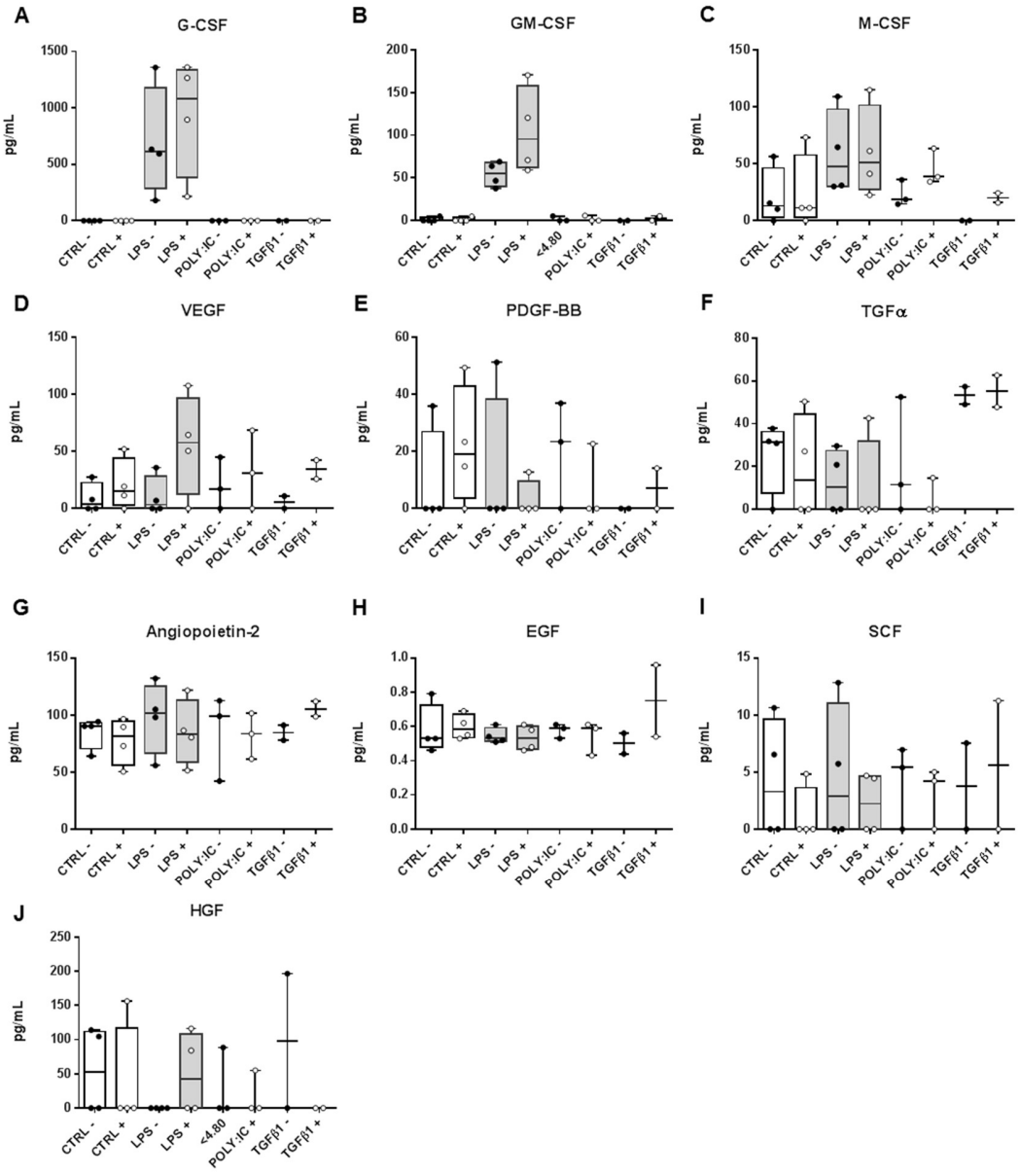


Figure 4.14: Production of growth factors comparing CD71- to CD71+ cells.
Growth factor production was measured in the supernatant of seperated and stimulated CD71- (•) and CD71+ (o) cells. Cells were left unstimulated (ctrl, n=4), or stimulated with LPS (n=4,10 ng/mL), or Poly:IC (n=3, 10 µg/ml), or rhTGFβ1 (n=2, 10 ng/mL) for 24 hours. Cell supernatant was analysed to examine the production of growth factor by mulitplex. G-CSF, GM-CSF, M-CSF, VEGF, PDGF-AA, PDGF-BB, TGFα, Angiopoeitin-1, EGF, SCF and HGF (pg/mL) are shown in A-J respectively. Wilcoxon's ranked paired test was used to compare unstimulated to paired stimulated cells and Mann-Whitney U T test was used to compare same stimulus CD71- to CD71+. No significant differences were found.

4.4.11. Co-culturing CD71- and CD71+ cells with BEC down regulates BEC genes involved in extracellular matrix production

In order to examine how the CD71- and CD71+ cells influence BECs, co-cultures were set up with CD71- and CD71+ cells isolated from 5 individuals with IPF and added to confluent primary BECs, which were isolated from a healthy individual. CD71- and CD71+ cells were cultured with BECs for 6 hrs at which point the BEC and macrophages were then separated. BEC gene expression fold change was analysed at 6 hours and compared to BEC which were cultured alone (**Figure 4.15**). Examination of BEC gene expression of pro-inflammatory/fibrotic cytokine IL-6, and chemokines IL-8 and CCL2 revealed no significant changes after co-culture with CD71- and CD71+ cells (**Figure 4.15A-C** respectively). Analysis of TGFβ1 expression revealed a down-regulation in the co-cultured BEC (**Figure 4.15D**). With the expression of one of TGFβ1 receptors, TGFβR1 remaining unchanged (**Figure 4.15E**). Extracellular mediator, connective tissue growth factor (CTGF), gene expression appeared down-regulated by BECs in co-culture (**Figure 4.15F**). Extracellular matrix gene expression, collagen 1α1 (COL1A1) and fibronectin (FN1) was also decreased in BECs after co-culture for 6 hours (**Figure 4.15G-H** respectively).

IL-6, IL-8 and CCL2 proteins were measured in the supernatant of the co-culture at 6 hours. IL-6 was increased in the co-cultured supernatant compared to BEC, CD71- or CD71+ alone (**Figure 4.16A**). IL-8 levels look similar in the BEC cultured alone compared to the BEC in co-culture (**Figure 4.16B**). CCL2 was not detected at 6 hours in the supernatant (data not shown).

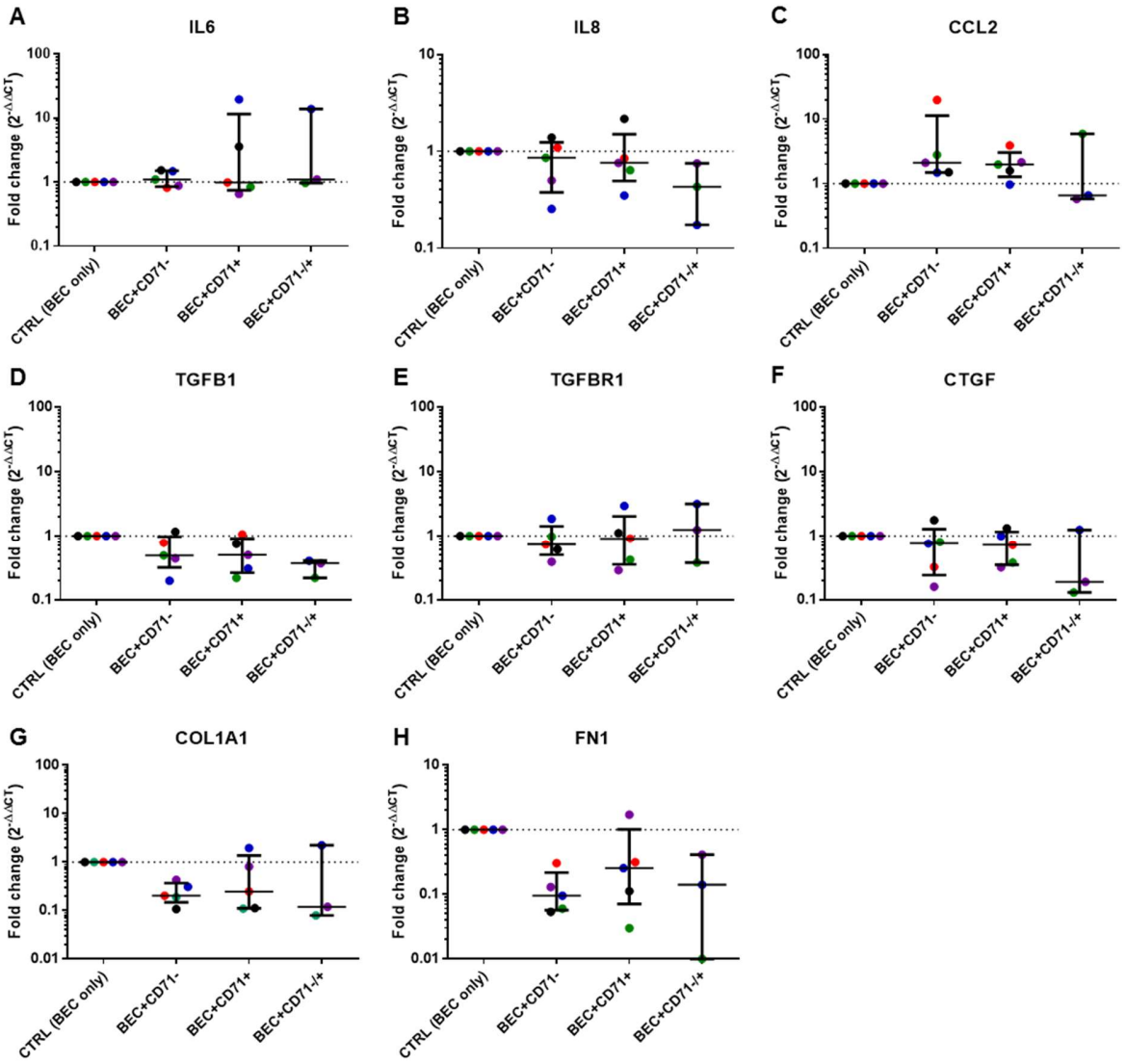


Figure 4.15: Gene expression fold change analysis of BEC after co-culture with CD71- and CD71+ cells for 6 hours.

IL-6, IL-8, CCL2, TGFβ1, TGFβR1, CTGF, COL1A1 and FN1 gene expression measured and fold change to BEC alone shown in A-H respectively. Median and interquartile range shown. Wilcoxon paired T test was used to compare BEC cultured alone to each BEC co-culture condition. No significant differences were found. Coloured circles represent individual IPF patients CD71- and CD71+ cells which were sorted and used in co-culture (•=patient ID #14, •= patient ID #15, •= patient ID #16 , •= patient ID #17 and •= patient ID #18).

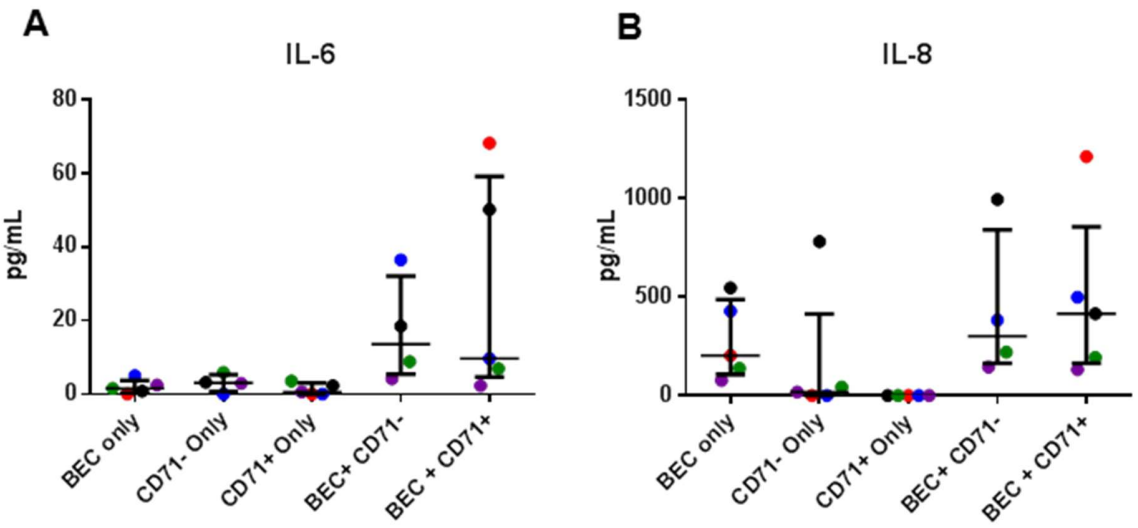


Figure 4.16: Measurement of IL-6 and IL-8 in the supernatant of BEC alone, CD71- and CD71+ alone, and BEC and CD71- or CD71+ in co-culture.
IL-6 (A) and IL-8 (B) was measured in the supernatant (pg/mL) at 6 hours post co-culture or single culture. Median and interquartile range shown. Wilcoxon paired T test was used to compare BEC cultured alone to each BEC co-culture condition. No significant differences were found. Coloured circles represent individual IPF patient CD71- and CD71+ cells which were sorted and used in co-culture (•=patient ID #14, •= patient ID #15, •= patient ID #16 , •= patient ID #17 and •= patient ID #18).

4.4.12. Stimulation of epithelial cell and fibroblast co-culture with CD71- cell supernatants results in increased collagen IV deposition

Co-cultures of primary small airway epithelial cells (SAEpC) and IPF fibroblasts (IPF134) result in deposition of quantifiable ECM (Appendix 8.2; **Figure 8.2.1**), which can be increased or inhibited by soluble factors. To assess whether CD71- or CD71+ cells induced ECM deposition, supernatants from FACS separated CD71- and CD71+ cells from 5 IPF patients were used to stimulate the SAEpC and IPF134 co-culture. Isolated CD71-/+ cells were either unstimulated for 48 hours or stimulated with LPS for 48 hours. The supernatants were then harvested and added to the SAEpC/IPF134 co-culture to examine the effect of mediators produced by CD71-/+ cells on ECM deposition. After 6 days of culture approximate cell viability was measured as a surrogate marker of cell growth using presto blue stain, which stains live cells, and fluorescence was quantified revealing no differences in the co-culture stimulated compared to unstimulated (Appendix 8.2; **Figure 8.2.2**). After presto blue staining the SAEpC and fibroblast were removed from the wells and fibronectin, collagen I and III, and collagen IV proteins were labelled and stained for quantification. A resulting increase in total fluorescent intensity (TFI) indicates an increase in the specific ECM proteins. Example images with CD71- cell supernatant stimulation are shown in **Figure 4.17**. No differences were found in TFI comparing stimulations to controls for either collagen I and III or fibronectin (data not shown). Analysis of geomean of TFI revealed an increase collagen IV deposition after stimulation of co-culture with CD71- cell supernatants but not CD71+ supernatants (**Figure 4.18A**). Both CD71- and CD71+ LPS stimulated supernatants increased collagen IV deposition compared to LPS baseline control (**Figure 4.18B**). Regardless of stimulation CD71- supernatants

significantly increased collagen IV deposition compared to CD71+ supernatants (**Figure 4.18C**) suggesting different roles by the cells in regulated collagen IV deposition.

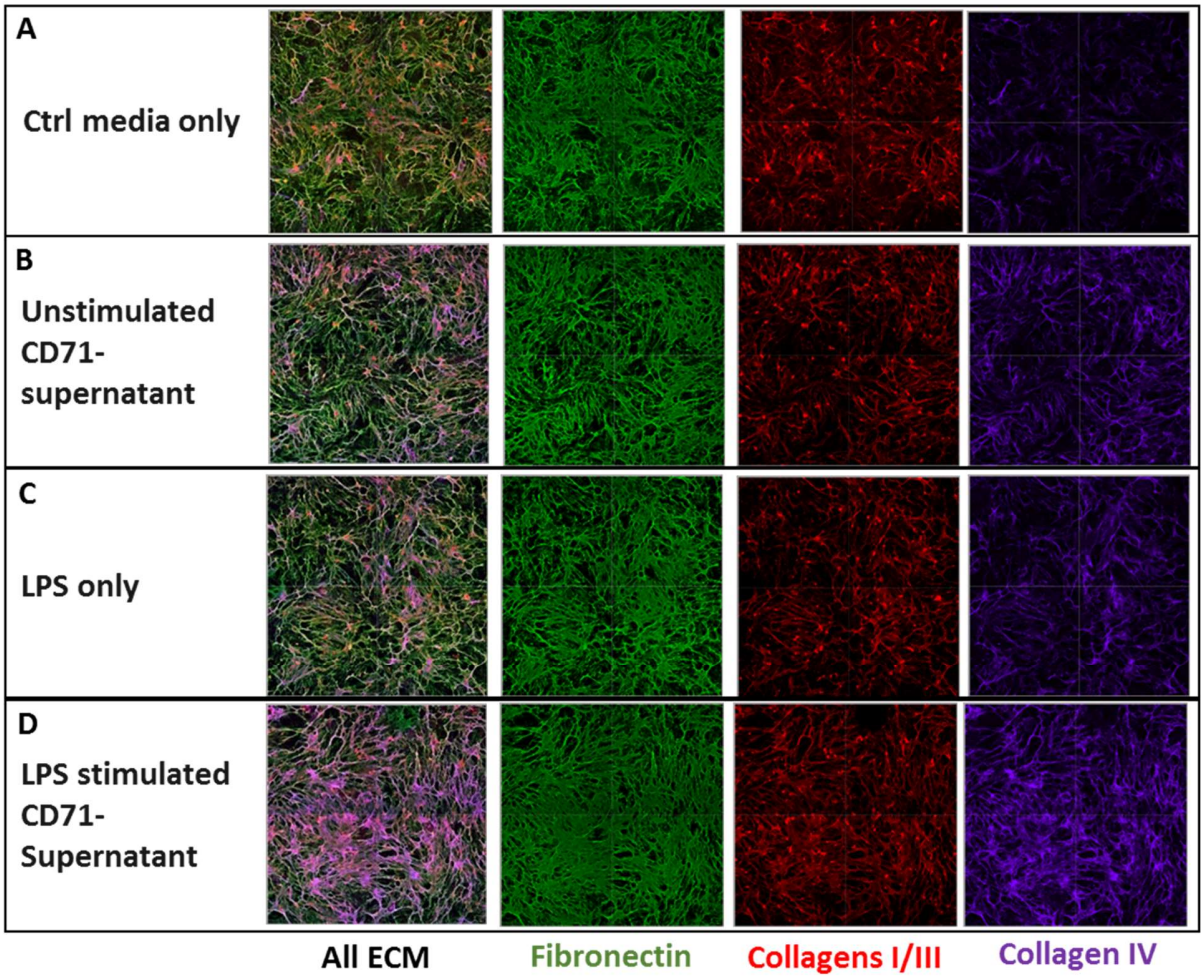


Figure 4.17: Example of fluorescent staining of extracellular matrix produced by primary small airway epithelial cells (SAEpC) and IPF fibroblasts (IPF134).
Representative images shown. Panel A shows extracellular matrix (ECM) deposited by co-culture with control media, panel B shows ECM deposition after stimulation of with CD71- unstimulated supernatants, panel C shows ECM deposition after stimulation with LPS only and panel D shows ECM deposition after stimulation with LPS stimulated CD71- supernatants. Fibronectin is shown in green, Collagens I and III are in red and collagen IV is in purple.

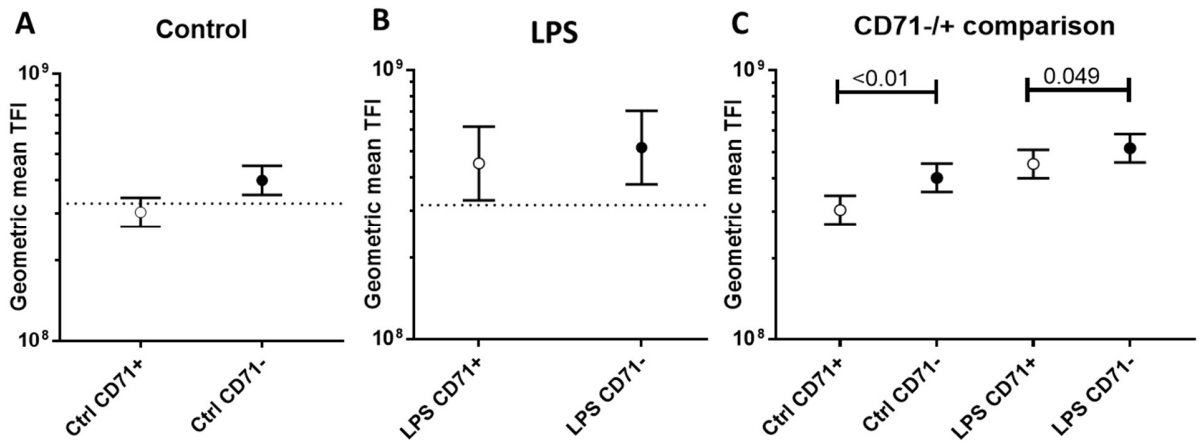


Figure 4.18: Collagen IV deposition is increased by CD71- cell supernatants compared to CD71+ cell supernatants.

Geometric total fluorescence intensity (TFI) reveals an increased collagen IV deposition by primary small airway epithelial cell (SAEpC) and IPF fibroblasts (IPF134) co-culture in response to CD71- unstimulated supernatants compared to the baseline geomean collagen deposition illustrated by the dashed line (A). Stimulation of co-culture with LPS alone, or supernatants from LPS stimulated CD71- and CD71+ cells reveal an increase in collagen IV deposition with stimulation with supernatants compared to LPS only (B). LPS only geomean value illustrated by dashed line (B). CD71- supernatants significantly increased collagen IV deposition compared to CD71+ supernatants, as measured by geometric TFI, in both control and LPS stimulated conditions (C). Geomean ± upper and lower 95% confidence interval shown from IPF isolated CD71- and CD71+ supernatants. Supernatants from 5 patients, with each patient supernatant carried out in quadruplicate wells (n=20 wells per supernatant cell condition). Geomean dashed line for control wells (n=16 wells) (A) and dashed line of LPS only stimulated control wells (n=4 wells) (B).

4.5. Discussion

Macrophages have been shown to play key roles in the progression of pathology in *in vivo* models of fibrosis [187, 341, 347, 362, 363] and in IPF [193]. The data from the previous results chapter revealed increased numbers of macrophages and monocytes in the airways of IPF patients. To evaluate this further results from this chapter analysing macrophages revealed phenotypically and functionally distinct macrophage populations which were increased in IPF, correlated with clinical decline and differentially stimulated collagen IV deposition by epithelial and fibroblast co-cultures. This data provides novel findings identifying differing macrophage phenotypes in IPF, the results of which will be discussed in detail.

As evidence in mouse models of IPF suggest an increase in the M2 'remodelling' macrophage phenotype [345-347], combined with data suggesting there is an increase in M2 phenotype in man [57, 346, 349, 350], the M1/M2 phenotypes of macrophages in IPF and other ILDs were first investigated. Contrary to previous reports here the evidence from FACS data suggests no clear M2 phenotype. However, this could in part be explained as a result of methods employed for analysis. One such discrepancy is the markers used to phenotype cells, for example CD204 has been used in literature to investigate M2 phenotypes [346] and CD40 has been used to identify M1 phenotypes [349]. Using these markers may have revealed additional phenotypic differences in IPF macrophages. Understanding different macrophage phenotypes is useful to identify cells specific to a disease. This enables the identification and isolation of specific cells to further interrogate roles in pathogenesis. Analysing a range of markers, rather than the more traditional M1/M2 status may prove valuable in the identification of disease specific populations.

Research examining macrophage phenotypes is moving away from the M1/M2 paradigm, instead focusing on examining activation of macrophages from environmental cues [180]. CD71 has been reported as a marker of mature macrophages [358, 359], with increased expression reported on macrophages from the bleomycin model of fibrosis [360] and increased expression on macrophages in patients with ILD [357]. Conversely to the latter two reports the data shows a decrease in the percentage of macrophages (CD11c+) expressing CD71 in IPF compared to healthy controls, however, the overall number of CD71+ cells was increased in the IPF BAL compared to healthy control BAL. Analysis of macrophages in IPF BAL revealed an increase in both macrophage CD71- proportion and CD71- cell number. Interestingly the increase in CD71- cell number correlated with FVC decline in ILD patients. However, it remains unclear whether the cell increase is a result of increasingly damaged tissue or whether they are contributing to fibrotic decline. Analysis of (CD11c+) CD71- and CD71+ cell phenotypes using FACS revealed an increase in the expression of both M1 (HLA-DR and CD86) and M2 (CD163 and CD206) markers on CD71+ cells, and an increase in the expression of monocyte marker (CD14) on the CD71- cells. This data, combined with previous reports suggesting CD71 is a marker of maturation on macrophages, suggests the CD71- cells may represent a less mature more monocyte-like cell. However, approximately 70% of CD71- cells express CD206, which is both an M2 marker, but also reported as a marker of airway macrophages in general [148]. The expression of CD71 appeared to develop in a gradient spectrum as opposed to a clear definitive positive/negative expression phenotype. This suggests some CD71- cells may be upregulating CD71 in the airways. Interestingly studies examining cells in the early 1990s using IHC, identified an increase in a monocyte-like-cell in IPF BAL [145, 147]. Although the origins of AMs were thought to be

embryonically derived in healthy mice [156, 157], recent evidence has shown bone marrow derived monocytes are able to differentiate into AMs [158]. This evidence combined with data from **Chapter 1** showing an increase in monocytes in IPF BAL, correlating with an increase in CCL2 in the BAL, and an increase in M-CSF compared to healthy controls, indicates a recruitment of monocytes and differentiation process which may be occurring in the lung. Examination of the morphology of the cells showed that in general the CD71- cells were smaller and less granular but did not appear to be distinctly monocytic in appearance, unlike the CD206-CD14+ cells described in **Chapter 1**. This suggests either a monocyte-macrophage transition, or a distinct slightly smaller macrophage subset, which CD71- cells may represent. Interestingly a series of recent publications have shown that specific deletion of monocyte-derived alveolar macrophages in the bleomycin model of lung fibrosis ameliorate the progression of pathology [72, 364, 365].

As the expression of CD71 was so abundant on AMs next the role of the receptor was examined. CD71 is a transferrin receptor and is involved in the uptake of transferrin into cells, it is expressed on numerous cell types [366], with high levels of expression, as shown, on AMs. As transferrin is a protein which binds iron, preventing it from being freely available to bacteria, which require iron to proliferate [367], genes related to iron were examined in the separated CD71+ and CD71- cells. As expected the gene which encodes the protein CD71 (TFRC) was increased on the CD71+ cells, and the gene encoding iron regulatory protein (IRP) 1, which binds to and stabilises CD71 mRNA [368], was also significantly increased. No differences were observed examining IPR2 expression, suggesting IRP1 is regulating CD71 expression in CD71+ macrophages. The decreased expression of the gene encoding ferriportin, an iron exporter, in CD71+ cells suggests these cells are actively importing and storing iron. A significantly increased percentage of CD71+ cells,

compared to CD71- cells, imported transferrin as measured by FACS. Interestingly iron-laden macrophages have been reported as increased in IPF [369] and here the data shows an increase in the number per mL of BAL of CD11c+CD71+ cells. Transferrin and ferritin are both produced by the liver and are increased/decreased in response to iron homeostasis and during infection [370, 371]. Increased ferritin levels are often used as a marker of low grade inflammation [372], however, transferrin, but not ferritin, levels are significantly increased in IPF BAL. The pathological impact of increased transferrin in IPF airways remains to be elucidated. Studies examining transferrin in animal models of respiratory failure have shown iron laden transferrin exacerbates respiratory failure as a consequence of decreasing surface activity of normal surfactant whereas non-iron laden transferrin showed no effect [373]. Therefore, assessing whether transferrin isolated from IPF patients contained iron may indicate whether or not it is having a direct effect on normal gas exchange. Finally, the expression of CD71 on CD11c cells inversely correlated with transferrin in the airways, suggesting the CD71+ cells are regulating transferrin levels. Taken together the data highlights the important role of CD71+ macrophages in maintaining the homeostasis of iron in the airways. A summary of the possible role of CD71+ cells in the uptake of transferrin and storage of iron is outlined in **Figure 4.19**.

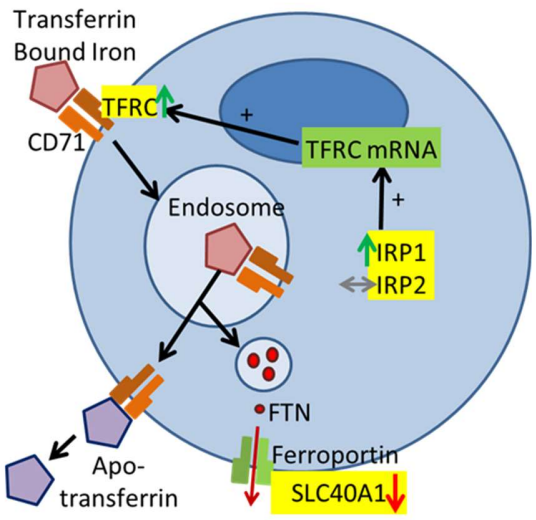


Figure 4.19: Summary of CD71+ cells role in transferrin bound iron uptake.
Illustration of gene up/downregulation in CD71+ cells compared to CD71- cells suggests independent roles in airway iron homeostasis. The arrows show increased (↑), decreased (↓) or the similar expression (↔) on CD71+ cells compared to CD71- cells.

The detection and elimination of pathogens is a key role of the airway macrophage. As the microbiome in IPF patients has been reported as altered, and that an increase in bacterial burden correlated with clinical decline [2, 3], the ability of macrophages to detect and eliminate pathogens in IPF patients and healthy controls, and in the CD71- and CD71+ cells were next examined. The expression of toll like receptor genes TLR2 and TLR3 were significantly increased in the CD71- cells, unfortunately analysis of healthy controls compared to IPF patients could not be performed owing to too few cells for this analysis from the healthy controls. The differences suggest that the ability of the cells to detect gram positive bacteria (TLR2) and to detect viral double stranded RNA (TLR3) differs in the CD71- and CD71+ cells. It is possible that the differing expression results in an altered ability to eliminate infectious agents. Analysis of nitric oxide production and phagocytosis were next examined. The percentage of CD71- cells that were nitric

oxide positive were significantly higher than CD71+ cells, conversely a higher percentage of CD71+ cells phagocytosed bacteria suggesting different roles in the elimination of pathogens. NOS2 involved in nitric oxide production in macrophages [374] was undetected in either cell type and phagocytosis related gene expression including ELMO expression, which is involved in phagocytosis and cell motility [375], and FCGR1 expression, involved in antibody mediated phagocytosis [376] were not differentially expressed comparing the cells. It is possible that other mechanisms could be altered in these cells explaining the differences in nitric oxide production, for example NOS1 and NOS3 involvement [374]. Alternative phagocytosis mechanisms, such as mannose detection linked phagocytosis, may explain why a greater proportion of CD71+ cells phagocytosed bacteria as they expressed significantly more mannose receptor compared to CD71- cells [377]. The ability of IPF derived CD71- and CD71+ cells to phagocytose did not differ compared to healthy controls suggesting increases in bacterial burden in IPF is not as a consequence of impaired phagocytosis. Interestingly nitric oxide production appeared significantly increased in healthy controls compared to IPF patients by both by CD71+ and CD71- cells. Previous studies have shown that nitric oxide inhibits the epithelial to mesenchymal transition, whereby alveolar epithelial cells transition into ECM producing myofibroblasts in the airway [378]. With some clinical reports suggesting that inhaled NO may be beneficial to IPF patients [379], an impaired ability to produce NO by the IPF macrophages may therefore be detrimental in disease pathogenesis.

As the TLR expression significantly differed between CD71- and CD71+ cells, to investigate whether CD71- and CD71+ cells responded in a similar manner to TLR stimulation, CD71- and CD71+ cells were isolated and stimulated with TLR ligands LPS (bacterial gram negative, TLR4

ligand) and Poly: IC (viral dsRNA, TLR3 ligand), and pro-inflammatory mediators were measured in stimulated cell supernatant. Unfortunately, the CD71- cells were virtually absent from the healthy control BAL and the number of CD71+ cells per ml of BAL were too low to carry out separations to compare to ILD, but comparison between the CD71- and CD71+ cells, regardless of diagnosis at baseline and post stimulation revealed no significant differences in pro-inflammatory mediator production. Both CD71- and CD71+ cells increased production of pro-inflammatory mediators in response to LPS stimulation and increased the production of CCL2 and IL-8 in response to Poly: IC stimulation. As previously discussed, Schupp et al (2015), examined total BAL cell production of a number of pro-inflammatory mediators including CCL2, IL-8 and TNFα at baseline demonstrating an increased production of pro-inflammatory mediators in BAL cells from AE IPF compared to stable IPF. The cause for AE in IPF patients is currently unknown; it is possible that AE could be caused by infection, cells isolated from AE IPF patients may have been primed with a bacterial or viral stimulus prior to isolation from the BAL, which would result in the increased production of the pro-inflammatory mediators observed in AE, similar to the increase in pro-inflammatory mediators observed with TLR stimulations here.

Understanding the role of the CD71- and CD71+ cells in the progression of fibrosis is critical in delineating possible sources of disease exacerbation. In order to understand what role the cells may play in fibrosis CD71- and CD71+ cells were separated from 3 IPF patients and examined for expression of fibrotic genes. Analysis of fibrotic gene expression highlighted key differences in expression profiles of the two cell types. The CD71- and CD71+ cells clustered together showing significantly different expression profiles of specific genes related to fibrosis. Examination of chemokine and chemokine receptor expression revealed increased expression of CCL2 and its

receptor CCR2 on CD71- cells. CCR2 expression is thought to be increased on monocytes and involved in M-CSF mediated M2 polarisation [380]. Similarly, there was an increase in the expression of chemokine receptor CXCR4 and chemokine CCL3 (MIP-1α) on CD71- cells. Taken together this suggests CD71- cells may have been recruited into the lung and they may play a role in actively recruiting more cells. Supporting this quantification of IL-8 and CCL2 in CD71- cell supernatant appeared slightly increased compared to CD71+. Conversely expression of pro-inflammatory cytokines such as IL-1α and TNFα was increased in the CD71+ cells suggesting a divergence in the inflammatory roles on these cells.

Expression of integrins significantly differed comparing CD71- and CD71+ cells with expression of ITGB5 and ITGB8 significantly increased, and ITGB1 and ITGAV expression increased on CD71+ cells. Integrins comprise of an alpha chain and a beta chain [381]. ITGB5 and ITGB8 are known to complex with ITGAV to form integrins αVβ5 and αVβ8, which interact with ECM ligands and activate pro-fibrotic mediator TGFβ. αVβ5 and αVβ8 have been shown to be able to bind to Latency associated peptide (LAP) bound TGFβ and activate TGFβ from its inactive LAP bound form [382, 383]. Activation of TGFβ is essential for TGFβ to exert its pro-fibrotic effects. It is interesting that alongside an increase in integrin expression on the CD71+ cells there is also an increase in the expression of members of the TGFβ superfamily including TGFβ1, the receptor TGFβR2, and downsteam signalling proteins SMAD2, SMAD4 and SMAD7, indicating both the production of, and ability to respond to, TGFβ1 signalling [384]. THBS1 which encode thrombospondin 1 (TSP-1) expression is also increased on the CD71+ cells. TSP-1 is known to bind fibrinogen, fibronectin and αVβ1. Interactions of LAP-TGFβ with CD36 and TSP-1 on the surface of macrophages result in the activation and release of TGFβ from LAP-TGFβ [385]. Alongside integrin-dependent

activation of TGFβ there are various integrin independent activation processes. MMP-2 and MMP-9 have been shown to cleave LAP-TGFβ releasing active TGFβ [386]. Interestingly expression of MMP-2 and MMP-9 is increased in CD71- cells suggesting these cells may act in concert with the CD71+ cells, releasing increased concentrations of MMP-2 and MMP-9 further activating TGFβ in the fibrotic lung.

TIMP2 expression was shown to be significantly increased in CD71+ cells whereas TIMP1 expression was increased in CD71- cells. Tissue inhibitors of metalloproteinases (TIMPS) are known to inhibit the MMPs and it was widely believed that an imbalance of TIMPs and MMPs led to fibrosis i.e. increased TIMPs in fibrotic tissue leads to decreased MMP activity resulting in increased ECM deposition [387]. TIMP-2 has also been shown to be increased in areas of pulmonary fibrosis and is known to inhibit MMP-2 [387]. TIMP1 has been shown to be increased in pulmonary fibrosis [387] and is known to inhibit MMP-9, however, their roles are more complex than just MMP inhibition. TIMP-1 KO mice were not protected from bleomycin induced fibrosis, instead knocking out TIMP-1 appeared to exert a pro-inflammatory damaging effect [388]. Contrary to these findings, pro-fibrotic roles for TIMP-1 include promoting fibroblast activation and proliferation though integrin β1 and CD63 [389]. Additional remodelling genes were shown increased on CD71- cells including VEGFA involved in angiogenesis and SERPINE1 encoding plasminogen activator inhibitor-1 (PAI-1). PAI-1 inhibits the enzyme urokinase plasminogen activator (uPA), which is responsible for the cleavage of plasminogen to form plasmin, which in turn mediates the degradation of the ECM [390]. Therefore, PAI-1 plays an important pro-fibrotic role in the inhibition of ECM degradation. SERPINA1, which encodes α-1-antitrypsin, acts in a similar way to PAI-1, primarily inhibiting elastase, but to a lesser extent also

inhibits plasmin and thrombin by irreversibly inhibiting trypsin, chymotrypsin and plasminogen activator [391]. SERPINA1 gene expression is increased on CD71+ cells suggesting divergent production of serine proteases by these cells.

A number of transcription factors were differentially expressed in the CD71- and CD71+ cells. The expression of CEBPB was significantly increased in CD71+ cells and is critically involved in acute phase cytokine production in macrophages, interestingly STAT6 expression is also increased, which has been shown to interact with CEBPB and is critical for IL-4 mediated responses [392]. STAT1 expression is also increased in CD71+ cells and is required for responses to IFN type I, II and III inflammatory responses [393]. Increased expression of both STAT1 and STAT6 in CD71+ cells suggests that these macrophages are able to react to multiple environmental signals as opposed to existing in a polarised state. SP1 and JUN expression is increased in CD71+ cells, which play roles in multiple cellular processes including cell growth, differentiation and apoptosis [394, 395]. Conversely MYC expression is increased in CD71- cells. MYC plays a key role in cell cycle progression and has been shown to be critical in differentiating monocytes into osteoclasts [396], a specialised bone tissue macrophage, suggesting a possible role for MYC differentiation in CD71- cells. BCL2 is also increased in CD71- cells, which plays role exerting anti-apoptotic effects [397]. Interestingly the AKT1 encoding serine-threonine kinase is increased in CD71+ compared to CD71-. This gene was reported increased in macrophages from IPF patients compared to healthy by Larson-Casey and colleagues (2016) leading to mitophagy, anti-apoptotic effects and TGFβ1 release in mouse [193]. It would be interesting to examine genes from isolated macrophages from healthy controls to further understand the differential role of the macrophage in fibrosis.

Growth factors play key roles in mediating pro-fibrotic effects such as matrix remodelling and also aid cellular differentiation [398]. Analysis of growth factors produced by CD71- and CD71+ cells at baseline and in response to TLR stimulation with LPS revealed an increase in G-CSF, GM-CSF and M-CSF production. G-CSF, GM-CSF and M-CSF are important mediators of granulocyte and macrophage differentiation [399] suggesting CD71- and CD71+ cells are able to produce and respond to these mediators in the presence of bacterial stimulation. Poly: IC increased the production of M-CSF without increasing the production of any other growth factor. Data from **Chapter 1** showed an increase in the levels of M-CSF in the BAL supernatant of IPF patients compared to healthy controls and this growth factor is thought to aid the differentiation of macrophage into an M2 phenotype [380]. Concentrations of M-CSF appeared higher in the CD71+ Poly: IC stimulated supernatant compared to CD71-. Stimulation of both CD71- and CD71+ cells with rhTGFβ1 induced an increase in TGFα expression, but not other growth factors. Interestingly a mouse model overexpressing TGFα resulted in a pulmonary fibrotic phenotype [400], alongside this TGFα staining in IPF patient lung is increased compared to healthy lungs [387] suggesting a role promoting fibrosis.

To examine CD71- and CD71+ macrophages in context with cells they would interact with in the airways, a co-culture was set up whereby CD71- and CD71+ cells isolated from IPF patient BAL were cultured separately or in combination with the same healthy donor isolated BEC. Gene expression in the BEC was then examined to see if either or both cell types induced an upregulation of pro-fibrotic mediators in the BECs. Key pro-fibrotic mediator TGFβ1 expression in BECs was down-regulated in co-culture as well as genes encoding components of ECM such as COL1A1, encoding collagen type 1 α1 chain, FN1, encoding fibronectin and CTGF, encoding

connective tissue growth factor, which promotes ECM deposition [401]. Taken together this data suggest that the CD71- and CD71+ cells play a protective role in fibrosis. However, there are a number of caveats with this work, firstly the BECs used for the interaction were from another donor and so the macrophages may have adversely reacted with the BECs, secondly BECs may have interacted differently with the CD71-/+macrophages compared to other epithelial cell types such as small airway or alveolar epithelial cells. Furthermore, examination of the response of an IPF-BEC may differ compared to observations reported here from a healthy control BEC. Additionally, fibroblasts are still widely regarded as the drivers of ECM matrix deposition, so examination of the interactions of CD71- and CD71+ cells with fibroblasts may highlight a role for the CD71-/+ cells in promoting ECM deposition by fibroblasts. It is likely AMs would directly interact with fibroblasts owing to the epithelial cell death and aberrant fibroblast proliferation in the IPF lung. Finally, the time point for gene examination may have not been the most appropriate, with gene changes perhaps differing at later or even earlier time points.

In order to examine the impact of the CD71- and CD71+ cell on ECM deposition an assay quantifying the deposition of collagens I and III, fibronectin and collagen IV by primary small airway epithelial cell (SAEpC) and IPF fibroblasts (IPF134) co-culture was used to examine the effects of CD71-/+ cellular mediators on ECM production. This assay revealed CD71- cell mediators in supernatants stimulated increased collagen IV deposition compared to CD71+ cell mediators, both from unstimulated cells, and from CD71-/+ LPS stimulated cells. Collagen IV forms the basement membrane of the ECM, acting to anchor and polarise epithelial cells [402]. Interestingly, increased serum levels of collagen IV have been reported in IPF patients, with increased collagen IV serum levels associated with poor prognosis [403] and dry collagen IV

weight is reported increased in other fibrotic diseases including liver fibrosis [404]. However, collagens I and III have been previously reported as increased in the fibrotic lung, not collagen IV [405]. It is also possible the window for collagen I and III and fibronectin quantification was missed as increased deposition may have been found at an earlier time point. This data may represent an earlier phenomenon in the development of fibrosis or indicate the importance of CD71- cells in wound healing. It is possible that the CD71- cells have been recruited into the lung as they share a phenotype similar to both monocytes and macrophages as previously discussed. The aforementioned publications indicated recruited monocytes into the murine bleomycin induced lung fibrosis, contributed to the fibrotic pathology, with the resident macrophage population playing a limited role in progression of fibrosis [72, 364, 365]. CD71- cells identified here may represent a recruited monocyte transitioning into an AM highlighted in the murine fibrotic model. The increased collagen IV deposition in response to CD71- derived mediators suggests a possible mechanism by which these cells may contribute to IPF. It would be interesting to examine how whole CD71-/+ cells would influence matrix deposition in the SAEpC/IPF134 cell co-culture.

In conclusion CD11c+ macrophage subsets have been identified in IPF patients and are separated by high or low levels of CD71 expression. Analysis of the proportion of either CD11c+ CD71-/+ macrophages which phagocytose fluorescently labelled bacteria revealed no differences comparing healthy control macrophages to IPF macrophages. However, production of NO appeared increased in both CD11c+ CD71-/+ healthy control macrophages compared to IPF CD11c+ CD71-/+ macrophages. Further analysis would be necessary to confirm the functional phenotype of IPF derived macrophages in host airway defence, including examination of the

production of proinflammatory mediators by healthy controls macrophages compared to IPF macrophages. The proportion of CD11c+ cells which are CD71- is significantly increased in IPF compared to healthy controls and both CD71- and CD71+ cell numbers are increased in IPF compared to healthy controls. An increase in CD71- cell number correlated with FVC clinical decline in ILD patients, suggesting a marker of poor prognosis, or possible contribution of CD71- cells to pathology. CD71- and CD71+ cells differ from one another significantly in protein expression, gene expression and function in the airways, with several differences found analysing the expression of fibrotic genes, suggesting divergent roles in fibrosis pathology. Finally, CD71- cell supernatants appeared to increase collagen IV deposition by SAEpC and IPF fibroblasts suggesting mediators produced by CD71- cells are able to drive fibrotic ECM deposition by SAEpC and IPF fibroblasts. Further interrogation of the CD11c+CD71- cells in lung fibrotic tissue would provide clues as to whether they are increased in fibrotic regions. Additionally, a direct comparison of supernatant stimulation of SAEpC and IPF fibroblasts with healthy control CD11c+CD71- supernatants would validate whether this is an IPF specific function of the CD11c+CD71- cells or a more general function of the cells in inducing ECM deposition.

4.5.1. Summary of CD71- and CD71+ functional phenotypes

Figure 4.20 summarises differences in protein expression, gene expression and function of the CD71- and CD71+ cells.

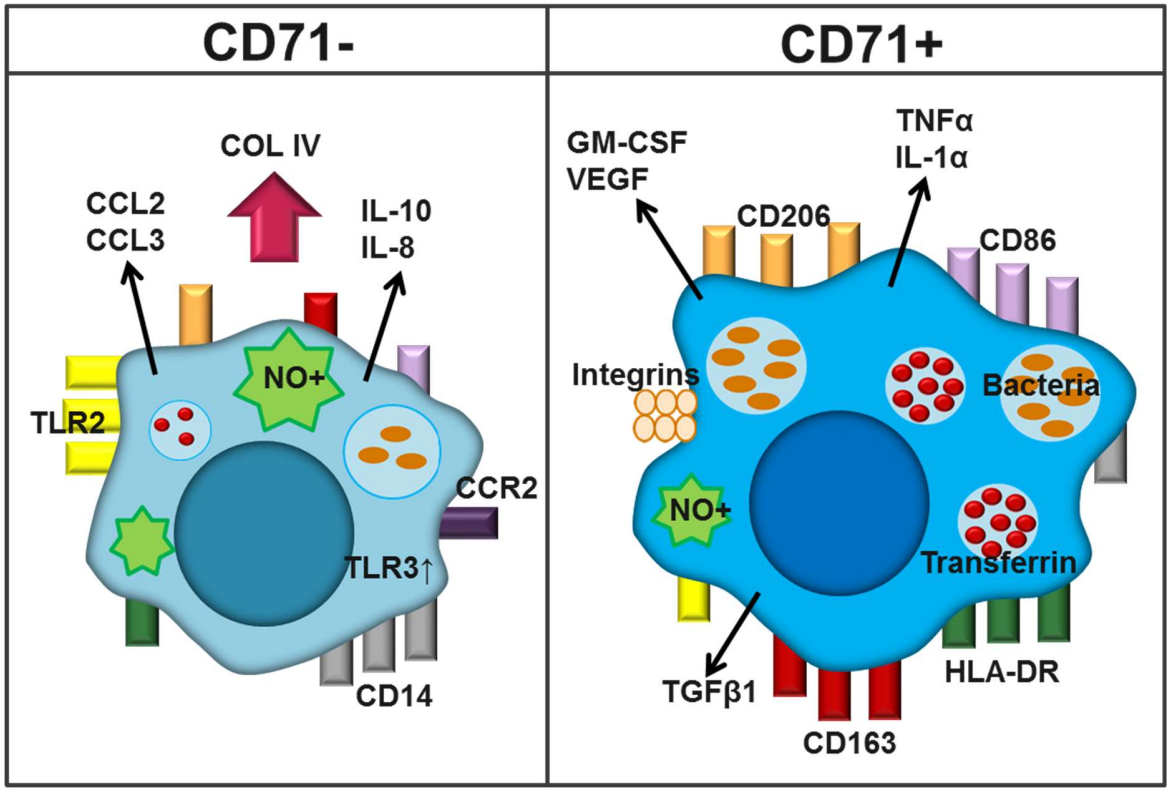


Figure 4.20: Summary of CD11c+ CD71+/CD71- Macrophage phenotypic and functional differences.

5. Investigation into the effects of TLR stimulation on IPF and healthy bronchial epithelial cells and fibroblasts

5.1. Introduction

Maintaining homeostasis within the airways is critical in preserving healthy lung function. Complex processes involving a multitude of different mediators, multi-cellular interactions, activation of appropriate cellular pathways and recruitment of specific cells after injury act in concert to maintain equilibrium. Continual insults to the airways can result in the onset of pathologies such as ILD, which may progress into lung fibrosis. Although the cause of onset of specific ILDs have been determined, such as specific repeat environmental exposure in cHP, or autoimmune antibody interactions in UCTD, the causal insult that initiates and potentiates IPF remains to be elucidated. Data from previous chapters have highlighted an altered environment in both the presence of extracellular mediators in IPF BAL fluid but also the composition and activation of specific leukocytes in the airways, however, the direct contribution of the stromal cells remain to be determined. Stromal cells have been shown to be important not only in airway defence and leukocyte recruitment but also in direct contribution to IPF pathology. Epithelial cells and fibroblasts are known to be able to produce chemokines that recruit cells into the airways and may act as pro- or anti-angiogenics [406]. The initiation of fibrosis in IPF is believed to result from continual damage to the alveolar epithelial layer, leading to an aberrant wound healing response involving the activation and differentiation of fibroblasts into myofibroblasts with a subsequent overproduction of extracellular matrix (ECM). The initial and subsequent insults to the epithelium remain to be determined.

As bacterial and viral infections are reportedly increased in IPF [26, 257-260, 266-268] it is essential to investigate the role they might play in fibrosis. Investigation into whether a variety of different stimuli, with focus on bacterial or viral ligand stimulation, inducing an appropriate pro-inflammatory and/or inappropriate pro-fibrotic response in primary stromal cells isolated from healthy controls compared to IPF patients is therefore required.

Progression of IPF is a complex multifaceted sequence of events involving combinations of multiple cell types, signalling pathways, mechanical stress, genetic susceptibility and environmental damage. The initiation of IPF is thought to involve damage to the epithelial cells and progression is believed to result from the proliferation of myofibroblasts producing excessive and dysregulated ECM. The initial trigger, or indeed the triggers, that progress the disease remain to be elucidated. With multiple polymorphisms associated with TLR and defence signalling, combined with data showing an increase in bacterial burden and possible viral exacerbation, investigation in to how epithelial cells and fibroblasts from IPF patients respond to bacterial and viral challenges is critical.

5.2. Hypothesis

The increased bacterial burden reported in the IPF airways results from impaired host inflammatory responses. IPF primary stromal cells, compared to healthy control primary stromal cells, will exhibit a defective inflammatory response to stimulation with bacteria and bacterial mimetic TLR ligands, as a result of abnormal TLR signalling. Furthermore, bacterial stimulation will result in increased pro-fibrotic gene and protein expression in IPF stromal cells compared to healthy control stromal cells.

5.3. Aims

- Examine inflammatory and fibrotic changes using gene and protein expression analysis of mediators involved in TLR signalling, inflammation and fibrosis, in primary healthy control and IPF epithelial cells and fibroblasts, in response to challenge with heat killed bacterial and TLR stimulation.
- Investigate pro-inflammatory and pro-fibrotic responses to paracrine signalling between epithelial cells and fibroblasts in response to bacterial and TLR ligand stimulation.
- Quantify fibroblast proliferation in response to direct heat killed bacterial or TLR ligand stimulation. Furthermore, investigate the effects of paracrine signalling from healthy and IPF epithelial cells stimulated with heat killed bacteria or TLR ligands on fibroblast proliferation.

5.4. Results

In order to investigate the response of the bronchial epithelial cells (BEC) to viral or bacterial pathogens, primary BECs from 5 healthy individuals and 6 individuals with IPF were isolated, cultured and stimulated with either of the following; TLR ligands, LPS (bacterial, TLR4 ligand) or Poly: IC (viral, TLR3 ligand); heat killed bacteria genera known to be increased in IPF, *Streptococcus pneumonia* (HKSP) or *Haemophilus influenzae B* (HKHIB); or pro-fibrotic stimulation with recombinant human (rh)TGFβ1. These conditions were then compared to unstimulated controls. Relative gene expressions (relative to housekeeping gene) were determined to compare the expression of genes in IPF BECs to healthy BECs. All relative gene expression analysis for BECs is included in the appendix 8.3; **Figure 8.3.1- 8.3.3**. Any significant differences in relative gene expression are highlighted and discussed in these results.

5.4.1. BEC stimulation pro-inflammatory gene analysis

Fold-change in gene expression of pro-inflammatory mediators were investigated post stimulation to assess BEC response to TLR agonists. BECs from both healthy controls and IPF patients showed significant upregulation of genes encoding IL-6 (**Figure 5.1A**), IL-8 (**Figure 5.1B**) and CCL2 (**Figure 5.1C**) in response to Poly: IC stimulation. rhTGFβ1 stimulation increased expression of IL-6 in healthy controls and IPF BECs (**Figure 5.1A**). The observed similarities in response to these specific TLR stimulations suggests IPF BECs respond in a similar manner to healthy controls BECs.

Analysis of the aforementioned pro-inflammatory genes provides a snap shot into pro-inflammatory mediator production by BECs. To investigate broader aspects of TLR signalling both

TLR gene expression (**Figure 5.2**) and genes downstream of TLR signalling were next determined (**Figure 5.3**). In IPF BECs TLR2 fold regulation was significantly increased in response to Poly: IC stimulation (**Figure 5.2A**). Similarly, Poly: IC stimulated cells showed increased expression of TLR3 compared to unstimulated controls in both healthy control and IPF BECs (**Figure 5.2B**). Conversely, TLR4 expression remained similar comparing stimulated to unstimulated cells (**Figure 5.2C**), indicating TLR4 gene regulation is not altered with the investigated TLR stimulation.

Further to TLR receptor gene expression analysis, genes involved in the TLR signalling pathway including; IRAK1, which is downstream of both TLR2 and TLR4 signalling, TOLLIP, which negatively regulates TLR signalling, and IRF3, which is downstream of TLR3 signalling, were investigated. IRAK1 fold regulation was increased in IPF LPS stimulated cells compared to IPF unstimulated control (**Figure 5.3A**). Relative to housekeeping control gene, expression of IRAK1 was significantly decreased in unstimulated IPF BECs compared to unstimulated healthy control BECs (**Figure 5.3B**). This data highlights baseline differences between healthy control and IPF BECs, suggesting signalling with IRAK1 may be impaired in IPF BECs. TOLLIP fold regulation did not differ in stimulated compared to unstimulated controls (**Figure 5.3C**). Interestingly the relative expression of TOLLIP was significantly decreased in unstimulated IPF BECs compared to unstimulated healthy control BECs (**Figure 5.3D**), indicating the negative regulator TOLLIP is decreased at baseline in IPF BECs, possibly resulting in aberrant TLR signalling in IPF BECs. The expression of IRF3 did not differ with stimulations or comparing healthy controls to IPF BECs (**Figure 5.3E**).

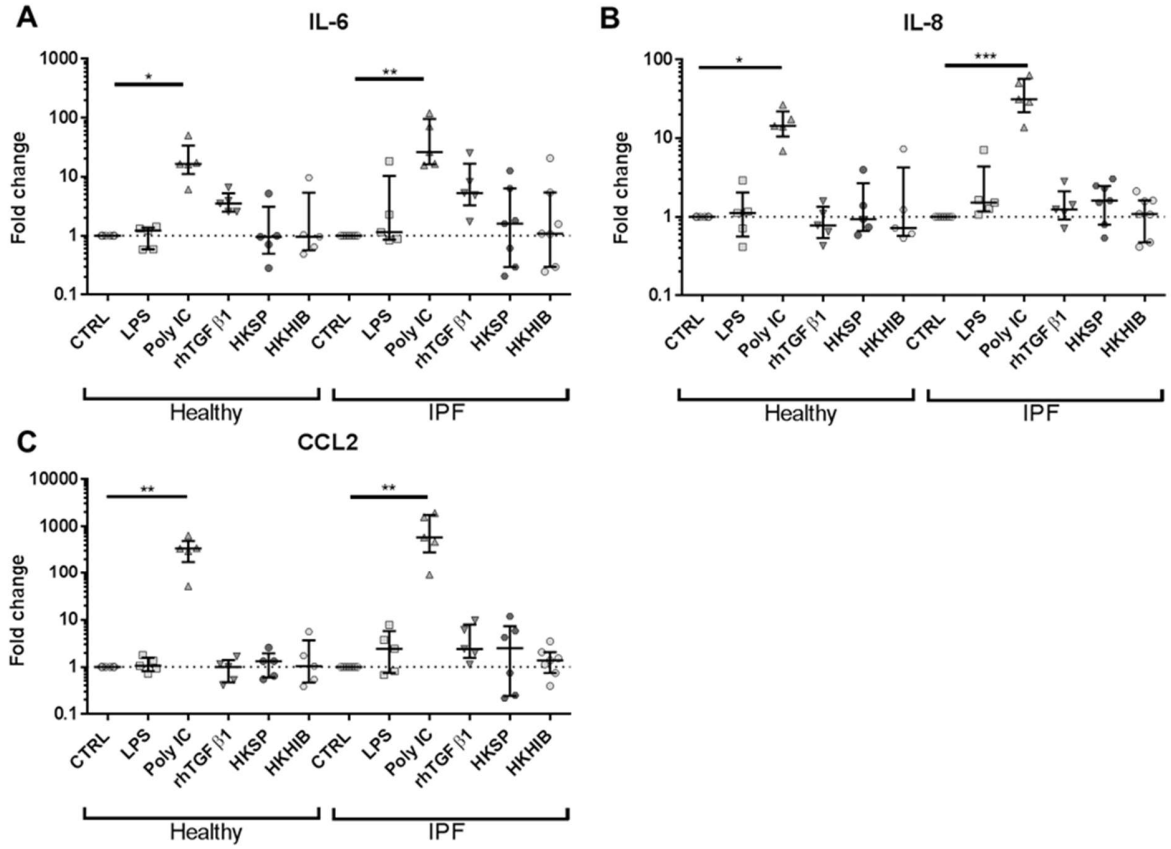


Figure 5.1: BEC stimulation: Pro-inflammatory gene expression analysis.
Gene expression analysis showing fold change of genes IL-6 (A), IL-8 (B) and CCL2 (C) in stimulated healthy (n=5) and IPF BECs (n=6). Fold change expression examines unstimulated controls compared to stimulated LPS, POLY: IC, recombinant human TGFβ1 (TGFB1), heat killed streptococcus pneumoniae (HKSP) and heat killed haemophilus influenza B (HKHIB) cells. Median and interquartile range is shown. Statistical analysis Kruskal-Wallis test with Dunn's multiple comparison was used to compare healthy or IPF cell stimulations * $p<0.05$, ** $p<0.01$, ***$p<0.001$.

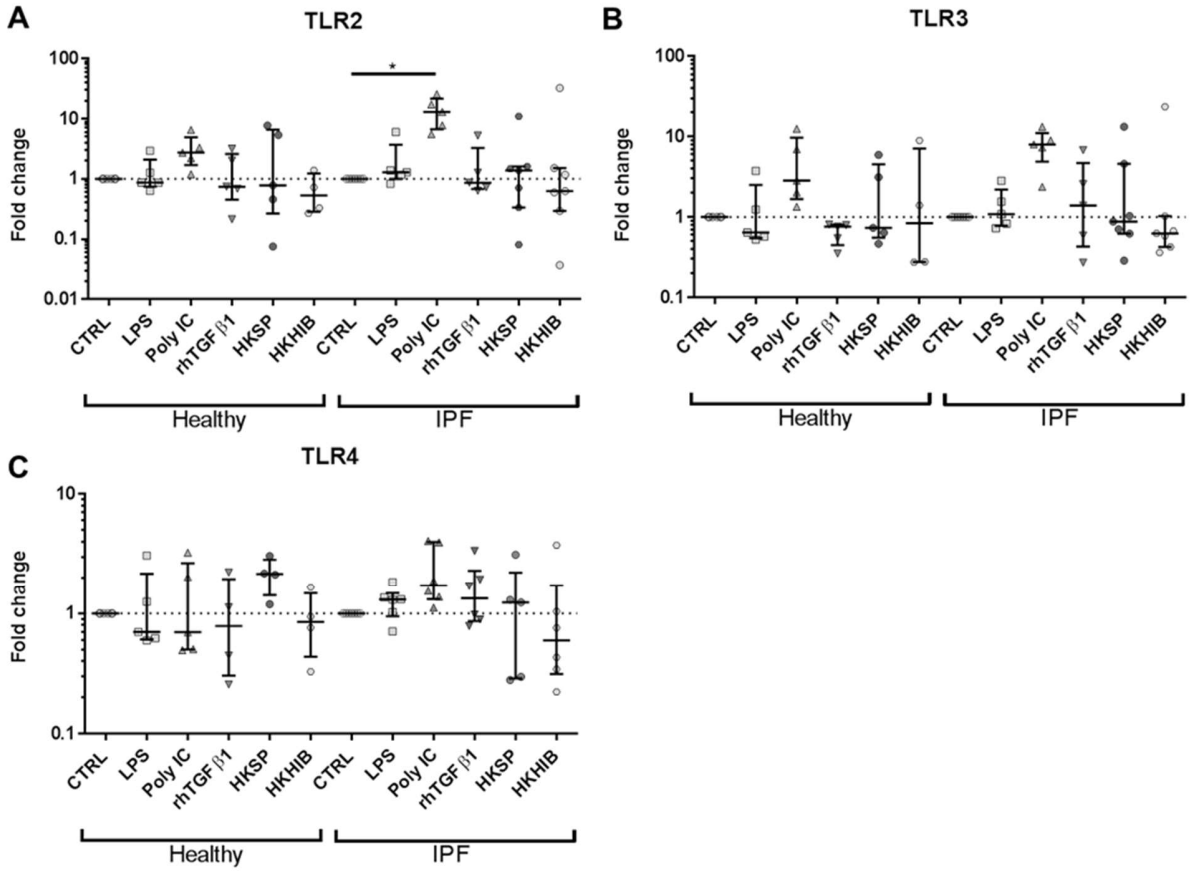


Figure 4: BEC stimulation: TLR gene expression analysis.
Gene expression analysis showing fold change of genes TLR2 (A), TLR3 (B) and TLR4 (C) in stimulated healthy and IPF BECs. Fold change expression examines unstimulated controls compared to LPS, POLY: IC, recombinant human TGFβ1 (TGFB1), heat killed streptococcus pneumoniae (HKSP) and heat killed haemophilus influenza B (HKHIB) stimulated cells. Median and interquartile range shown for healthy (n=5) and IPF BECs (n=6). Statistical analysis Kruskal-Wallis test with Dunn's multiple comparison was used to compare healthy or IPF cell stimulations * $p<0.05$.

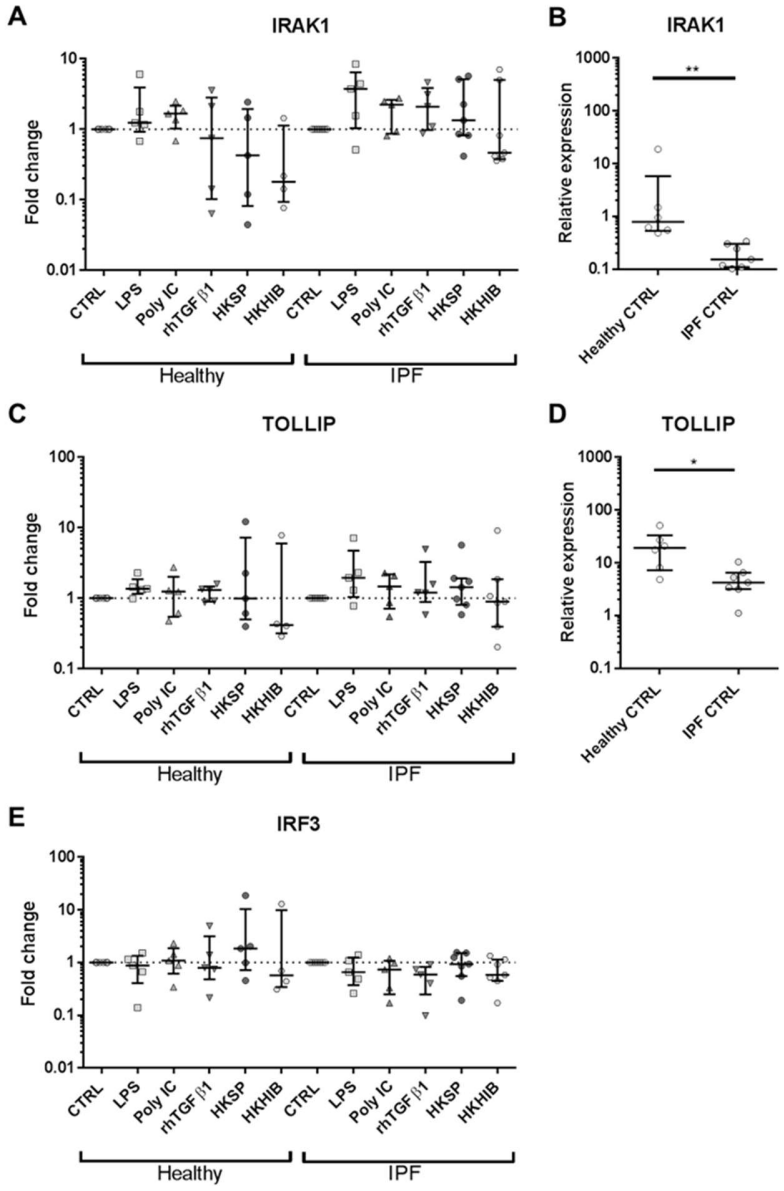


Figure 5.3: BEC stimulation: TLR mediator gene expression analysis.
Gene expression analysis showing fold change and relative expression of genes IRAK1 (A-B), TOLLIP (C-D) and fold change only for IRF3 (E). Fold change expression examines unstimulated controls compared to LPS, POLY: IC, recombinant human TGFβ1 (TGFB1), heat killed streptococcus pneumoniae (HKSP) and heat killed haemophilus influenza B (HKHIB) stimulated cells. Relative expression, relative to housekeeping control GAPDH, compares unstimulated controls. Median and interquartile range shown for healthy (n=5, or unstimulated n=6) and IPF BECs (n=5, or unstimulated n=7). Statistical analysis Kruskal-Wallis test with Dunn's multiple comparison was used to compare healthy or IPF cell stimulations. Comparison between healthy and IPF controls were examined using Mann Whitney T test * $p<0.05$, ** $p<0.01$.

5.4.1. BEC stimulation pro-fibrotic gene analysis

In order to examine how stimulation of BEC TLRs may influence the progression of fibrosis, both specific TLR ligands; gram negative bacterial wall component and TLR4 ligand, LPS, and viral synthetic dsRNA TLR3 ligand, Poly: IC, or heat killed bacterial challenge, were used to stimulate primary BECs from healthy controls and IPF patients. Following from stimulation expression of key pro-fibrotic mediators including TGFβ1 and TGFβ receptor 2, (TGFβR2) were examined. TGFβ1 gene expression was assessed post Poly: IC stimulation revealing a significant fold upregulation of TGFβ1 in IPF BECs (**Figure 5.4A**). Likewise, rhTGFβ1 stimulation induced a significant increase in fold expression of TGFβ1 in IPF BECs (**Figure 5.4A**). Taken together this suggests Poly: IC stimulation is pro-fibrotic. TGFβR2 analysis of fold change revealed no differences (**Figure 5.4B**).

Increased deposition of ECM is a hallmark feature of fibrosis. Stimulation with pro-fibrotic rhTGFβ1 resulted in an increase in expression of CTGF, a mediator of ECM, in healthy BECs, with a significant increase in expression in stimulated IPF BECs, compared to paired unstimulated controls (**Figure 5.5A**). LPS stimulation of IPF BECs, but not LPS stimulation of healthy control BECs, appeared to increase CTGF expression (**Figure 5.5A**). Examination of genes encoding ECM proteins fibronectin and collagen-1α1 (COL1A1) revealed all stimulations of IPF BECs induced an upregulation in Fibronectin-1 gene expression compared to unstimulated controls (**Figure 5.5B**). COL1A1 fold expression after Poly: IC and rhTGFβ1 stimulation appeared to increase in healthy control and IPF BECs compared to unstimulated controls (**Figure 5.5C**).

A summary of the median values of all gene fold up/down-regulation in healthy and IPF BEC, including fold change in gene expression comparing healthy controls and IPF controls, are shown in **Table 5.1**.

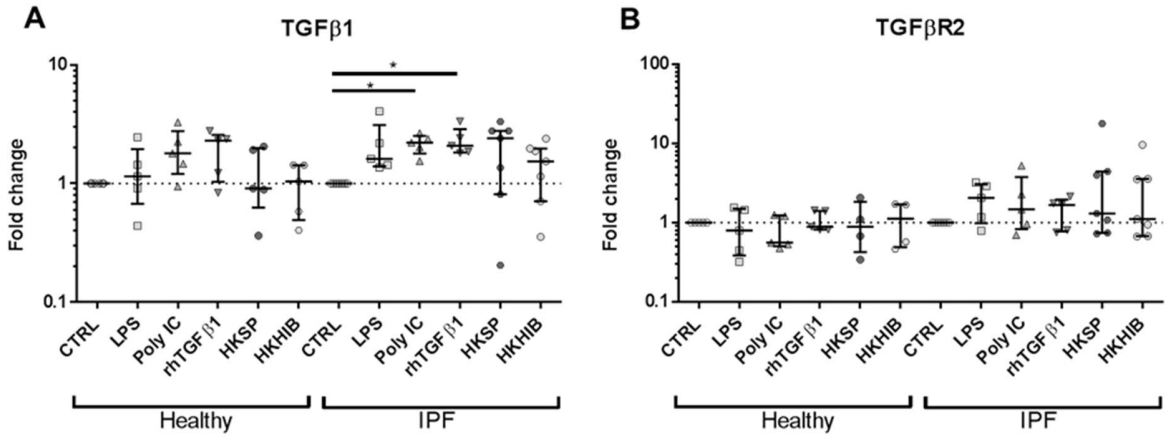


Figure 5.4: BEC stimulation: TGFβ gene expression analysis.
Gene expression analysis showing fold change of genes TGFβ1 (A) and TGFβR2 (B) in stimulated; LPS, POLY: IC, recombinant human TGFβ1 (TGFB1), heat killed streptococcus pneumoniae (HKSP) and heat killed haemophilus influenza B (HKHIB) conditions in healthy and IPF BECs compared to paired unstimulated controls (CTRL). Median and interquartile range is shown for healthy (n=5) and IPF BECs (n=5). Statistical analysis Kruskal-Wallis test with Dunn's multiple comparison was used to compare healthy or IPF cell stimulations * $p<0.05$.

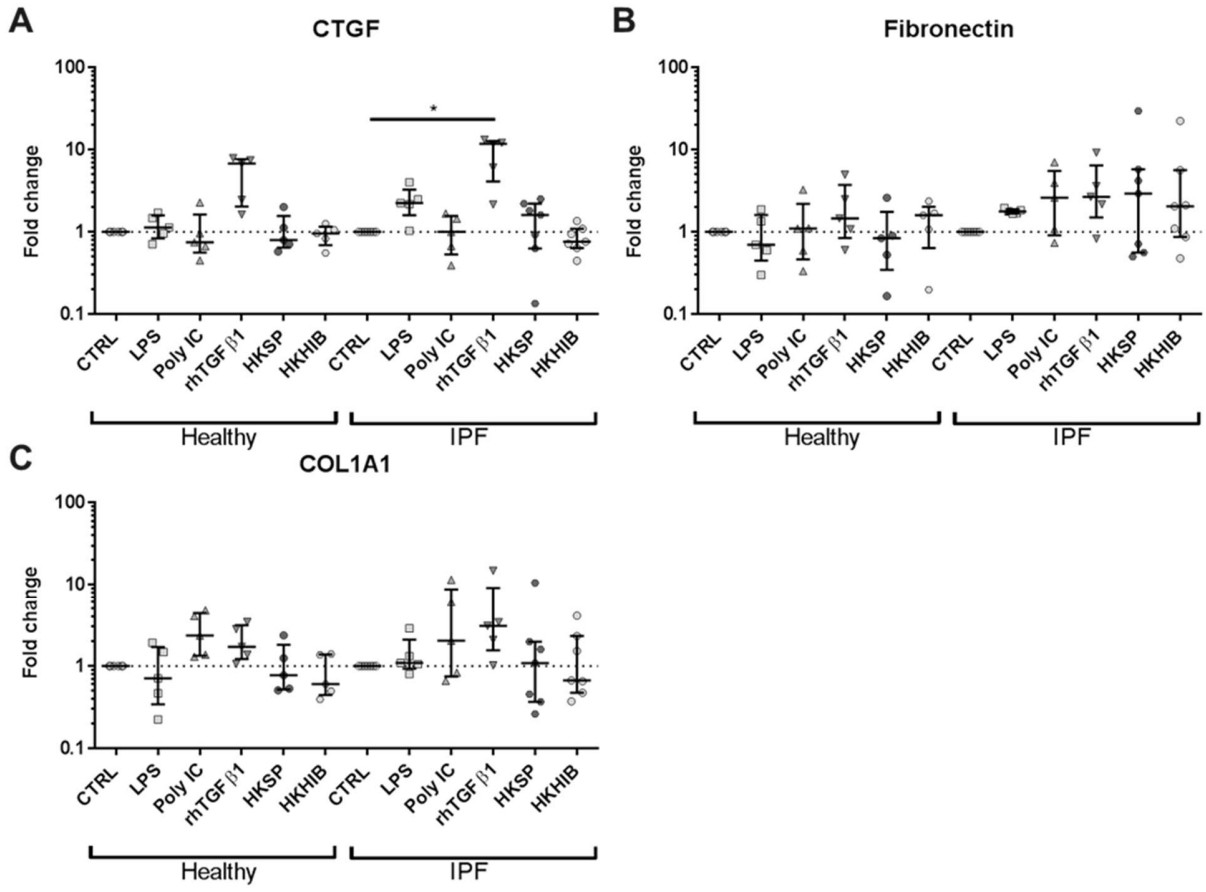


Figure 5.5: BEC stimulation: ECM gene expression analysis.
Gene expression analysis showing fold change of genes CTGF (A), FN1 (fibronectin) (B) and COL1A1 (C) in stimulated; LPS, POLY: IC, recombinant human TGFβ1 (TGFB1), heat killed streptococcus pneumoniae (HKSP) and heat killed haemophilus influenza B (HKHIB) conditions in healthy and IPF BECs compared to paired unstimulated controls (CTRL). Median and interquartile range is shown for healthy (n=5) and IPF BECs (n=5). Statistical analysis Kruskal-Wallis test with Dunn's multiple comparison was used to compare healthy or IPF cell stimulations * $p<0.05$.

		Fold change ($2^{-\Delta\Delta CT}$) compared to healthy unstimulated												
		Healthy n=5/6						IPF n=5/7						
Gene Role	Gene	Ctrl	LPS	Poly: IC	rh-TGFβ1	HK SP	HK HIB	Ctrl	LPS	Poly: IC	rh-TGFβ1	HK SP	HK HIB	Ctrl IPF vs Ctrl Healthy
TGFB1	TGFβ1	1	1.34	2.80	1.04	1.31	0.68	1	1.07	1.62	1.64	1.64	1.48	0.50
	TGFβ-R2	1	0.80	0.54	0.82	0.83	0.75	1	1.50	2.74	1.67	3.11	3.58	0.22
Collagen ECM	COL-1A1	1	0.85	2.50	2.06	0.98	0.90	1	0.91	1.21	1.09	0.72	0.64	0.94
ECM	CTGF	1	1.85	1.43	4.00	1.84	1.83	1	3.89	1.54	12.23	0.82	0.99	0.50
	FN1	1	1.28	1.26	3.12	1.00	1.28	1	0.75	1.51	1.98	0.94	1.31	0.31
Pro-inflam mediator	IL-6	1	1.19	16.77	4.98	0.69	0.94	1	0.84	15.80	8.21	0.74	0.62	1.27
	IL-8	1	1.37	17.68	0.98	1.93	1.76	1	1.64	23.01	0.95	2.31	1.28	1.28
	CCL2	1	0.97	408.73	0.92	0.76	2.03	1	1.17	491.14	2.01	4.56	1.38	0.51
TLR	TLR2	1	0.73	3.28	0.70	1.96	0.48	1	0.69	6.42	0.56	1.03	0.72	0.67
	TLR3	1	1.15	5.04	0.59	1.44	0.55	1	0.47	3.92	0.38	2.00	1.31	0.56
	TLR4	1	1.27	1.34	0.70	2.91	0.37	1	0.69	0.81	0.50	1.32	0.76	0.47
TLR Signalling	TOL-LIP	1	0.91	0.52	0.84	0.57	0.27	1	1.95	1.34	1.30	1.43	1.11	0.22
	IRAK1	1	1.30	1.49	1.51	0.35	0.13	1	2.89	1.84	2.20	2.64	0.74	0.20
	IRF3	1	0.52	1.19	0.43	0.62	0.38	1	0.88	0.64	0.39	1.02	0.73	0.52

Table 5.1: Summary of BEC stimulation median gene fold change compared to unstimulated control cells.

Red cells indicate an increase of over 2 fold (≥2) expression and blue represent a 2 fold decrease (≤0.5) or lower. The last column represents median gene fold change for unstimulated cell gene expression comparing IPF to healthy, showing decreased expression of a number of genes in IPF BECs.

5.4.2. BEC stimulation chemokine and cytokine analysis

To verify gene expression analysis of up-regulated pro-inflammatory genes, and to further examine the pro-inflammatory response of BEC to TLR stimulation, chemokines and cytokines were measured in the supernatant of stimulated healthy control and IPF BECs 24 hours post stimulation. Analysis of chemokines in the supernatant revealed an increased production of a number of chemokines in response to Poly: IC stimulation only. CXCL9, CXCL10, CXCL11, CCL3, CCL4, CCL5, CCL11, CCL17, CCL20, CXCL1 and CXCL5 were all increased in the supernatant post Poly: IC stimulation compared to unstimulated controls in both healthy control and IPF BEC supernatants (**Figure 5.6A-K** respectively). Chemokine production of CCL3, CCL4 and CCL20 in response to Poly: IC stimulation appeared increased in healthy compared to IPF (**Figure 5.6D-E** and **I** respectively). Examination of IL-6, IL-8 and CCL2 levels in the supernatants post stimulation revealed increased levels in the supernatants of healthy control and IPF Poly: IC stimulated cell supernatants compared to unstimulated cell supernatants (**Figure 5.7A, B** and **C** respectively). Taken together the inflammatory chemokine and cytokine data suggests Poly: IC, TLR3 stimulation, but not LPS, TLR4 or bacterial stimulation, induces BEC mediated inflammation.

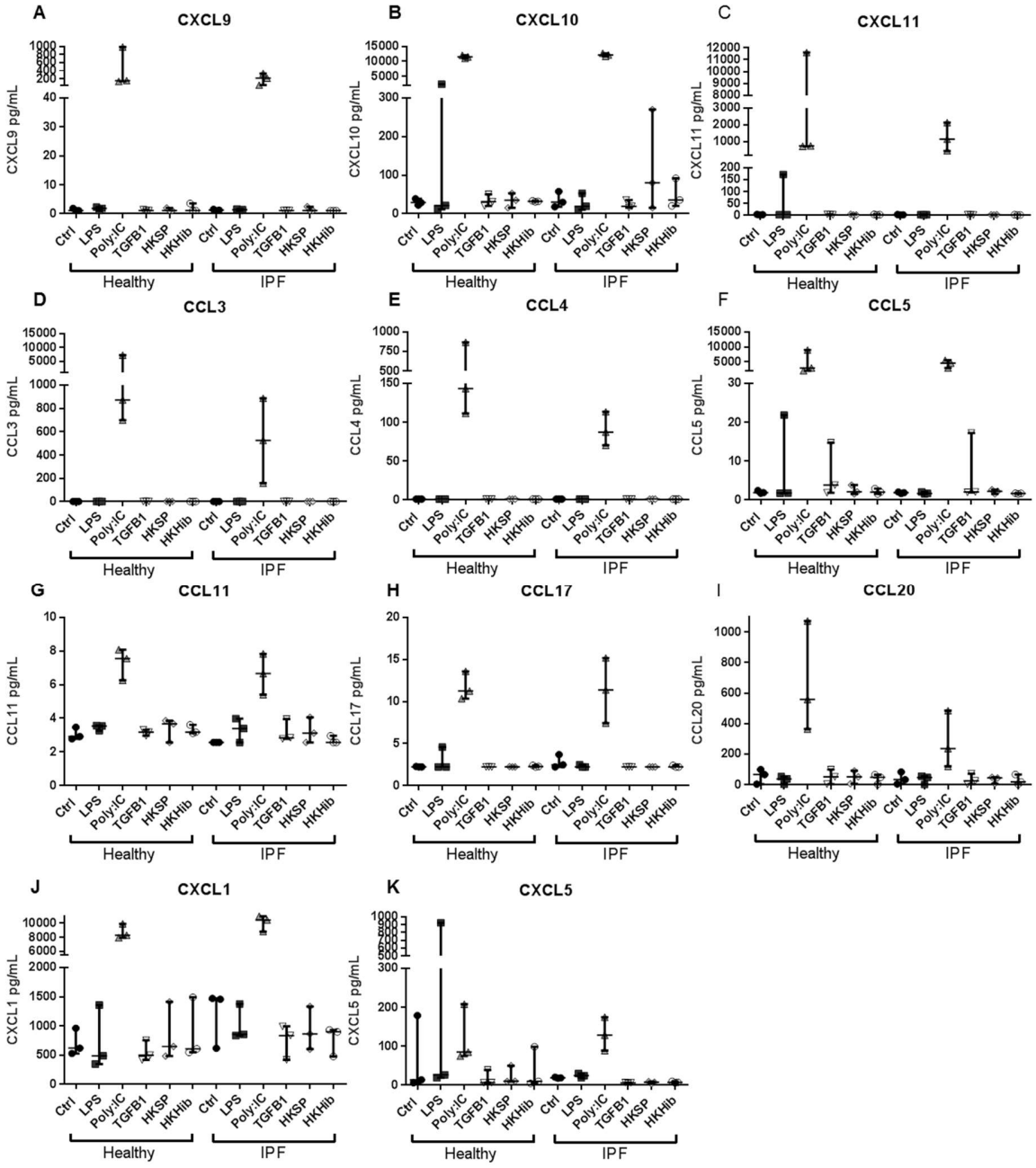


Figure 5.6: BEC stimulation: Chemokine production analysis.
Chemokines from supernatant of BEC (pg/mL) in unstimulated control (CTRL) and stimulated; LPS, POLY: IC, recombinant human TGFβ1 (TGFB1), heat killed streptococcus pneumoniae (HKSP) and heat killed haemophilus influenza B (HKHib) conditions. Median and interquartile range (pg/mL) is shown for CXCL9, CXCL10, CXCL11, CCL3, CCL4, CCL5, CCL11, CCL17, CCL20, CXCL1 and CXCL5 in A-K respectively. Statistical analysis using Friedman test with Dunn's multiple comparison to compare healthy (n=3) or IPF (n=3) cell stimulations. Comparison between the same stimulation in healthy and IPF was examined using Mann Whitney U T test.

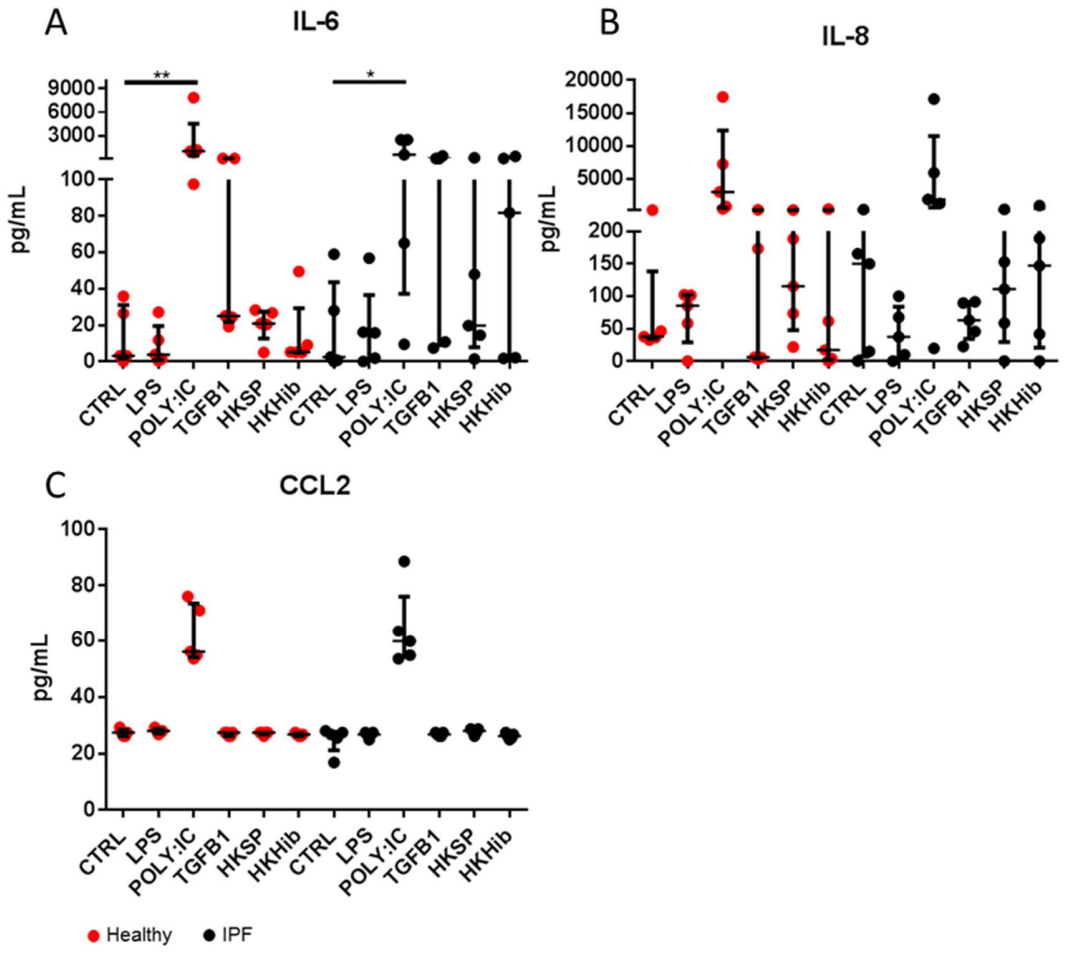


Figure 5.7: BEC stimulation: Pro-inflammatory cytokine and chemokine production analysis. IL-6 (A), IL-8 (B) and CCL2 (C) pg/mL were measured in healthy (n=5) (●) and IPF (n=5) (●) BEC supernatants in unstimulated control (CTRL) and stimulated LPS, POLY: IC, recombinant human TGFβ1 (TGFB1), heat killed *streptococcus pneumoniae* (HKSP) and heat killed *haemophilus influenza B* (HKHib) conditions. Median and interquartile range is shown. Statistical analysis using Friedman test with Dunn's multiple comparison to compare cell stimulations * $p<0.05$, ** $p<0.01$. Comparison between the same stimulation in healthy and IPF was examined using Mann Whitney U T test revealing no significant differences.

5.4.3. BEC stimulation growth factor analysis

BECs play active roles in the wound healing process, and therefore fibrosis, by the production of growth factors which influence angiogenesis [407], fibroblast proliferation and differentiation [408]. Alongside these direct effects, BECs produce growth factors which differentiate leukocytes, such as macrophages [409], which play a role in fibrosis [193]. To examine the impact of bacterial or viral TLR ligand stimulations on growth factor production, multiplex analysis of BEC supernatants post stimulation were conducted. G-CSF and GM-CSF were increased in response to Poly: IC stimulation (**Figure 5.8A** and **B** respectively). M-CSF was increased in response to both LPS and Poly: IC stimulation in healthy and IPF BEC supernatants (**Figure 5.8C**). Angiopoietin, FGF basic and SCF levels remained similar across stimulations (**Figure 5.8D, E** and **F** respectively), and VEGF was significantly increased in response to Poly: IC stimulation in IPF BECs (**Figure 5.8G**). PDGF-AA and PDGF-BB levels remain the same (**Figure 5.8H** and **I** respectively). TGFα levels were significantly increased in response to Poly: IC stimulation in both healthy and IPF BEC supernatants (**Figure 5.8J**) with levels of TGFα higher in IPF Poly: IC compared to healthy Poly: IC supernatant (**Figure 5.8J**). TGFβ1 concentration in the supernatant of the rhTGFβ1 stimulated BECs were increased compared to unstimulated control. The levels of TGFβ1 in the supernatant were higher than the levels of rhTGFβ1 spiked supernatant alone (spiked at the same concentration as stimulation, indicated by the dashed lines on graph) (**Figure 5.9**).

Figure 5.10 illustrates a summary of pro-inflammatory and pro-fibrotic changes in response to stimulation in BECs isolated from individuals who are healthy or have IPF.

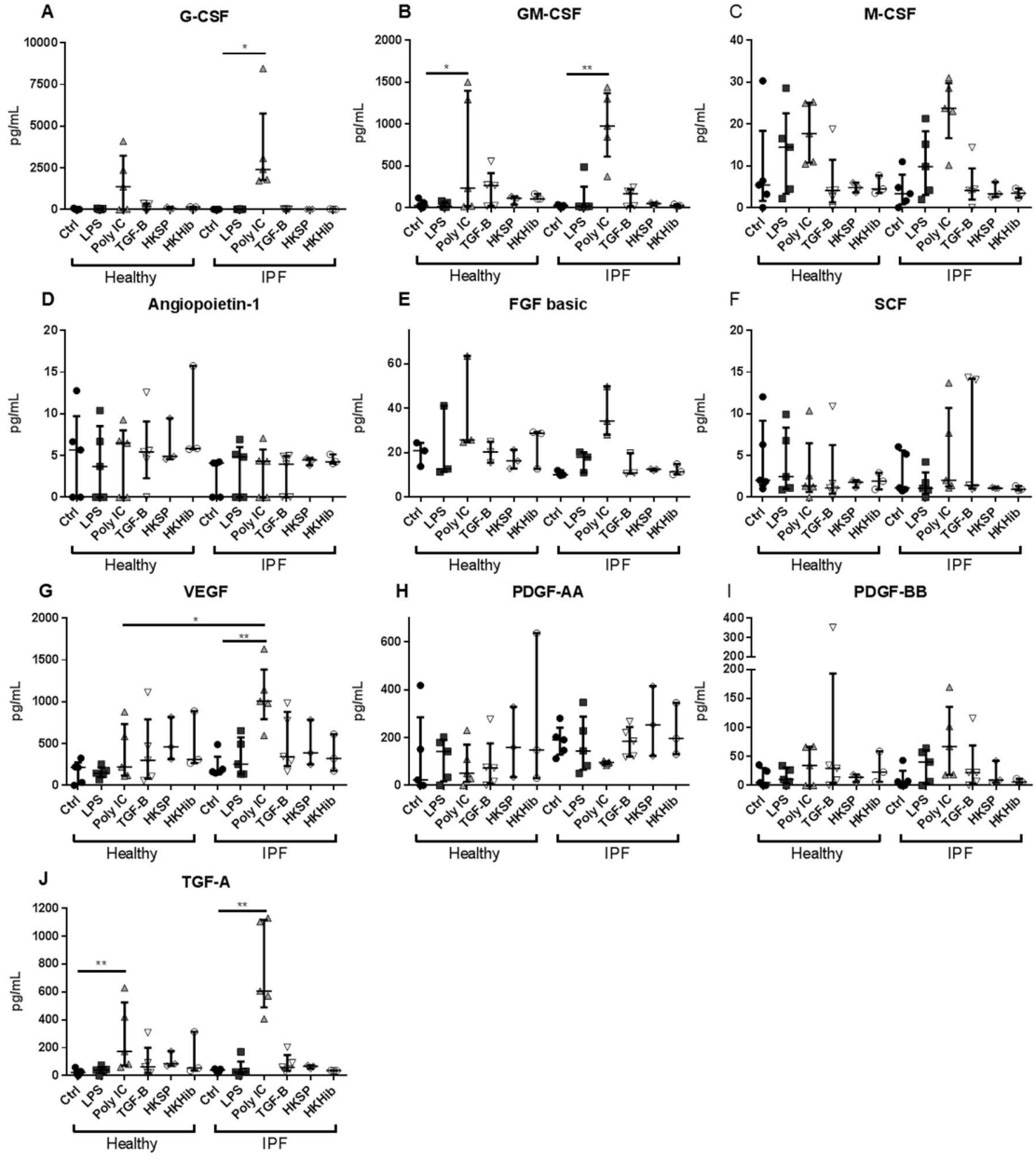


Figure 5.8: BEC stimulation: Growth factor analysis.
Growth factors from supernatant of stimulated healthy (n=5) and IPF (n=5) BEC (pg/mL) in unstimulated control (CTRL) and stimulated; LPS, POLY: IC, recombinant human TGFβ1 (TGFB1), heat killed streptococcus pneumoniae (HKSP) and heat killed haemophilus influenza B (HKHib) conditions. G-CSF, GM-CSF, M-CSF, Angiopoietin-1, FGF basic, SCF, VEGF, PDGF-AA, PDGF-BB and TGF-α (A-J respectively). Median and interquartile range shown. Statistical analysis using Friedman test with Dunn's multiple comparison to compare healthy or IPF cell stimulations. Comparison between the same stimulation in healthy and IPF was examined using Mann Whitney T test * $p<0.05$, ** $p<0.01$.

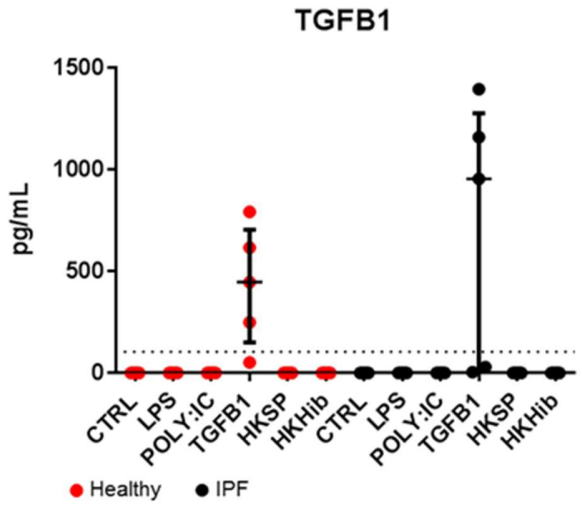


Figure 5.9: TGFβ1 levels post BEC stimulation.
TGFβ1 (pg/mL) was measured in stimulated healthy (n=5) (●) and IPF (n=5) (●) BEC supernatant 24 hours post stimulation. Median and interquartile range of separated healthy and IPF and BEC responses to unstimulated control (CTRL) and stimulated; LPS, POLY: IC, recombinant human TGFβ1 (TGFB1), heat killed streptococcus pneumoniae (HKSP) and heat killed haemophilus influenza B (HKHib) conditions are shown. Dashed line represents baseline rhTGFβ1 used for stimulation (median of 3 spiked supernatants). Statistical analysis using Friedman test with Dunn's multiple comparison to compare cell stimulations ** $p<0.01$.

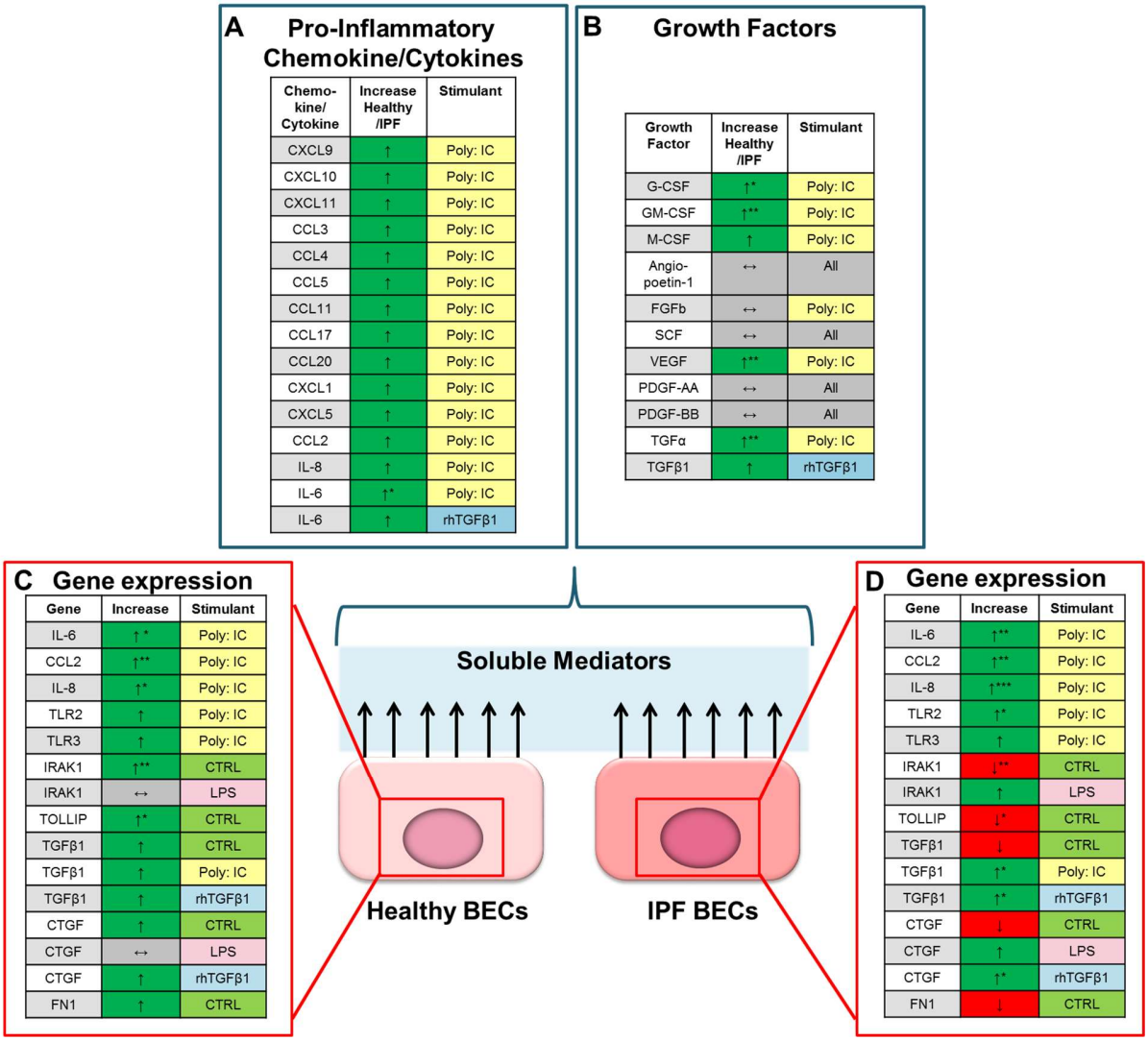


Figure 5.10: Summary of gene changes and mediator production by healthy and IPF BECs in response to stimulations.
Summary of soluble proinflammatory chemokines/cytokines (A) and growth factors (B) produced by BECs in response to highlighted stimulations. Gene expression fold change to highlighted stimulations compared to controls are outlined for healthy (C) and IPF (D) BECs.

5.4.4. Fibroblast stimulation pro-inflammatory gene analysis

In the IPF lung there is considerable tissue damage with loss of integrity to the epithelial layer combined with an excessive proliferation of invasive fibroblasts and myofibroblasts, which leads to the abnormal and excessive deposition of ECM. The effects of bacterial and viral TLR ligand stimulation of fibroblasts were next examined and the response of healthy and IPF fibroblasts to these challenges were assessed. Relative gene expression analysis for fibroblasts are included in appendix 8.3; **Figure 8.3.4-8.3.5** revealing no differences in gene expression in healthy control compared to IPF fibroblasts in unstimulated condition. Fold change was first determined examining stimulated IPF and healthy control fibroblasts to unstimulated controls. Pro-inflammatory genes IL-6, IL-8 and CCL2 were measured revealing no significant fold differences for IL-6 or IL-8 gene expression (**Figure 5.11A** and **B** respectively). However, CCL2 gene expression revealed a significant fold upregulation comparing IPF unstimulated cells to IPF Poly: IC stimulated cells (**Figure 5.11C**).

Complimentary to the pro-inflammatory gene expression analysis, TLR genes post stimulation were next examined. TLR receptor gene expression analysis revealed a decrease in expression of TLR2 in response to rhTGFβ1 stimulation in both healthy control and IPF fibroblasts (**Figure 5.12A**). TLR3 expression increased in response to Poly: IC stimulation of healthy control and IPF fibroblasts (**Figure 5.12B**), while TLR4 expression remained consistent across groups (**Figure 5.12C**). TLR downstream signalling genes including IRAK1 and TOLLIP were examined but expression did not change in response to stimulation (**Figure 5.13**). Overall the fibroblast response to TLR simulation appears reduced compared to BEC response.

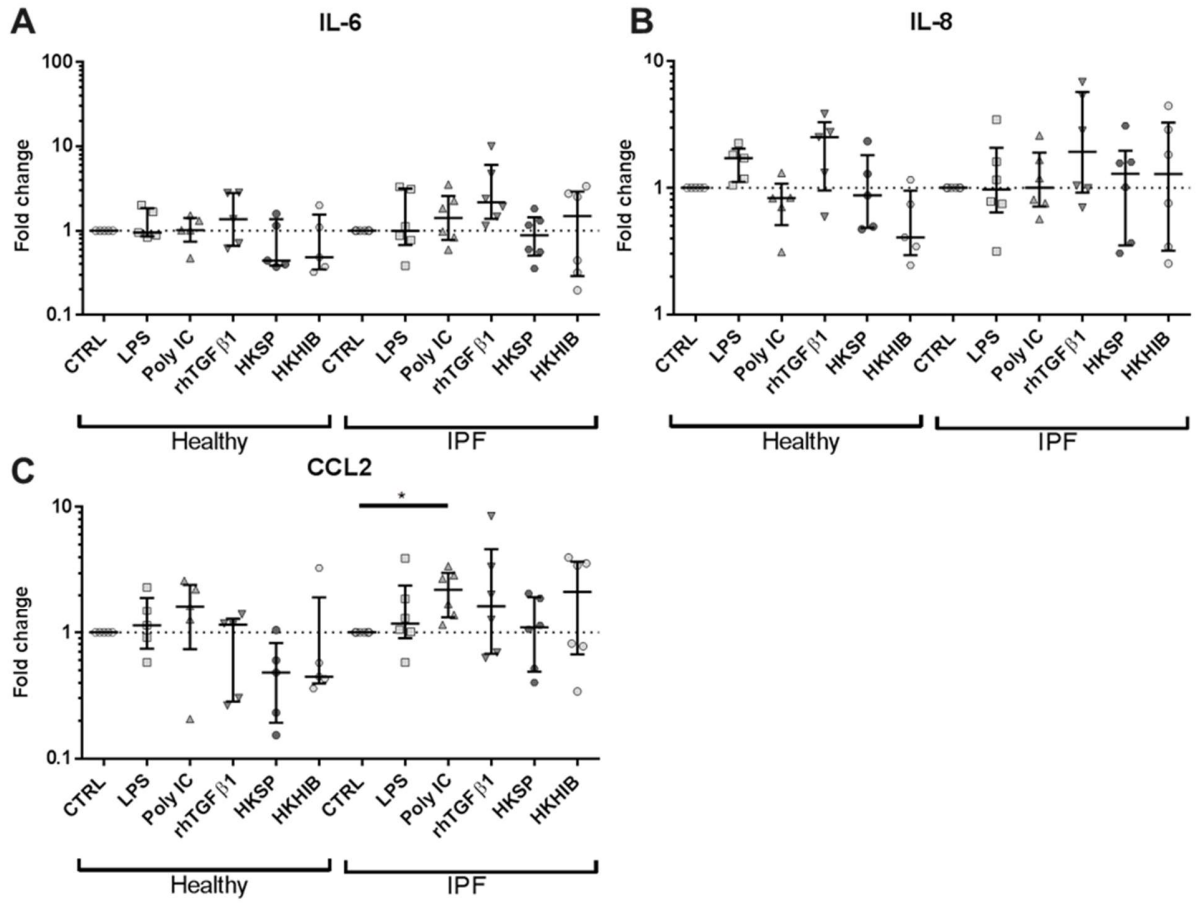


Figure 5.11: Fibroblast stimulation: Pro-inflammatory gene expression analysis.
Median and interquartile range gene expression analysis showing fold change of genes IL-6 (A), IL-8 (B) and CCL2 (C) in stimulated LPS, POLY: IC, recombinant human TGFβ1 (TGFB1), heat killed streptococcus pneumoniae (HKSP) and heat killed haemophilus influenza B (HKHIB) conditions in healthy control (n=5) and IPF (n=6) fibroblasts compared to unstimulated controls (CTRL). Statistical analysis using Friedman test with Dunn's multiple comparison was used to compare healthy or IPF cell stimulations.

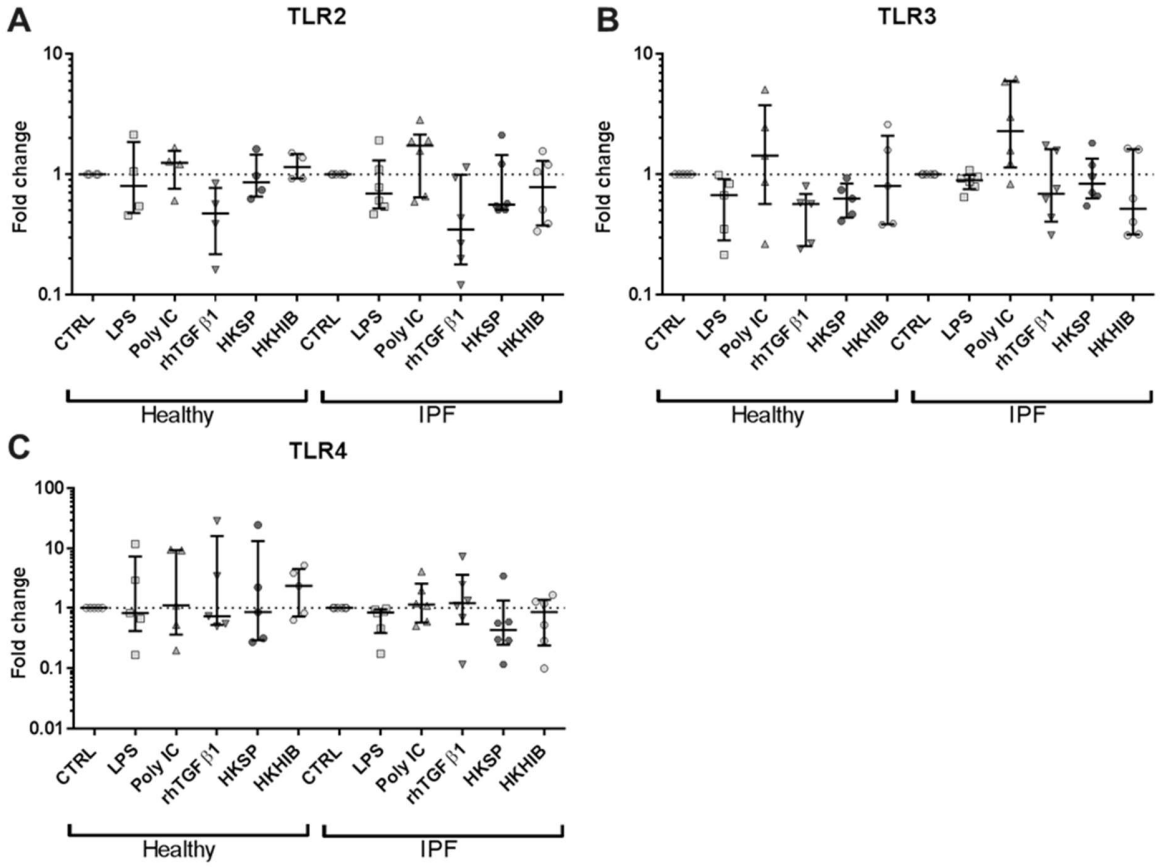


Figure 5.12: Fibroblast stimulation: TLR gene expression analysis.
Median and interquartile range gene expression analysis showing fold change of genes TLR2 (A), TLR3 (B) and TLR4 (C) in stimulated LPS, POLY: IC, recombinant human TGFβ1 (TGFB1), heat killed streptococcus pneumoniae (HKSP) and heat killed haemophilus influenza B (HKHIB) conditions in healthy control (n=4 TLR2, n=5 TLR3 and TLR4) and IPF (n=6) fibroblasts compared to unstimulated controls (CTRL). Statistical analysis using Friedman test with Dunn's multiple comparison was used to compare healthy or IPF cell stimulations.

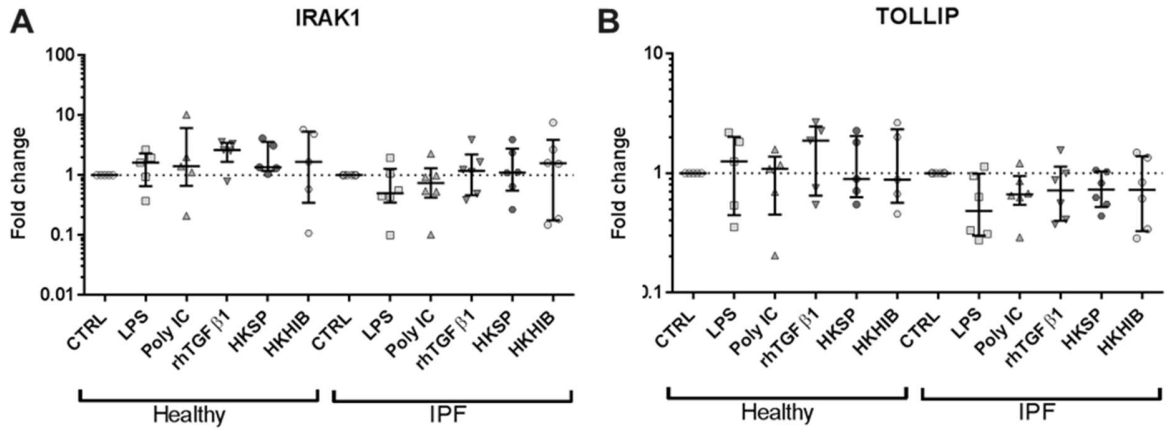


Figure 5.13: Fibroblast stimulation: TLR mediator gene expression analysis.
Median and interquartile range gene expression analysis showing fold change of genes IRAK1 (A) and TOLLIP (B) in stimulated LPS, POLY: IC, recombinant human TGFβ1 (TGFB1), heat killed streptococcus pneumoniae (HKSP) and heat killed haemophilus influenza B (HKHIB) conditions in healthy control (n=5) and IPF (n=6) fibroblasts compared to unstimulated controls (CTRL). Statistical analysis using Friedman test with Dunn's multiple comparison was used to compare healthy or IPF cell stimulations.

5.4.5. Fibroblast stimulation pro-fibrotic gene analysis

To examine the impact of stimulation of fibroblasts with bacterial and viral ligand TLR stimulation on fibrosis, fibrotic gene fold changes were next examined in response to stimulation of fibroblasts. Firstly, the expression of ACTA2, a gene encoding αSMA, a protein upregulated on myofibroblasts, was examined. ACTA2 gene expression was increased post stimulation with rhTGFβ1 in healthy fibroblasts and significantly increased in rhTGFβ1 stimulated IPF fibroblasts (**Figure 5.14**). Similarly, TGFβ1 and TGFβR1 expression were increased in both healthy and IPF fibroblasts stimulated with rhTGFβ1 (**Figure 5.15A** and **B** respectively). TGFβR2 was decreased in response to rhTGFβ1 stimulation (**Figure 5.15C**).

Further to genes associated with myofibroblast differentiation and TGFβ signalling ECM mediator CTGF and ECM genes encoding ECM collagens, COL1A1, COL3A1, and fibronectin, FN1, were next examined. CTGF expression was significantly increased in healthy fibroblasts in response to rhTGFβ1 stimulation and was also increased in IPF fibroblasts in response to rhTGFβ1 stimulation (**Figure 5.16A**). COL1A1, COL3A1 and the gene encoding fibronectin (FN1) did not differ significantly across the range of stimuli or between groups (**Figure 5.16B, C** and **D** respectively). Taken together the data demonstrates a pro-fibrotic role for TGFβ1 as expected, with no pro-fibrotic changes induced with TLR stimulation.

In addition to fold change examining the impact of stimulation, relative gene expression analysis of fibroblasts is included in appendix 8.3; **Figure 8.3.6-8.3.8** showing no significant differences in gene expression comparing paired conditions in IPF to healthy control fibroblasts.

A summary of fibroblast gene expression is outlined in **Table 5.2**.

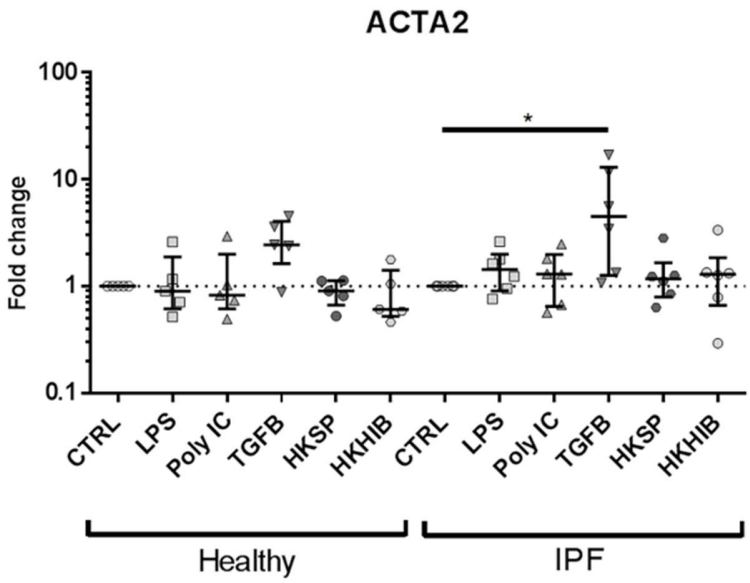


Figure 5.14: ACTA2 gene expression analysis.
Median and interquartile range gene expression analysis showing fold change of ACTA2 in stimulated LPS, POLY: IC, recombinant human TGFβ1 (TGFB1), heat killed streptococcus pneumoniae (HKSP) and heat killed haemophilus influenza B (HKHIB) conditions in healthy control (n=5) and IPF (n=6) fibroblasts compared to unstimulated controls (CTRL). Statistical analysis using Friedman test with Dunn's multiple comparison was used to compare healthy or IPF cell stimulations.

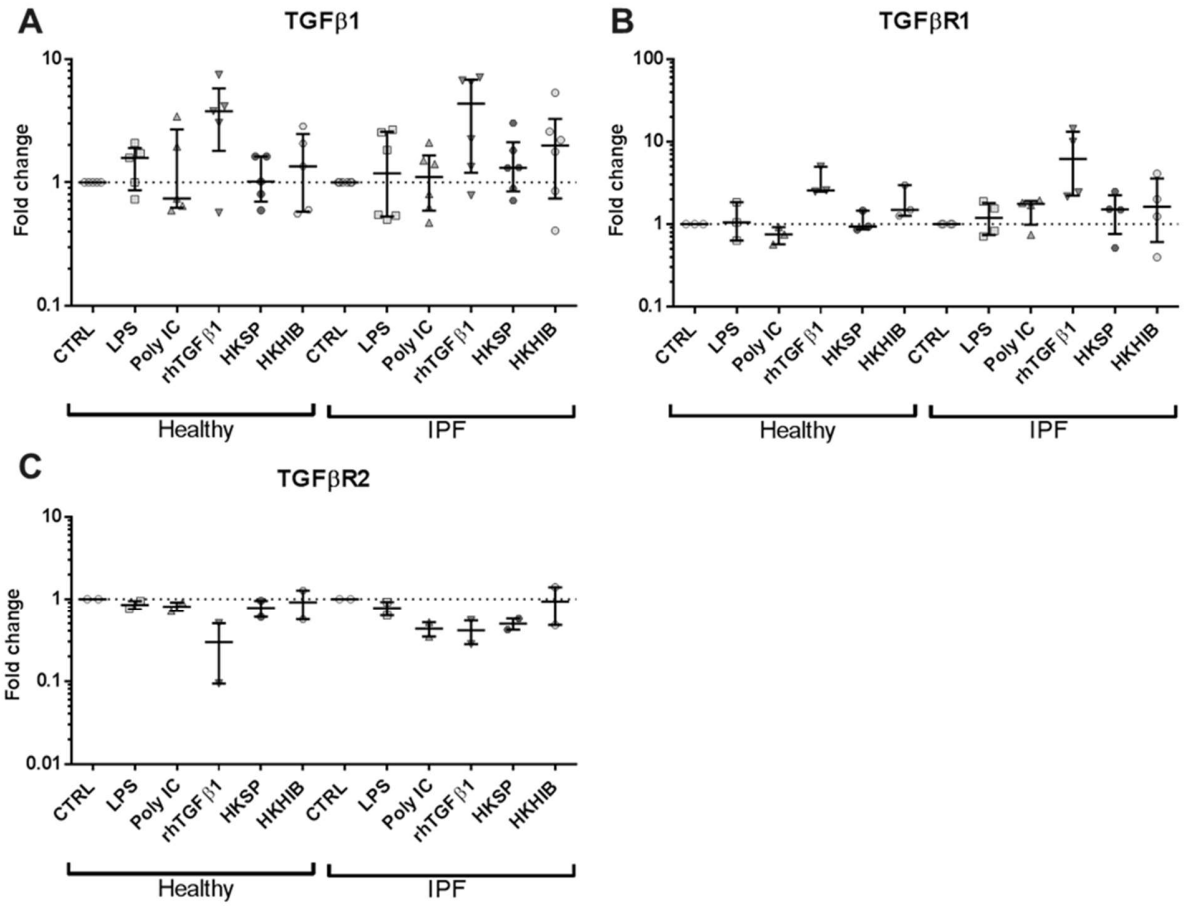


Figure 6: Fibroblast stimulation: TGFβ superfamily gene expression analysis.
Median and interquartile range gene expression analysis showing fold change of TGFβ1 (A), TGFβR1 (B) and TGFβR2 (C) in stimulated LPS, POLY: IC, recombinant human TGFβ1 (TGFB1), heat killed streptococcus pneumoniae (HKSP) and heat killed haemophilus influenza B (HKHIB) conditions in healthy control (n=5/3/2 for respective genes) and IPF (n=6/4/2 for respective genes) fibroblasts compared to unstimulated controls (CTRL). Statistical analysis using Friedman test with Dunn's multiple comparison was used to compare healthy or IPF cell stimulations.

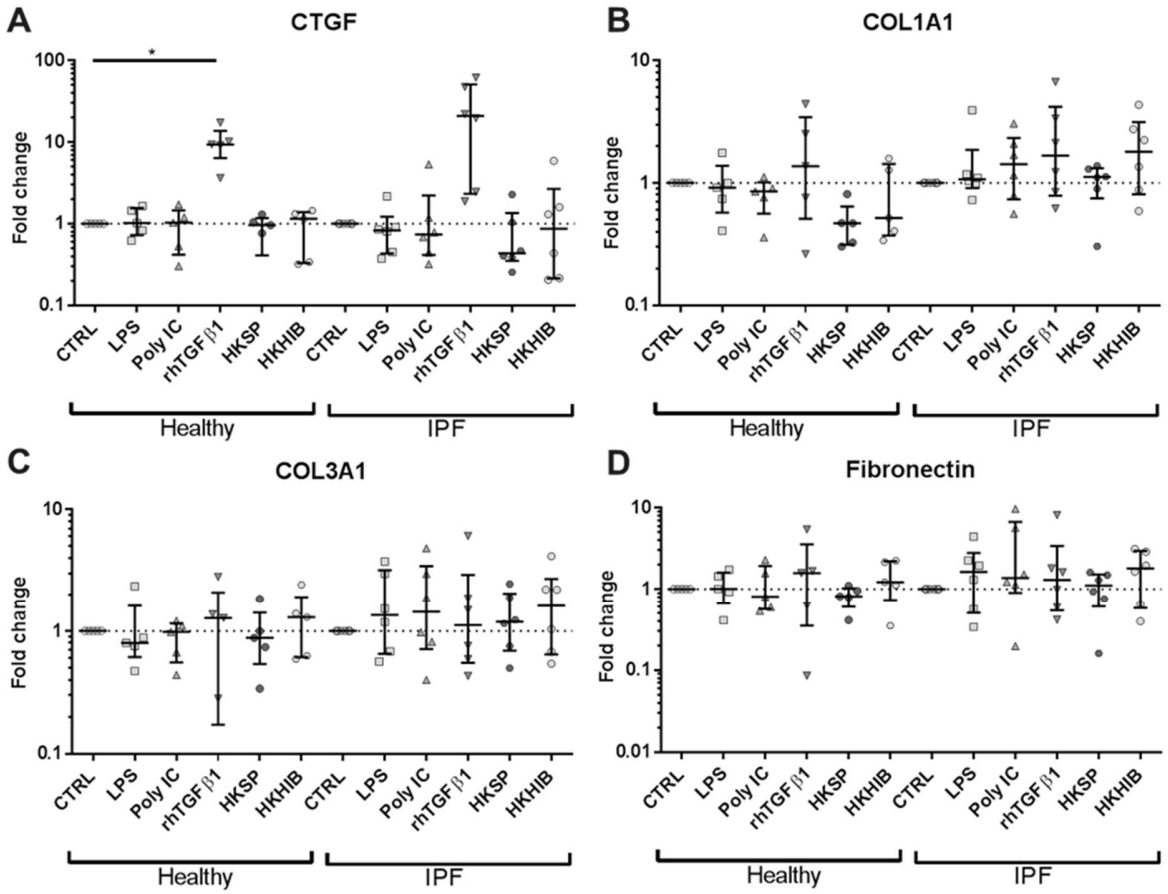


Figure 5.16: Fibroblast stimulation: ECM gene expression analysis.
Median and interquartile range gene expression analysis showing fold change of CTGF (A), COL1A1 (B), COL3A1 (C) in stimulated LPS, POLY: IC, recombinant human TGFβ1 (TGFB1), heat killed streptococcus pneumoniae (HKSP) and heat killed haemophilus influenza B (HKHIB) conditions in healthy control (n=5) and IPF (n=6) fibroblasts compared to unstimulated controls (CTRL). Statistical analysis using Friedman test with Dunn's multiple comparison was used to compare healthy or IPF cell stimulations.

		Fold change ($2^{-\Delta\Delta CT}$) compared to healthy unstimulated												
		Healthy n=5						IPF n=6						
Gene Role	**Gene**	**Ctrl**	**LPS**	**Poly: IC**	**rh-TGFβ 1**	**HKSP**	**HKHIB**	**Ctrl**	**LPS**	**Poly: IC**	**rh-TGFβ 1**	**HKSP**	**HKHIB**	**Ctrl IPF vs Healthy**
Myofibro-blast	ACTA2	1	2.59	1.28	3.60	1.13	1.77	1	1.04	1.17	2.99	0.87	1.15	0.81
TGFB1	TGFβ1	1	1.52	2.26	3.32	1.07	1.91	1	0.73	0.84	2.09	1.12	1.32	1.70
	TGFβR1	1	0.89	0.57	2.48	1.09	1.43	1	0.95	1.36	3.01	1.05	1.19	0.75
	TGFβR2	1	0.85	0.81	0.22	0.76	0.85	1	0.76	0.42	0.39	0.49	0.82	1.51
ECM	CTGF	1	1.45	0.77	9.36	0.34	1.24	1	0.57	0.92	12.97	0.46	0.95	0.62
	COL1A1	1	1.25	0.93	1.78	0.58	1.06	1	1.09	1.89	2.23	1.20	1.81	0.90
	COL3A1	1	1.25	0.98	1.28	0.82	1.16	1	1.15	1.14	1.09	0.93	0.90	0.87
	FN	1	1.45	0.75	0.97	0.95	1.99	1	1.41	2.67	1.54	1.07	1.11	1.03
Pro-inflam mediator	IL-6	1	1.47	1.52	2.05	0.84	1.10	1	1.15	1.25	3.23	0.58	0.94	1.53
	IL-8	1	1.14	0.71	2.51	0.95	0.27	1	0.98	1.12	1.85	0.77	1.08	2.18
	CCL2	1	0.91	0.39	0.44	0.26	0.61	1	1.48	1.94	1.83	1.10	1.42	0.35
TLR	TLR2	1	0.55	1.13	0.69	0.85	1.13	1	0.55	1.31	0.24	0.74	0.59	3.02
	TLR3	1	0.59	0.87	0.36	0.63	0.96	1	0.84	3.23	1.08	0.97	0.49	1.35
	TLR4	1	2.37	3.02	3.12	1.59	3.85	1	0.65	1.46	1.63	0.71	1.10	1.35
TLR Signalling	TOLLIP	1	1.20	0.73	1.88	1.20	0.71	1	0.67	0.73	0.81	0.92	1.07	1.57
	IRAK1	1	1.31	2.82	2.40	2.09	2.07	1	1.03	0.93	1.46	1.84	1.96	1.61

Table 5.2: Summary of Fibroblast stimulation median gene fold change compared to unstimulated cells.

Red cells indicate an increase of over 2-fold (≥2) expression and blue represent a 2 fold decrease (≤0.5) or lower. The last column represents median gene fold change for unstimulated cell gene expression comparing IPF to healthy.

5.4.1. Fibroblast stimulation chemokine and cytokine analysis

Defence against potentially tissue damaging infection is essential in maintaining normal tissue homeostasis, thus the inflammatory response of fibroblasts were next assessed by examining the production of chemokines and cytokines following stimulation. Multiplex analysis of CXCL9, CXCL10, CXCL11, CCL3, CCL5, CCL11, CCL17, CXCL1, CXCL5 and CCL20 in cell supernatants revealed no differences in chemokine production in response to stimulation or comparing healthy to IPF fibroblasts (**Figure 5.17A-I** respectively). Examination of IL-6 revealed a significant increase in IL-6 in the supernatant of IPF rhTGFβ1 stimulated fibroblasts compared to controls (**Figure 5.18A**). IL-8 and CCL2 levels appeared similar across stimulation groups in healthy and IPF fibroblasts (**Figure 5.18B** and **C** respectively).

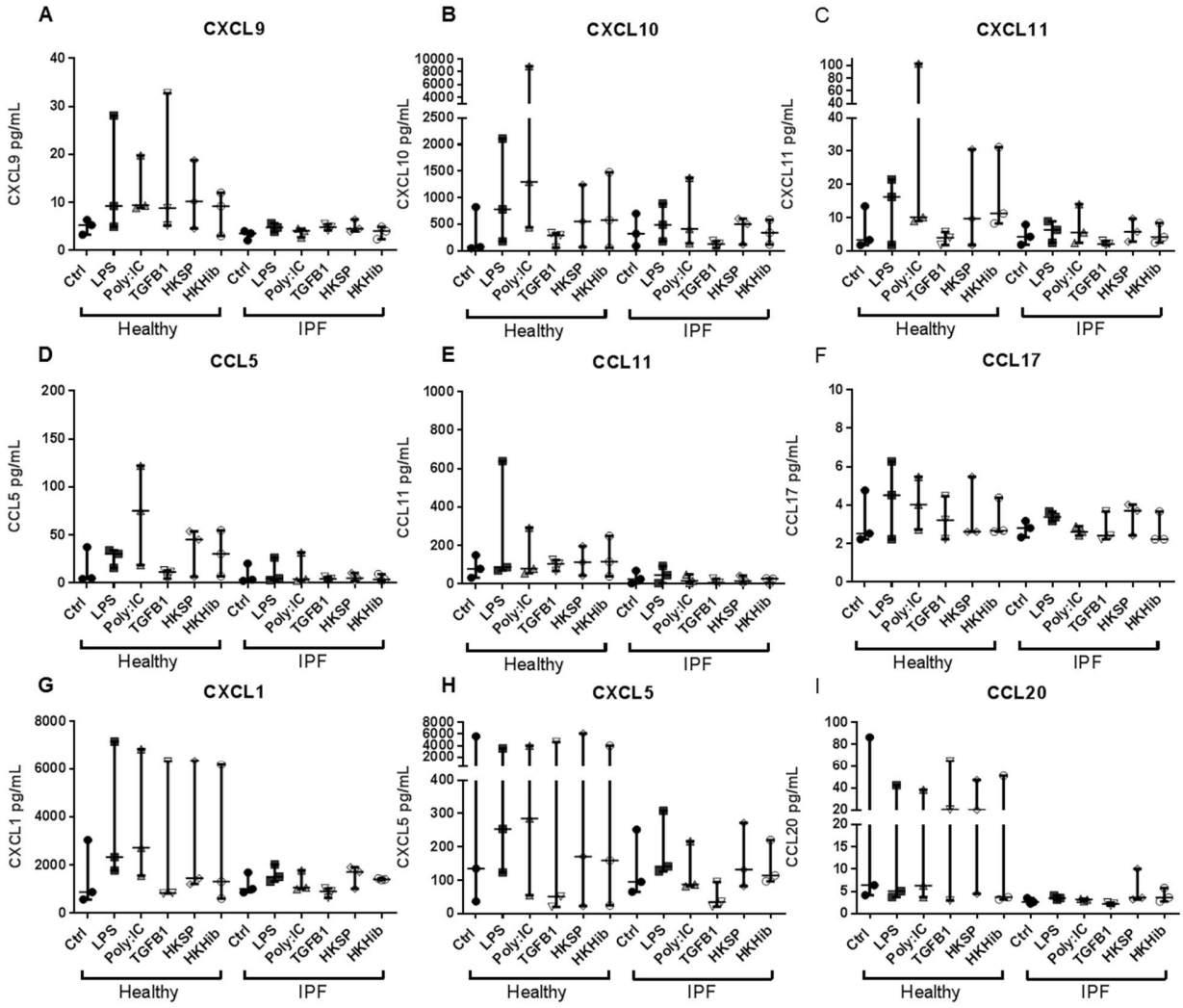


Figure 5.17: Fibroblast stimulation: Chemokine production analysis.
Chemokines from supernatant of fibroblasts (pg/mL) in unstimulated control (CTRL) and stimulated; LPS, POLY: IC, recombinant human TGFβ1 (TGFB1), heat killed streptococcus pneumoniae (HKSP) and heat killed haemophilus influenza B (HKHib) conditions. Median and interquartile range (pg/mL) is shown for CXCL9, CXCL10, CXCL11, CCL3, CCL4, CCL5, CCL11, CCL17, CCL20, CXCL1 and CXCL5 in A-K respectively. Statistical analysis using Friedman test with Dunn's multiple comparison to compare healthy (n=3) or IPF (n=3) cell stimulations. Comparison between the same stimulation in healthy and IPF was examined using Mann Whitney U T test.

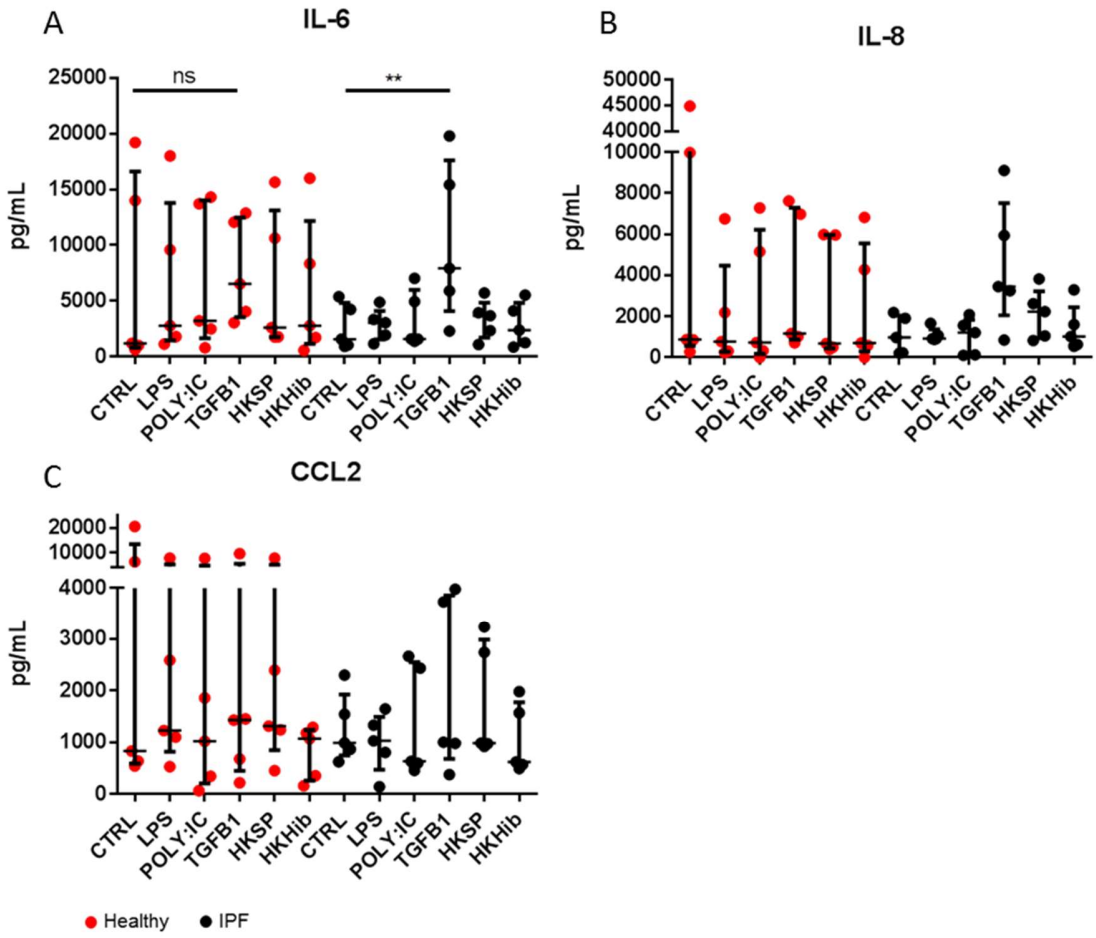


Figure 5.18: Fibroblast stimulation: Pro-inflammatory cytokine and chemokine production analysis.

IL-6 (A), IL-8 (B) and CCL2 (C) pg/mL were measured in healthy (n=5) (●) and IPF (n=5) (●) fibroblast supernatants in unstimulated control (CTRL) and stimulated LPS, POLY: IC, recombinant human TGFβ1 (TGFB1), heat killed *streptococcus pneumoniae* (HKSP) and heat killed *haemophilus influenza B* (HKHib) conditions. Median and interquartile range is shown. Statistical analysis using Friedman test with Dunn's multiple comparison to compare cell stimulations ** $p<0.01$. Comparison between the same stimulation in healthy and IPF fibroblasts were examined using Mann Whitney U T test revealing no significant differences.

5.4.2. Fibroblast stimulation growth factor analysis

Fibroblasts are fundamental in driving ECM deposition, influencing surrounding epithelial cells, endothelial cells, and leukocytes in both the lung parenchyma and the airways. Examination of fibroblast production of a range of growth factors, which drive tissue remodelling and immune cell activation, is therefore critical to understand which pro-fibrotic factors are released following specific stimulations, highlighting potential pathogenic stimuli. To further examine possible pro-fibrotic effects as a result of TLR stimulation of healthy and IPF fibroblasts, production of growth factors were next examined. G-CSF, GM-CSF and M-CSF levels appeared similar across stimulation groups in healthy and IPF fibroblasts (**Figure 5.19A-C** respectively). Angiopoietin-1, FGF basic and SCF levels were reduced in the IPF rhTGFβ1 stimulated fibroblast supernatant (**Figure 5.19D-F** respectively). VEGF and PDGF-AA production was increased in response to rhTGFβ1 stimulation in both healthy and IPF fibroblasts (**Figure 5.19G-H**), conversely PDGF-BB and HGF concentrations appeared lower in the rhTGFβ1 stimulated IPF fibroblasts (**Figure 5.19I-J**). Finally, TGFβ1 was increased in the rhTGFβ1 stimulated supernatants, with levels in many samples higher than spiked rhTGFβ1 stimulation supernatant control (same concentration of TGFβ1 as that used in stimulation) as indicated by the dashed line (**Figure 5.20A** and **B**).

A summary of pro-inflammatory and pro-fibrotic changes in response to stimulation in fibroblasts isolated from individuals who are healthy or have IPF is shown in **Figure 5.21**.

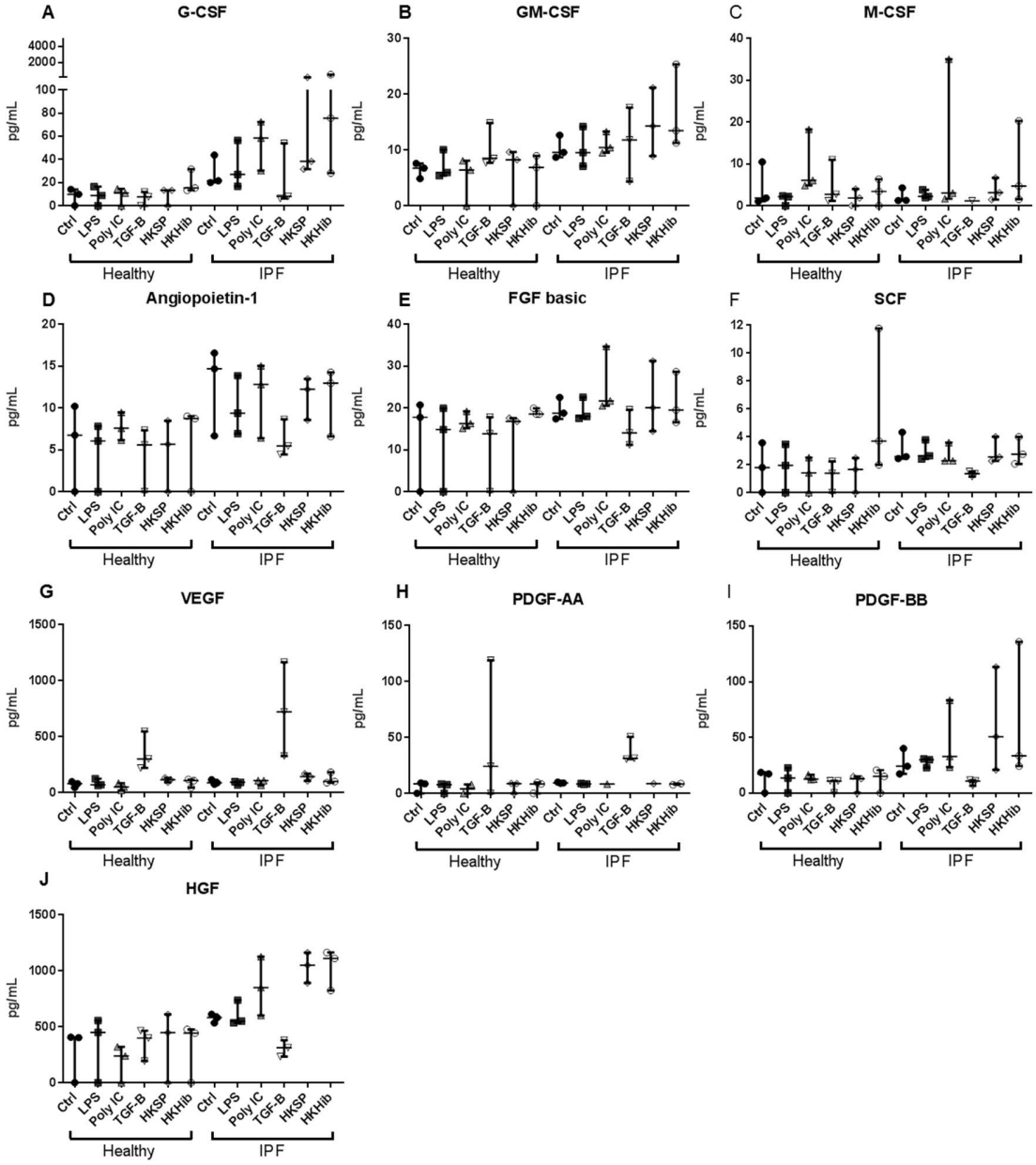


Figure 5.19: Fibroblast stimulation: Growth factor analysis.
Growth factors from supernatant of stimulated healthy (n=5) and IPF (n=5) fibroblasts (pg/mL) in unstimulated control (CTRL) and stimulated; LPS, POLY: IC, recombinant human TGFβ1 (TGFB1), heat killed streptococcus pneumoniae (HKSP) and heat killed haemophilus influenza B (HKHib) conditions. G-CSF, GM-CSF, M-CSF, Angiopoietin-1, FGF basic, SCF, VEGF, PDGF-AA, PDGF-BB and TGF-α (A-J respectively). Median and interquartile range shown. Statistical analysis using Friedman test with Dunn's multiple comparison to compare healthy or IPF cell stimulations. Comparison between the same stimulation in healthy and IPF was examined using Mann Whitney T test * $p<0.05$, ** $p<0.01$.

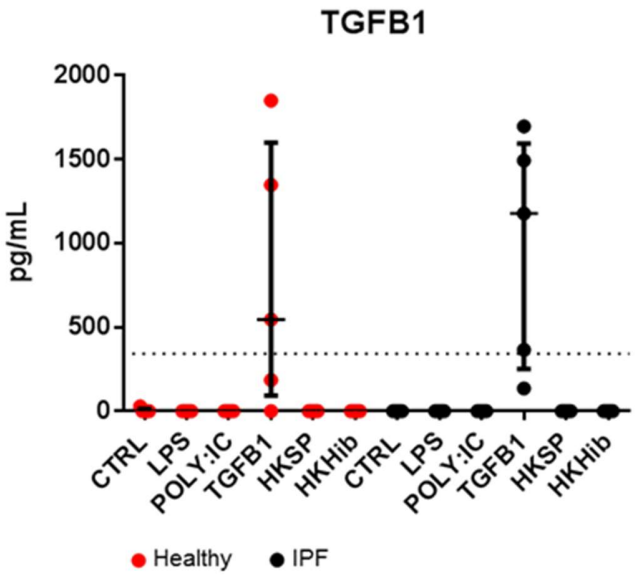


Figure 5.20: TGFβ1 levels post fibroblast stimulation.
TGFβ1 (pg/mL) was measured in stimulated healthy (n=5) (●) and IPF (n=5) (●) fibroblast supernatant 24 hours post stimulation. Median and interquartile range of separated healthy and IPF and BEC responses to unstimulated control (CTRL) and stimulated; LPS, POLY: IC, recombinant human TGFβ1 (TGFB1), heat killed streptococcus pneumoniae (HKSP) and heat killed haemophilus influenza B (HKHib) conditions are shown. Dashed line represents baseline rhTGFβ1 used for stimulation (median of 3 spiked supernatants). Statistical analysis using Friedman test with Dunn's multiple comparison to compare cell stimulations ** $p<0.01$.

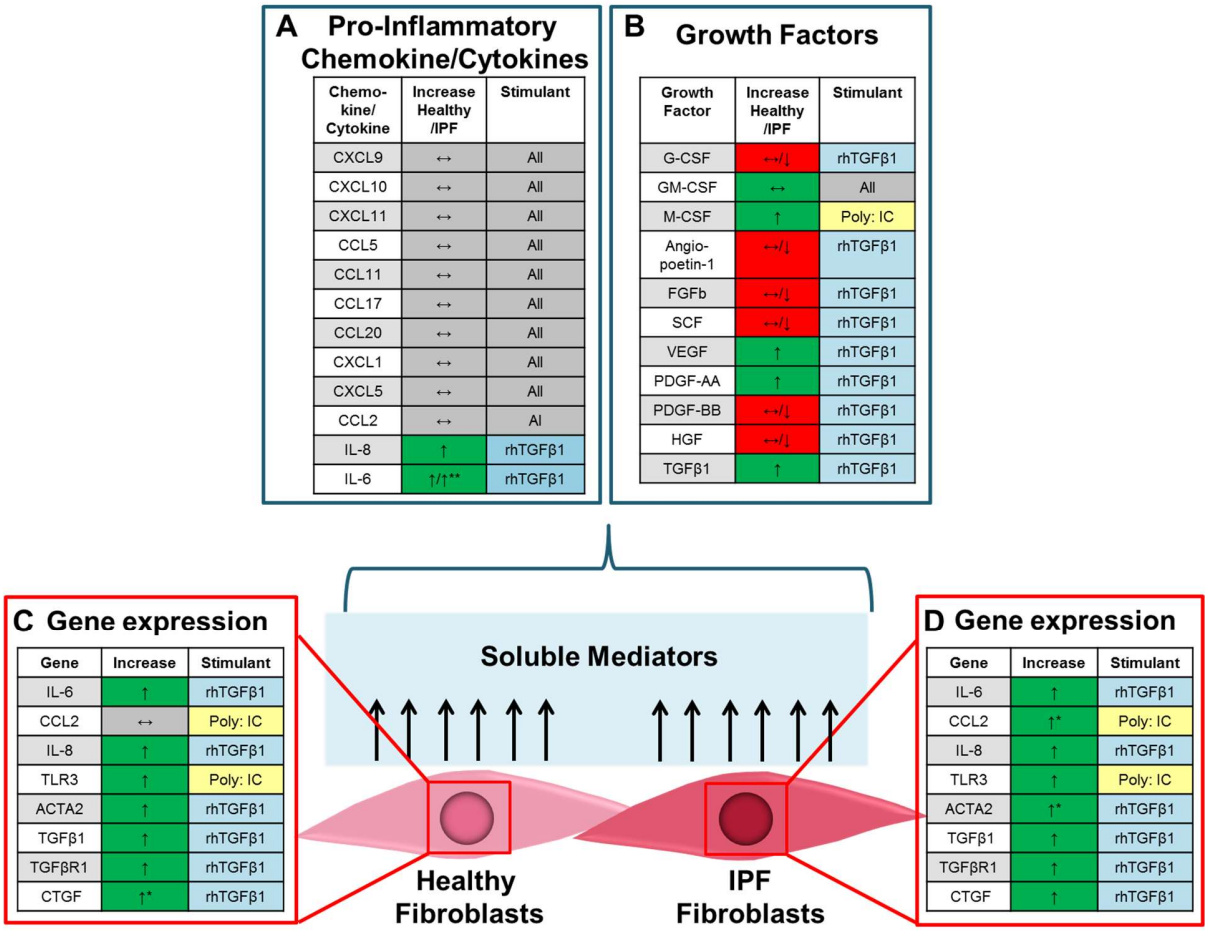


Figure 5.21: Summary of gene changes and mediator production by healthy and IPF BECs in response to stimulations.

Summary of soluble proinflammatory chemokines/cytokines (A) and growth factors (B) produced by fibroblasts in response to highlighted stimulations. Gene expression fold change to highlighted stimulations compared to controls are outlined for healthy (C) and IPF (D) fibroblasts.

5.4.3. Proinflammatory response of fibroblasts stimulated with conditioned BEC media

Stimulation of fibroblasts directly does not address the impact of cross talk between epithelial cells and fibroblasts that would occur *in vivo*. In a normal healthy *in vivo* setting inhaled infectious agents would likely first encounter leukocytes in the airways, such as airway macrophages, or other members of the innate immune system including the epithelial cell barrier. The release of mediators by the epithelial cells may impact on the function of the underlying fibroblasts in the airways. To examine this, healthy primary fibroblasts were stimulated with conditioned BEC supernatant, i.e. the supernatant taken from BECs which had been stimulated with mediators previously described, or the same concentration of stimulus alone in BEBM media without cell contact (see **Figure 2.8**). Pro-inflammatory gene expression in fibroblasts were first examined after stimulation with control stimulants (stimulants alone with no BEC conditioning) revealing an increase in fold regulation of IL-6 gene expression post LPS and TGFβ1 stimulation (**Figure 5.22A**). IL-8 expression was significantly increased post LPS stimulation and increased post Poly: IC and rhTGFβ1 stimulation (**Figure 5.22B**). CCL2 was increased post LPS, Poly: IC, TGFβ1 stimulation and decreased post HKSP and HKHIB stimulation (**Figure 5.22C**). In comparison, the same fibroblast stimulated with n=3 healthy and n=3 and IPF BEC conditioned supernatants revealed an increase in IL-6, IL-8 and CCL2 gene expression in response to Poly: IC BEC conditioned supernatant (**Figure 5.23A-C** respectively).

In addition to fold change examining the impact of stimulation, relative gene expression analysis of fibroblasts is included in appendix 8.3; **Figure 8.3.9-8.3.12**.

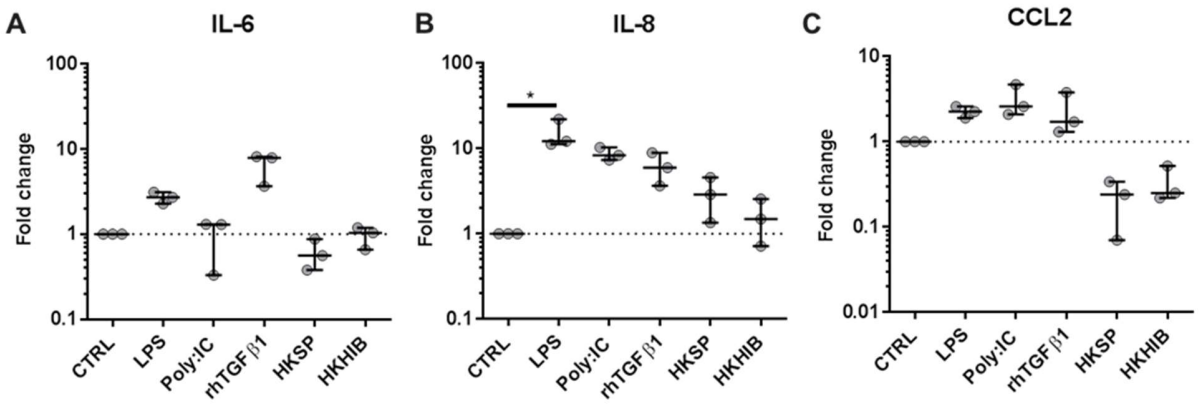


Figure 5.22: Fibroblast BEC conditioned media stimulation control: pro-inflammatory gene expression analysis.

Gene expression analysis showing fold change of genes IL-6 (A), IL-8 (B) and CCL2 (C) after stimulation of the same healthy fibroblast with unstimulated control (CTRL) and stimulated; LPS, POLY: IC, recombinant human TGFβ1 (TGFB1), heat killed streptococcus pneumoniae (HKSP) and heat killed haemophilus influenza B (HKHIB) conditions in BEBM media alone (n=3). Median and interquartile range is shown. Statistical analysis used Friedman test with Dunn's multiple comparison to compare healthy or IPF cell stimulations.

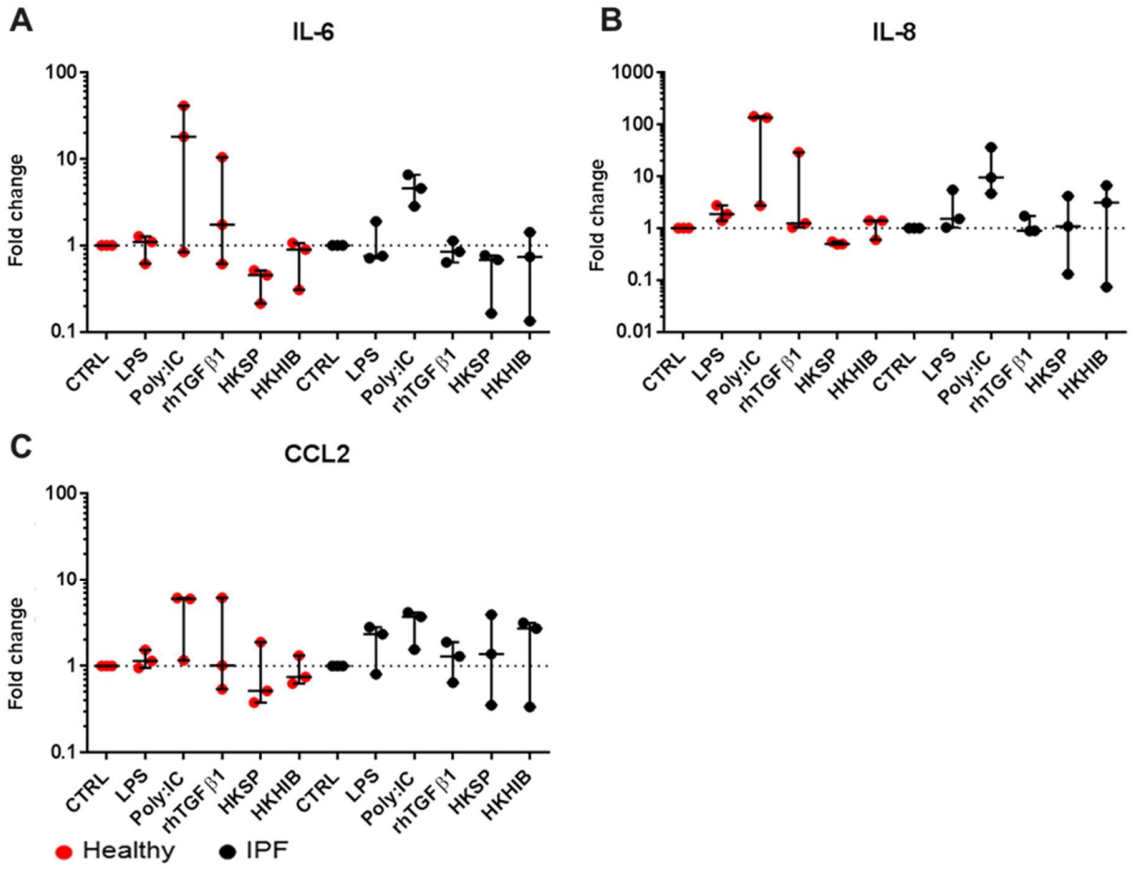


Figure 5.23: Fibroblast stimulation with conditioned healthy and IPF BEC supernatant: pro-inflammatory gene expression analysis.

Gene expression analysis showing fold change of genes IL-6 (A), IL-8 (B) and CCL2 (C) after stimulation the same fibroblast with conditioned supernatant from healthy (n=3) and IPF (n=3) BECs unstimulated control (CTRL) and stimulated; LPS, POLY: IC, recombinant human TGFβ1 (TGFB1), heat killed streptococcus pneumoniae (HKSP) and heat killed haemophilus influenza B (HKHIB). Median and interquartile range is shown. Statistical analysis used Friedman test with Dunn's multiple comparison to compare healthy or IPF cell stimulations.

Complementary to the gene expression analysis, pro-inflammatory cytokine IL-6, chemokines IL-8 and CCL2, alongside pro-fibrotic TGFβ1 were measured in fibroblast supernatant post stimulation with BEC conditioned supernatants, or control stimulants. To ensure the levels of the soluble mediators were not attributable to BEC release, the concentrations reported here were compared to those previously reported by BEC alone (see **Figure 5.7**). These supernatants were diluted 1 in 2 and used for fibroblast stimulation. In all cases the stimulated fibroblast supernatants contained higher concentrations than the BEC conditioned media alone suggesting the increased concentrations are attributable to release from the fibroblasts. Concentrations of IL-6 were increased in fibroblasts stimulated with rhTGFβ1 alone (**Figure 5.24A**). Contrary to this IL-6 levels post stimulation with conditioned BEC supernatant resulted in higher levels of IL-6 in response to Poly: IC BEC conditioned media (**Figure 5.24B**). CCL2 levels in stimulation only conditions did not change (**Figure 5.24C**), however, CCL2 concentrations post stimulation with healthy Poly: IC conditioned supernatant resulted in significantly higher levels of CCL2 compared to healthy control conditioned media (**Figure 5.24D**). Fibroblasts stimulated with IPF control BEC conditioned media, released significantly more CCL2 than fibroblasts stimulated with healthy control conditioned BEC media, suggesting that mediators released specifically by IPF BECs induce an increased production of CCL2 by fibroblasts at baseline (**Figure 5.24D**). IL-8 was not detected by ELISA in supernatant of fibroblast stimulation controls (data not shown). However, IL-8 production was increased post stimulation with Poly: IC BEC conditioned media compared to the unstimulated controls (**Figure 5.24E**). The aforementioned gene expression analysis measuring IL-6, CCL2 and IL-8 compliments this protein expression data showing the same increases (**Figure 5.23** and **Figure 5.24** respectively). Finally, TGFβ1 was not detected in the

supernatant of stimulus only controls (data not shown) but was detected and increased in the fibroblast supernatant post stimulation with rhTGFβ1 IPF BEC conditioned media but not in response to rhTGFβ1 healthy BEC conditioned media (**Figure 5.24F**). Taken together the fibroblasts increased proinflammatory gene expression and protein production in response to BEC conditioned media suggests soluble factors produced by BECs alter the fibroblast proinflammatory response. Comparisons between different conditioned BEC media stimulations revealed Poly: IC conditioned media induced the greatest fibroblast inflammatory response.

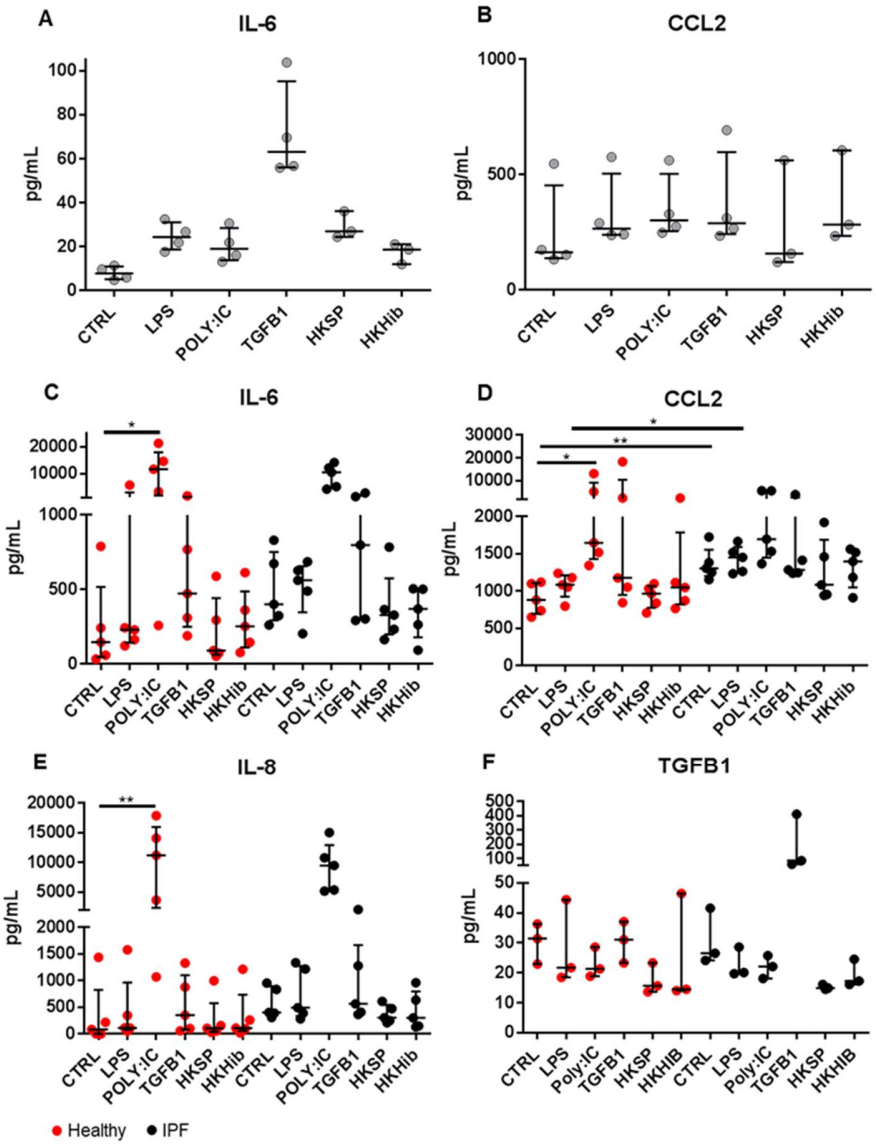


Figure 5.24: Fibroblast pro-inflammatory cytokine and chemokine production analysis post stimulation with conditioned BEC Media.

Levels of IL-6 and CCL2 (pg/mL) produced by directly stimulated fibroblasts are shown in A and B respectively (n=4 wells). Levels of IL-6 and CCL2 (C and D respectively) were measured in the supernatant of a fibroblast stimulated with BEC supernatants from healthy (n=5) (●) and IPF (n=5) (●) BEC supernatants. E and F show the levels of IL-8 in the supernatant of a fibroblasts stimulated with BEC supernatants from healthy (n=5) (●) and IPF (n=5) (●), and TGFβ1 levels in the supernatant of a fibroblasts stimulated with BEC supernatants from healthy (n=3) (●) and IPF (n=3) (●). Median and interquartile range for unstimulated control (CTRL) and stimulated; LPS, POLY: IC, recombinant human TGFβ1 (TGFB1), heat killed streptococcus pneumoniae (HKSP) and heat killed haemophilus influenza B (HKHIB) is shown. Statistical analysis using Friedman test with Dunn's multiple comparison to compare cell stimulations *p<0.05, ** p<0.01.

5.4.4. Pro-fibrotic gene expression analysis in fibroblasts stimulated with conditioned BEC media

Expression of the genes ACTA2 and COL1A1 remained consistent in all stimulation conditions in the fibroblast stimulation control (**Figure 5.26A** and **B** respectively). CTGF expression was increased post rhTGFβ1 stimulation (**Figure 5.26C**) and TGFβ1 expression appeared similar or decreased post LPS, Poly: IC, HKSP and HKHIB stimulation compared to control (**Figure 5.26D**). Expression of the same fibrotic genes post fibroblast stimulation with conditioned BEC media appeared silmilar to the stimulation control (**Figure 5.27**), with no change in the expression of ACTA2 (**Figure 5.27A**), COL1A1 (**Figure 5.27B**), CTGF (**Figure 5.27C**) and TGFβ1 expression (**Figure 5.27D**).

In order to examine whether different fibroblasts would respond in a similar manner to conditioned BEC media, conditioned BEC media from one healthy and one IPF BEC donor was used to stimulate healthy primary fibroblasts from three different donors. **Table 5.3** illustrates gene increase/decrease in fold expression compared to unstimulated BEC conditioned control, highlighting similar trends with pro-inflammatory mediators IL-6, IL-8 and CCL2 gene expression increased in response to Poly: IC conditioned BEC media.

A summary of gene expression changes and mediator production by stimulated fibroblasts with conditioned BEC media is outlined in **Figure 5.28**.

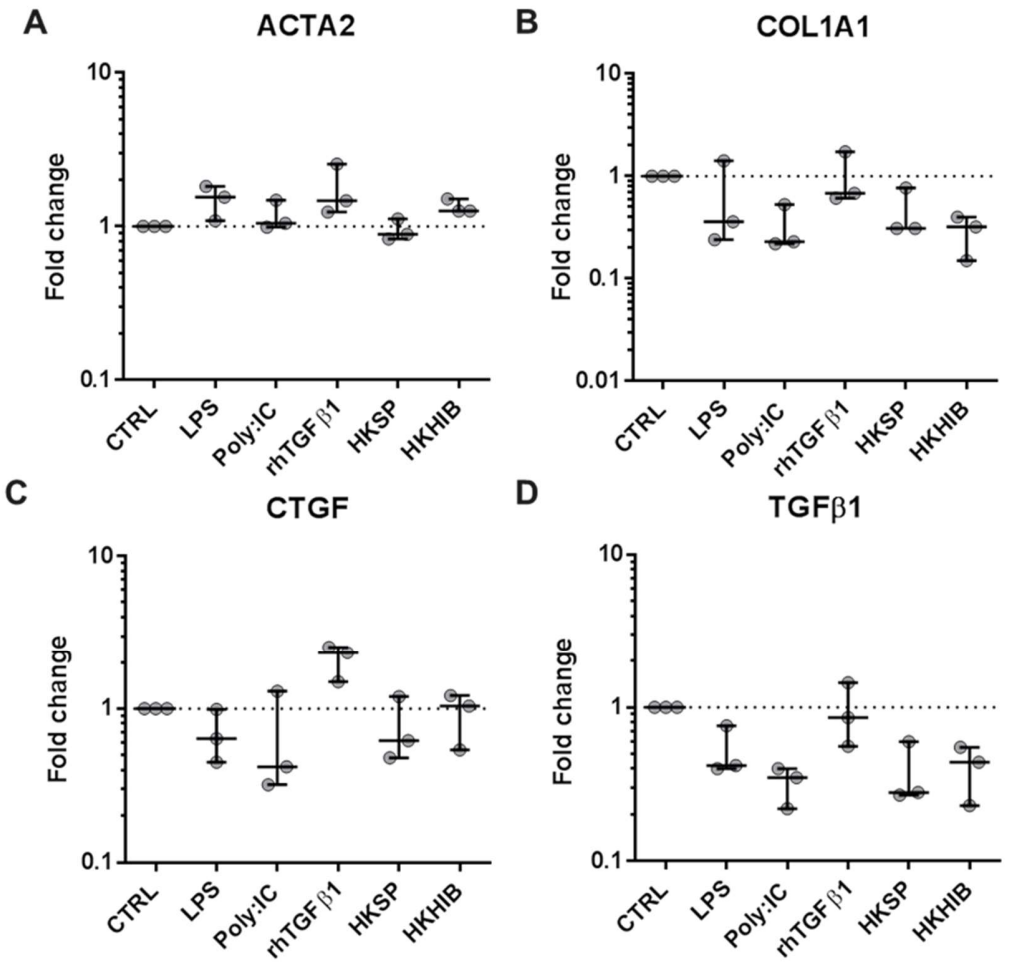


Figure 5.25: Fibroblast stimulated controls for conditioned BEC supernatant pro-fibrotic gene expression analysis.

Gene expression analysis showing fold change of genes ACTA2 (A), COL1A1 (B) CTGF (C) and TGFβ1 (D) after stimulation of the same healthy fibroblast with unstimulated control (CTRL) and stimulated; LPS, POLY: IC, recombinant human TGFβ1 (TGFB1), heat killed streptococcus pneumoniae (HKSP) and heat killed haemophilus influenza B (HKHIB) conditions in BEBM media alone (n=3). Median and interquartile range is shown. Statistical analysis used Friedman test with Dunn's multiple comparison to compare healthy or IPF cell stimulations.

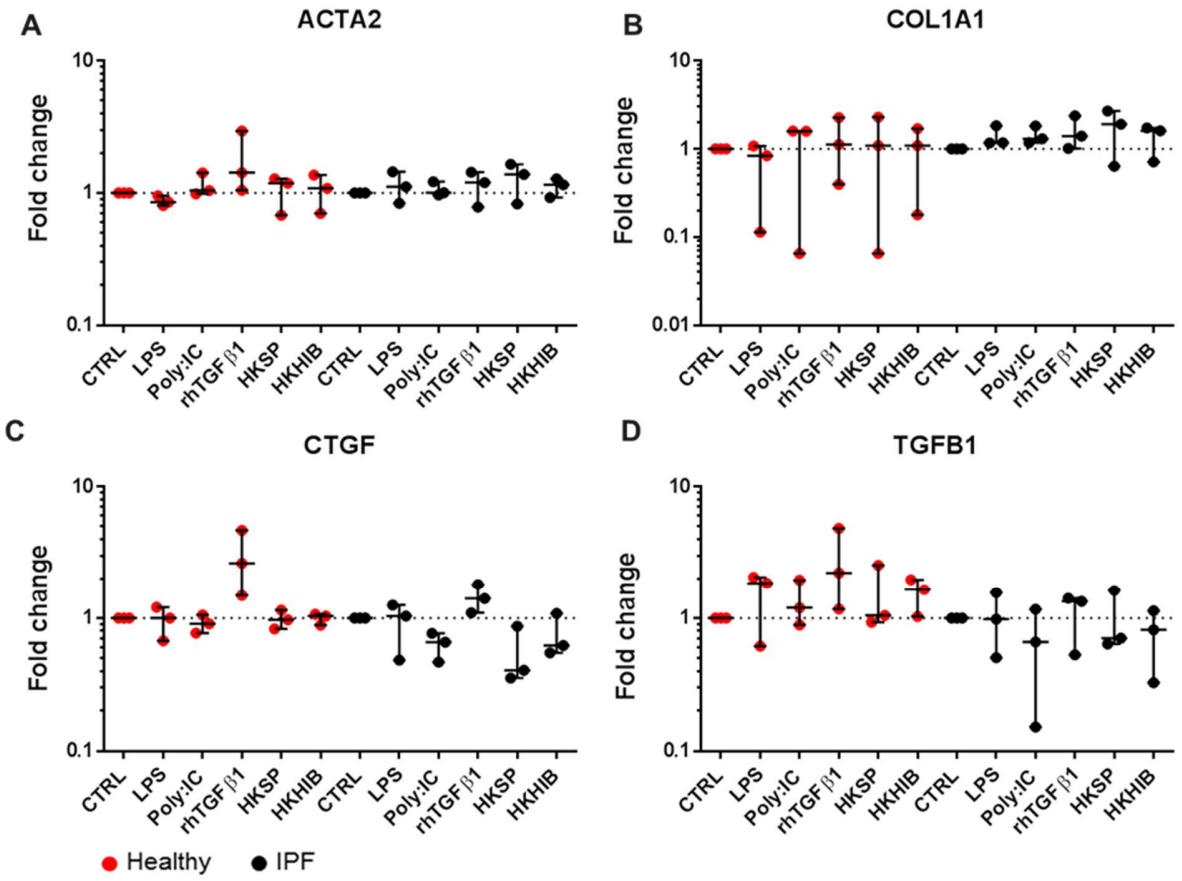


Figure 5.26: Pro-fibrotic gene expression analysis in fibroblasts stimulated with conditioned BEC media.

Gene expression analysis showing fold change of genes ACTA2 (A), COL1A1 (B) CTGF (C) and TGFβ1 (D). The same healthy fibroblast was stimulated with supernatant from stimulated healthy (n=3) and IPF (n=3) BEC conditioned media unstimulated control (CTRL) and stimulated; LPS, POLY: IC, recombinant human TGFβ1 (TGFB1), heat killed streptococcus pneumoniae (HKSP) and heat killed haemophilus influenza B (HKHIB). Median and interquartile range is shown. Statistical analysis using Friedman test with Dunn's multiple comparison to compare healthy or IPF cell stimulations.

Fibroblast	26789											
BEC	26993						191015-1					
Stimulation	CTRL	LPS	POLY: IC	rh-TGFB1	HKSP	HKHIB	CTRL	LPS	POLY: IC	rh-TGFB1	HKSP	HKHIB
ASMA	1	0.80	0.99	2.95	0.68	0.70	1	1.12	0.97	1.20	1.38	1.28
CTGF	1	1.00	0.77	4.67	0.83	1.04	1	1.26	0.66	1.10	0.87	1.08
IL8	1	2.75	135.06	29.14	0.55	1.41	1	5.50	9.53	0.90	1.08	6.66
IL6	1	1.28	18.16	10.48	0.45	1.07	1	1.90	4.59	0.64	0.77	1.43
MCP-1	1	1.53	6.11	6.15	1.89	1.32	1	2.80	3.70	1.29	1.37	3.16
TGFB1	1	2.05	0.89	4.84	0.93	1.97	1	0.98	0.66	1.34	1.63	1.14
COL1A1	1	0.11	0.07	0.40	0.06	0.18	1	1.18	1.18	1.40	1.91	1.73

Fibroblast	27068											
BEC	26993						191015-1					
Stimulation	CTRL	LPS	POLY: IC	rh-TGFB1	HKSP	HKHIB	CTRL	LPS	POLY: IC	rh-TGFB1	HKSP	HKHIB
ASMA	1	0.97	0.47	0.79	0.36	0.64	1	1.12	0.77	1.28	0.99	0.87
CTGF	1	0.31	0.10	1.47	0.08	0.09	1	0.60	0.10	1.14	0.34	0.23
IL8	1	0.48	3.88	3.32	0.28	0.37	1	0.36	0.39	0.26	0.41	0.21
IL6	1	0.37	9.91	0.67	0.10	0.68	1	2.14	5.28	2.60	2.43	5.06
MCP-1	1	1.04	1.71	0.95	0.23	0.81	1	2.17	4.02	1.83	2.14	2.75
TGFB1	1	0.54	0.39	0.76	0.36	0.62	1	1.33	0.65	1.39	1.52	2.26
COL1A1	1	0.38	0.20	0.37	0.22	0.47	1	1.75	0.77	2.25	1.14	1.82

Fibroblast	27913											
BEC	26993						191015-1					
Stimulation	CTRL	LPS	POLY: IC	rh-TGFB1	HKSP	HKHIB	CTRL	LPS	POLY: IC	rh-TGFB1	HKSP	HKHIB
ASMA	1	0.42	0.36	0.73	1.07	1.88	1	1.24	0.92	0.71	1.49	5.10
CTGF	1	0.82	0.44	2.64	0.40	0.18	1	0.21	0.17	1.34	0.32	1.60
IL8	1	4.32	3.12	1.54	1.06	0.72	1	0.52	0.76	0.49	1.94	1.06
IL6	1	2.85	10.97	4.52	2.44	2.73	1	0.84	2.60	0.51	2.39	1.03
MCP-1	1	0.92	2.34	1.09	0.68	1.28	1	0.78	1.38	0.73	2.30	1.25
TGFB1	1	0.50	0.39	1.20	1.03	1.20	1	1.25	1.07	2.38	2.01	3.46
COL1A1	1	1.10	0.78	1.15	1.50	1.83	1	0.90	0.65	1.18	1.33	2.04

Table 5.3: Summary of Gene fold change with three different primary healthy fibroblasts 26789, 27065 and 27913, stimulated with the one healthy (26993) and one IPF (191015-1) primary BEC conditioned media.

Red cells indicate an increase of over 2 fold (≥2) expression and blue represent a 2 fold decrease (≤0.5) or lower. Last column represents median gene fold change for unstimulated cell gene expression comparing IPF to healthy.

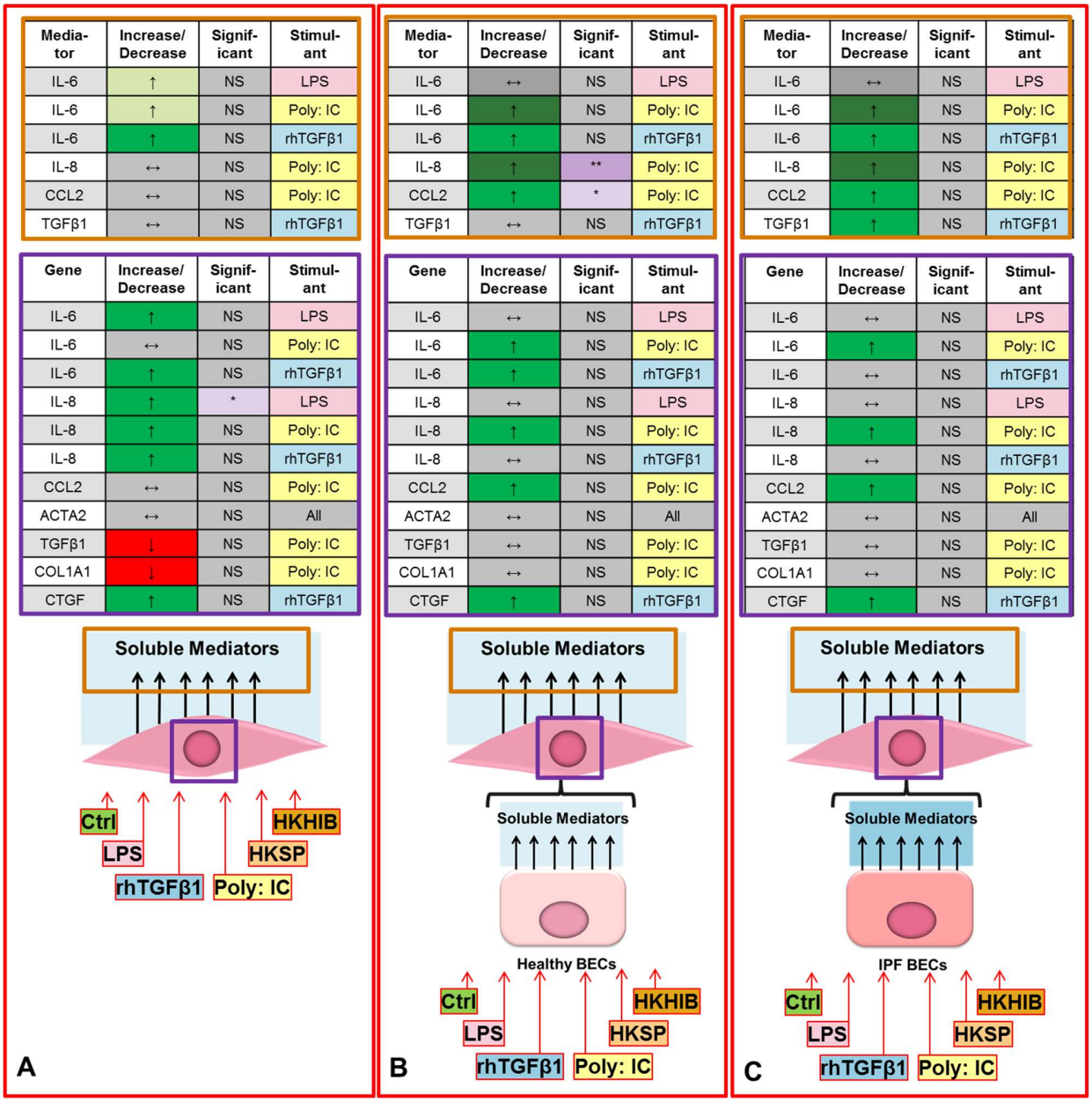


Figure 5.27: Summary of gene expression change and mediator production by fibroblasts stimulated with conditioned BEC media.

Fibroblasts stimulated with stimulus alone (A), stimulated with healthy conditioned BEC media (B) or stimulated with IPF conditioned BEC media (C). Darker green indicates greater increase.

5.4.5. Fibroblast proliferation assay

Excessive proliferation of fibroblasts is a hallmark feature of IPF, therefore the proliferation capacity of fibroblasts was quantified in the presence of bacterial, TLR ligand and rhTGFβ1 stimulation. Furthermore, to examine the effects of epithelial-fibroblast paracrine signalling, fibroblast proliferation was measured in the presence of healthy or IPF BEC conditioned media. Fibroblasts were cultured in 96 well plates and the percentage confluence of the cells were calculated over 72 hours. **Figure 5.28** shows the median values for growth curves of 3 healthy primary fibroblasts stimulated directly or with conditioned media from (n=3) healthy BECs or conditioned media from (n=3) IPF BECs. Comparison of control groups revealed increased proliferation of fibroblasts growing in the healthy/IPF BEC media compared to media alone (**Figure 5.28A**). Fibroblast growth was increased in response to LPS IPF BEC conditioned media compared to either LPS alone or LPS healthy BEC conditioned media (**Figure 5.28B**). rhTGFβ1 and Poly: IC stimulations were comparable across groups (**Figure 5.28C** and **D** respectively). HKSP direct stimulation increased proliferation compared to HKSP healthy/IPF BEC conditioned media (**Figure 5.28E**). Conversely direct HKHIB stimulation decreased proliferation compared to HKHIB healthy/IPF BEC conditioned media (**Figure 5.28F**).

Comparison of stimulation conditions revealed an increase in the proliferation of fibroblasts in response to LPS and rhTGFβ1 compared to control media, with Poly: IC showing no effect (**Figure 5.29A**). Similar to the observed effects examining direct stimulus, rhTGFβ1 and LPS conditioned BEC media increased proliferation of fibroblasts (**Figure 5.29B**). Stimulation of fibroblasts with HKSP and HKHIB conditioned BEC media did not alter fibroblast proliferation (**Figure 5.29C** and **D** respectively).

The area under the curve illustrating the proliferation of fibroblasts is shown in **Figure 5.30.** There were no significant increases/decreases in fibroblast proliferation comparing controls to stimulations.

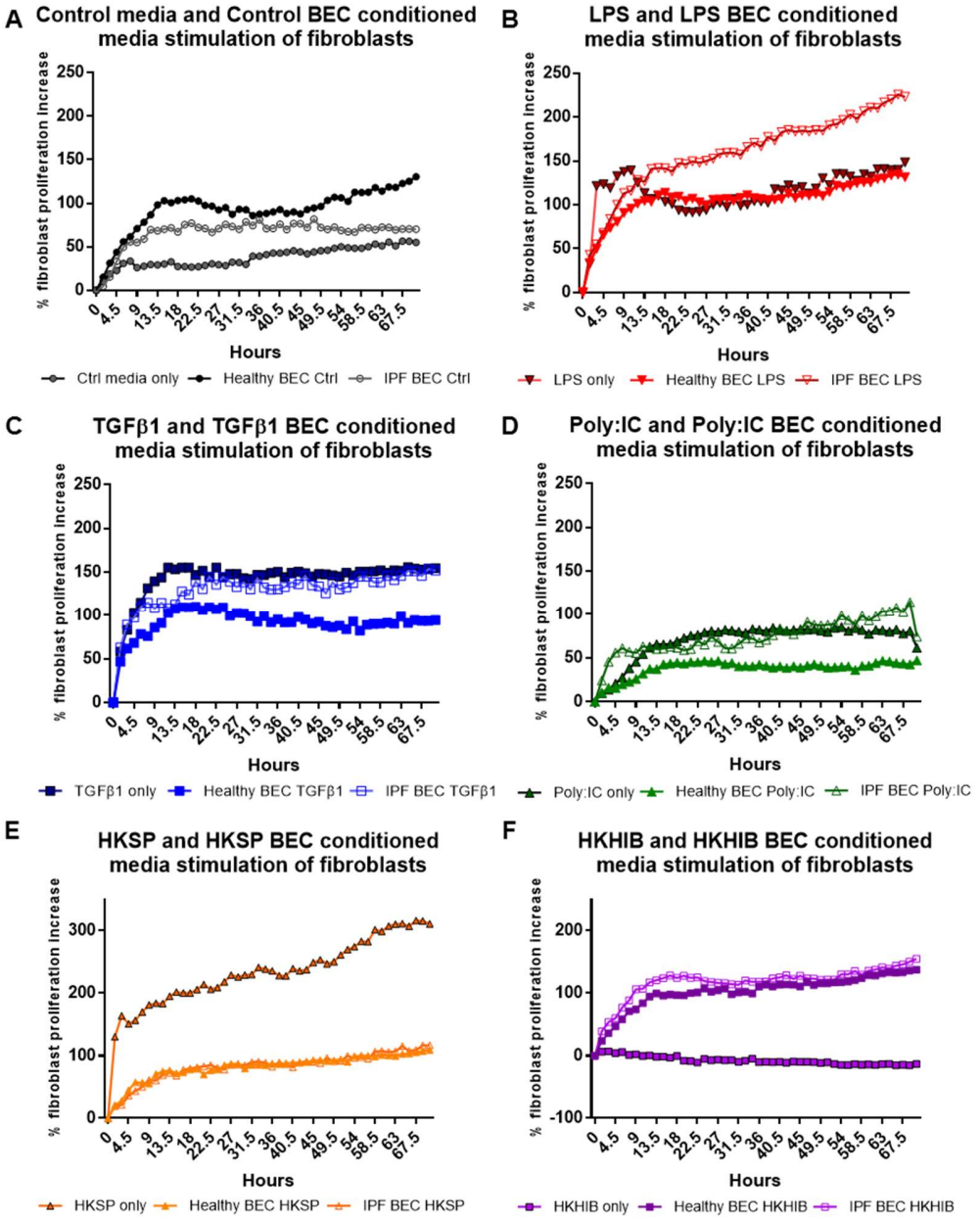


Figure 5.28: Fibroblast growth curve stimulation analysis.
The median percentage of proliferation increase/decrease over time (hours) shown for each stimulus; Ctrl media only (n=3), Healthy Ctrl (n=3), IPF Ctrl (n=3) (A), LPS, Healthy LPS, IPF LPS (B), (rh)TGFβ1 only, Healthy (rh)TGFβ1, IPF (rh)TGFβ1 (C), Poly: IC only, Healthy Poly: IC, IPF Poly: IC (D), HKSP only, Healthy HKSP, IPF HKSP (E), HKHIB only, Healthy HKHIB, IPF HKHIB (F).

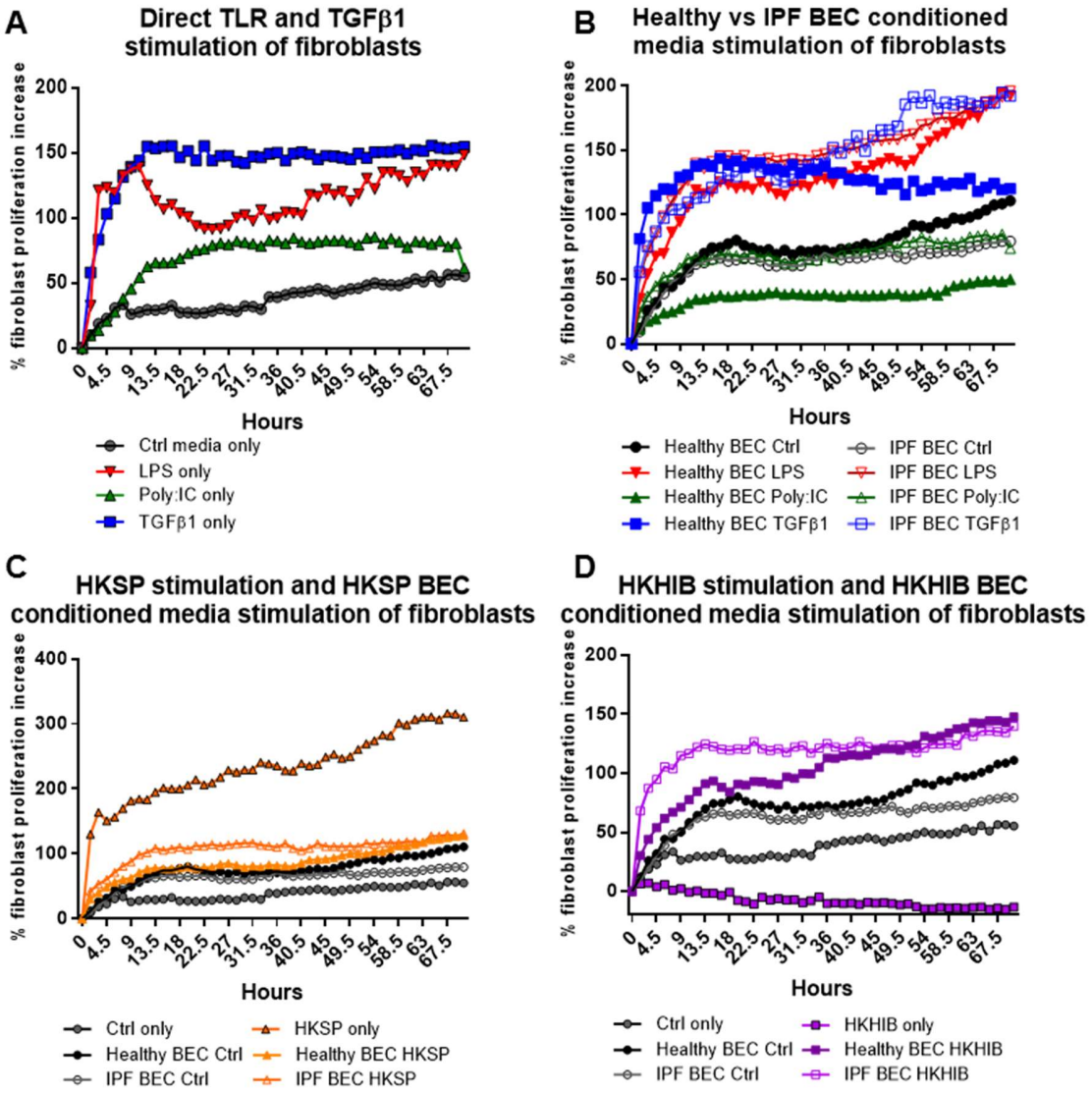


Figure 5.29: Fibroblast growth curve stimulation comparison.
The median percentage of proliferation increase/decrease over time (hours) shown for different stimulation conditions; Ctrl media only, LPS only, Poly: IC only, (rh)TGFβ1 only (A), Healthy Ctrl, IPF Ctrl, Healthy LPS, IPF LPS, Healthy Poly: IC, IPF Poly: IC, Healthy (rh)TGFβ1, IPF (rh)TGFβ1 (B), Ctrl media only, Healthy Ctrl, IPF Ctrl, HKSP, Healthy HKSP, IPF HKSP (C), Ctrl media only, Healthy Ctrl, IPF Ctrl, HKHIB, Healthy HKHIB, IPF HKHIB (D).

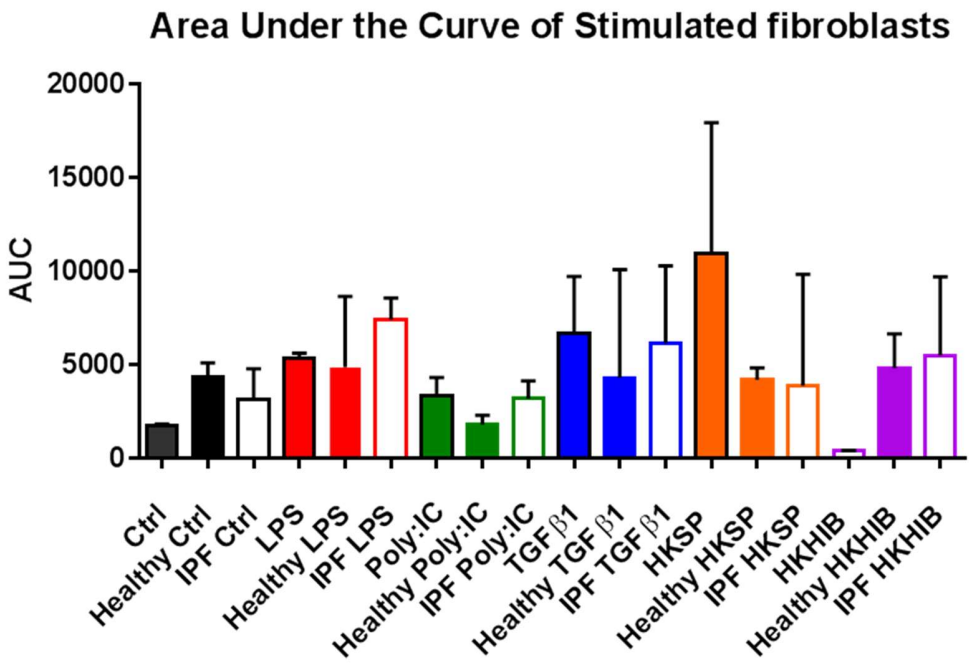


Figure 5.30: Percentage growth area under the curve of fibroblasts stimulated with conditioned BEC media.

Area under the curve for proliferation curves of fibroblasts. Median and interquartile range is shown for different stimulation conditions; Ctrl media only, LPS only, Poly: IC only, (rh)TGFβ1 only (A), Healthy Ctrl, IPF Ctrl, Healthy LPS, IPF LPS, Healthy Poly: IC, IPF Poly: IC, Healthy (rh)TGFβ1, IPF (rh)TGFβ1 (B), Ctrl media only, Healthy Ctrl, IPF Ctrl, HKSP, Healthy HKSP, IPF HKSP (C), Ctrl media only, Healthy Ctrl, IPF Ctrl, HKHIB, Healthy HKHIB, IPF HKHIB (D).

5.5. Discussion

Epithelial cells, alongside airway macrophages, form one of the first lines of defence against invading pathogens. IPF is thought to result from repetitive damage to the epithelial cell layer resulting in epithelial cell apoptosis, however, the source or sources initiating and potentiating this damage remain to be elucidated. One possible factor promoting epithelial cell damage is bacterial infection. IPF patients exhibit an altered lung microbiome, with increased bacterial burden correlating with clinical decline [26]. Alongside changes to the lung bacterial microbiome, increasing evidence has suggested a role for viral infection in IPF, with the presence of specific viruses in IPF patients [257-260]. However, reports investigating the response of healthy and IPF epithelial cells to bacterial and viral stimuli are lacking. In order to address this, the response of healthy and IPF primary bronchial epithelial cells (BECs) were examined after challenge with either; whole heat killed (HK) bacteria reported increased in IPF; *Streptococcus pneumonia*e (HKSP) or *Haemophilus influenzae* type b (HKHIB) [26], a bacterial cell wall component and TLR4 ligand; LPS, a double stranded (ds)RNA viral TLR3 ligand; Poly: IC or pro-fibrotic mediator; recombinant human (rh)TGFβ1.

Mounting an appropriate inflammatory response is critical to eliminate pathogens. Evaluation of the defence response to stimuli was first assessed investigating pro-inflammatory mediator IL-6, CCL2 and IL-8 gene expression. Healthy and IPF BECs increased expression of IL-6, IL-8 and CCL2 significantly in response to Poly: IC stimulation, with limited response to either LPS, HKSP or HKHIB. The fold increase in IL-6 and IL-8 gene expression was greater in the IPF patients; however, quantification of protein in the supernatant was comparable between IPF and healthy people. Production of inflammatory mediators by healthy primary human BECs in literature have shown

an increase in the release of IL-6, IL-8, CCL5 [410] and CCL2 [411] in response to Poly: IC, corroborating gene expression data, however, examination of the response of IPF alveolar epithelial cells or BECs in response to Poly: IC, or indeed bacterial stimulation, has never been investigated to our knowledge. Examination of chemokine production revealed an increase in all examined chemokines including CXCL1, CXCL5, CXCL9, CXCL10, CXCL11, CCL3, CCL4, CCL5, CCL11, CCL17 and CCL20 in Poly: IC stimulated BEC supernatant. The concentrations of CCL3, CCL4 and CCL20 were lower in supernatants of the Poly: IC stimulated IPF BECs compared to Poly: IC stimulated healthy supernatants. Contrary to these findings CCL3 has been shown to be increased in IPF [205, 213, 214], correlating with clinical decline and exerting pro-fibrotic effects in the bleomycin model of fibrosis [195, 213]. However, there are multiple sources for this chemokine including macrophages, which were shown to be increased in IPF in previous results (**3.4** and **4.4**). Quantification of CCL4 and CCL20 has not been examined in IPF, however, our examination of chemokines in the BAL (**3.4.3**) showed slightly decreased median levels of CCL4 in IPF BAL and similar levels of CCL20. CCL4 is thought to attract NK cells [412] to site of injury and CCL20 is thought to attract lymphocytes to the epithelium [413]. It is possible that the reduced production of these two chemokines by the BEC in IPF may result in an impaired defence response to virus by the IPF BECs. Increasing the sample numbers would be required to validate these findings. Stimulation of BEC with rhTGFβ1, regardless of disease profile, appeared to increase the release of IL-6 into the supernatant, which may indicate BECs as a possible source of IL-6, which has been found to be increased in IPF [414], and has been shown to induce proliferation of fibroblasts, enhancing matrix deposition [221].

Appropriate responses to bacterial and/or viral PAMPs, requires effective signalling through PRRs like the TLRs. As the bacterial burden and viral incidence have been reported as increased in IPF, components of the TLR signalling cascade, comparing healthy to IPF BECs, were next examined. TLR3 expression was increased in both healthy and IPF BECs in response to stimulation with TLR3 ligand, Poly: IC. Alongside TLR3, TLR2 expression was also increased in response to Poly: IC stimulation in healthy BECs and significantly upregulated in response to Poly: IC in IPF. Previous research examining the response of normal human airway epithelial cells to Poly: IC stimulation also showed an increase in the expression of TLR2 in response to Poly: IC, TLR3 stimulation, suggesting cross talk between the TLR pathways [415]. Melkamu et al (2009) went on to show an enhanced response to the TLR1/2 ligand Pam3CSK4 (a synthetic triacylated lipopeptide (LP) that mimics the acylated amino terminus of bacterial LPs) by epithelial cells post Poly: IC (TLR3) stimulation [415], suggesting TLR3 stimulation may enhance TLR2 signalling. It would be interesting to see if IPF BECs show an enhanced response to sequential TLR2 stimulation post TLR3 stimulation in order to examine whether viral challenge may lead to exacerbated bacterial/DAMP/fungal responses in IPF BECs. Expression of IRAK-1, which is downstream of TLR2 and TLR4 signalling, and TOLLIP, a negative regulator of TLR signalling [416] were both significantly decreased at baseline in IPF BECs compared to healthy. TLR canonical signalling pathway involves the MyD88 adapter protein and IRAK complex, comprised of IRAK-1 and IRAK-4 active kinases [417]. Deficiency of IRAK-1 in human fibroblasts results in an impaired TLR2/6, TLR1/2 and TLR4 stimulation [418]. Reduced TLR2 and IRAK-1 expression is a characteristic feature of cells that have become tolerant to bacterial lipoprotein stimulation, which can be rescued by overexpressing IRAK-1 [419]. It is therefore possible the reduced expression of IRAK1

has occurred as a result of increased bacterial exposure in the IPF airways. Alternatively viral dsRNA ligand, Poly: IC, has been shown to decrease expression of both IRAK1 and TOLLIP in epithelial cells [420]. It is possible the decrease in expression of IRAK1 and TOLLIP at baseline in IPF cells may be due to pre-exposure to viral stimulation *in vivo* prior to cell isolation. Examination of the bacterial microbiome or virome from the matched patients' lavage may identify possible differences in bacterial and/or viral exposure, providing a more comprehensive picture of the environment the BECs were isolated from.

In order to elucidate the roles TLR or bacterial signalling may have on fibrosis, pro-fibrotic responses to the stimulations were investigated, examining expression of genes known to be involved in fibrosis combined with the release of growth factors by the BECs. Perhaps surprisingly TGFβ1 expression in unstimulated IPF BECs was lower compared to healthy BECs, as TGFβ1 is a key driver of fibrosis one might expect IPF BECs to express increased TGFβ1 compared to healthy at baseline. TGFβ1 expression was increased compared to unstimulated controls in response to both Poly: IC stimulation and rhTGFβ1 stimulation in healthy BECs, and significantly increased in IPF BECs in response to both Poly: IC and rhTGFβ1 stimulation. A dose response increase of TGFβ1 has been previously reported in human BECs stimulated with Poly: IC, which was reduced by inhibiting TLR3 using siRNA [421]. These data suggest a role for viral stimulation in the production of TGFβ1, which may be contributing to the fibrotic pathology in IPF. TGFβ1 may be positively regulating further TGFβ1 expression in BECs, as both the gene expression, and detection of TGFβ1, appeared increased post rhTGFβ1 stimulation. Both connective tissue growth factor (CTGF) and fibronectin (FN1) expression were lower in IPF unstimulated BEC compared to unstimulated healthy BEC. This is unexpected as both fibronectin and CTGF are thought to play

important roles in the production of ECM, which is increased in IPF [422]. Stimulation with rhTGFβ1 resulted in an increase in the expression of CTGF in healthy BEC and a significant and greater fold increase in expression in rhTGFβ1 stimulated IPF BECs compared to unstimulated controls. LPS stimulation also appeared to increase the fold expression of CTGF and IRAK1, but only in IPF BECs, suggesting a divergent and possibly increased response to TLR4 stimulation in IPF BECs.

Growth factor production by BECs were quantified revealing an increase in G-CSF, which was significant in IPF, a significant increase in GM-CSF, which was higher in IPF and increased production of M-CSF in response to Poly: IC. These growth factors are involved in the maturation of granulocytes [225] and macrophages [380, 399]. rhTGFβ1 stimulation increased the production of GM-CSF, albeit marginally, and LPS increased the production of M-CSF. The significant increase in GM-CSF production in response to Poly: IC stimulation is expected, and has been reported in healthy primary lung epithelial cells previously [420, 423]. GM-CSF has been shown to play a protective role *in vivo* models of human influenza A virus pneumonia using mouse-adapted influenza virus A/Puerto Rico/8/34 (PR8) (H1N1) strain, acting to protect against infection by stimulating alveolar macrophages [424]. It is likely the BECs release increased GM-CSF in response to Poly: IC to activate alveolar macrophages in man in a similar manner. It is quite interesting that both LPS and Poly: IC induced release of M-CSF, which is increased in IPF [228]. This may point to viral and/or bacterial infection in IPF patients as the levels of M-CSF are significantly increased in the BAL (**Figure 3.17**). FGFb, PDGF-BB, VEGF and TGFα are increased in response to Poly: IC stimulation in IPF BECs suggesting Poly: IC dsRNA stimulation of BEC result in an increase in the release of pro-fibrotic growth factors [222, 233, 247, 400, 421].

Taken together the data suggests that Poly: IC stimulation, rather than bacterial stimulation, enhances the production and upregulation of pro-fibrotic mediators by BECs. Furthermore, evidence in literature has shown the human lung epithelial cell line, the A549 cell line, co-treated with latent membrane protein-1 (expressed by the Epstein-Barr virus, which is increased in IPF[260]) and low levels of TGFβ1 resulted in a synergistic induction of EMT [274]. Additionally a study investigating the impact of EBV stimulation on A549 and primary human AT2 cells showed an increase in TGFβ1 transcript post stimulation [275]. This data from human *in vitro* experiments combined with evidence from *in vivo* models [255, 256, 272, 273], suggests a role for viruses in IPF pathology.

Further to the investigation of BEC responses to bacterial and viral ligand stimulation, stimulations were investigated in primary fibroblasts from healthy and IPF donors. As the epithelial layer in the IPF lung is severely disrupted, combined with excessive proliferation of fibroblasts, it is possible fibroblasts would directly encounter infectious challenge. Examinations of pro-inflammatory responses were next assessed in primary fibroblasts both from healthy and IPF individuals. Neither Poly: IC, LPS nor bacterial stimulation resulted in an increase in protein expression of any pro-inflammatory mediator or chemokine measured. Stimulation with rhTGFβ1 resulted in an increase IL-8 and IL-6 production suggesting a potentiation of pro-fibrotic responses by fibroblasts, as both IL-8 and IL-6 are increased in IPF, and have been shown to exacerbate fibrosis [112, 204, 205, 221]. Pro-fibrotic genes were upregulated, as expected, in response to rhTGFβ1 stimulation, resulting in increased expression of ACTA2 (αSMA, upregulated on ECM producing myofibroblasts), TGFβ1, TGFβ receptor gene, TGFβR1, and CTGF. This supports the wealth of literature highlighting TGFβ1 as a pro-fibrotic mediator in IPF [425].

Complimentary to gene expression a number of pro-fibrotic growth factors were increased in response to rhTGFβ1 stimulation including TGFβ1, VEGF and PDGF-AA. Specific growth factors were decreased in response to rhTGFβ1 stimulation in IPF fibroblasts, but not healthy fibroblasts, including G-CSF, Angiopoietin-1, FGFb, SCF, PDGF-BB and HGF. Alongside pro-fibrotic effects, TGFβ1 is pivotal in immune-regulation, dampening inflammatory responses [426], therefore it is perhaps unsurprising that G-CSF production is decreased. Angiopoietin-1 levels are decreased in IPF BAL [231], and FGFb and HGF are thought to play a role in epithelial proliferation [234, 240] with HGF production previously reported as reduced in IPF fibroblasts [241], and FGFb administration reported to ameliorate the bleomycin model [234]. Taken together a reduction in these growth factors may result in exacerbation of fibrosis in response to TGFβ1 stimulation. Conversely PDGF-BB and SCF have been reported as pro-fibrotic [150, 247], with PDGF-BB promoting mesenchymal survival [224] and SCF promoting the survival of mast cells, which have been found to be pro-fibrotic [150]. This data highlights the complex role of TGFβ1 in promoting and possible mitigating specific aspects of fibrosis.

In a normal healthy lung, fibroblasts would not encounter pathogens in the airways, instead responding to signals from the epithelial cells and infiltrating leukocytes. To examine epithelial-mesenchymal cross talk the supernatants of stimulated IPF BECS and healthy BECs (BEC conditioned media) were used to stimulate fibroblasts from healthy controls. Fibroblast pro-fibrotic and pro-inflammatory responses were examined in response to the IPF and healthy conditioned BEC media. Interestingly, stimulation with Poly: IC conditioned BEC media, compared to direct Poly: IC stimulation, resulted in in an increase in IL-6, IL-8 and CCL2 gene expression and secretion. This suggests that dsRNA stimulation of epithelial cells alters the capacity of fibroblasts

to produce pro-inflammatory/pro-fibrotic mediators. Fibroblast CCL2 production was significantly increased in response to stimulation with IPF BEC conditioned control media compared to healthy BEC conditioned media. This indicates factors released by IPF BECs are increasing fibroblast production of the CCL2, which is increased in the IPF BAL. Further dissection of protein expression in the BEC media would be required to elucidate the mechanisms which lead to CCL2 release by fibroblasts. Finally, fibroblasts were stimulated with BEC conditioned media or stimulation alone to examine whether stimulation would change proliferation. Stimulation with rhTGFβ1 alone, or healthy/IPF rhTGFβ1 conditioned BEC media resulted in increased proliferation, with a similar observation noted with LPS stimulation conditions. Additional experimental sample stimulation and analysis would be required to confirm these observations. Measurement of collagen and other components of the ECM by fibroblasts following stimulation may provide evidence indicating whether there is a pro-fibrotic effect.

In summary, bacterial or bacterial ligand stimulation did not induce fibrotic change or the production of pro-inflammatory mediators in either the BECs or fibroblasts. Instead data generated suggest that the viral TLR ligand, Poly: IC, induces pro-fibrotic changes in IPF BECs (Summarised in **Figure 5.31**), with mediators produced by BECs inducing an up-regulation of pro-fibrotic mediators in fibroblasts. To investigate this further it would be interesting to stimulate these cells with a virus, such as herpes simplex virus type-1, which is shown to be increased in IPF [103], and examine the responses of IPF and healthy BECs. Furthermore, the development of co-cultures and the measurement of ECM deposition with BEC and fibroblasts may further validate pro-fibrotic findings. Finally blockade of specific components of the TLR signalling cascade could be utilised to investigate important components of these pathways which may be

inducing a pro-fibrotic response. It would also be interesting to examine the response of BECs with a bacterial challenge post viral challenge, as the viral challenge resulted in increased TLR2 expression in IPF BECs. Finally, as the main site of injury is in the alveoli, examination of these stimulations and response by AT1 and AT2 cells, measuring apoptosis in response to these challenges would help to dissect the possible role of viral and bacterial stimulation at site of injury.

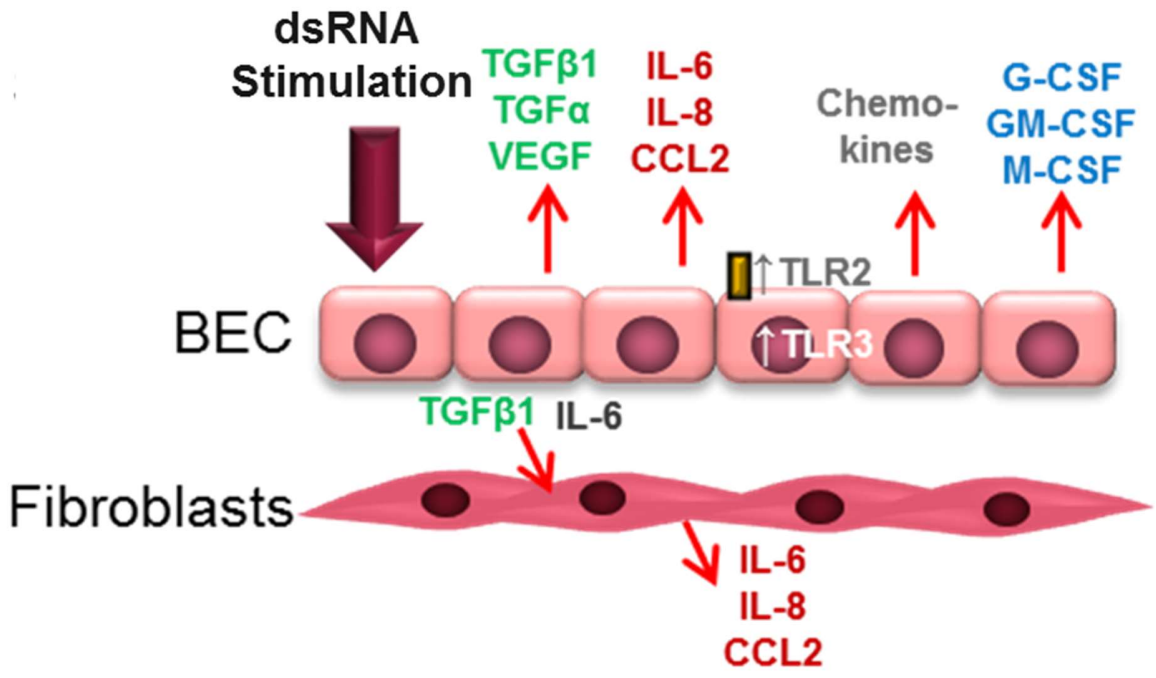


Figure 5.31: Summary of IPF airway response to Poly: IC (dsRNA) stimulation.
In response to viral stimulation BECs upregulate TGFβ1, TLR3 and TLR2 expression and release profibrotic mediators including VEGF, TGFα, IL-6, IL-8 and CCL2. Multiple other chemokines are released into the airways likely to initiate an influx of leukocytes. Granulocytes and macrophages in the airways would be matured interacting with the released BEC produced growth factors G-CSF, GM-CSF and M-CSF. Mediators released by BECs in response to Poly: IC stimulation induces the release of profibrotic mediators IL-6, IL-8 and CCL2 by fibroblasts.

6. Discussion

Collectively the data presented in this thesis provide a valuable and comprehensive overview of the IPF airways, with detailed analysis of the roles of specific cells in response to stimulations resulting in pro-fibrotic changes. The main aims of this research were to; examine BAL leukocyte and mediator profiles, to investigate airway macrophage (AM) function and phenotype, and to assess the role of primary epithelial cells and fibroblasts in response to differing TLR and bacterial stimuli. Investigations into these areas have led to several novel findings including:

- Analysis of key leukocyte populations with paired analysis of extracellular mediators in healthy compared to IPF, UCTD and cHP ILD BAL. Identification of increased monocytes in the IPF airways compared to healthy BAL correlating with increased CCL2. Finally, the observed increased monocyte/macrophage populations, CCL2 and growth factor M-CSF correlated with reduced FVC.
- Identification of a CD11c+CD71- airway macrophage, which were significantly increased in IPF and virtually absent in healthy controls. Additionally, CD11c+CD71- cells exhibited significantly different phenotypes and functional roles compared CD11c+CD71+ airway. Supernatants from isolated CD71- macrophages compared to CD71+ macrophages were shown to stimulate a significant increase in collagen IV deposition by epithelial cells and fibroblasts.
- TLR stimulation of isolated primary BECs from IPF airways have not been investigated previously to our knowledge. The data illustrated significant differences in IPF BEC response and gene expression to specific stimulations compared to healthy BECs. Bacterial or bacterial TLR stimulation of stromal cells did not induce a profibrotic

response, however, Poly: IC stimulation of BECs led to an increase in the expression of multiple pro-fibrotic genes and mediators.

Collectively this work suggests that viral stimulation may potentiate IPF progression and should be investigated further. Furthermore, the increased monocytes, CCL2 and M-CSF correlating with clinical decline suggests an important role for macrophages and possibly monocyte derived macrophages in IPF. Findings highlighting that CD71- macrophage supernatants induced increased collagen IV deposition indicates a possible cell type that may be targeted and inhibited to prevent further ECM deposition.

6.1. Innate immune responses to bacterial and TLR stimulation

The original hypothesis speculated that the defective clearance of bacteria may lead to a pro-fibrotic response driven by bacterial stimulation, and that the reported increases in bacteria would correspond to defective elimination of bacterial pathogens by innate immune cells in IPF patients. Taken together the data presented does not appear to support this hypothesis. There were limited observations pointing to a defective response to bacterial stimuli in IPF compared to healthy control innate immune cells, with no observed increases in the investigated fibrotic genes or mediators analysed post bacterial and bacterial TLR stimulation of primary healthy and IPF bronchial epithelial cells (BECs) or fibroblasts. However, ECM production in response to bacterial stimuli was not measured, nor was live bacterial stimulus. This could be utilised in order to investigate the roles of bacteria in fibrotic progression. In addition, stimulation of epithelial and fibroblasts in co-culture may induce a different response. However, there did appear to be

an induction of pro-fibrotic mediators in response to viral TLR3 ligand Poly: IC stimulation of BECs which influenced an upregulation and increased production of fibrotic mediators by fibroblasts.

In vitro systems enable a simplified investigation into how mediators may induce changes in specific cell types, facilitating the dissection of specific roles of cells; however, they do not accurately recapitulate the multiple mechanisms and complex cellular interactions that occur in an *in vivo* setting, which is an important consideration when interpreting this research. It is possible the microbiome is altered in IPF as a consequence of the altered architecture in fibrotic airways, providing an environment that facilitates the proliferation of bacteria, which this research does not address. Responses by the cells investigated could differ in an *in vivo* setting as opposed to the examined *in vitro* setting used in this research. However, findings in murine models of fibrosis appear to corroborate observations reported here with limited reports on bacterial exacerbation [427], but numerous reports indicating possible viral exacerbation in murine models of fibrosis [255, 256, 272, 273]. Nevertheless, it is possible there may be an ongoing indirect effect of bacteria in influencing fibrosis, by inducing the recruitment and differentiation of leukocytes into the airways, such as monocytes, and by the activation of macrophages, which respond robustly to bacterial TLR4 ligand, LPS, inducing the production of cytokines, chemokine and growth factors. Unfortunately, small cell numbers and yields from healthy controls prevented separation and stimulation of AMs to examine mediator production, which may have highlighted differences in IPF macrophage ability to respond to bacterial stimulation. Assessment of phagocytosis appeared comparable between healthy and IPF, which is perhaps unsurprising with previous investigations highlighting that IPF macrophages exhibited normal phagocytosis, but suggested an impaired bactericidal and bacteriostatic activity post

infection with intracellular bacteria [428]. Interestingly the percentage of AMs positive for nitric oxide (NO) was significantly greater in healthy AMs compared to IPF, which suggests a mechanism by which IPF AMs exhibit impaired intracellular pathogen defence as NO plays a role in intracellular bacterial killing [429]. Further investigation, with focus on intracellular bacteria, would be necessary to dissect the impaired bacterial defence in IPF macrophages.

It is also possible the mediators the bacteria produce exert a pro-fibrotic response in primary fibroblasts or BECs. The stimulations were carried out with heat killed bacteria so the interactions will differ from that of live bacteria. The up-regulation of TLR2 post TLR3 viral stimulation of BECs suggests the response of the BECs to bacterial challenge after viral challenge may differ, with a possible increase in responsiveness to bacterial challenge by BECs. It would be interesting to investigate how viral stimulation may affect the responsiveness of cells to bacterial challenge.

Comparatively to bacterial ligand LPS stimulation, viral ligand Poly: IC stimulation of AMs did not increase production of many key pro-inflammatory mediators including IL-1β, TNFα and IL-6 but did induce an increase in CCL2 and IL-8, suggesting that AM may act to recruit leukocytes in response to direct viral stimulations. Similarly, BECs increased production of chemokines following Poly: IC stimulation, but differed to AMs as they did not respond to LPS stimulations. Cells known to be important in the elimination of virus such as NK cells were found increased in IPF patient BAL compared to healthy controls, which may have been recruited due to viral infection of the BECs, other epithelial cells or AMs. Poly: IC stimulation of BECs also increased production of a number of growth factors including VEGF and PDGF-BB, which are thought to play a role in the progression of IPF. Furthermore, gene expression analysis of BECs showed an

increase in the expression of a number of pro-fibrotic mediators including TGFβ1 and IL-6 in response to Poly: IC stimulations. Stimulation of fibroblasts with conditioned Poly: IC stimulated BEC supernatant, but not bacterial stimulated BEC supernatant, resulted in the increase of IL-6, IL-8 and CCL2 gene expression and protein production by fibroblasts, whereas direct stimulation of fibroblasts with Poly: IC alone showed a limited or reduced response compared to conditioned BEC media. This suggests that BECs soluble mediators influence the production of pro-fibrotic mediators by fibroblasts in response to Poly: IC. Alongside supporting evidence of viral exacerbation in murine fibrosis models, evidence supporting the role of viral stimulation in man have suggested an increased presence of virus in IPF patients including herpes virus (HV) [257-259] and Epstein-Barr virus (EBV) [260]. Conversely some reports show no presence for viruses EBV and HHV-8 from IPF biopsies and as such concluded no involvement of virus in IPF pathogenesis [430]. Methods of detection between studies vary, it is important to consider there may not be an ongoing virus present at time of BAL or tissue biopsy but presence of viral infection may still be detected. For example Kelly et al (2002) found increased presence of EBV genomes, which is a sign of productive EBV replication, in IPF lung biopsies [431], and measurement of viral capsid IgA antibodies in the BAL of IPF has also been reported increased [432]. Nevertheless, further research into this field is necessary to validate these findings, including stimulation of cells with live virus, rather than a viral mimetic, and subsequent quantification of ECM deposition to further examine roles in pathology. Elucidation by blockade of components of TLR signalling would help to determine which parts of the TLR3 pathway are required in the upregulation of pro-fibrotic mediators. Furthermore, examination of responses by other epithelial cell types may highlight differences in cellular response.

6.2. Identification of distinct macrophage populations and functional role in IPF

Observations examining AM macrophage function and phenotype, combined with general leukocyte analysis highlighted key differences comparing AMs in IPF to healthy controls. Significant increases in monocytes and CD71- macrophages were found in IPF BAL, which correlated with clinical decline. The increase in monocytes in the airways correlated with CCL2 suggesting these cells were being attracted into the airways by this chemokine. This is further supported by *in vivo* observations that have shown inhibition of CCL2 [433], or knocking out its receptor CCR2 [209-211], prevents the recruitment of monocytes into the airways, attenuating the bleomycin model of fibrosis, suggesting a possible pathological role of these cells. M-CSF levels were also increased in IPF, which may be differentiating the monocytes to macrophages in the airways. Interestingly the CD71- cells had an appearance of smaller less granular macrophages and expressed significantly increased monocyte marker CD14 compared to CD71+ AMs, suggesting they may represent a more immature monocyte-derived-macrophage. CD71- cells also expressed significantly more CCR2, the receptor for CCL2, expressed by monocytes [434], than the CD71+. The function of the CD71- and CD71+ cells in the airways differed in terms of transferrin bound iron regulation, pathogen detection and defence. Furthermore, the cells expressed significantly different fibrotic genes suggesting divergent roles in disease progression. However, co-culture of CD71- or CD71+ cells with BECs appeared to down-regulate the production of a number of pro-fibrotic genes by the BECs. It is possible that the cells play a protective role in IPF and are recruited as a response to fibrotic pathology; however, these findings conflict with the pro-fibrotic effects demonstrated by macrophages in both the bleomycin model and in IPF. The time point chosen for examination of gene expression post co-

culture may not have been optimal and perhaps co-culture with fibroblasts may have shown different effects. The data did suggest that the combined culture of CD71- cells and BECs resulted in increased IL-6 production, which is an important mediator in fibrosis.

Following from direct co-culture of CD71- and CD71+ cells with BECS, investigation into the production of ECM by small airway epithelial cells and IPF fibroblasts grown in co-culture revealed CD71- cell supernatants induced an increase in collagen IV deposition, suggesting the CD71- cells may play a role in the increased deposition of collagen in the IPF airways.

6.3. Summary and future work

The first chapter of the thesis aimed to characterise the BAL inflammatory profiles in ILD compared to healthy controls. To achieve this immune cell composition was examined using multicolour flow cytometry, with paired quantification of soluble mediators by multiplex analysis, combined with clinical lung function readouts in patients with ILD and healthy controls. This data was analysed to evaluate the BAL profiles revealing an increased monocyte and macrophage signature in IPF and UCTD compared to healthy controls, and an increased lymphocyte signature in cHP. However, the methods employed could be improved further with more sophisticated analytical techniques. For example, the examination of the BAL cellular infiltrate could be evaluated using mass cytometry, a technique which enables the labelling and quantification of over 40 intracellular and extracellular mediators with antibodies conjugated to isotopically pure elements. This allows the accurate quantification of extensive panels of markers without fluorescence compensation, which is required using FACS analysis.

Analysis of extracellular mediators could also be improved. Rather than examining specific mediators in the BAL using multiplex analysis, utilising mass spectrometry to comprehensively evaluate proteomic profiles in BAL would indiscriminately determine and quantify a multitude of proteins, providing additional clues as to what is driving these poorly understood pathologies. Additionally, pairing analysis of the BAL to systemic and relatively non-invasive compartments such as the peripheral blood, and/or induced sputum, would enable extensive correlations between different sites, possibly identifying novel biomarkers, allowing for future analysis to be conducted using less invasive sampling techniques. Combining these analyses with longitudinal study of patient acute exacerbations and pathological progression could identify cell types or protein biomarkers which may be predictive of a poor or improved disease course, allowing for more focused future protein/cellular analysis predictive of patient disease outcome.

Collectively the second chapter highlights a possible pro-fibrotic role for an infiltrating monocyte-macrophage population, which has been highlighted in mouse models, with the increased CD11c+CD71- 'immature' macrophages releasing mediators which enhanced the expression of specific collagens. In order to verify whether the CD71- cells represent a true 'immature' monocyte-derived-macrophage the CD71- cells could be cultured in conditions which as closely as possible recapitulate those that are found in the airways to see if they differentiate into a more mature airway macrophage. Nevertheless, this data suggests that the CD71- cells may play a role directly in IPF pathogenesis. Elegant studies in the bleomycin murine model of fibrosis have identified monocyte-derived-macrophages driving fibrosis supporting a role for these cells in pathology in man [72, 364, 365]. Additionally, murine models have shown that viral challenge can exacerbate or induce fibrosis [255, 256, 272, 273]. The increase in pro-fibrotic mediators by

direct and indirect Poly: IC stimulation of stromal cells suggests a role for viral infection in IPF pathogenesis. Key chemokines such as CCL2 were increased in these stimulations. It would be interesting to see if monocytes were attracted to the Poly: IC stimulated BEC supernatants using chemotaxis assays. Furthermore, neutralisation of specific chemokines such as CCL2 may prevent this chemotaxis, highlighting which chemokines specifically are important in attracting monocytes into the airways. This would also verify Poly: IC stimulated BECs as a possible source for monocyte recruitment. Further examination of both human airway macrophages and the examination of viral infection in man in exacerbation of fibrosis is essential. To further delineate the roles of the macrophages and viral stimulus, co-culturing of the CD71+ and CD71- macrophage populations in the ECM producing epithelial and fibroblast co-culture system would highlight whether direct cell interactions influence ECM deposition in a similar way to the supernatants. Equally stimulating the ECM producing epithelial-fibroblast co-culture with the healthy and IPF BEC conditioned supernatant may result in increased ECM deposition. Examining conditioned supernatants used to stimulate the ECM co-culture using proteomic analysis would help identify specific elevated proteins which may contribute to the observed increased ECM production. Blockade of the specific proteins identified as increased in the cell supernatants may help identify possible novel soluble therapeutic targets.

Characterisation of the macrophage in the BAL did not reveal a distinct M1/M2 profile examining the M1 markers HLA-DR and CD86 or M2 markers CD163 and CD206. Additional M2 markers such as extracellular CD209, and intracellular cytokines including TGFβ and IL-10 could be used to further assess the M2 phenotype. Similarly, inclusion of additional M1 markers such as CD80 and the production of TNFα and IL-1β could be used to further examine the M1 phenotype. Using

techniques, such as the aforementioned mass cytometry, would enable the evaluation of an extensive range of macrophage surface and intracellular markers building a comprehensive macrophage profile. In addition, isolation of macrophages from patients with ILD and healthy individuals, could be used to examine the transcriptome using RNA-seq, which would provide a comprehensive gene profile of macrophages in health compared to disease.

Finally, the third chapter highlights the direct stimulation of IPF and healthy primary BECs with viral mimetic, Poly: IC a TLR3 ligand, but not gram negative bacterial cell wall component, LPS, a TLR4 ligand, or heat killed bacterial stimulation, induced an upregulation in multiple pro-fibrotic mediators. It would be interesting to validate this work using live bacteria and live viral infection. Additionally, using more complex and tissue relevant cultures, such as air liquid interface (ALI) cultures co-culturing fibroblasts with epithelial cells from healthy and diseased individuals would help to validate these findings in a more tissue relevant assay. Furthermore, quantification of ECM post stimulation is necessary as a hallmark pathological feature of fibrotic ILD.

Differences in responses in primary healthy compared to IPF isolated fibroblasts suggest a possible decrease in the production of proinflammatory mediators by the IPF fibroblasts, however, an increase in the n numbers would be necessary to validate these observations.

Taken together the work suggests research into IPF pathogenesis should focus on viral exacerbation and the role of monocytes and monocyte-derived-macrophages in driving IPF pathology. A proposed model of viral stimulation and cellular interactions driving IPF pathology is illustrated in **Figure 6.1**.

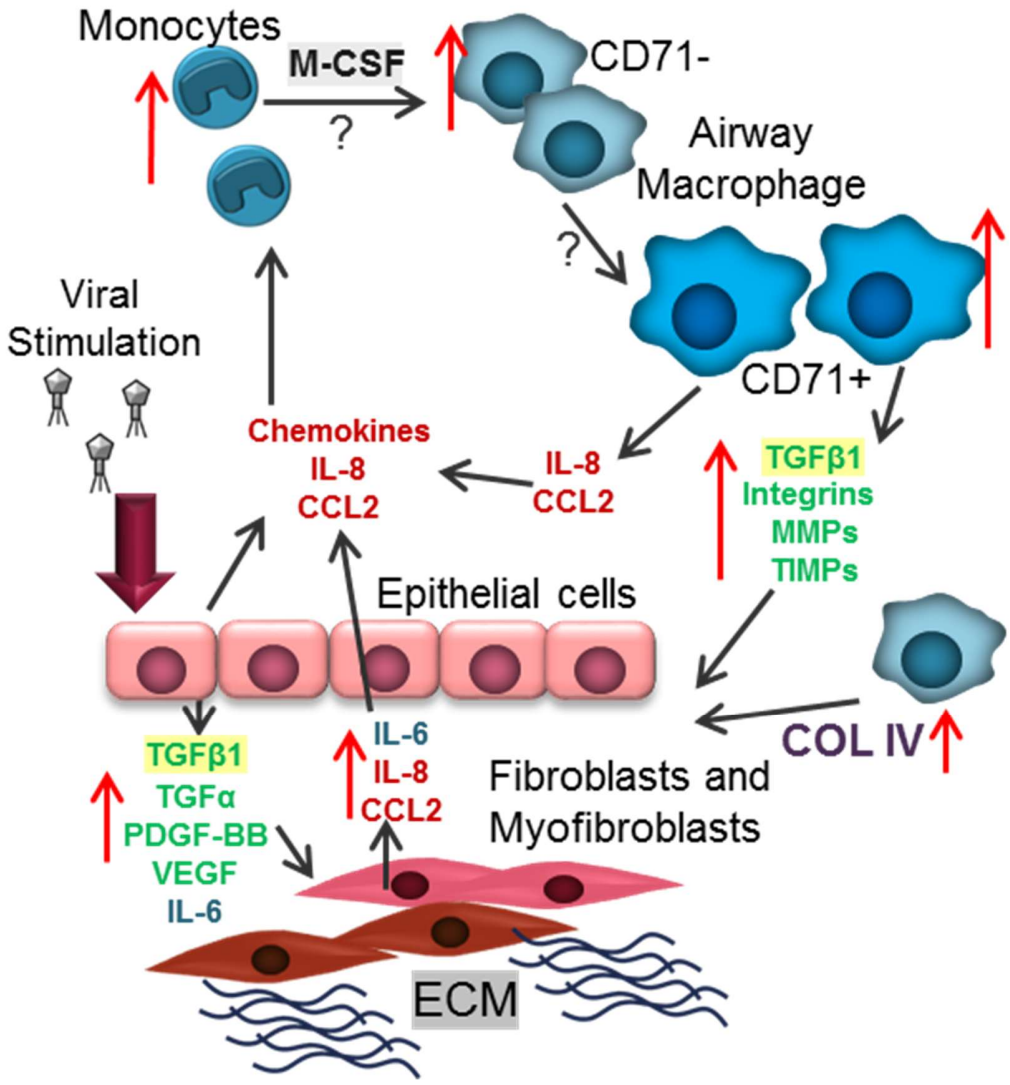


Figure 6.1: Proposed model of viral stimulation and cellular interactions driving IPF pathology. Stimulation of BECs with Poly: IC results in the upregulation of pro-fibrotic mediators including TGFβ1, TGFα, PDGF-BB and IL-6, which have been shown to differentiate fibroblasts into myofibroblasts. Activation of fibroblasts with stimulated Poly: IC BEC supernatant results in fibroblast IL-6, CCL2 and IL-8 production. CCL2 release from BEC and fibroblasts result in the recruitment of monocytes into the airways, which may differentiate into macrophages with the presence of M-CSF and GM-CSF produced by Poly: IC stimulated BECs. Monocytes may differentiate into CD71- macrophages which induce collagen IV deposition by epithelial cells and fibroblasts. Growth factors, integrins and pro-fibrotic mediators expressed and released by macrophages further activate fibroblasts. Direct stimulation of AMs by Poly: IC results in the release chemokines including CCL2 further attracting monocytes into the airways.

7. References

1. Nalysnyk, L., et al., *Incidence and prevalence of idiopathic pulmonary fibrosis: review of the literature.* Eur Respir Rev, 2012. **21**(126): p. 355-61.
2. Molyneaux, P.L., et al., *The role of bacteria in the pathogenesis and progression of idiopathic pulmonary fibrosis.* Am J Respir Crit Care Med, 2014. **190**(8): p. 906-13.
3. Han, M.K., et al., *Lung microbiome and disease progression in idiopathic pulmonary fibrosis: an analysis of the COMET study.* Lancet Respir Med, 2014. **2**(7): p. 548-56.
4. Meyer, K.C., *Diagnosis and management of interstitial lung disease.* Transl Respir Med, 2014. **2**: p. 4.
5. Suki, B. and J.H. Bates, *Extracellular matrix mechanics in lung parenchymal diseases.* Respir Physiol Neurobiol, 2008. **163**(1-3): p. 33-43.
6. Liang, B.M., D.C. Lam, and Y.L. Feng, *Clinical applications of lung function tests: a revisit.* Respirology, 2012. **17**(4): p. 611-9.
7. Espoladore, L.M., et al., *Cytological analysis of bronchoalveolar lavage in patients with interstitial lung diseases and the relation of cytological analysis to fibrosis in high-resolution computed tomography.* Anal Quant Cytopathol Histpathol, 2014. **36**(4): p. 206-12.
8. Cottin, V., *Eosinophilic Lung Diseases.* Clin Chest Med, 2016. **37**(3): p. 535-56.
9. McLennan, G., M.W. Stevens, and R.L. Walsh, *Bronchoalveolar lavage.* Aust N Z J Med, 1985. **15**(5): p. 659-67.
10. Selman, M., A. Pardo, and T.E. King, Jr., *Hypersensitivity pneumonitis: insights in diagnosis and pathobiology.* Am J Respir Crit Care Med, 2012. **186**(4): p. 314-24.
11. Lazarus, A.A. and A. Philip, *Asbestosis.* Dis Mon, 2011. **57**(1): p. 14-26.
12. Ekstrom, M., et al., *Effects of smoking, gender and occupational exposure on the risk of severe pulmonary fibrosis: a population-based case-control study.* BMJ Open, 2014. **4**(1): p. e004018.
13. Koo, J.W., et al., *Occupational exposure and idiopathic pulmonary fibrosis: a multicentre case-control study in Korea.* Int J Tuberc Lung Dis, 2017. **21**(1): p. 107-112.
14. Awadalla, N.J., et al., *Occupational and environmental risk factors for idiopathic pulmonary fibrosis in Egypt: a multicenter case-control study.* Int J Occup Environ Med, 2012. **3**(3): p. 107-16.
15. Muggia, F.M., A.C. Louie, and B.I. Sikic, *Pulmonary toxicity of antitumor agents.* Cancer Treat Rev, 1983. **10**(4): p. 221-43.
16. Camus, P., et al., *Interstitial lung disease induced by drugs and radiation.* Respiration, 2004. **71**(4): p. 301-26.
17. Cordier, J.F., *Cryptogenic organizing pneumonia.* Clin Chest Med, 2004. **25**(4): p. 727-38, vi-vii.
18. Drakopanagiotakis, F., et al., *Cryptogenic and secondary organizing pneumonia: clinical presentation, radiographic findings, treatment response, and prognosis.* Chest, 2011. **139**(4): p. 893-900.

19. Mukhopadhyay, S. and J.G. Parambil, *Acute interstitial pneumonia (AIP): relationship to Hamman-Rich syndrome, diffuse alveolar damage (DAD), and acute respiratory distress syndrome (ARDS).* Semin Respir Crit Care Med, 2012. **33**(5): p. 476-85.
20. Mathai, S.K., et al., *Pulmonary fibrosis in the era of stratified medicine.* Thorax, 2016. **71**(12): p. 1154-1160.
21. Chakraborty, S., et al., *Emerging therapeutic interventions for idiopathic pulmonary fibrosis.* Expert Opin Investig Drugs, 2014. **23**(7): p. 893-910.
22. Woodcock, H.V. and T.M. Maher, *The treatment of idiopathic pulmonary fibrosis.* F1000Prime Rep, 2014. **6**: p. 16.
23. Richeldi, L., et al., *Efficacy and safety of nintedanib in idiopathic pulmonary fibrosis.* N Engl J Med, 2014. **370**(22): p. 2071-82.
24. Kligerman, S.J., et al., *Nonspecific interstitial pneumonia: radiologic, clinical, and pathologic considerations.* Radiographics, 2009. **29**(1): p. 73-87.
25. Akira, M., et al., *Non-specific interstitial pneumonia: findings on sequential CT scans of nine patients.* Thorax, 2000. **55**(10): p. 854-9.
26. Nishino, M., et al., *Clinicopathologic features associated with relapse in cryptogenic organizing pneumonia.* Hum Pathol, 2014. **45**(2): p. 342-51.
27. Godbert, B., M.P. Wissler, and J.M. Vignaud, *Desquamative interstitial pneumonia: an analytic review with an emphasis on aetiology.* Eur Respir Rev, 2013. **22**(128): p. 117-23.
28. Drent, M., J.P. Cremers, and T.L. Jansen, *Pulmonology meets rheumatology in sarcoidosis: a review on the therapeutic approach.* Curr Opin Rheumatol, 2014. **26**(3): p. 276-84.
29. Bussone, G. and L. Mouthon, *Interstitial lung disease in systemic sclerosis.* Autoimmun Rev, 2011. **10**(5): p. 248-55.
30. Cottin, V., *Significance of connective tissue diseases features in pulmonary fibrosis.* Eur Respir Rev, 2013. **22**(129): p. 273-80.
31. Montgomery, N.D., et al., *Diagnostic complexities of eosinophilia.* Arch Pathol Lab Med, 2013. **137**(2): p. 259-69.
32. Barker, A.F., et al., *Obliterative bronchiolitis.* N Engl J Med, 2014. **370**(19): p. 1820-8.
33. Sgalla, G., A. Biffi, and L. Richeldi, *Idiopathic pulmonary fibrosis: Diagnosis, epidemiology and natural history.* Respirology, 2016. **21**(3): p. 427-37.
34. Raghu, G., et al., *Incidence and prevalence of idiopathic pulmonary fibrosis in US adults 18-64 years old.* Eur Respir J, 2016. **48**(1): p. 179-86.
35. Navaratnam, V., et al., *The rising incidence of idiopathic pulmonary fibrosis in the U.K.* Thorax, 2011. **66**(6): p. 462-7.
36. Swigris, J.J., et al., *Ethnic and racial differences in the presence of idiopathic pulmonary fibrosis at death.* Respir Med, 2012. **106**(4): p. 588-93.
37. Sisson, T.H., et al., *Increased survivin expression contributes to apoptosis-resistance in IPF fibroblasts.* Adv Biosci Biotechnol, 2012. **3**(6a): p. 657-664.
38. Huang, S.K. and J.C. Horowitz, *Outstaying their Welcome: The Persistent Myofibroblast in IPF.* Austin J Pulm Respir Med, 2014. **1**(1): p. 3.
39. Habiel, D.M. and C. Hogaboam, *Heterogeneity in fibroblast proliferation and survival in idiopathic pulmonary fibrosis.* Front Pharmacol, 2014. **5**: p. 2.
40. Horowitz, J.C., et al., *Activation of the pro-survival phosphatidylinositol 3-kinase/AKT pathway by transforming growth factor-beta1 in mesenchymal cells is mediated by p38*

MAPK-dependent induction of an autocrine growth factor. J Biol Chem, 2004. **279**(2): p. 1359-67.

41. Horowitz, J.C., et al., *Survivin expression induced by endothelin-1 promotes myofibroblast resistance to apoptosis.* Int J Biochem Cell Biol, 2012. **44**(1): p. 158-69.
42. Horowitz, J.C., et al., *Combinatorial activation of FAK and AKT by transforming growth factor-beta1 confers an anoikis-resistant phenotype to myofibroblasts.* Cell Signal, 2007. **19**(4): p. 761-71.
43. Kulasekaran, P., et al., *Endothelin-1 and transforming growth factor-beta1 independently induce fibroblast resistance to apoptosis via AKT activation.* Am J Respir Cell Mol Biol, 2009. **41**(4): p. 484-93.
44. Parker, M.W., et al., *Fibrotic extracellular matrix activates a profibrotic positive feedback loop.* J Clin Invest, 2014. **124**(4): p. 1622-35.
45. Willis, B.C., et al., *Induction of epithelial-mesenchymal transition in alveolar epithelial cells by transforming growth factor-beta1: potential role in idiopathic pulmonary fibrosis.* Am J Pathol, 2005. **166**(5): p. 1321-32.
46. Yang, T., M. Chen, and T. Sun, *Simvastatin attenuates TGF-beta1-induced epithelial-mesenchymal transition in human alveolar epithelial cells.* Cell Physiol Biochem, 2013. **31**(6): p. 863-74.
47. O'Beirne, S.L., et al., *CXCL9 Regulates TGF-beta1-Induced Epithelial to Mesenchymal Transition in Human Alveolar Epithelial Cells.* J Immunol, 2015. **195**(6): p. 2788-96.
48. Funke, M., et al., *The lysophosphatidic acid receptor LPA1 promotes epithelial cell apoptosis after lung injury.* Am J Respir Cell Mol Biol, 2012. **46**(3): p. 355-64.
49. Hagimoto, N., et al., *TGF-beta 1 as an enhancer of Fas-mediated apoptosis of lung epithelial cells.* J Immunol, 2002. **168**(12): p. 6470-8.
50. Kim, S.J., et al., *The Role of Mitochondrial DNA in Mediating Alveolar Epithelial Cell Apoptosis and Pulmonary Fibrosis.* Int J Mol Sci, 2015. **16**(9): p. 21486-519.
51. Garcia-Alvarez, J., et al., *Membrane type-matrix metalloproteinases in idiopathic pulmonary fibrosis.* Sarcoidosis Vasc Diffuse Lung Dis, 2006. **23**(1): p. 13-21.
52. Meyer, K.C., et al., *An official American Thoracic Society clinical practice guideline: the clinical utility of bronchoalveolar lavage cellular analysis in interstitial lung disease.* Am J Respir Crit Care Med, 2012. **185**(9): p. 1004-14.
53. Costabel, U. and J. Guzman, *Bronchoalveolar lavage in interstitial lung disease.* Curr Opin Pulm Med, 2001. **7**(5): p. 255-61.
54. Wells, A.U., *Managing diagnostic procedures in idiopathic pulmonary fibrosis.* Eur Respir Rev, 2013. **22**(128): p. 158-62.
55. Borensztajn, K., B. Crestani, and M. Kolb, *Idiopathic pulmonary fibrosis: from epithelial injury to biomarkers--insights from the bench side.* Respiration, 2013. **86**(6): p. 441-52.
56. Rottoli, P., et al., *Cytokine profile and proteome analysis in bronchoalveolar lavage of patients with sarcoidosis, pulmonary fibrosis associated with systemic sclerosis and idiopathic pulmonary fibrosis.* Proteomics, 2005. **5**(5): p. 1423-30.
57. Schupp, J.C., et al., *Macrophage activation in acute exacerbation of idiopathic pulmonary fibrosis.* PLoS One, 2015. **10**(1): p. e0116775.
58. Rabeyrin, M., et al., *Usual interstitial pneumonia end-stage features from explants with radiologic and pathological correlations.* Ann Diagn Pathol, 2015. **19**(4): p. 269-76.

59. Cavazza, A., et al., *The role of histology in idiopathic pulmonary fibrosis: an update.* Respir Med, 2010. **104 Suppl 1**: p. S11-22.
60. Mubarak, K.K., et al., *Parenchymal trafficking of pleural mesothelial cells in idiopathic pulmonary fibrosis.* Eur Respir J, 2012. **39**(1): p. 133-40.
61. Fernandez, I.E., et al., *Systematic phenotyping and correlation of biomarkers with lung function and histology in lung fibrosis.* Am J Physiol Lung Cell Mol Physiol, 2016. **310**(10): p. L919-27.
62. Warsinske, H.C., et al., *Computational Modeling Predicts Simultaneous Targeting of Fibroblasts and Epithelial Cells Is Necessary for Treatment of Pulmonary Fibrosis.* Front Pharmacol, 2016. **7**: p. 183.
63. Beach, T.A., et al., *Radiation induced pulmonary fibrosis as a model of progressive fibrosis: Contributions of DNA damage, inflammatory response and cellular senescence genes.* Exp Lung Res, 2017. **43**(3): p. 134-149.
64. Davis, G.S., K.O. Leslie, and D.R. Hemenway, *Silicosis in mice: effects of dose, time, and genetic strain.* J Environ Pathol Toxicol Oncol, 1998. **17**(2): p. 81-97.
65. Roberts, S.N., et al., *A novel model for human interstitial lung disease: hapten-driven lung fibrosis in rodents.* J Pathol, 1995. **176**(3): p. 309-18.
66. Chua, F., J. Gauldie, and G.J. Laurent, *Pulmonary fibrosis: searching for model answers.* Am J Respir Cell Mol Biol, 2005. **33**(1): p. 9-13.
67. Umezawa, H., *Chemistry and mechanism of action of bleomycin.* Fed Proc, 1974. **33**(11): p. 2296-302.
68. Schrier, D.J., R.G. Kunkel, and S.H. Phan, *The role of strain variation in murine bleomycin-induced pulmonary fibrosis.* Am Rev Respir Dis, 1983. **127**(1): p. 63-6.
69. Scotton, C.J., et al., *Ex vivo micro-computed tomography analysis of bleomycin-induced lung fibrosis for preclinical drug evaluation.* Eur Respir J, 2013. **42**(6): p. 1633-45.
70. Janick-Buckner, D., G.E. Ranges, and M.P. Hacker, *Alteration of bronchoalveolar lavage cell populations following bleomycin treatment in mice.* Toxicol Appl Pharmacol, 1989. **100**(3): p. 465-73.
71. Jones, H.A., et al., *In vivo measurement of neutrophil activity in experimental lung inflammation.* Am J Respir Crit Care Med, 1994. **149**(6): p. 1635-9.
72. Satoh, T., et al., *Identification of an atypical monocyte and committed progenitor involved in fibrosis.* Nature, 2017. **541**(7635): p. 96-101.
73. Izbicki, G., et al., *Time course of bleomycin-induced lung fibrosis.* Int J Exp Pathol, 2002. **83**(3): p. 111-9.
74. Lawson, W.E., et al., *Increased and prolonged pulmonary fibrosis in surfactant protein C-deficient mice following intratracheal bleomycin.* Am J Pathol, 2005. **167**(5): p. 1267-77.
75. Raghu, G., et al., *Prednisone, azathioprine, and N-acetylcysteine for pulmonary fibrosis.* N Engl J Med, 2012. **366**(21): p. 1968-77.
76. Bellaye, P.S. and M. Kolb, *Why do patients get idiopathic pulmonary fibrosis? Current concepts in the pathogenesis of pulmonary fibrosis.* BMC Med, 2015. **13**: p. 176.
77. Daccord, C. and T.M. Maher, *Recent advances in understanding idiopathic pulmonary fibrosis.* F1000Res, 2016. **5**.
78. Wynn, T.A., *Cellular and molecular mechanisms of fibrosis.* J Pathol, 2008. **214**(2): p. 199-210.

79. Wynn, T.A. and T.R. Ramalingam, *Mechanisms of fibrosis: therapeutic translation for fibrotic disease.* Nat Med, 2012. **18**(7): p. 1028-40.
80. Coghlan, M.A., et al., *Sequencing of idiopathic pulmonary fibrosis-related genes reveals independent single gene associations.* BMJ Open Respir Res, 2014. **1**(1): p. e000057.
81. Mulugeta, S., S. Nureki, and M.F. Beers, *Lost after translation: insights from pulmonary surfactant for understanding the role of alveolar epithelial dysfunction and cellular quality control in fibrotic lung disease.* Am J Physiol Lung Cell Mol Physiol, 2015. **309**(6): p. L507-25.
82. Thomas, A.Q., et al., *Heterozygosity for a surfactant protein C gene mutation associated with usual interstitial pneumonitis and cellular nonspecific interstitial pneumonitis in one kindred.* Am J Respir Crit Care Med, 2002. **165**(9): p. 1322-8.
83. Noth, I., et al., *Genetic variants associated with idiopathic pulmonary fibrosis susceptibility and mortality: a genome-wide association study.* Lancet Respir Med, 2013. **1**(4): p. 309-317.
84. Yang, I.V., et al., *MUC5B and Idiopathic Pulmonary Fibrosis.* Ann Am Thorac Soc, 2015. **12 Suppl 2**: p. S193-9.
85. Yang, I.V., et al., *Expression of cilium-associated genes defines novel molecular subtypes of idiopathic pulmonary fibrosis.* Thorax, 2013. **68**(12): p. 1114-21.
86. Kim, K.C., *Role of epithelial mucins during airway infection.* Pulm Pharmacol Ther, 2012. **25**(6): p. 415-9.
87. Peljto, A.L., et al., *Association between the MUC5B promoter polymorphism and survival in patients with idiopathic pulmonary fibrosis.* Jama, 2013. **309**(21): p. 2232-9.
88. Mathai, S.K., et al., *Desmoplakin Variants Are Associated with Idiopathic Pulmonary Fibrosis.* Am J Respir Crit Care Med, 2016. **193**(10): p. 1151-60.
89. Fingerlin, T.E., et al., *Genome-wide association study identifies multiple susceptibility loci for pulmonary fibrosis.* Nat Genet, 2013. **45**(6): p. 613-20.
90. Borie, R., et al., *Prevalence and characteristics of TERT and TERC mutations in suspected genetic pulmonary fibrosis.* Eur Respir J, 2016. **48**(6): p. 1721-1731.
91. Mushiroda, T., et al., *A genome-wide association study identifies an association of a common variant in TERT with susceptibility to idiopathic pulmonary fibrosis.* J Med Genet, 2008. **45**(10): p. 654-6.
92. Marrone, A., et al., *Functional characterization of novel telomerase RNA (TERC) mutations in patients with diverse clinical and pathological presentations.* Haematologica, 2007. **92**(8): p. 1013-20.
93. Takeda, K. and S. Akira, *TLR signaling pathways.* Semin Immunol, 2004. **16**(1): p. 3-9.
94. Chilosi, M., et al., *Premature lung aging and cellular senescence in the pathogenesis of idiopathic pulmonary fibrosis and COPD/emphysema.* Transl Res, 2013. **162**(3): p. 156-73.
95. Yanai, H., et al., *Cellular senescence-like features of lung fibroblasts derived from idiopathic pulmonary fibrosis patients.* Aging (Albany NY), 2015. **7**(9): p. 664-72.
96. Minagawa, S., et al., *Accelerated epithelial cell senescence in IPF and the inhibitory role of SIRT6 in TGF-beta-induced senescence of human bronchial epithelial cells.* Am J Physiol Lung Cell Mol Physiol, 2011. **300**(3): p. L391-401.
97. Brand-Saberi, B.E. and T. Schafer, *Trachea: anatomy and physiology.* Thorac Surg Clin, 2014. **24**(1): p. 1-5.

98. Wong, A.P., A. Keating, and T.K. Waddell, *Airway regeneration: the role of the Clara cell secretory protein and the cells that express it.* Cytotherapy, 2009. **11**(6): p. 676-87.
99. Birchenough, G.M., et al., *New developments in goblet cell mucus secretion and function.* Mucosal Immunol, 2015. **8**(4): p. 712-9.
100. Camelo, A., et al., *The epithelium in idiopathic pulmonary fibrosis: breaking the barrier.* Front Pharmacol, 2014. **4**: p. 173.
101. Konishi, S., et al., *Directed Induction of Functional Multi-ciliated Cells in Proximal Airway Epithelial Spheroids from Human Pluripotent Stem Cells.* Stem Cell Reports, 2016. **6**(1): p. 18-25.
102. Knudsen, L., C. Ruppert, and M. Ochs, *Tissue remodelling in pulmonary fibrosis.* Cell Tissue Res, 2017. **367**(3): p. 607-626.
103. Renois, F., et al., *Respiratory echovirus 30 and coxsackievirus B5 can induce production of RANTES, MCP-1 and IL-8 by human bronchial epithelial cells.* Virus Res, 2010. **152**(1-2): p. 41-9.
104. Dosanjh, A., *Connective tissue growth factor expression in human bronchial epithelial cells.* Acta Biochim Biophys Sin (Shanghai), 2006. **38**(1): p. 53-7.
105. Pan, L.H., et al., *Type II alveolar epithelial cells and interstitial fibroblasts express connective tissue growth factor in IPF.* Eur Respir J, 2001. **17**(6): p. 1220-7.
106. Thaikoottathil, J.V., et al., *Cigarette smoke extract reduces VEGF in primary human airway epithelial cells.* Eur Respir J, 2009. **33**(4): p. 835-43.
107. Shimizu, S., et al., *Thrombin stimulates the expression of PDGF in lung epithelial cells.* Am J Physiol Lung Cell Mol Physiol, 2000. **279**(3): p. L503-10.
108. Xu, Y.D., et al., *Release of biologically active TGF-beta1 by alveolar epithelial cells results in pulmonary fibrosis.* Am J Physiol Lung Cell Mol Physiol, 2003. **285**(3): p. L527-39.
109. Tatler, A.L. and G. Jenkins, *TGF-beta activation and lung fibrosis.* Proc Am Thorac Soc, 2012. **9**(3): p. 130-6.
110. Volckaert, T. and S. De Langhe, *Lung epithelial stem cells and their niches: Fgf10 takes center stage.* Fibrogenesis Tissue Repair, 2014. **7**: p. 8.
111. Phan, S.H., *Genesis of the myofibroblast in lung injury and fibrosis.* Proc Am Thorac Soc, 2012. **9**(3): p. 148-52.
112. Keane, M.P., et al., *The CXC chemokines, IL-8 and IP-10, regulate angiogenic activity in idiopathic pulmonary fibrosis.* J Immunol, 1997. **159**(3): p. 1437-43.
113. Coppe, J.P., et al., *Secretion of vascular endothelial growth factor by primary human fibroblasts at senescence.* J Biol Chem, 2006. **281**(40): p. 29568-74.
114. Burgess, J.K., et al., *The extracellular matrix - the under-recognized element in lung disease?* J Pathol, 2016. **240**(4): p. 397-409.
115. Nho, R.S. and V. Polunovsky, *Translational control of the fibroblast-extracellular matrix association: An application to pulmonary fibrosis.* Translation (Austin), 2013. **1**(1): p. e23934.
116. Sousa, A.M., et al., *Smooth muscle alpha-actin expression and myofibroblast differentiation by TGFbeta are dependent upon MK2.* J Cell Biochem, 2007. **100**(6): p. 1581-92.

117. Katzenstein, A.L., S. Mukhopadhyay, and J.L. Myers, *Diagnosis of usual interstitial pneumonia and distinction from other fibrosing interstitial lung diseases.* Hum Pathol, 2008. **39**(9): p. 1275-94.
118. Waisberg, D.R., et al., *Abnormal expression of telomerase/apoptosis limits type II alveolar epithelial cell replication in the early remodeling of usual interstitial pneumonia/idiopathic pulmonary fibrosis.* Hum Pathol, 2010. **41**(3): p. 385-91.
119. Yamaguchi, M., et al., *Fibroblastic foci, covered with alveolar epithelia exhibiting epithelial-mesenchymal transition, destroy alveolar septa by disrupting blood flow in idiopathic pulmonary fibrosis.* Lab Invest, 2017. **97**(3): p. 232-242.
120. Wynn, T.A., *Integrating mechanisms of pulmonary fibrosis.* J Exp Med, 2011. **208**(7): p. 1339-50.
121. Ekert, J.E., et al., *Chemokine (C-C motif) ligand 2 mediates direct and indirect fibrotic responses in human and murine cultured fibrocytes.* Fibrogenesis Tissue Repair, 2011. **4**(1): p. 23.
122. Moore, B.B., et al., *The role of CCL12 in the recruitment of fibrocytes and lung fibrosis.* Am J Respir Cell Mol Biol, 2006. **35**(2): p. 175-81.
123. Andersson-Sjoland, A., et al., *Fibrocytes are a potential source of lung fibroblasts in idiopathic pulmonary fibrosis.* Int J Biochem Cell Biol, 2008. **40**(10): p. 2129-40.
124. Kasai, H., et al., *TGF-beta1 induces human alveolar epithelial to mesenchymal cell transition (EMT).* Respir Res, 2005. **6**: p. 56.
125. Chapman, H.A., *Epithelial-mesenchymal interactions in pulmonary fibrosis.* Annu Rev Physiol, 2011. **73**: p. 413-35.
126. Balbi, B., et al., *Bronchoalveolar lavage, sputum and exhaled clinically relevant inflammatory markers: values in healthy adults.* Eur Respir J, 2007. **30**(4): p. 769-81.
127. Heron, M., et al., *Bronchoalveolar lavage cell pattern from healthy human lung.* Clin Exp Immunol, 2012. **167**(3): p. 523-31.
128. Papakosta, D., et al., *Bronchoalveolar lavage fluid and blood natural killer and natural killer T-like cells in cryptogenic organizing pneumonia.* Respirology, 2014. **19**(5): p. 748-54.
129. Papiris, S.A., et al., *Relationship of BAL and lung tissue CD4+ and CD8+ T lymphocytes, and their ratio in idiopathic pulmonary fibrosis.* Chest, 2005. **128**(4): p. 2971-7.
130. Barrera, L., et al., *Functional diversity of T-cell subpopulations in subacute and chronic hypersensitivity pneumonitis.* Am J Respir Crit Care Med, 2008. **177**(1): p. 44-55.
131. Murayama, J., et al., *Lung fibrosis in hypersensitivity pneumonitis. Association with CD4+ but not CD8+ cell dominant alveolitis and insidious onset.* Chest, 1993. **104**(1): p. 38-43.
132. Caillaud, D.M., et al., *Bronchoalveolar lavage in hypersensitivity pneumonitis: a series of 139 patients.* Inflamm Allergy Drug Targets, 2012. **11**(1): p. 15-9.
133. Shimizu, Y., et al., *Intracellular Th1/Th2 balance of pulmonary CD4(+) T cells in patients with active interstitial pneumonia evaluated by serum KL-6.* Immunopharmacol Immunotoxicol, 2006. **28**(2): p. 295-304.
134. Murray, L.A., et al., *Hyper-responsiveness of IPF/UIP fibroblasts: interplay between TGFbeta1, IL-13 and CCL2.* Int J Biochem Cell Biol, 2008. **40**(10): p. 2174-82.
135. Vasakova, M., et al., *Correlation of IL-1alpha and IL-4 gene polymorphisms and clinical parameters in idiopathic pulmonary fibrosis.* Scand J Immunol, 2007. **65**(3): p. 265-70.

136. Vasakova, M., et al., *IL-4 polymorphisms, HRCT score and lung tissue markers in idiopathic pulmonary fibrosis.* Hum Immunol, 2013. **74**(10): p. 1346-51.
137. Vasakova, M., et al., *Cytokine gene polymorphisms and high-resolution-computed tomography score in idiopathic pulmonary fibrosis.* Respir Med, 2007. **101**(5): p. 944-50.
138. Parker, J.M., et al., *A Phase 2 Randomized Controlled Study of Tralokinumab in Subjects with Idiopathic Pulmonary Fibrosis.* Am J Respir Crit Care Med, 2017.
139. Chizzolini, C., *T cells, B cells, and polarized immune response in the pathogenesis of fibrosis and systemic sclerosis.* Curr Opin Rheumatol, 2008. **20**(6): p. 707-12.
140. Xue, J., et al., *Plasma B lymphocyte stimulator and B cell differentiation in idiopathic pulmonary fibrosis patients.* J Immunol, 2013. **191**(5): p. 2089-95.
141. Esposito, I., et al., *Natural killer cells in Bal and peripheral blood of patients with idiopathic pulmonary fibrosis (IPF).* Int J Immunopathol Pharmacol, 2005. **18**(3): p. 541-5.
142. Korosec, P., et al., *Expansion of pulmonary CD8+CD56+ natural killer T-cells in hypersensitivity pneumonitis.* Chest, 2007. **132**(4): p. 1291-7.
143. Kotsianidis, I., et al., *Global impairment of CD4+CD25+FOXP3+ regulatory T cells in idiopathic pulmonary fibrosis.* Am J Respir Crit Care Med, 2009. **179**(12): p. 1121-30.
144. Gruber, R., et al., *Determination of gamma/delta and other T-lymphocyte subsets in bronchoalveolar lavage fluid and peripheral blood from patients with sarcoidosis and idiopathic fibrosis of the lung.* Apmis, 1996. **104**(3): p. 199-205.
145. Hoogsteden, H.C., et al., *Phenotype of blood monocytes and alveolar macrophages in interstitial lung disease.* Chest, 1989. **95**(3): p. 574-7.
146. Kiemle-Kallee, J., et al., *Alveolar macrophages in idiopathic pulmonary fibrosis display a more monocyte-like immunophenotype and an increased release of free oxygen radicals.* Eur Respir J, 1991. **4**(4): p. 400-6.
147. Hoogsteden, H.C., et al., *Differences in expression of monocyte/macrophage surface antigens in peripheral blood and bronchoalveolar lavage cells in interstitial lung diseases.* Lung, 1993. **171**(3): p. 149-60.
148. Yu, Y.R., et al., *Flow Cytometric Analysis of Myeloid Cells in Human Blood, Bronchoalveolar Lavage, and Lung Tissues.* Am J Respir Cell Mol Biol, 2016. **54**(1): p. 13-24.
149. Andersson, C.K., et al., *Activated MCTC mast cells infiltrate diseased lung areas in cystic fibrosis and idiopathic pulmonary fibrosis.* Respir Res, 2011. **12**: p. 139.
150. Wygrecka, M., et al., *Mast cells and fibroblasts work in concert to aggravate pulmonary fibrosis: role of transmembrane SCF and the PAR-2/PKC-alpha/Raf-1/p44/42 signaling pathway.* Am J Pathol, 2013. **182**(6): p. 2094-108.
151. Kinder, B.W., et al., *Baseline BAL neutrophilia predicts early mortality in idiopathic pulmonary fibrosis.* Chest, 2008. **133**(1): p. 226-32.
152. Gregory, A.D., et al., *Neutrophil elastase promotes myofibroblast differentiation in lung fibrosis.* J Leukoc Biol, 2015. **98**(2): p. 143-52.
153. Wei, Y.R., et al., *Establishment of the mouse model of acute exacerbation of idiopathic pulmonary fibrosis.* Exp Lung Res, 2016. **42**(2): p. 75-86.
154. Fujimoto, K., et al., *Eosinophil activation in patients with pulmonary fibrosis.* Chest, 1995. **108**(1): p. 48-54.
155. Boomars, K.A., et al., *Relationship between cells obtained by bronchoalveolar lavage and survival in idiopathic pulmonary fibrosis.* Thorax, 1995. **50**(10): p. 1087-92.

156. Guilliams, M., et al., *Alveolar macrophages develop from fetal monocytes that differentiate into long-lived cells in the first week of life via GM-CSF.* J Exp Med, 2013. **210**(10): p. 1977-92.
157. Yona, S., et al., *Fate mapping reveals origins and dynamics of monocytes and tissue macrophages under homeostasis.* Immunity, 2013. **38**(1): p. 79-91.
158. van de Laar, L., et al., *Yolk Sac Macrophages, Fetal Liver, and Adult Monocytes Can Colonize an Empty Niche and Develop into Functional Tissue-Resident Macrophages.* Immunity, 2016. **44**(4): p. 755-68.
159. Morales-Nebreda, L., et al., *The heterogeneity of lung macrophages in the susceptibility to disease.* Eur Respir Rev, 2015. **24**(137): p. 505-9.
160. Kaur, M., et al., *Macrophage adaptation in airway inflammatory resolution.* Eur Respir Rev, 2015. **24**(137): p. 510-5.
161. Martinez, F.O., et al., *Transcriptional profiling of the human monocyte-to-macrophage differentiation and polarization: new molecules and patterns of gene expression.* J Immunol, 2006. **177**(10): p. 7303-11.
162. Beyer, M., et al., *High-resolution transcriptome of human macrophages.* PLoS One, 2012. **7**(9): p. e45466.
163. te Velde, A.A., et al., *Modulation of phenotypic and functional properties of human peripheral blood monocytes by IL-4.* J Immunol, 1988. **140**(5): p. 1548-54.
164. McBride, W.H., et al., *Influences of interleukins 2 and 4 on tumor necrosis factor production by murine mononuclear phagocytes.* Cancer Res, 1990. **50**(10): p. 2949-52.
165. Cao, H., et al., *Differential regulation of class II MHC determinants on macrophages by IFN-gamma and IL-4.* J Immunol, 1989. **143**(11): p. 3524-31.
166. Donnelly, R.P., et al., *Differential regulation of IL-1 production in human monocytes by IFN-gamma and IL-4.* J Immunol, 1990. **145**(2): p. 569-75.
167. Stein, M., et al., *Interleukin 4 potently enhances murine macrophage mannose receptor activity: a marker of alternative immunologic macrophage activation.* J Exp Med, 1992. **176**(1): p. 287-92.
168. Liew, F.Y., et al., *Resistance to Leishmania major infection correlates with the induction of nitric oxide synthase in murine macrophages.* Eur J Immunol, 1991. **21**(12): p. 3009-14.
169. Oswald, I.P., et al., *Low response of BALB/c macrophages to priming and activating signals.* J Leukoc Biol, 1992. **52**(3): p. 315-22.
170. Stenger, S., et al., *Tissue expression of inducible nitric oxide synthase is closely associated with resistance to Leishmania major.* J Exp Med, 1994. **180**(3): p. 783-93.
171. Dileepan, K.N., et al., *Direct activation of murine peritoneal macrophages for nitric oxide production and tumor cell killing by interferon-gamma.* J Interferon Cytokine Res, 1995. **15**(5): p. 387-94.
172. Lavin, Y., et al., *Tissue-resident macrophage enhancer landscapes are shaped by the local microenvironment.* Cell, 2014. **159**(6): p. 1312-26.
173. Gosselin, D., et al., *Environment drives selection and function of enhancers controlling tissue-specific macrophage identities.* Cell, 2014. **159**(6): p. 1327-40.
174. Mills, C.D., et al., *M-1/M-2 macrophages and the Th1/Th2 paradigm.* J Immunol, 2000. **164**(12): p. 6166-73.

175. Sans-Fons, M.G., et al., *Arginine transport is impaired in C57Bl/6 mouse macrophages as a result of a deletion in the promoter of Slc7a2 (CAT2), and susceptibility to Leishmania infection is reduced.* J Infect Dis, 2013. **207**(11): p. 1684-93.
176. Martinez, F.O. and S. Gordon, *The M1 and M2 paradigm of macrophage activation: time for reassessment.* F1000Prime Rep, 2014. **6**: p. 13.
177. Wang, N., H. Liang, and K. Zen, *Molecular mechanisms that influence the macrophage m1-m2 polarization balance.* Front Immunol, 2014. **5**: p. 614.
178. Kaku, Y., et al., *Overexpression of CD163, CD204 and CD206 on alveolar macrophages in the lungs of patients with severe chronic obstructive pulmonary disease.* PLoS One, 2014. **9**(1): p. e87400.
179. Ferrante, C.J. and S.J. Leibovich, *Regulation of Macrophage Polarization and Wound Healing.* Adv Wound Care (New Rochelle), 2012. **1**(1): p. 10-16.
180. Murray, P.J., et al., *Macrophage activation and polarization: nomenclature and experimental guidelines.* Immunity, 2014. **41**(1): p. 14-20.
181. Lucattelli, M., et al., *Collagen phagocytosis by lung alveolar macrophages in animal models of emphysema.* Eur Respir J, 2003. **22**(5): p. 728-34.
182. Ji, W.J., et al., *Temporal and spatial characterization of mononuclear phagocytes in circulating, lung alveolar and interstitial compartments in a mouse model of bleomycin-induced pulmonary injury.* J Immunol Methods, 2014. **403**(1-2): p. 7-16.
183. Ueno, M., et al., *Hypoxia-inducible factor-1alpha mediates TGF-beta-induced PAI-1 production in alveolar macrophages in pulmonary fibrosis.* Am J Physiol Lung Cell Mol Physiol, 2011. **300**(5): p. L740-52.
184. Khalil, N., et al., *Plasmin regulates the activation of cell-associated latent TGF-beta 1 secreted by rat alveolar macrophages after in vivo bleomycin injury.* Am J Respir Cell Mol Biol, 1996. **15**(2): p. 252-9.
185. Denholm, E.M. and S.M. Rollins, *Expression and secretion of transforming growth factor-beta by bleomycin-stimulated rat alveolar macrophages.* Am J Physiol, 1993. **264**(1 Pt 1): p. L36-42.
186. Khalil, N., et al., *Macrophage production of transforming growth factor beta and fibroblast collagen synthesis in chronic pulmonary inflammation.* J Exp Med, 1989. **170**(3): p. 727-37.
187. Murray, L.A., et al., *TGF-beta driven lung fibrosis is macrophage dependent and blocked by Serum amyloid P.* Int J Biochem Cell Biol, 2011. **43**(1): p. 154-62.
188. Uhal, B.D., et al., *Angiotensin-TGF-beta 1 crosstalk in human idiopathic pulmonary fibrosis: autocrine mechanisms in myofibroblasts and macrophages.* Curr Pharm Des, 2007. **13**(12): p. 1247-56.
189. Cao, B., et al., *The potential role of PDGF, IGF-1, TGF-beta expression in idiopathic pulmonary fibrosis.* Chin Med J (Engl), 2000. **113**(9): p. 776-82.
190. Craig, V.J., et al., *Mononuclear phagocytes and airway epithelial cells: novel sources of matrix metalloproteinase-8 (MMP-8) in patients with idiopathic pulmonary fibrosis.* PLoS One, 2014. **9**(5): p. e97485.
191. Fujishima, S., et al., *Production and activation of matrix metalloproteinase 7 (matrilysin 1) in the lungs of patients with idiopathic pulmonary fibrosis.* Arch Pathol Lab Med, 2010. **134**(8): p. 1136-42.

192. Lemjabbar, H., et al., *Overexpression of alveolar macrophage gelatinase B (MMP-9) in patients with idiopathic pulmonary fibrosis: effects of steroid and immunosuppressive treatment.* Am J Respir Cell Mol Biol, 1999. **20**(5): p. 903-13.
193. Larson-Casey, J.L., et al., *Macrophage Akt1 Kinase-Mediated Mitophagy Modulates Apoptosis Resistance and Pulmonary Fibrosis.* Immunity, 2016. **44**(3): p. 582-96.
194. Willems, S., et al., *Multiplex protein profiling of bronchoalveolar lavage in idiopathic pulmonary fibrosis and hypersensitivity pneumonitis.* Ann Thorac Med, 2013. **8**(1): p. 38-45.
195. Shinoda, H., et al., *Elevated CC chemokine level in bronchoalveolar lavage fluid is predictive of a poor outcome of idiopathic pulmonary fibrosis.* Respiration, 2009. **78**(3): p. 285-92.
196. Cai, M., et al., *CCL18 in serum, BAL fluid and alveolar macrophage culture supernatant in interstitial lung diseases.* Respir Med, 2013. **107**(9): p. 1444-52.
197. Cui, A., et al., *Angiogenic and angiostatic chemokines in idiopathic pulmonary fibrosis and granulomatous lung disease.* Respiration, 2010. **80**(5): p. 372-8.
198. Yogo, Y., et al., *Macrophage derived chemokine (CCL22), thymus and activation-regulated chemokine (CCL17), and CCR4 in idiopathic pulmonary fibrosis.* Respir Res, 2009. **10**: p. 80.
199. Vasakova, M., et al., *Bronchoalveolar lavage fluid cellular characteristics, functional parameters and cytokine and chemokine levels in interstitial lung diseases.* Scand J Immunol, 2009. **69**(3): p. 268-74.
200. Car, B.D., et al., *Elevated IL-8 and MCP-1 in the bronchoalveolar lavage fluid of patients with idiopathic pulmonary fibrosis and pulmonary sarcoidosis.* Am J Respir Crit Care Med, 1994. **149**(3 Pt 1): p. 655-9.
201. Tzouvelekis, A., S. Anevlavis, and D. Bouros, *Angiogenesis in interstitial lung diseases: a pathogenetic hallmark or a bystander?* Respir Res, 2006. **7**: p. 82.
202. Keane, M.P., et al., *ENA-78 is an important angiogenic factor in idiopathic pulmonary fibrosis.* Am J Respir Crit Care Med, 2001. **164**(12): p. 2239-42.
203. Phillips, R.J., et al., *Circulating fibrocytes traffic to the lungs in response to CXCL12 and mediate fibrosis.* J Clin Invest, 2004. **114**(3): p. 438-46.
204. Lynch, J.P., 3rd, et al., *Neutrophilic alveolitis in idiopathic pulmonary fibrosis. The role of interleukin-8.* Am Rev Respir Dis, 1992. **145**(6): p. 1433-9.
205. Ziegenhagen, M.W., et al., *Increased expression of proinflammatory chemokines in bronchoalveolar lavage cells of patients with progressing idiopathic pulmonary fibrosis and sarcoidosis.* J Investig Med, 1998. **46**(5): p. 223-31.
206. Burdick, M.D., et al., *CXCL11 attenuates bleomycin-induced pulmonary fibrosis via inhibition of vascular remodeling.* Am J Respir Crit Care Med, 2005. **171**(3): p. 261-8.
207. Keane, M.P., et al., *IFN-gamma-inducible protein-10 attenuates bleomycin-induced pulmonary fibrosis via inhibition of angiogenesis.* J Immunol, 1999. **163**(10): p. 5686-92.
208. Zhang, K., et al., *Lung monocyte chemoattractant protein-1 gene expression in bleomycin-induced pulmonary fibrosis.* J Immunol, 1994. **153**(10): p. 4733-41.
209. Moore, B.B., et al., *Protection from pulmonary fibrosis in the absence of CCR2 signaling.* J Immunol, 2001. **167**(8): p. 4368-77.
210. Gharaee-Kermani, M., et al., *CC-chemokine receptor 2 required for bleomycin-induced pulmonary fibrosis.* Cytokine, 2003. **24**(6): p. 266-76.

211. Okuma, T., et al., *C-C chemokine receptor 2 (CCR2) deficiency improves bleomycin-induced pulmonary fibrosis by attenuation of both macrophage infiltration and production of macrophage-derived matrix metalloproteinases.* J Pathol, 2004. **204**(5): p. 594-604.
212. Inoshima, I., et al., *Anti-monocyte chemoattractant protein-1 gene therapy attenuates pulmonary fibrosis in mice.* Am J Physiol Lung Cell Mol Physiol, 2004. **286**(5): p. L1038-44.
213. Smith, R.E., et al., *Production and function of murine macrophage inflammatory protein-1 alpha in bleomycin-induced lung injury.* J Immunol, 1994. **153**(10): p. 4704-12.
214. Standiford, T.J., et al., *Macrophage inflammatory protein-1 alpha expression in interstitial lung disease.* J Immunol, 1993. **151**(5): p. 2852-63.
215. Kodama, N., et al., *Expression of RANTES by bronchoalveolar lavage cells in nonsmoking patients with interstitial lung diseases.* Am J Respir Cell Mol Biol, 1998. **18**(4): p. 526-31.
216. Belperio, J.A., et al., *The role of the Th2 CC chemokine ligand CCL17 in pulmonary fibrosis.* J Immunol, 2004. **173**(7): p. 4692-8.
217. Keane, M.P., et al., *Neutralization of the CXC chemokine, macrophage inflammatory protein-2, attenuates bleomycin-induced pulmonary fibrosis.* J Immunol, 1999. **162**(9): p. 5511-8.
218. Fernandez, I.E. and O. Eickelberg, *The impact of TGF-beta on lung fibrosis: from targeting to biomarkers.* Proc Am Thorac Soc, 2012. **9**(3): p. 111-6.
219. Warshamana, G.S., M. Corti, and A.R. Brody, *TNF-alpha, PDGF, and TGF-beta(1) expression by primary mouse bronchiolar-alveolar epithelial and mesenchymal cells: tnf-alpha induces TGF-beta(1).* Exp Mol Pathol, 2001. **71**(1): p. 13-33.
220. Redente, E.F., et al., *Tumor necrosis factor-alpha accelerates the resolution of established pulmonary fibrosis in mice by targeting profibrotic lung macrophages.* Am J Respir Cell Mol Biol, 2014. **50**(4): p. 825-37.
221. Le, T.T., et al., *Blockade of IL-6 Trans signaling attenuates pulmonary fibrosis.* J Immunol, 2014. **193**(7): p. 3755-68.
222. Yan, Z., Z. Kui, and Z. Ping, *Reviews and prospectives of signaling pathway analysis in idiopathic pulmonary fibrosis.* Autoimmun Rev, 2014. **13**(10): p. 1020-5.
223. Smadja, D.M., et al., *Increase in both angiogenic and angiostatic mediators in patients with idiopathic pulmonary fibrosis.* Pathol Biol (Paris), 2014. **62**(6): p. 391-4.
224. Bonner, J.C., *Regulation of PDGF and its receptors in fibrotic diseases.* Cytokine Growth Factor Rev, 2004. **15**(4): p. 255-73.
225. Roberts, A.W., *G-CSF: a key regulator of neutrophil production, but that's not all!* Growth Factors, 2005. **23**(1): p. 33-41.
226. Auffray, C., M.H. Sieweke, and F. Geissmann, *Blood monocytes: development, heterogeneity, and relationship with dendritic cells.* Annu Rev Immunol, 2009. **27**: p. 669-92.
227. Ashitani, J., et al., *Granulocyte-colony stimulating factor levels in bronchoalveolar lavage fluid from patients with idiopathic pulmonary fibrosis.* Thorax, 1999. **54**(11): p. 1015-20.
228. Baran, C.P., et al., *Important roles for macrophage colony-stimulating factor, CC chemokine ligand 2, and mononuclear phagocytes in the pathogenesis of pulmonary fibrosis.* Am J Respir Crit Care Med, 2007. **176**(1): p. 78-89.
229. Thomas, M. and H.G. Augustin, *The role of the Angiopoietins in vascular morphogenesis.* Angiogenesis, 2009. **12**(2): p. 125-37.

230. Uehara, M., et al., *Impact of angiopoietin-1 and -2 on clinical course of idiopathic pulmonary fibrosis.* Respir Med, 2016. **114**: p. 18-26.
231. Margaritopoulos, G.A., et al., *Investigation of angiogenetic axis Angiopoietin-1 and -2/Tie-2 in fibrotic lung diseases: a bronchoalveolar lavage study.* Int J Mol Med, 2010. **26**(6): p. 919-23.
232. Nugent, M.A. and R.V. Iozzo, *Fibroblast growth factor-2.* Int J Biochem Cell Biol, 2000. **32**(2): p. 115-20.
233. Zhang, S., et al., *Growth factors secreted by bronchial epithelial cells control myofibroblast proliferation: an in vitro co-culture model of airway remodeling in asthma.* Lab Invest, 1999. **79**(4): p. 395-405.
234. Guzy, R.D., et al., *Fibroblast growth factor 2 is required for epithelial recovery, but not for pulmonary fibrosis, in response to bleomycin.* Am J Respir Cell Mol Biol, 2015. **52**(1): p. 116-28.
235. Dabusti, M., et al., *CD116 (granulocyte-macrophage colony stimulating factor receptor).* J Biol Regul Homeost Agents, 2001. **15**(1): p. 86-9.
236. Hamilton, J.A. and G.P. Anderson, *GM-CSF Biology.* Growth Factors, 2004. **22**(4): p. 225-31.
237. Taniguchi, H., et al., *Interleukin 5 and granulocyte-macrophage colony-stimulating factor levels in bronchoalveolar lavage fluid in interstitial lung disease.* Eur Respir J, 2000. **16**(5): p. 959-64.
238. Moore, B.B., et al., *GM-CSF regulates bleomycin-induced pulmonary fibrosis via a prostaglandin-dependent mechanism.* J Immunol, 2000. **165**(7): p. 4032-9.
239. Bottaro, D.P., et al., *Identification of the hepatocyte growth factor receptor as the c-met proto-oncogene product.* Science, 1991. **251**(4995): p. 802-4.
240. Nakamura, T. and S. Mizuno, *The discovery of hepatocyte growth factor (HGF) and its significance for cell biology, life sciences and clinical medicine.* Proc Jpn Acad Ser B Phys Biol Sci, 2010. **86**(6): p. 588-610.
241. Marchand-Adam, S., et al., *Defect of hepatocyte growth factor secretion by fibroblasts in idiopathic pulmonary fibrosis.* Am J Respir Crit Care Med, 2003. **168**(10): p. 1156-61.
242. Dariusz Ziora, M.A., Zenon Czuba, Dariusz Jastrzębski, Karolina Zeleznik, Slawomir Kasperczyk, Jerzy Kozielski and Wojciech Krol, *Increased Serum Hepatocyte Growth Factor (HGF) Levels in Patients with Idiopathic Pulmonary Fibrosis (IPF) or Progressive Sarcoidosis.* J Mol Biomark Diagn, 2014. **5**(167).
243. Nagaoka, I., B.C. Trapnell, and R.G. Crystal, *Upregulation of platelet-derived growth factor-A and -B gene expression in alveolar macrophages of individuals with idiopathic pulmonary fibrosis.* J Clin Invest, 1990. **85**(6): p. 2023-7.
244. Prasad, S., C.M. Hogaboam, and G. Jarai, *Deficient repair response of IPF fibroblasts in a co-culture model of epithelial injury and repair.* Fibrogenesis Tissue Repair, 2014. **7**: p. 7.
245. Abdollahi, A., et al., *Inhibition of platelet-derived growth factor signaling attenuates pulmonary fibrosis.* J Exp Med, 2005. **201**(6): p. 925-35.
246. Bergeron, A., et al., *Cytokine profiles in idiopathic pulmonary fibrosis suggest an important role for TGF-beta and IL-10.* Eur Respir J, 2003. **22**(1): p. 69-76.
247. Hetzel, M., et al., *Different effects of growth factors on proliferation and matrix production of normal and fibrotic human lung fibroblasts.* Lung, 2005. **183**(4): p. 225-37.

248. Ashman, L.K., *The biology of stem cell factor and its receptor C-kit.* Int J Biochem Cell Biol, 1999. **31**(10): p. 1037-51.
249. Kumar, V., S.A. Bustin, and I.A. McKay, *Transforming growth factor alpha.* Cell Biol Int, 1995. **19**(5): p. 373-88.
250. Burgel, P.R. and J.A. Nadel, *Epidermal growth factor receptor-mediated innate immune responses and their roles in airway diseases.* Eur Respir J, 2008. **32**(4): p. 1068-81.
251. Madtes, D.K., et al., *Elevated transforming growth factor-alpha levels in bronchoalveolar lavage fluid of patients with acute respiratory distress syndrome.* Am J Respir Crit Care Med, 1998. **158**(2): p. 424-30.
252. Baughman, R.P., et al., *Overexpression of transforming growth factor-alpha and epidermal growth factor-receptor in idiopathic pulmonary fibrosis.* Sarcoidosis Vasc Diffuse Lung Dis, 1999. **16**(1): p. 57-61.
253. Meyer, K.C., A. Cardoni, and Z.Z. Xiang, *Vascular endothelial growth factor in bronchoalveolar lavage from normal subjects and patients with diffuse parenchymal lung disease.* J Lab Clin Med, 2000. **135**(4): p. 332-8.
254. Johannson, K.A., et al., *Acute exacerbation of idiopathic pulmonary fibrosis associated with air pollution exposure.* Eur Respir J, 2014. **43**(4): p. 1124-31.
255. Ashley, S.L., et al., *gamma-Herpes virus-68, but not Pseudomonas aeruginosa or influenza A (H1N1), exacerbates established murine lung fibrosis.* Am J Physiol Lung Cell Mol Physiol, 2014. **307**(3): p. L219-30.
256. Lok, S.S., et al., *Murine gammaherpes virus as a cofactor in the development of pulmonary fibrosis in bleomycin resistant mice.* Eur Respir J, 2002. **20**(5): p. 1228-32.
257. Lasithiotaki, I., et al., *Detection of herpes simplex virus type-1 in patients with fibrotic lung diseases.* PLoS One, 2011. **6**(12): p. e27800.
258. Calabrese, F., et al., *Herpes virus infection is associated with vascular remodeling and pulmonary hypertension in idiopathic pulmonary fibrosis.* PLoS One, 2013. **8**(2): p. e55715.
259. Tang, Y.W., et al., *Herpesvirus DNA is consistently detected in lungs of patients with idiopathic pulmonary fibrosis.* J Clin Microbiol, 2003. **41**(6): p. 2633-40.
260. Tsukamoto, K., et al., *Involvement of Epstein-Barr virus latent membrane protein 1 in disease progression in patients with idiopathic pulmonary fibrosis.* Thorax, 2000. **55**(11): p. 958-61.
261. Beck, J.M., V.B. Young, and G.B. Huffnagle, *The microbiome of the lung.* Transl Res, 2012. **160**(4): p. 258-66.
262. Hilty, M., et al., *Disordered microbial communities in asthmatic airways.* PLoS One, 2010. **5**(1): p. e8578.
263. Surette, M.G., *The cystic fibrosis lung microbiome.* Ann Am Thorac Soc, 2014. **11 Suppl 1**: p. S61-5.
264. Pragman, A.A., et al., *The lung microbiome in moderate and severe chronic obstructive pulmonary disease.* PLoS One, 2012. **7**(10): p. e47305.
265. Dickson, R.P., J.R. Erb-Downward, and G.B. Huffnagle, *The role of the bacterial microbiome in lung disease.* Expert Rev Respir Med, 2013. **7**(3): p. 245-57.
266. Hewitt, R.J. and P.L. Molyneaux, *The respiratory microbiome in idiopathic pulmonary fibrosis.* Ann Transl Med, 2017. **5**(12): p. 250.

267. Salisbury, M.L., et al., *Microbiome in interstitial lung disease: from pathogenesis to treatment target.* Curr Opin Pulm Med, 2017.
268. Molyneaux, P.L., et al., *Changes in the respiratory microbiome during acute exacerbations of idiopathic pulmonary fibrosis.* Respir Res, 2017. **18**(1): p. 29.
269. Molyneaux, P.L., et al., *Host-Microbial Interactions in Idiopathic Pulmonary Fibrosis.* Am J Respir Crit Care Med, 2017. **195**(12): p. 1640-1650.
270. Bernasconi, E., et al., *Airway Microbiota Determines Innate Cell Inflammatory or Tissue Remodeling Profiles in Lung Transplantation.* Am J Respir Crit Care Med, 2016. **194**(10): p. 1252-1263.
271. Huang, Y., et al., *Microbes Are Associated with Host Innate Immune Response in Idiopathic Pulmonary Fibrosis.* Am J Respir Crit Care Med, 2017. **196**(2): p. 208-219.
272. Mora, A.L., et al., *Lung infection with gamma-herpesvirus induces progressive pulmonary fibrosis in Th2-biased mice.* Am J Physiol Lung Cell Mol Physiol, 2005. **289**(5): p. L711-21.
273. Mora, A.L., et al., *Activation of alveolar macrophages via the alternative pathway in herpesvirus-induced lung fibrosis.* Am J Respir Cell Mol Biol, 2006. **35**(4): p. 466-73.
274. Sides, M.D., et al., *The Epstein-Barr virus latent membrane protein 1 and transforming growth factor--beta1 synergistically induce epithelial--mesenchymal transition in lung epithelial cells.* Am J Respir Cell Mol Biol, 2011. **44**(6): p. 852-62.
275. Malizia, A.P., et al., *Alveolar epithelial cell injury with Epstein-Barr virus upregulates TGFbeta1 expression.* Am J Physiol Lung Cell Mol Physiol, 2008. **295**(3): p. L451-60.
276. Samara, K.D., et al., *Expression profiles of Toll-like receptors in non-small cell lung cancer and idiopathic pulmonary fibrosis.* Int J Oncol, 2012. **40**(5): p. 1397-404.
277. Yang, H.Z., et al., *Targeting TLR2 attenuates pulmonary inflammation and fibrosis by reversion of suppressive immune microenvironment.* J Immunol, 2009. **182**(1): p. 692-702.
278. O'Dwyer, D.N., et al., *The Toll-like receptor 3 L412F polymorphism and disease progression in idiopathic pulmonary fibrosis.* Am J Respir Crit Care Med, 2013. **188**(12): p. 1442-50.
279. Trujillo, G., et al., *TLR9 differentiates rapidly from slowly progressing forms of idiopathic pulmonary fibrosis.* Sci Transl Med, 2010. **2**(57): p. 57ra82.
280. Capelluto, D.G., *Tollip: a multitasking protein in innate immunity and protein trafficking.* Microbes Infect, 2012. **14**(2): p. 140-7.
281. Gharaee-Kermani, M., et al., *Recent advances in molecular targets and treatment of idiopathic pulmonary fibrosis: focus on TGFbeta signaling and the myofibroblast.* Curr Med Chem, 2009. **16**(11): p. 1400-17.
282. Macias-Barragan, J., et al., *[Effects of alpha lipoic acid and pirfenidone on liver cells antioxidant modulation against oxidative damage].* Rev Med Chil, 2014. **142**(12): p. 1553-64.
283. Oku, H., et al., *Antifibrotic action of pirfenidone and prednisolone: different effects on pulmonary cytokines and growth factors in bleomycin-induced murine pulmonary fibrosis.* Eur J Pharmacol, 2008. **590**(1-3): p. 400-8.
284. Inomata, M., et al., *Pirfenidone inhibits fibrocyte accumulation in the lungs in bleomycin-induced murine pulmonary fibrosis.* Respir Res, 2014. **15**: p. 16.
285. Knuppel, L., et al., *A Novel Antifibrotic Mechanism of Nintedanib and Pirfenidone. Inhibition of Collagen Fibril Assembly.* 2017. **57**(1): p. 77-90.

286. Xie, Y., et al., *Upregulation of RGS2: a new mechanism for pirfenidone amelioration of pulmonary fibrosis.* 2016. **17**(1): p. 103.
287. Noble, P.W., et al., *Pirfenidone in patients with idiopathic pulmonary fibrosis (CAPACITY): two randomised trials.* Lancet, 2011. **377**(9779): p. 1760-9.
288. Nagai, S., et al., *Open-label compassionate use one year-treatment with pirfenidone to patients with chronic pulmonary fibrosis.* Intern Med, 2002. **41**(12): p. 1118-23.
289. Chaudhary, N.I., et al., *Inhibition of PDGF, VEGF and FGF signalling attenuates fibrosis.* Eur Respir J, 2007. **29**(5): p. 976-85.
290. Wollin, L., et al., *Mode of action of nintedanib in the treatment of idiopathic pulmonary fibrosis.* Eur Respir J, 2015. **45**(5): p. 1434-45.
291. Hilberg, F., et al., *BIBF 1120: triple angiokinase inhibitor with sustained receptor blockade and good antitumor efficacy.* Cancer Res, 2008. **68**(12): p. 4774-82.
292. Rangarajan, S. and A. Kurundkar, *Novel Mechanisms for the Antifibrotic Action of Nintedanib.* 2016. **54**(1): p. 51-9.
293. Ogura, T., et al., *Safety and pharmacokinetics of nintedanib and pirfenidone in idiopathic pulmonary fibrosis.* Eur Respir J, 2015. **45**(5): p. 1382-92.
294. Mosca, M., et al., *The diagnosis and classification of undifferentiated connective tissue diseases.* J Autoimmun, 2014. **48-49**: p. 50-2.
295. Szodoray, P., et al., *Altered Th17 cells and Th17/regulatory T-cell ratios indicate the subsequent conversion from undifferentiated connective tissue disease to definitive systemic autoimmune disorders.* Hum Immunol, 2013. **74**(12): p. 1510-8.
296. Ferri, C., et al., *Interstitial pneumonia with autoimmune features and undifferentiated connective tissue disease: Our interdisciplinary rheumatology-pneumology experience, and review of the literature.* Autoimmun Rev, 2016. **15**(1): p. 61-70.
297. Kinder, B.W., et al., *Idiopathic nonspecific interstitial pneumonia: lung manifestation of undifferentiated connective tissue disease?* Am J Respir Crit Care Med, 2007. **176**(7): p. 691-7.
298. Kim, H.C., et al., *Interstitial pneumonia related to undifferentiated connective tissue disease: pathologic pattern and prognosis.* Chest, 2015. **147**(1): p. 165-172.
299. Alberti, M.L., et al., *Undifferentiated connective tissue disease and interstitial lung disease: Trying to define patterns.* Reumatol Clin, 2016.
300. Kinder, B.W., et al., *Undifferentiated connective tissue disease-associated interstitial lung disease: changes in lung function.* Lung, 2010. **188**(2): p. 143-9.
301. Pan, L., et al., *Comparison of characteristics of connective tissue disease-associated interstitial lung diseases, undifferentiated connective tissue disease-associated interstitial lung diseases, and idiopathic pulmonary fibrosis in Chinese Han population: a retrospective study.* Clin Dev Immunol, 2013. **2013**: p. 121578.
302. Szodoray, P., et al., *Progressive divergent shifts in natural and induced T-regulatory cells signify the transition from undifferentiated to definitive connective tissue disease.* Int Immunol, 2008. **20**(8): p. 971-9.
303. Suda, T., et al., *Distinct prognosis of idiopathic nonspecific interstitial pneumonia (NSIP) fulfilling criteria for undifferentiated connective tissue disease (UCTD).* Respir Med, 2010. **104**(10): p. 1527-34.

304. Kumanovics, G., et al., *Simultaneous presence of neutrophil alveolitis and Ki-67 positivity of alveolar macrophages in dermato-/polymyositis and systemic sclerosis.* Rheumatol Int, 2003. **23**(1): p. 6-10.
305. Solaymani-Dodaran, M., et al., *Extrinsic allergic alveolitis: incidence and mortality in the general population.* Qjm, 2007. **100**(4): p. 233-7.
306. Spagnolo, P., et al., *Hypersensitivity Pneumonitis: A Comprehensive Review.* J Investig Allergol Clin Immunol, 2015. **25**(4): p. 237-50; quiz follow 250.
307. Hanak, V., J.M. Golbin, and J.H. Ryu, *Causes and presenting features in 85 consecutive patients with hypersensitivity pneumonitis.* Mayo Clin Proc, 2007. **82**(7): p. 812-6.
308. Ando, M., et al., *HLA-DQw3 in Japanese summer-type hypersensitivity pneumonitis induced by Trichosporon cutaneum.* Am Rev Respir Dis, 1989. **140**(4): p. 948-50.
309. Camarena, A., et al., *Major histocompatibility complex and tumor necrosis factor-alpha polymorphisms in pigeon breeder's disease.* Am J Respir Crit Care Med, 2001. **163**(7): p. 1528-33.
310. Camarena, A., et al., *PSMB8 (LMP7) but not PSMB9 (LMP2) gene polymorphisms are associated to pigeon breeder's hypersensitivity pneumonitis.* Respir Med, 2010. **104**(6): p. 889-94.
311. Aquino-Galvez, A., et al., *Transporter associated with antigen processing (TAP) 1 gene polymorphisms in patients with hypersensitivity pneumonitis.* Exp Mol Pathol, 2008. **84**(2): p. 173-7.
312. Dakhama, A., et al., *Common respiratory viruses in lower airways of patients with acute hypersensitivity pneumonitis.* Am J Respir Crit Care Med, 1999. **159**(4 Pt 1): p. 1316-22.
313. Cormier, Y., et al., *Long-term viral enhancement of lung response to Saccharopolyspora rectivirgula.* Am J Respir Crit Care Med, 1994. **149**(2 Pt 1): p. 490-4.
314. Park, Y., S.J. Oh, and D.H. Chung, *CD4(+)CD25(+) regulatory T cells attenuate Hypersensitivity Pneumonitis by suppressing IFN-gamma production by CD4(+) and CD8(+) T cells.* J Leukoc Biol, 2009. **86**(6): p. 1427-37.
315. Girard, M., E. Israel-Assayag, and Y. Cormier, *Impaired function of regulatory T-cells in hypersensitivity pneumonitis.* Eur Respir J, 2011. **37**(3): p. 632-9.
316. Selman, M., et al., *Gene expression profiles distinguish idiopathic pulmonary fibrosis from hypersensitivity pneumonitis.* Am J Respir Crit Care Med, 2006. **173**(2): p. 188-98.
317. Joshi, A.D., et al., *Interleukin-17-mediated immunopathogenesis in experimental hypersensitivity pneumonitis.* Am J Respir Crit Care Med, 2009. **179**(8): p. 705-16.
318. Mitaka, K., et al., *Th2-biased immune responses are important in a murine model of chronic hypersensitivity pneumonitis.* Int Arch Allergy Immunol, 2011. **154**(3): p. 264-74.
319. Simonian, P.L., et al., *gammadelta T cells protect against lung fibrosis via IL-22.* J Exp Med, 2010. **207**(10): p. 2239-53.
320. Holdsworth, G., et al., *Quantitative and organisational changes in mature extracellular matrix revealed through high-content imaging of total protein fluorescently stained in situ.* Sci Rep, 2017. **7**(1): p. 9963.
321. Giavarina, D., *Understanding Bland Altman analysis.* Biochem Med (Zagreb), 2015. **25**(2): p. 141-51.
322. Jia, Y., et al., *Expression of ligands for Siglec-8 and Siglec-9 in human airways and airway cells.* J Allergy Clin Immunol, 2015. **135**(3): p. 799-810.e7.

323. Abbasi-Kenarsari, H., et al., *Cloning and Expression of CD19, a Human B-Cell Marker in NIH-3T3 Cell Line.* Avicenna J Med Biotechnol, 2015. **7**(1): p. 39-44.
324. Jacobsen, E.A., N.A. Lee, and J.J. Lee, *Re-defining the unique roles for eosinophils in allergic respiratory inflammation.* Clin Exp Allergy, 2014. **44**(9): p. 1119-36.
325. Hizawa, N., et al., *Genetic polymorphisms at FCER1B and PAI-1 and asthma susceptibility.* Clin Exp Allergy, 2006. **36**(7): p. 872-6.
326. Shin, J.S. and A.M. Greer, *The role of FcepsilonRI expressed in dendritic cells and monocytes.* Cell Mol Life Sci, 2015. **72**(12): p. 2349-60.
327. Messingham, K.N., et al., *Human eosinophils express the high affinity IgE receptor, FcepsilonRI, in bullous pemphigoid.* PLoS One, 2014. **9**(9): p. e107725.
328. Yin, X., et al., *Human Blood CD1c+ Dendritic Cells Encompass CD5high and CD5low Subsets That Differ Significantly in Phenotype, Gene Expression, and Functions.* J Immunol, 2017. **198**(4): p. 1553-1564.
329. Fragoulis, G.E., S. Siebert, and I.B. McInnes, *Therapeutic Targeting of IL-17 and IL-23 Cytokines in Immune-Mediated Diseases.* Annu Rev Med, 2016. **67**: p. 337-53.
330. Obradovic, H., et al., *Doxycycline Inhibits IL-17-Stimulated MMP-9 Expression by Downregulating ERK1/2 Activation: Implications in Myogenic Differentiation.* Mediators Inflamm, 2016. **2016**: p. 2939658.
331. Zundler, S. and M.F. Neurath, *Interleukin-12: Functional activities and implications for disease.* Cytokine Growth Factor Rev, 2015. **26**(5): p. 559-68.
332. Dinarello, C.A. and G. Fantuzzi, *Interleukin-18 and host defense against infection.* J Infect Dis, 2003. **187 Suppl 2**: p. S370-84.
333. Moore, B.B. and T.A. Moore, *Viruses in Idiopathic Pulmonary Fibrosis. Etiology and Exacerbation.* Ann Am Thorac Soc, 2015. **12 Suppl 2**: p. S186-92.
334. Hunninghake, G.W., et al., *Mechanisms of neutrophil accumulation in the lungs of patients with idiopathic pulmonary fibrosis.* J Clin Invest, 1981. **68**(1): p. 259-69.
335. Murray, L.A., et al., *Targeting interleukin-13 with tralokinumab attenuates lung fibrosis and epithelial damage in a humanized SCID idiopathic pulmonary fibrosis model.* Am J Respir Cell Mol Biol, 2014. **50**(5): p. 985-94.
336. Passalacqua, G., et al., *IL-13 and idiopathic pulmonary fibrosis: Possible links and new therapeutic strategies.* Pulm Pharmacol Ther, 2017. **45**: p. 95-100.
337. Huaux, F., et al., *Eosinophils and T lymphocytes possess distinct roles in bleomycin-induced lung injury and fibrosis.* J Immunol, 2003. **171**(10): p. 5470-81.
338. Suga, M., et al., *Clinical significance of MCP-1 levels in BALF and serum in patients with interstitial lung diseases.* Eur Respir J, 1999. **14**(2): p. 376-82.
339. Rose, C.E., Jr., S.S. Sung, and S.M. Fu, *Significant involvement of CCL2 (MCP-1) in inflammatory disorders of the lung.* Microcirculation, 2003. **10**(3-4): p. 273-88.
340. Mia, S., et al., *An optimized protocol for human M2 macrophages using M-CSF and IL-4/IL-10/TGF-beta yields a dominant immunosuppressive phenotype.* Scand J Immunol, 2014. **79**(5): p. 305-14.
341. Gibbons, M.A., et al., *Ly6Chi monocytes direct alternatively activated profibrotic macrophage regulation of lung fibrosis.* Am J Respir Crit Care Med, 2011. **184**(5): p. 569-81.

342. Hansel, T.T., et al., *A Comprehensive Evaluation of Nasal and Bronchial Cytokines and Chemokines Following Experimental Rhinovirus Infection in Allergic Asthma: Increased Interferons (IFN-gamma and IFN-lambda) and Type 2 Inflammation (IL-5 and IL-13).* EBioMedicine, 2017. **19**: p. 128-138.
343. Hussell, T. and T.J. Bell, *Alveolar macrophages: plasticity in a tissue-specific context.* Nat Rev Immunol, 2014. **14**(2): p. 81-93.
344. Jones, C.V., et al., *M2 macrophage polarisation is associated with alveolar formation during postnatal lung development.* Respir Res, 2013. **14**: p. 41.
345. Yao, Y., et al., *Chop Deficiency Protects Mice Against Bleomycin-induced Pulmonary Fibrosis by Attenuating M2 Macrophage Production.* Mol Ther, 2016. **24**(5): p. 915-25.
346. Stahl, M., et al., *Lung collagens perpetuate pulmonary fibrosis via CD204 and M2 macrophage activation.* PLoS One, 2013. **8**(11): p. e81382.
347. Ballinger, M.N., et al., *IRAK-M promotes alternative macrophage activation and fibroproliferation in bleomycin-induced lung injury.* 2015. **194**(4): p. 1894-904.
348. Etzerodt, A. and S.K. Moestrup, *CD163 and inflammation: biological, diagnostic, and therapeutic aspects.* Antioxid Redox Signal, 2013. **18**(17): p. 2352-63.
349. Wojtan, P., et al., *Macrophage polarization in interstitial lung diseases.* Cent Eur J Immunol, 2016. **41**(2): p. 159-64.
350. Murray, L.A., et al., *Serum amyloid P therapeutically attenuates murine bleomycin-induced pulmonary fibrosis via its effects on macrophages.* PLoS One, 2010. **5**(3): p. e9683.
351. Zaynagetdinov, R., et al., *Identification of myeloid cell subsets in murine lungs using flow cytometry.* Am J Respir Cell Mol Biol, 2013. **49**(2): p. 180-9.
352. Katsura, Y., et al., *Characteristics of alveolar macrophages from murine models of OVA-induced allergic airway inflammation and LPS-induced acute airway inflammation.* Exp Lung Res, 2015. **41**(7): p. 370-82.
353. Bosmann, M., et al., *CD11c+ alveolar macrophages are a source of IL-23 during lipopolysaccharide-induced acute lung injury.* Shock, 2013. **39**(5): p. 447-52.
354. Albert, R.K., et al., *Expression and function of beta 2 integrins on alveolar macrophages from human and nonhuman primates.* Am J Respir Cell Mol Biol, 1992. **7**(2): p. 182-9.
355. Striz, I., et al., *The phenotype of alveolar macrophages and its correlation with immune cells in bronchoalveolar lavage.* Eur Respir J, 1993. **6**(9): p. 1287-94.
356. Schaberg, T., et al., *Increased number of alveolar macrophages expressing surface molecules of the CD11/CD18 family in sarcoidosis and idiopathic pulmonary fibrosis is related to the production of superoxide anions by these cells.* Am Rev Respir Dis, 1993. **147**(6 Pt 1): p. 1507-13.
357. Taylor, M.L., et al., *Extensive surface phenotyping of alveolar macrophages in interstitial lung disease.* Clin Immunol, 2000. **94**(1): p. 33-41.
358. Andreesen, R., et al., *Surface phenotype analysis of human monocyte to macrophage maturation.* J Leukoc Biol, 1990. **47**(6): p. 490-7.
359. Andreesen, R., et al., *Expression of transferrin receptors and intracellular ferritin during terminal differentiation of human monocytes.* Blut, 1984. **49**(3): p. 195-202.
360. Misharin, A.V., et al., *Flow cytometric analysis of macrophages and dendritic cell subsets in the mouse lung.* Am J Respir Cell Mol Biol, 2013. **49**(4): p. 503-10.

361. Zanoni, I. and F. Granucci, *Role of CD14 in host protection against infections and in metabolism regulation.* Front Cell Infect Microbiol, 2013. **3**: p. 32.
362. Tao, B., et al., *Myeloid-specific disruption of tyrosine phosphatase Shp2 promotes alternative activation of macrophages and predisposes mice to pulmonary fibrosis.* J Immunol, 2014. **193**(6): p. 2801-11.
363. Leach, H.G., et al., *Endothelial cells recruit macrophages and contribute to a fibrotic milieu in bleomycin lung injury.* Am J Respir Cell Mol Biol, 2013. **49**(6): p. 1093-101.
364. McCubbrey, A.L., et al., *Deletion of c-FLIP from CD11b(hi) Macrophages Prevents Development of Bleomycin-induced Lung Fibrosis.* Am J Respir Cell Mol Biol, 2017.
365. Misharin, A.V., et al., *Monocyte-derived alveolar macrophages drive lung fibrosis and persist in the lung over the life span.* J Exp Med, 2017. **214**(8): p. 2387-2404.
366. Sargent, P.J., S. Farnaud, and R.W. Evans, *Structure/function overview of proteins involved in iron storage and transport.* Curr Med Chem, 2005. **12**(23): p. 2683-93.
367. Bruhn, K.W. and B. Spellberg, *Transferrin-mediated iron sequestration as a novel therapy for bacterial and fungal infections.* Curr Opin Microbiol, 2015. **27**: p. 57-61.
368. Theil, E.C., *Iron homeostasis and nutritional iron deficiency.* J Nutr, 2011. **141**(4): p. 724s-728s.
369. Puxeddu, E., et al., *Iron laden macrophages in idiopathic pulmonary fibrosis: the telltale of occult alveolar hemorrhage?* Pulm Pharmacol Ther, 2014. **28**(1): p. 35-40.
370. Ponka, P., C. Beaumont, and D.R. Richardson, *Function and regulation of transferrin and ferritin.* Semin Hematol, 1998. **35**(1): p. 35-54.
371. Ratledge, C., *Iron metabolism and infection.* Food Nutr Bull, 2007. **28**(4 Suppl): p. S515-23.
372. Kell, D.B. and E. Pretorius, *Serum ferritin is an important inflammatory disease marker, as it is mainly a leakage product from damaged cells.* Metallomics, 2014. **6**(4): p. 748-73.
373. Hallman, M., A. Sarnesto, and K. Bry, *Interaction of transferrin saturated with iron with lung surfactant in respiratory failure.* J Appl Physiol (1985), 1994. **77**(2): p. 757-66.
374. Bogdan, C., *Nitric oxide synthase in innate and adaptive immunity: an update.* Trends Immunol, 2015. **36**(3): p. 161-78.
375. Gumienny, T.L., et al., *CED-12/ELMO, a novel member of the CrkII/Dock180/Rac pathway, is required for phagocytosis and cell migration.* Cell, 2001. **107**(1): p. 27-41.
376. Aderem, A. and D.M. Underhill, *Mechanisms of phagocytosis in macrophages.* Annu Rev Immunol, 1999. **17**: p. 593-623.
377. Karavitis, J. and E.J. Kovacs, *Macrophage phagocytosis: effects of environmental pollutants, alcohol, cigarette smoke, and other external factors.* J Leukoc Biol, 2011. **90**(6): p. 1065-78.
378. Vyas-Read, S., et al., *Nitric oxide attenuates epithelial-mesenchymal transition in alveolar epithelial cells.* Am J Physiol Lung Cell Mol Physiol, 2007. **293**(1): p. L212-21.
379. Yoshida, M., et al., *The effect of low-dose inhalation of nitric oxide in patients with pulmonary fibrosis.* Eur Respir J, 1997. **10**(9): p. 2051-4.
380. Sierra-Filardi, E., et al., *CCL2 shapes macrophage polarization by GM-CSF and M-CSF: identification of CCL2/CCR2-dependent gene expression profile.* J Immunol, 2014. **192**(8): p. 3858-67.
381. Ginsberg, M.H., *Integrin activation.* BMB Rep, 2014. **47**(12): p. 655-9.

382. Munger, J.S. and D. Sheppard, *Cross talk among TGF-beta signaling pathways, integrins, and the extracellular matrix.* Cold Spring Harb Perspect Biol, 2011. **3**(11): p. a005017.
383. Wright, D.B., H. Meurs, and B.G. Dekkers, *Integrins: therapeutic targets in airway hyperresponsiveness and remodelling?* Trends Pharmacol Sci, 2014. **35**(11): p. 567-74.
384. Shi, Y. and J. Massague, *Mechanisms of TGF-beta signaling from cell membrane to the nucleus.* Cell, 2003. **113**(6): p. 685-700.
385. Yehualaeshet, T., et al., *Activation of rat alveolar macrophage-derived latent transforming growth factor beta-1 by plasmin requires interaction with thrombospondin-1 and its cell surface receptor, CD36.* Am J Pathol, 1999. **155**(3): p. 841-51.
386. Krstic, J. and J.F. Santibanez, *Transforming growth factor-beta and matrix metalloproteinases: functional interactions in tumor stroma-infiltrating myeloid cells.* ScientificWorldJournal, 2014. **2014**: p. 521754.
387. Selman, M., et al., *TIMP-1, -2, -3, and -4 in idiopathic pulmonary fibrosis. A prevailing nondegradative lung microenvironment?* Am J Physiol Lung Cell Mol Physiol, 2000. **279**(3): p. L562-74.
388. Kim, K.H., et al., *Tissue inhibitor of metalloproteinase-1 deficiency amplifies acute lung injury in bleomycin-exposed mice.* Am J Respir Cell Mol Biol, 2005. **33**(3): p. 271-9.
389. Dong, J. and Q. Ma, *TIMP1 promotes multi-walled carbon nanotube-induced lung fibrosis by stimulating fibroblast activation and proliferation.* Nanotoxicology, 2017. **11**(1): p. 41-51.
390. Gharaee-Kermani, M., et al., *The role of urokinase in idiopathic pulmonary fibrosis and implication for therapy.* Expert Opin Investig Drugs, 2008. **17**(6): p. 905-16.
391. Hunt, J.M. and R. Tuder, *Alpha 1 anti-trypsin: one protein, many functions.* Curr Mol Med, 2012. **12**(7): p. 827-35.
392. Tsao, C.H., et al., *Interleukin-4 regulates lipid metabolism by inhibiting adipogenesis and promoting lipolysis.* J Lipid Res, 2014. **55**(3): p. 385-97.
393. Ivashkiv, L.B. and L.T. Donlin, *Regulation of type I interferon responses.* Nat Rev Immunol, 2014. **14**(1): p. 36-49.
394. Cook, T., B. Gebelein, and R. Urrutia, *Sp1 and its likes: biochemical and functional predictions for a growing family of zinc finger transcription factors.* Ann N Y Acad Sci, 1999. **880**: p. 94-102.
395. Meng, Q. and Y. Xia, *c-Jun, at the crossroad of the signaling network.* Protein Cell, 2011. **2**(11): p. 889-98.
396. Battaglino, R., et al., *c-myc is required for osteoclast differentiation.* J Bone Miner Res, 2002. **17**(5): p. 763-73.
397. Hawkins, C.J. and D.L. Vaux, *Analysis of the role of bcl-2 in apoptosis.* Immunol Rev, 1994. **142**: p. 127-39.
398. Barrientos, S., et al., *Growth factors and cytokines in wound healing.* Wound Repair Regen, 2008. **16**(5): p. 585-601.
399. Barreda, D.R., P.C. Hanington, and M. Belosevic, *Regulation of myeloid development and function by colony stimulating factors.* Dev Comp Immunol, 2004. **28**(5): p. 509-54.
400. Hardie, W.D., et al., *Conditional expression of transforming growth factor-alpha in adult mouse lung causes pulmonary fibrosis.* Am J Physiol Lung Cell Mol Physiol, 2004. **286**(4): p. L741-9.

401. Ihn, H., *Pathogenesis of fibrosis: role of TGF-beta and CTGF.* Curr Opin Rheumatol, 2002. **14**(6): p. 681-5.
402. Karsdal, M.A., et al., *The good and the bad collagens of fibrosis - Their role in signaling and organ function.* Adv Drug Deliv Rev, 2017.
403. Su, Y., et al., *Association of serum levels of laminin, type IV collagen, procollagen III N-terminal peptide, and hyaluronic acid with the progression of interstitial lung disease.* Medicine (Baltimore), 2017. **96**(18): p. e6617.
404. Schuppan, D., *Structure of the extracellular matrix in normal and fibrotic liver: collagens and glycoproteins.* Semin Liver Dis, 1990. **10**(1): p. 1-10.
405. Raghu, G., et al., *Extracellular matrix in normal and fibrotic human lungs.* Am Rev Respir Dis, 1985. **131**(2): p. 281-9.
406. Amenomori, M., et al., *Differential effects of human neutrophil peptide-1 on growth factor and interleukin-8 production by human lung fibroblasts and epithelial cells.* Exp Lung Res, 2010. **36**(7): p. 411-9.
407. Lee, H.S. and J. Kim, *Constitutive expression of vascular endothelial cell growth factor (VEGF) gene family ligand and receptors on human upper and lower airway epithelial cells.* Int Forum Allergy Rhinol, 2014. **4**(1): p. 8-14.
408. Bosse, Y., et al., *Leukotriene D4-induced, epithelial cell-derived transforming growth factor beta1 in human bronchial smooth muscle cell proliferation.* Clin Exp Allergy, 2008. **38**(1): p. 113-21.
409. Ito, Y., et al., *Influenza induces IL-8 and GM-CSF secretion by human alveolar epithelial cells through HGF/c-Met and TGF-alpha/EGFR signaling.* Am J Physiol Lung Cell Mol Physiol, 2015. **308**(11): p. L1178-88.
410. Lever, A.R., et al., *Comprehensive evaluation of poly(I:C) induced inflammatory response in an airway epithelial model.* Physiol Rep, 2015. **3**(4).
411. Taima, K., et al., *Double-stranded RNA stimulates the expression of monocyte chemoattractant protein-1 in BEAS-2B bronchial epithelial cells.* Exp Lung Res, 2005. **31**(3): p. 361-75.
412. Maghazachi, A.A., *Role of chemokines in the biology of natural killer cells.* Curr Top Microbiol Immunol, 2010. **341**: p. 37-58.
413. Marcet, B., et al., *Extracellular nucleotides regulate CCL20 release from human primary airway epithelial cells, monocytes and monocyte-derived dendritic cells.* J Cell Physiol, 2007. **211**(3): p. 716-27.
414. Takizawa, H., et al., *Increased IL-6 and IL-8 in bronchoalveolar lavage fluids (BALF) from patients with sarcoidosis: correlation with the clinical parameters.* Clin Exp Immunol, 1997. **107**(1): p. 175-81.
415. Melkamu, T., et al., *Regulation of TLR2 expression and function in human airway epithelial cells.* J Membr Biol, 2009. **229**(2): p. 101-13.
416. McClure, R. and P. Massari, *TLR-Dependent Human Mucosal Epithelial Cell Responses to Microbial Pathogens.* Front Immunol, 2014. **5**: p. 386.
417. Cohen, P., *The TLR and IL-1 signalling network at a glance.* J Cell Sci, 2014. **127**(Pt 11): p. 2383-90.
418. Della Mina, E., et al., *Inherited human IRAK-1 deficiency selectively impairs TLR signaling in fibroblasts.* Proc Natl Acad Sci U S A, 2017. **114**(4): p. E514-e523.

419. Li, C.H., et al., *Bacterial lipoprotein-induced tolerance is reversed by overexpression of IRAK-1.* Immunol Cell Biol, 2012. **90**(3): p. 314-20.
420. Ritter, M., et al., *Characterization of Toll-like receptors in primary lung epithelial cells: strong impact of the TLR3 ligand poly(I:C) on the regulation of Toll-like receptors, adaptor proteins and inflammatory response.* J Inflamm (Lond), 2005. **2**: p. 16.
421. Jiang, J., et al., *Regulation of Viral Infection-induced Airway Remodeling Cytokine Production by the TLR3-EGFR Signaling Pathway in Human Bronchial Epithelial Cells.* Copd, 2016. **13**(6): p. 750-755.
422. Todd, N.W., I.G. Luzina, and S.P. Atamas, *Molecular and cellular mechanisms of pulmonary fibrosis.* Fibrogenesis Tissue Repair, 2012. **5**(1): p. 11.
423. Matsukura, S., et al., *Synthetic double-stranded RNA induces multiple genes related to inflammation through Toll-like receptor 3 depending on NF-kappaB and/or IRF-3 in airway epithelial cells.* Clin Exp Allergy, 2006. **36**(8): p. 1049-62.
424. Halstead, E.S., et al., *GM-CSF overexpression after influenza a virus infection prevents mortality and moderates M1-like airway monocyte/macrophage polarization.* Respir Res, 2018. **19**(1): p. 3.
425. Sakai, N. and A.M. Tager, *Fibrosis of two: Epithelial cell-fibroblast interactions in pulmonary fibrosis.* Biochim Biophys Acta, 2013. **1832**(7): p. 911-21.
426. Kehrl, J.H., *Transforming growth factor-beta: an important mediator of immunoregulation.* Int J Cell Cloning, 1991. **9**(5): p. 438-50.
427. Knippenberg, S., et al., *Streptococcus pneumoniae triggers progression of pulmonary fibrosis through pneumolysin.* Thorax, 2015. **70**(7): p. 636-46.
428. Savici, D., P.A. Campbell, and T.E. King, Jr., *Bronchoalveolar macrophages from patients with idiopathic pulmonary fibrosis are unable to kill facultative intracellular bacteria.* Am Rev Respir Dis, 1989. **139**(1): p. 22-7.
429. Weiss, G. and U.E. Schaible, *Macrophage defense mechanisms against intracellular bacteria.* Immunol Rev, 2015. **264**(1): p. 182-203.
430. Zamo, A., et al., *HHV-8 and EBV are not commonly found in idiopathic pulmonary fibrosis.* Sarcoidosis Vasc Diffuse Lung Dis, 2005. **22**(2): p. 123-8.
431. Kelly, B.G., et al., *A rearranged form of Epstein-Barr virus DNA is associated with idiopathic pulmonary fibrosis.* Am J Respir Crit Care Med, 2002. **166**(4): p. 510-3.
432. Manika, K., et al., *Epstein-Barr virus DNA in bronchoalveolar lavage fluid from patients with idiopathic pulmonary fibrosis.* Sarcoidosis Vasc Diffuse Lung Dis, 2007. **24**(2): p. 134-40.
433. Furonaka, M., et al., *Suplatast tosilate prevents bleomycin-induced pulmonary fibrosis in mice.* J Pharmacol Exp Ther, 2009. **328**(1): p. 55-61.
434. Mandl, M., et al., *Characterization of the CD14++CD16+ monocyte population in human bone marrow.* PLoS One, 2014. **9**(11): p. e112140.

8. Appendix

8.1. Supplementary data for results chapter 2.

	Cellular Differential Percentage						Cell # (x10^4)/mL BAL					
	Healthy	IPF	UCTD	HP	cHP	Sarcoid	Healthy	IPF	UCTD	HP	cHP	Sarcoid
Number of values	7	113	20	15	28	9	7	113	20	15	28	9
Macrophage												
Minimum	63.2	39.7	52.0	14.0	26.0	40.0	3.0	2.0	3.6	6.2	1.8	1.1
25% Percentile	82.6	67.9	67.3	60.3	52.0	54.0	3.2	11.9	7.3	9.1	4.6	5.2
Median	90.4	75.0	71.3	63.0	63.0	65.3	6.7	17.9	14.9	14.3	11.2	12.7
75% Percentile	92.6	81.5	81.7	73.0	71.4	72.7	12.3	26.7	29.3	21.1	17.9	15.7
Maximum	93.8	94.7	97.0	78.7	86.0	88.7	13.0	139	121	53.8	64.9	43.1
Mean	86.3	73.4	73.4	60.3	59.7	64.3	7.7	23.2	24.1	18.6	14.3	13.9
S.D.	10.8	11.3	10.9	18.5	14.7	14.1	4.2	19.8	27.3	12.8	13.6	12.2
S.E.M	4.1	1.1	2.4	4.8	2.8	4.7	1.6	1.9	6.1	3.3	2.6	4.1
Lymphocyte												
Minimum	5	0.3	0.7	12.7	3.7	2.7	0.2	0.2	0.1	2.2	0.1	0.1
25% Percentile	5.7	5.0	4.8	19.3	18.0	8.4	0.3	1.0	1.2	3.4	2.2	1.1
Median	6.3	9.3	8.7	22.0	22.9	23.0	0.5	2.0	1.6	5.8	3.8	3.4
75% Percentile	13.2	14.5	15.4	33.7	29.0	34.9	1.1	4.0	3.8	13.5	7.9	10.1
Maximum	33.4	54.7	27.0	67.0	54.7	44.7	6.9	56.4	9.3	67.0	25.8	16.1
Mean	11.3	10.9	9.8	27.7	24.6	23.1	1.5	3.4	2.4	11.9	6.7	5.4
S.D.	10.2	8.8	6.6	13.7	10.9	14.4	2.4	5.7	2.3	16.4	7.3	5.5
S.E.M	3.8	0.8	1.5	3.5	2.1	4.8	0.9	0.5	0.5	4.2	1.4	1.8
Neutrophil												
Minimum	0.3	0.3	2.0	1.0	1.0	1.0	0.01	0.13	0.11	0.14	0.07	0.14
25% Percentile	0.4	5.0	4.2	2.0	3.7	2.5	0.03	1.04	0.57	0.37	0.52	0.28
Median	1.0	8.0	7.0	3.7	8.0	8.0	0.07	1.83	1.46	1.24	1.35	0.56
75% Percentile	1.2	12.3	12.8	13.3	11.9	13.5	0.15	3.35	3.61	4.96	2.48	2.94
Maximum	1.3	31.0	31.7	22.7	25.0	26.0	0.3	15.4	19.3	14.0	35.8	15.9
Mean	0.9	9.4	9.6	7.1	9.0	9.1	0.10	2.89	3.47	3.15	3.07	2.76
S.D.	0.4	5.9	7.9	6.7	6.2	8.0	0.09	3.00	4.96	4.19	6.74	5.04
S.E.M	0.2	0.6	1.8	1.7	1.2	2.7	0.03	0.28	1.11	1.08	1.27	1.68
Eosinophil												
Minimum	0.2	0.0	0.3	0.0	0.0	0.7	0.01	0.00	0.08	0.00	0.00	0.01
25% Percentile	0.3	2.9	2.6	0.7	2.1	0.9	0.04	0.51	0.44	0.18	0.21	0.07
Median	1.2	5.0	4.7	2.7	4.2	1.7	0.07	1.10	0.90	1.06	0.77	0.43
75% Percentile	2.7	7.0	8.7	7.0	7.2	4.5	0.37	2.05	2.40	2.47	2.70	1.38
Maximum	3.2	21.7	21.0	15.0	27.3	7.7	0.4	19.6	11.9	4.6	15.8	2.3
Mean	1.6	5.5	6.5	4.0	5.5	2.6	0.2	1.7	2.1	1.4	1.7	0.7
S.D.	1.2	4.1	5.1	4.2	5.4	2.5	0.2	2.3	2.8	1.5	3.0	0.9
S.E.M	0.4	0.4	1.1	1.1	1.0	0.8	0.07	0.22	0.63	0.38	0.57	0.30

Table 8.1.1: Cellular differential raw data.
Abbreviations; S.D., Standard deviation, S.E.M., standard error of mean

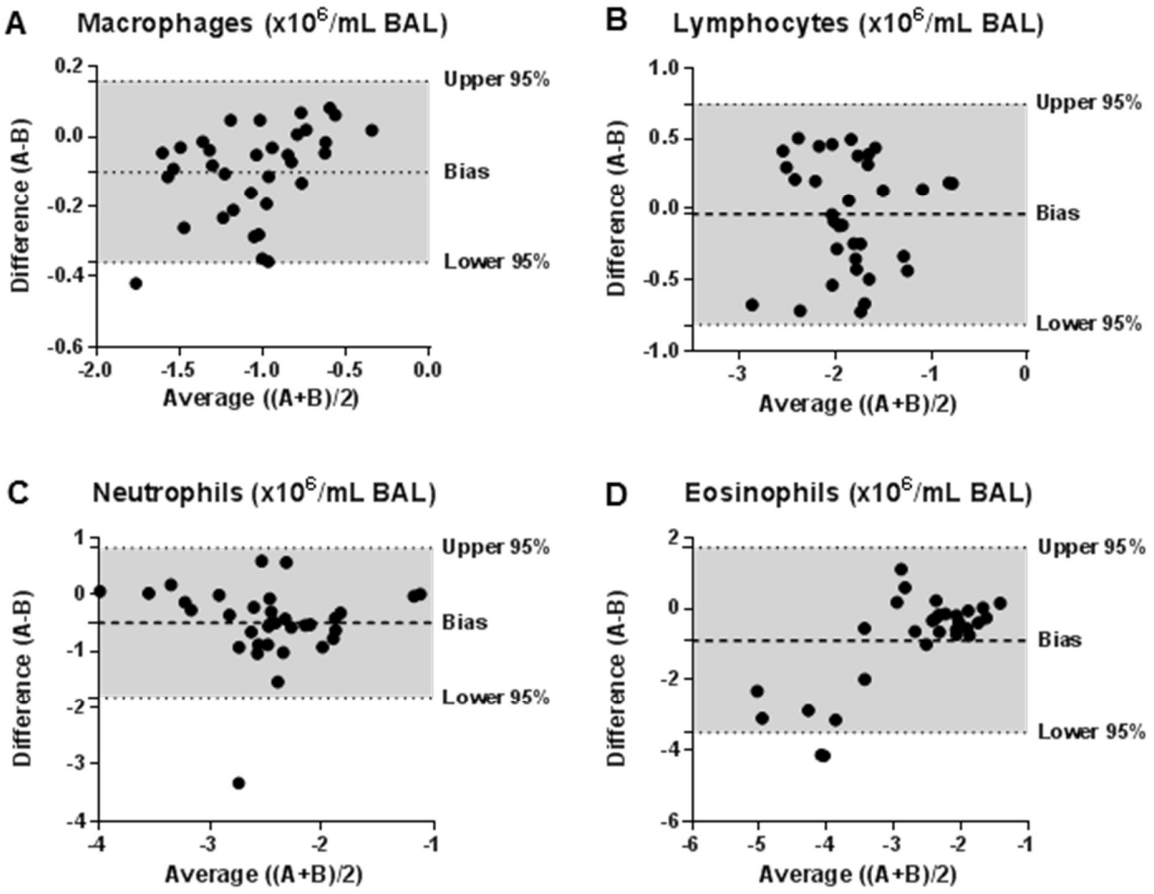


Figure 8.1.1: Bland-Altman comparison of methods reveals no significant difference comparing FACs analysis and differential analysis of cell number.

Bland-Altman plots comparing method A (differential analysis) to method B (FACs analysis) for macrophages, lymphocytes, neutrophils and eosinophils (A-D respectively). Bias, upper and lower 95% limits are illustrated on each graph. Points within the grey area indicate a non-significant difference in results comparing the two analysis methods.

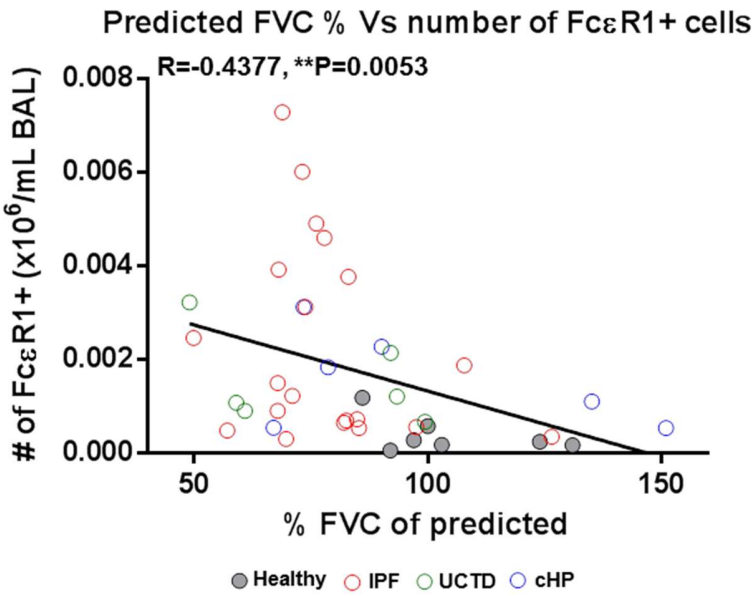


Figure 7: Increased numbers of FcεR1+ cells inversely correlate with percentage predicted forced vital capacity (FVC).

Correlations were carried out using Spearman's rank correlation with r values and p values written on the top left of graph. Linear regression is highlighted with a black line. Sample decode; healthy controls (●), IPF (O), UCTD (O) and cHP (O).

8.2. Supplementary data for results chapter 3.

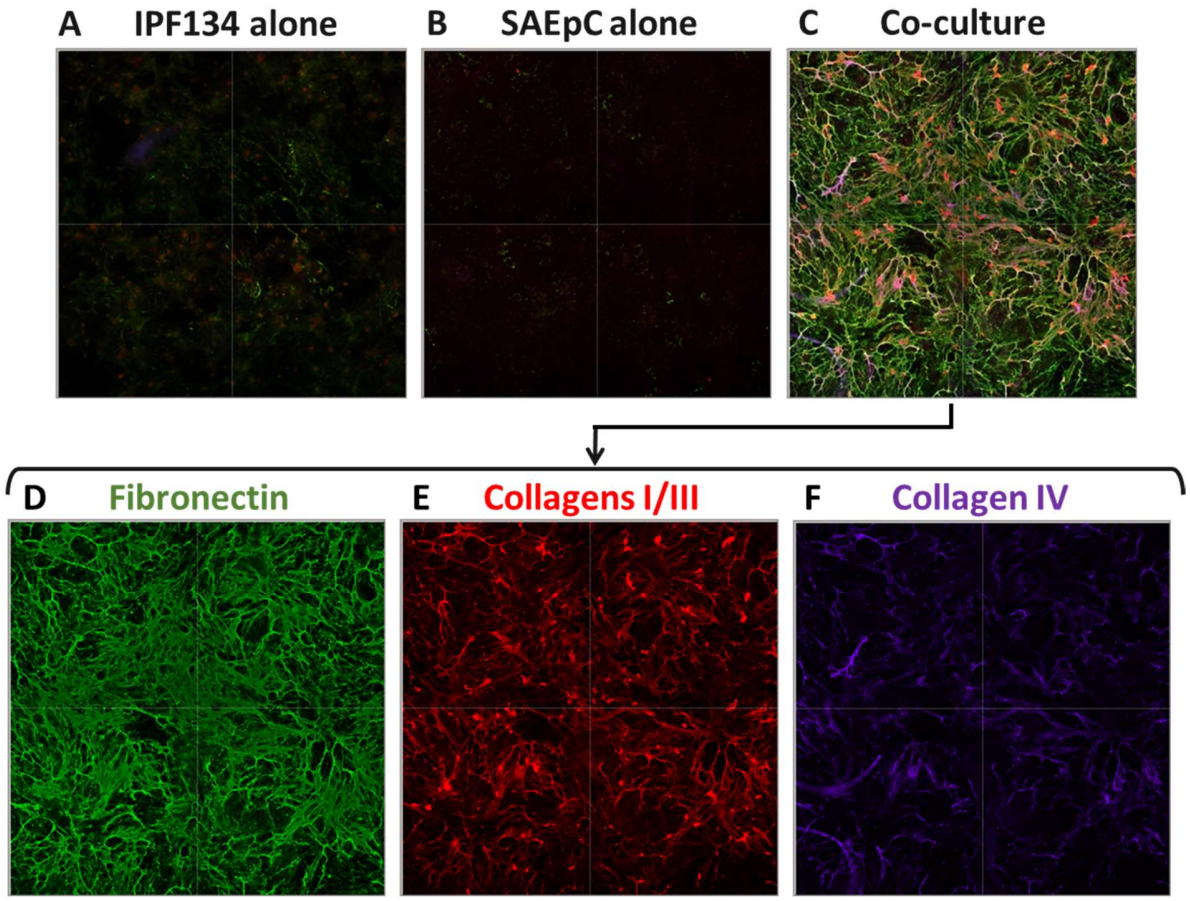


Figure 8.2.1: Co-culture of primary IPF fibroblasts (IPF134) and primary small airway epithelial cells (SAEpC) results in extracellular matrix (ECM) deposition.
Stained ECM from a culture of fibroblasts (IPF134) alone (A), SAEpC alone (B) and in co-culture (C) illustrating co-culture is necessary for complex matrix deposition. Fibronectin deposition is stained and illustrated green (D), collagens I and III are stained and illustrated in red (E) and collagen IV is stained and illustrated in purple (F).

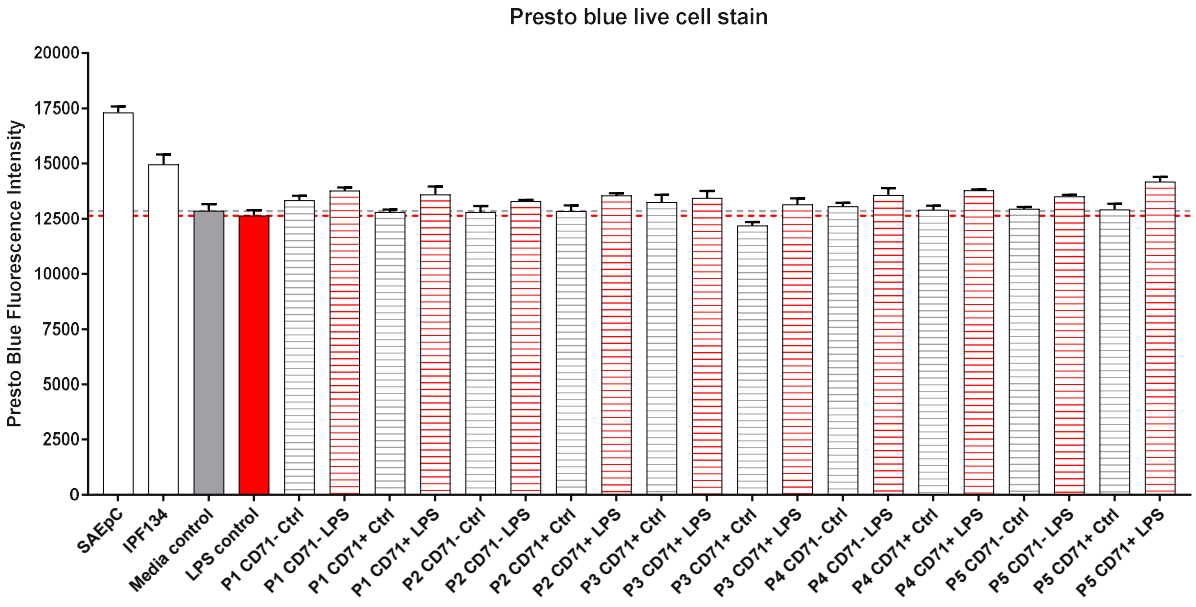


Figure 8.2.2: Examination of cell viability reveals no differences comparing co-culture control to CD71-/+ control unstimulated or LPS to CD71-/+ LPS stimulated.

Presto blue live cell staining fluorescent intensity providing an approximate measure of cell growth for primary small airway epithelial cell (SAEpC) cultured alone, fibroblasts (IPF134) cultured alone, co-culture (SAEpC + IPF134, media control), co-culture with LPS (LPS control), and co-cultures stimulated with either CD71-/+ ctrl unstimulated supernatants or CD71-/+ LPS stimulated supernatants isolated from 5 IPF patients. Values represent mean with standard deviation of quadruplicate wells, with media control representing 16 wells. The grey dashed line highlights the media control and the red dashed line highlights the LPS control.

8.3. Supplementary data for results chapter 4.

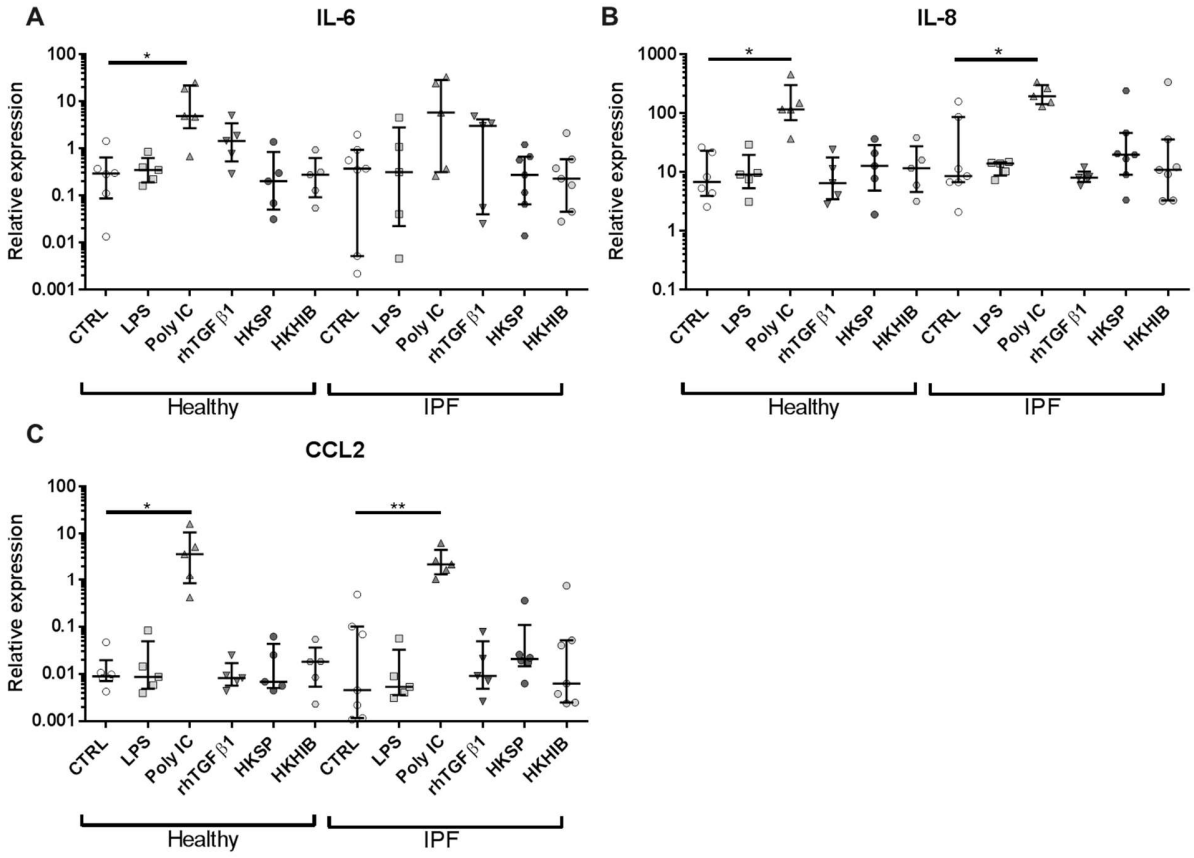


Figure 8.3.1: BEC stimulation: pro-inflammatory relative gene expression analysis.
Gene relative expression analysis showing relative expression of genes IL-6 (A), IL-8 (B) and CCL2 (C) in healthy (stimulated n=5, unstimulated n=6) and IPF BECs (stimulated n=5, unstimulated n=6). Median and interquartile range for unstimulated controls compared to stimulated LPS, POLY: IC, recombinant human TGFβ1 (TGFB1), heat killed streptococcus pneumoniae (HKSP) and heat killed haemophilus influenza B (HKHIB) cells is shown. Statistical analysis Kruskal-Wallis test with Dunn's multiple comparison was used to compare healthy or IPF cell stimulations. Mann Whitney U T test was used to compare Heathy to IPF same stimulus * $p<0.05$, ** $p<0.01$.

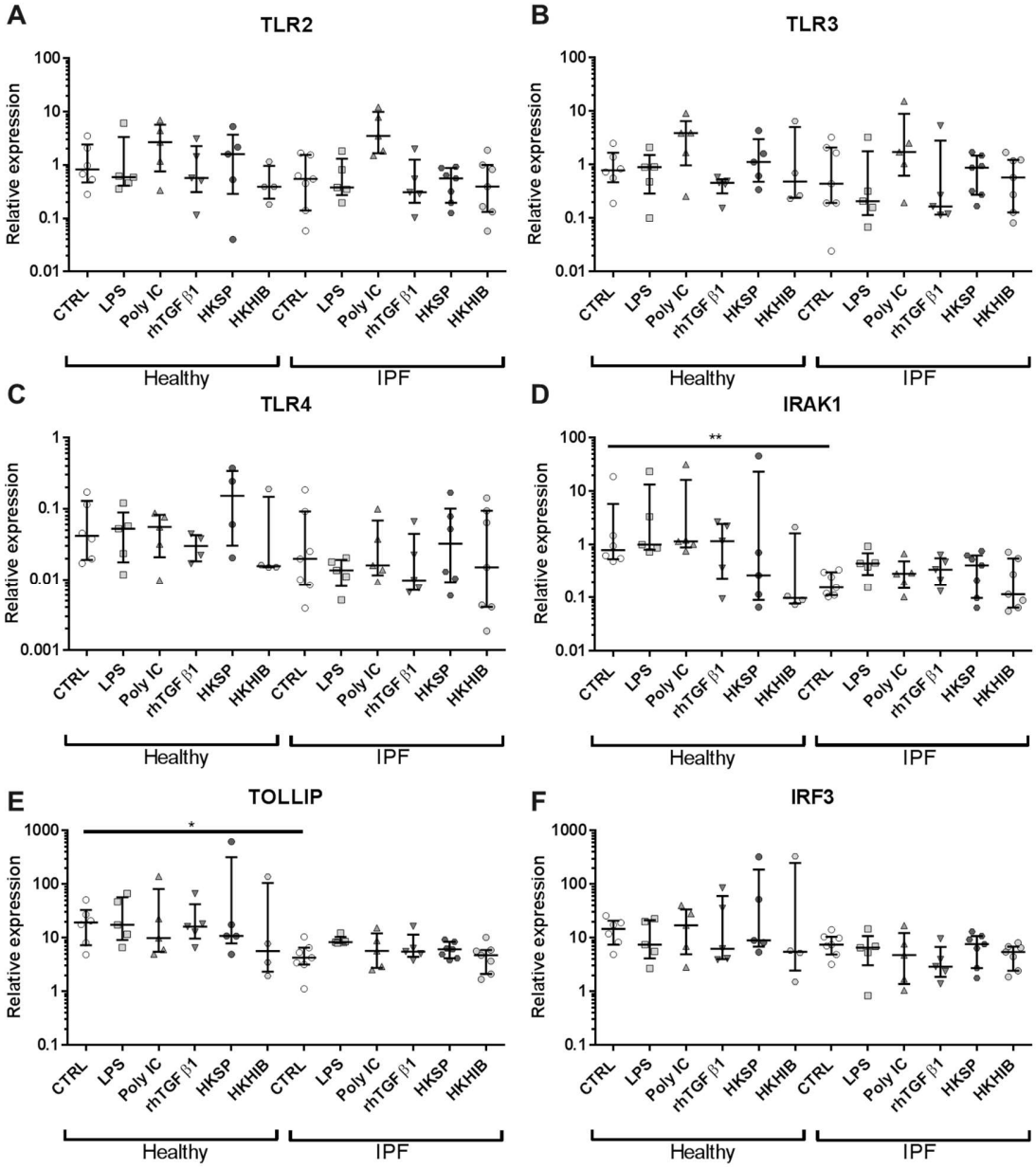


Figure 8.3.2: BEC stimulation: TLR and TLR signalling relative gene expression analysis.
Gene relative expression analysis showing relative expression of genes TLR2 (A), TLR3 (B), TLR4 (C), IRAK1 (D), TOLLIP (E) and IRF3 (F) in healthy (stimulated n=5, unstimulated n=6) and IPF BECs (stimulated n=5, unstimulated n=6). Median and interquartile range for unstimulated controls compared to stimulated LPS, POLY: IC, recombinant human TGFβ1 (TGFB1), heat killed streptococcus pneumoniae (HKSP) and heat killed haemophilus influenza B (HKHIB) cells is shown. Statistical analysis Kruskal-Wallis test with Dunn's multiple comparison was used to compare healthy or IPF cell stimulations. Mann Whitney U T test was used to compare Heathy to IPF same stimulus * $p<0.05$, ** $p<0.01$.

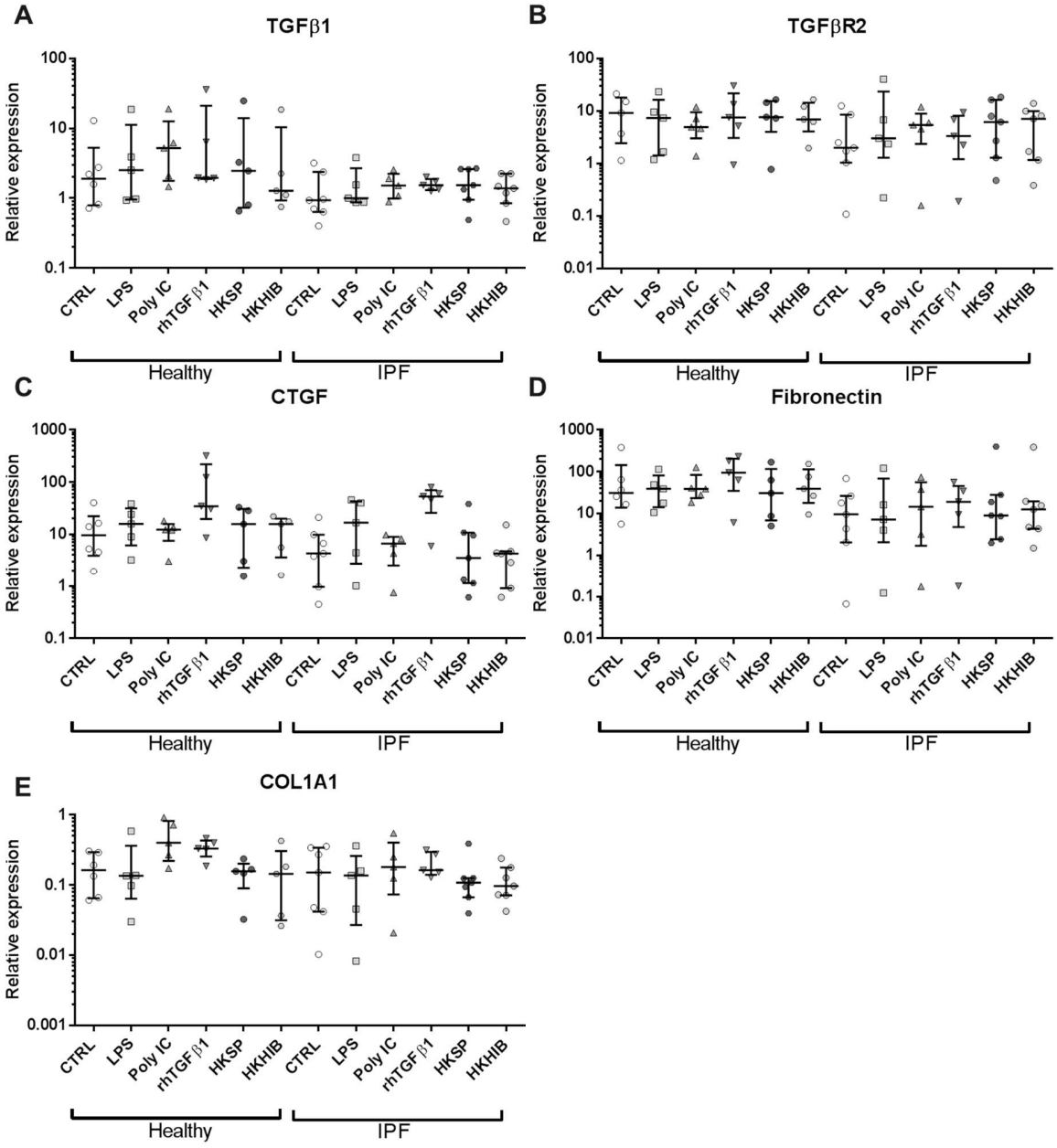


Figure 8.3.3: BEC stimulation: Pro-fibrotic relative gene expression analysis.
Gene relative expression analysis showing relative expression of genes TGFβ1 (A), TGFβR2 (B), CTGF (C), FN1 (fibronectin) (D) and COL1A1 (E) in healthy (stimulated n=5, unstimulated n=6) and IPF BECs (stimulated n=5, unstimulated n=6). Median and interquartile range for unstimulated controls compared to stimulated LPS, POLY: IC, recombinant human TGFβ1 (TGFB1), heat killed streptococcus pneumoniae (HKSP) and heat killed haemophilus influenza B (HKHIB) cells is shown. Statistical analysis Kruskal-Wallis test with Dunn's multiple comparison was used to compare healthy or IPF cell stimulations. Mann Whitney U T test was used to compare Heathy to IPF same stimulus.

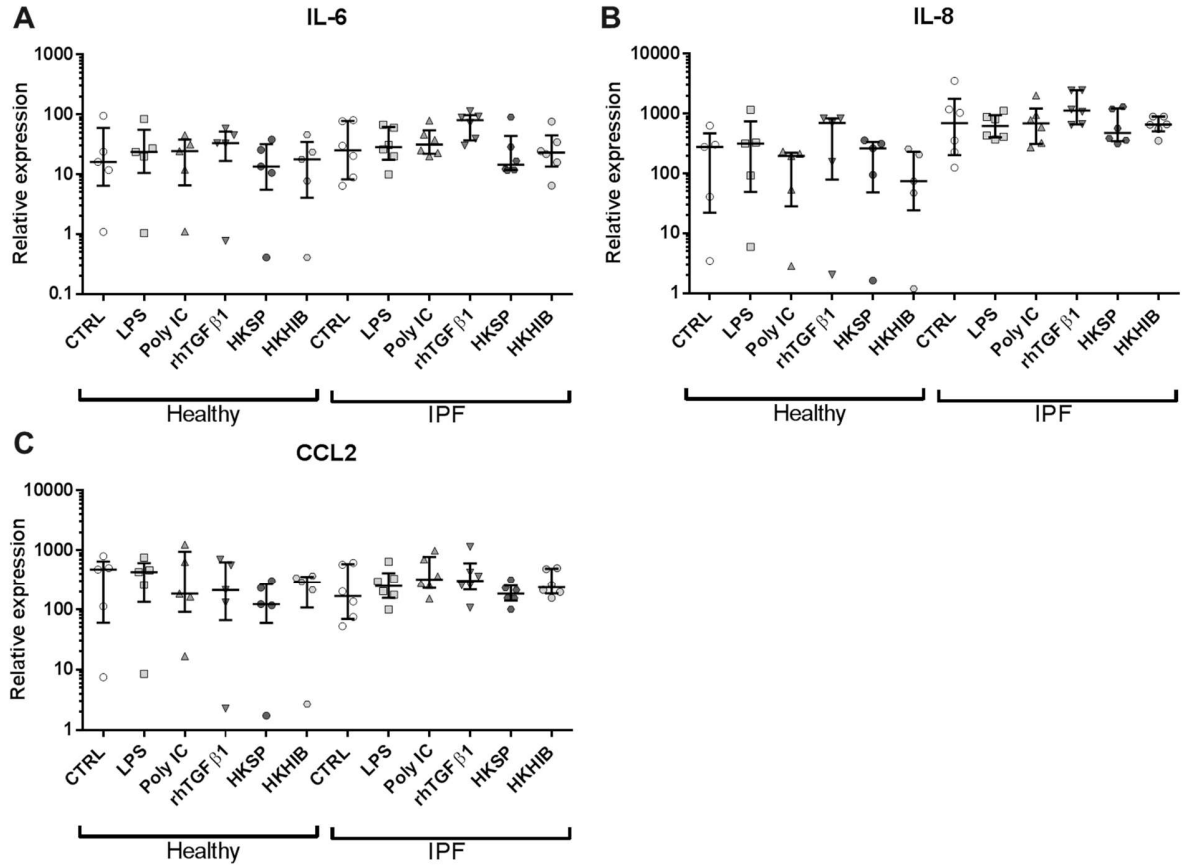


Figure 8.3.4: Fibroblast stimulation: pro-inflammatory relative gene expression analysis.
Gene relative expression analysis showing relative expression of genes IL-6 (A), IL-8 (B) and CCL2 (C) in healthy (n=5) and IPF fibroblasts (n=6). Median and interquartile range for unstimulated controls compared to stimulated LPS, POLY: IC, recombinant human TGFβ1 (TGFB1), heat killed streptococcus pneumoniae (HKSP) and heat killed haemophilus influenza B (HKHIB) cells is shown. Statistical analysis Kruskal-Wallis test with Dunn's multiple comparison was used to compare healthy or IPF cell stimulations. Mann Whitney U T test was used to compare Heathy to IPF same stimulus.

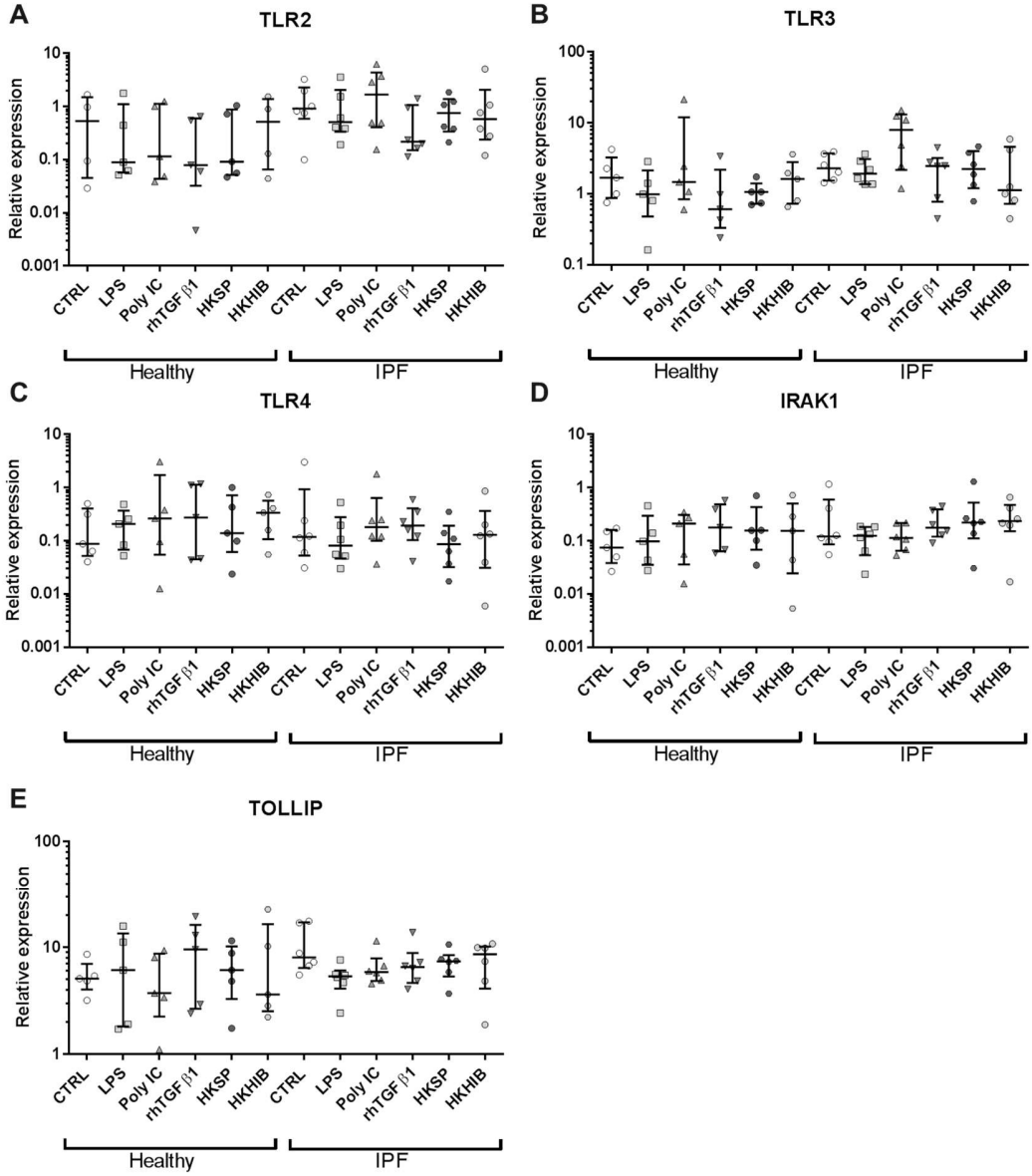


Figure 8.3.5: Fibroblast stimulation: TLR and TLR signalling relative gene expression analysis. Gene relative expression analysis showing relative expression of genes TLR2 (A), TLR3 (B), TLR4 (C), IRAK1 (D) and TOLLIP (E) in healthy (n=5) and IPF fibroblasts (n=6). Median and interquartile range for unstimulated controls compared to stimulated LPS, POLY: IC, recombinant human TGFβ1 (TGFB1), heat killed streptococcus pneumoniae (HKSP) and heat killed haemophilus influenza B (HKHIB) cells is shown Statistical analysis Kruskal-Wallis test with Dunn's multiple comparison was used to compare healthy or IPF cell stimulations. Mann Whitney U T test was used to compare Heathy to IPF same stimulus.

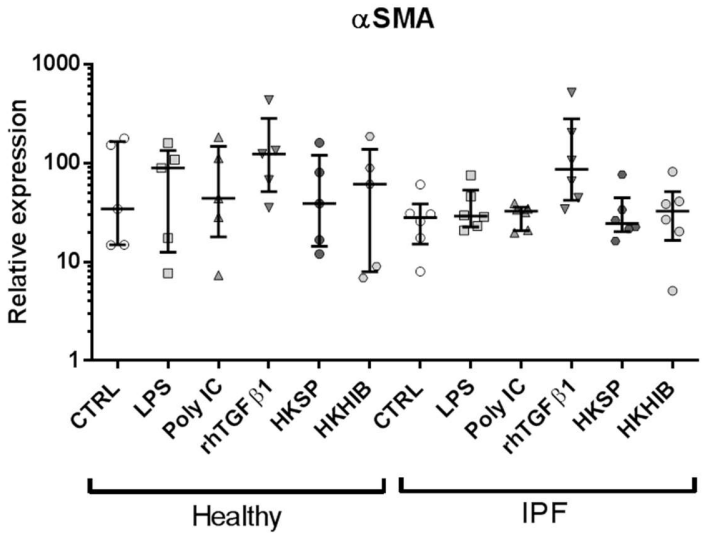


Figure 8.3.6: Fibroblast stimulation: ACTA2 (αSMA) relative gene expression analysis.
Gene relative expression analysis showing relative expression of gene ACTA2 (αSMA) in healthy (n=5) and IPF fibroblasts (n=6). Median and interquartile range for unstimulated controls compared to stimulated LPS, POLY: IC, recombinant human TGFβ1 (TGFB1), heat killed streptococcus pneumoniae (HKSP) and heat killed haemophilus influenza B (HKHIB) cells is shown. Statistical analysis Kruskal-Wallis test with Dunn's multiple comparison was used to compare healthy or IPF cell stimulations. Mann Whitney U T test was used to compare Heathy to IPF same stimulus.

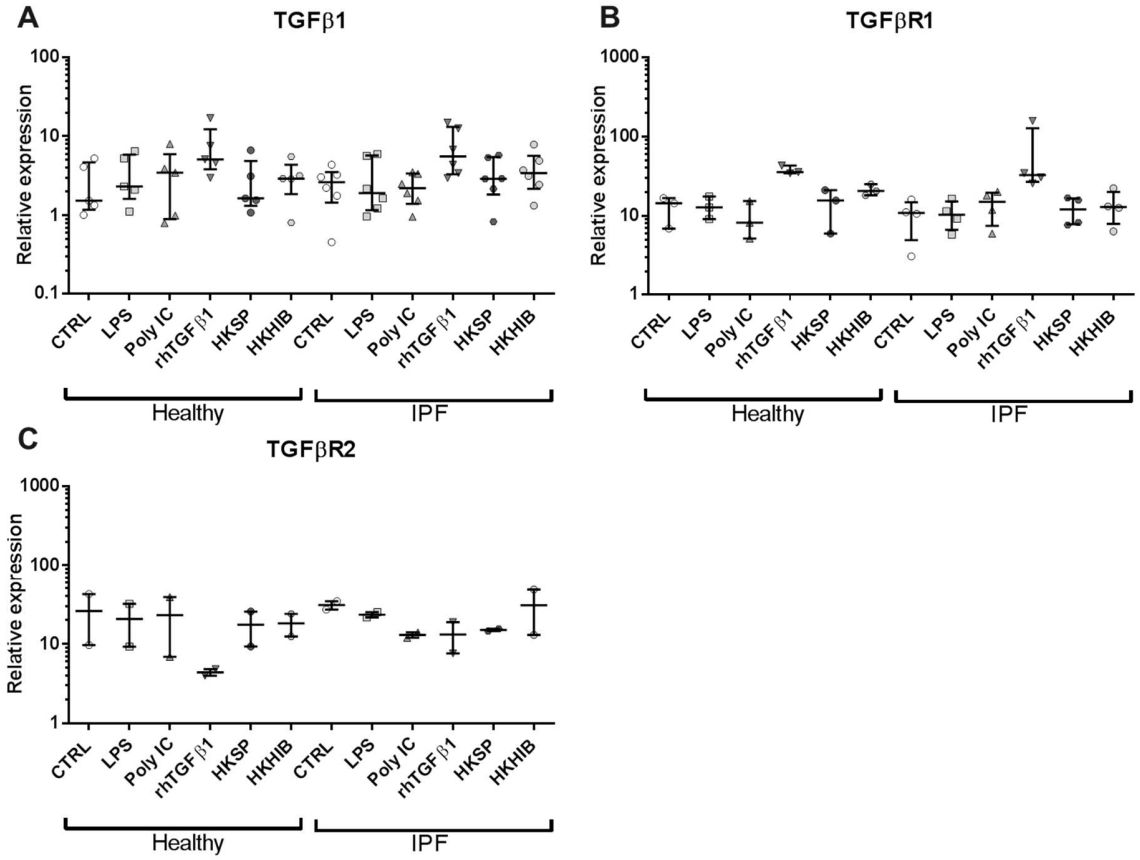


Figure 8.3.7: Fibroblast stimulation: TGFβ and TGFβ receptor relative gene expression analysis. Relative expression of genes TGFβ (A), TGFβR1 (B) and TGFβR2 (C) in healthy (n=5) and IPF fibroblasts (n=6). Median and interquartile range for unstimulated controls compared to stimulated LPS, POLY: IC, recombinant human TGFβ1 (TGFB1), heat killed streptococcus pneumoniae (HKSP) and heat killed haemophilus influenza B (HKHIB) cells is shown. Statistical analysis Kruskal-Wallis test with Dunn's multiple comparison was used to compare healthy or IPF cell stimulations. Mann Whitney U T test was used to compare Heathy to IPF same stimulus.

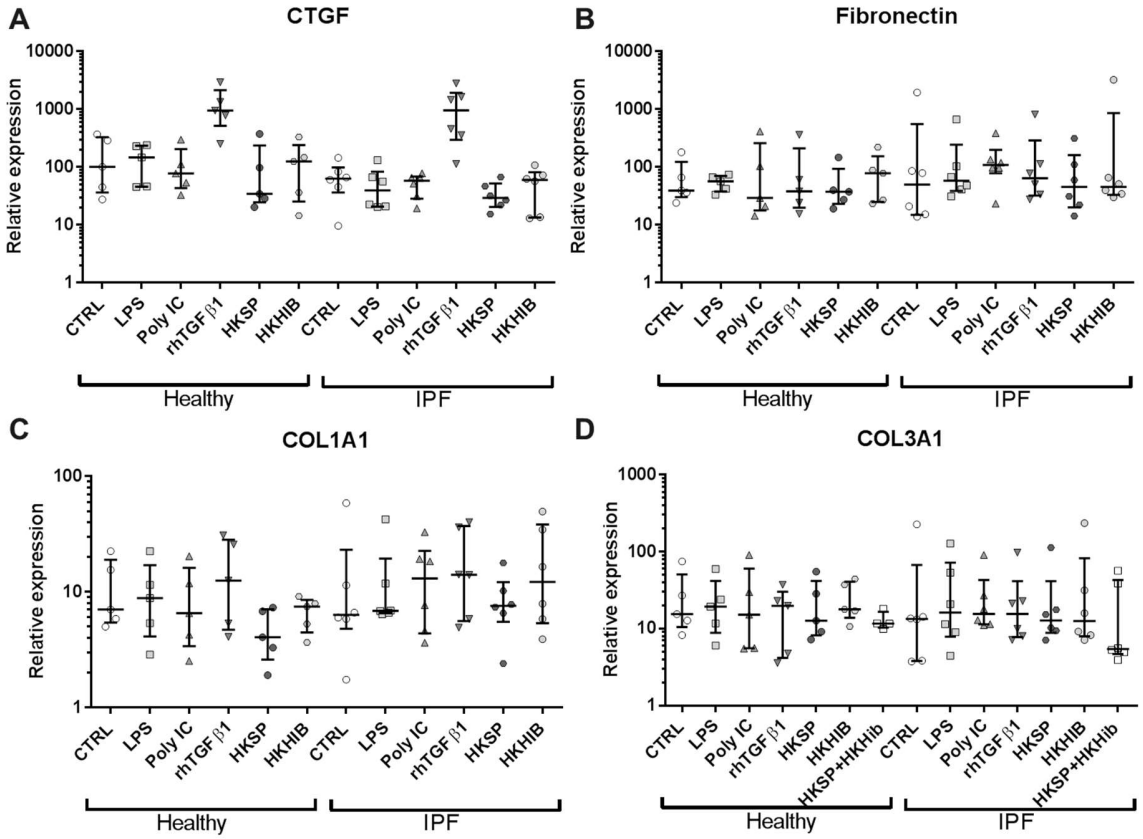


Figure 8.3.8: Fibroblast stimulation: ECM relative gene expression analysis.
Relative expression of genes CTGF (A), FN1 (fibronectin) (B), COL1A1 (C) and COL3A1 in healthy (n=5) and IPF fibroblasts (n=6). Median and interquartile range for unstimulated controls compared to stimulated LPS, POLY: IC, recombinant human TGFβ1 (TGFB1), heat killed streptococcus pneumoniae (HKSP) and heat killed haemophilus influenza B (HKHIB) cells is shown. Statistical analysis Kruskal-Wallis test with Dunn's multiple comparison was used to compare healthy or IPF cell stimulations. Mann Whitney U T test was used to compare Heathy to IPF same stimulus.

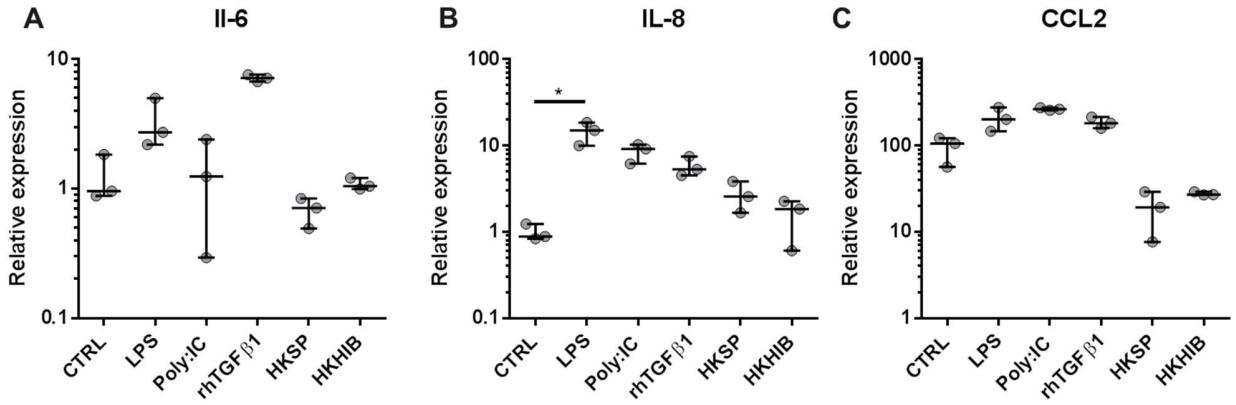


Figure 8.3.9: Fibroblast BEC conditioned media stimulation control pro-inflammatory relative gene expression analysis.

Relative gene expression analysis showing fold change of genes IL-6 (A), IL-8 (B) and CCL2 (C) after stimulation of the same healthy fibroblast with TLR ligands, rhTGFβ1 or heat killed bacteria in BEBM alone (n=3). Median and interquartile range for unstimulated controls compared to stimulated LPS, POLY: IC, recombinant human TGFβ1 (TGFB1), heat killed streptococcus pneumoniae (HKSP) and heat killed haemophilus influenza B (HKHIB) cells is shown. Statistical analysis used Friedman test with Dunn's multiple comparison to compare healthy or IPF cell stimulations.

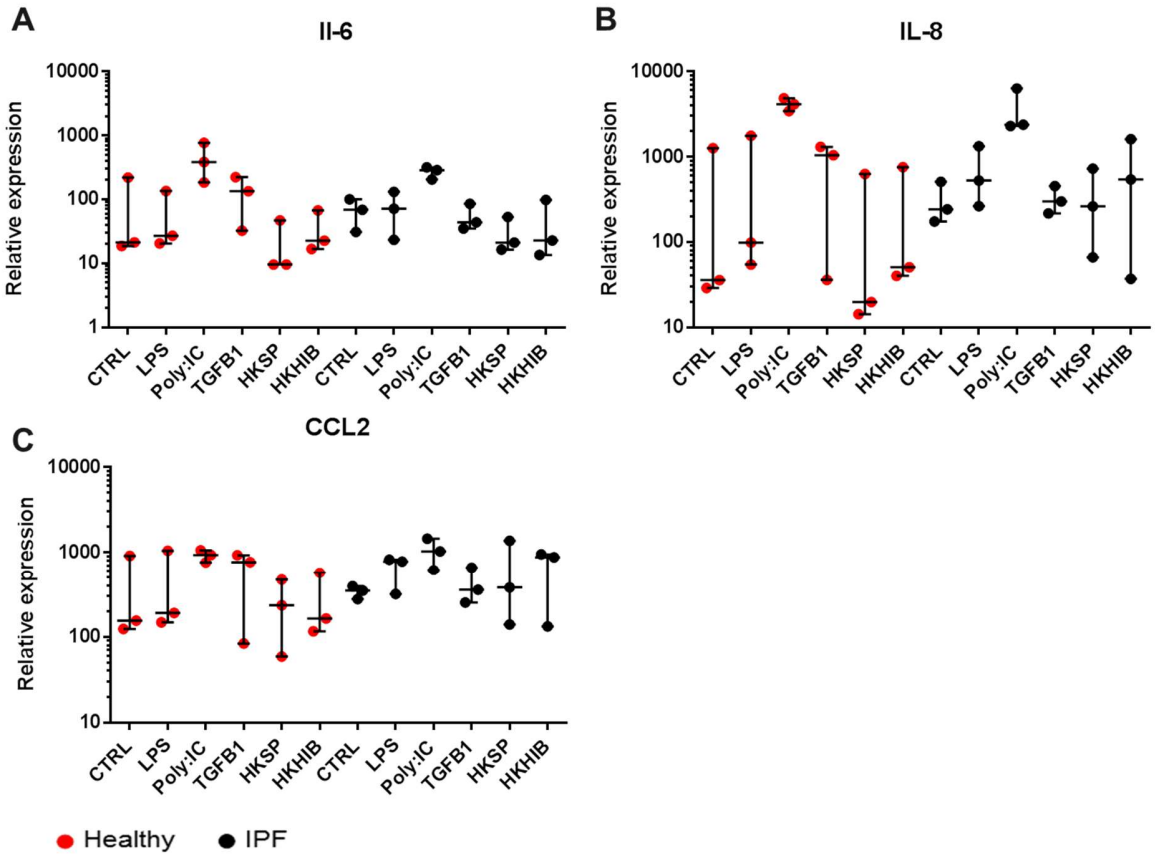


Figure 8.3.10: Fibroblast stimulation with conditioned healthy and IPF BEC supernatant pro-inflammatory relative gene expression analysis.

Relative gene expression analysis showing fold change of genes IL-6 (A), IL-8 (B) and CCL2 (C) after stimulation the same fibroblast with conditioned supernatant from healthy (n=3) and IPF (n=3) BECs. Median and interquartile range for unstimulated controls compared to stimulated LPS, POLY: IC, recombinant human TGFβ1 (TGFB1), heat killed streptococcus pneumoniae (HKSP) and heat killed haemophilus influenza B (HKHIB) cells is shown. Statistical analysis used Friedman test with Dunn's multiple comparison to compare healthy or IPF cell stimulations.

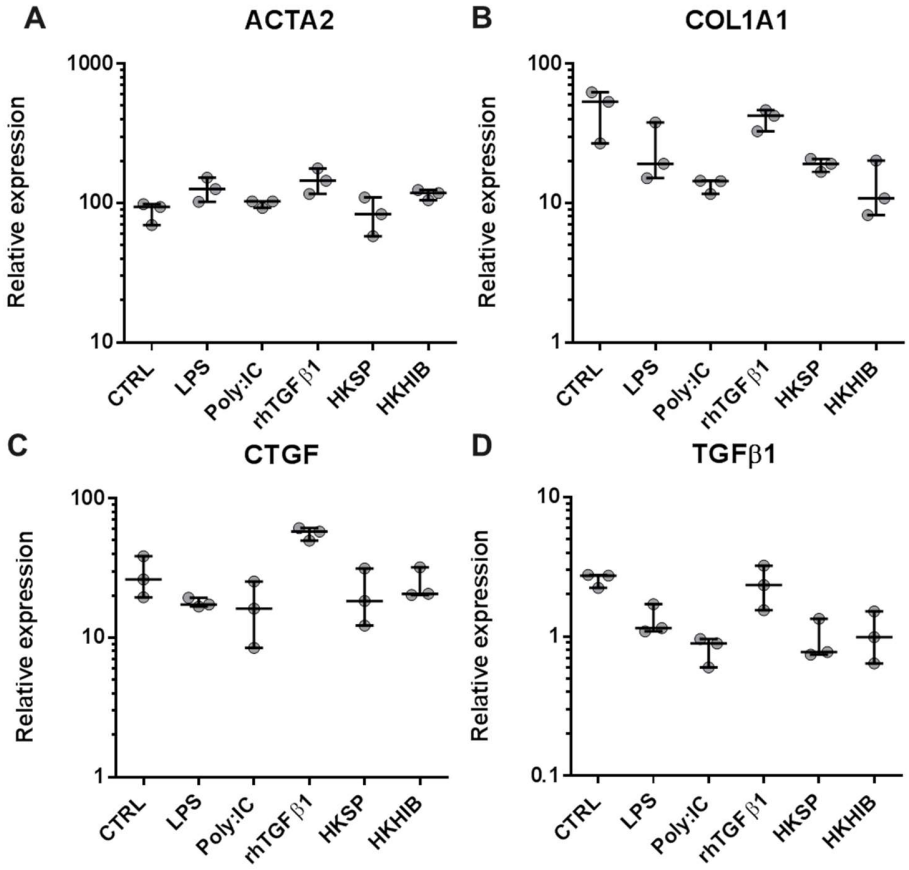


Figure 8.3.11: Fibroblast stimulated controls for conditioned BEC supernatant pro-fibrotic relative gene expression analysis.

Relative gene expression analysis showing fold change of genes ACTA2 (A), COL1A1 (B) CTGF (C) and TGFβ1 (D), stimulating the same fibroblast with the same concentration of stimulus only. Median and interquartile range for unstimulated controls compared to stimulated LPS, POLY: IC, recombinant human TGFβ1 (TGFB1), heat killed streptococcus pneumoniae (HKSP) and heat killed haemophilus influenza B (HKHIB) cells is shown. Statistical analysis using Friedman test with Dunn's multiple comparison to compare healthy or IPF cell stimulations.

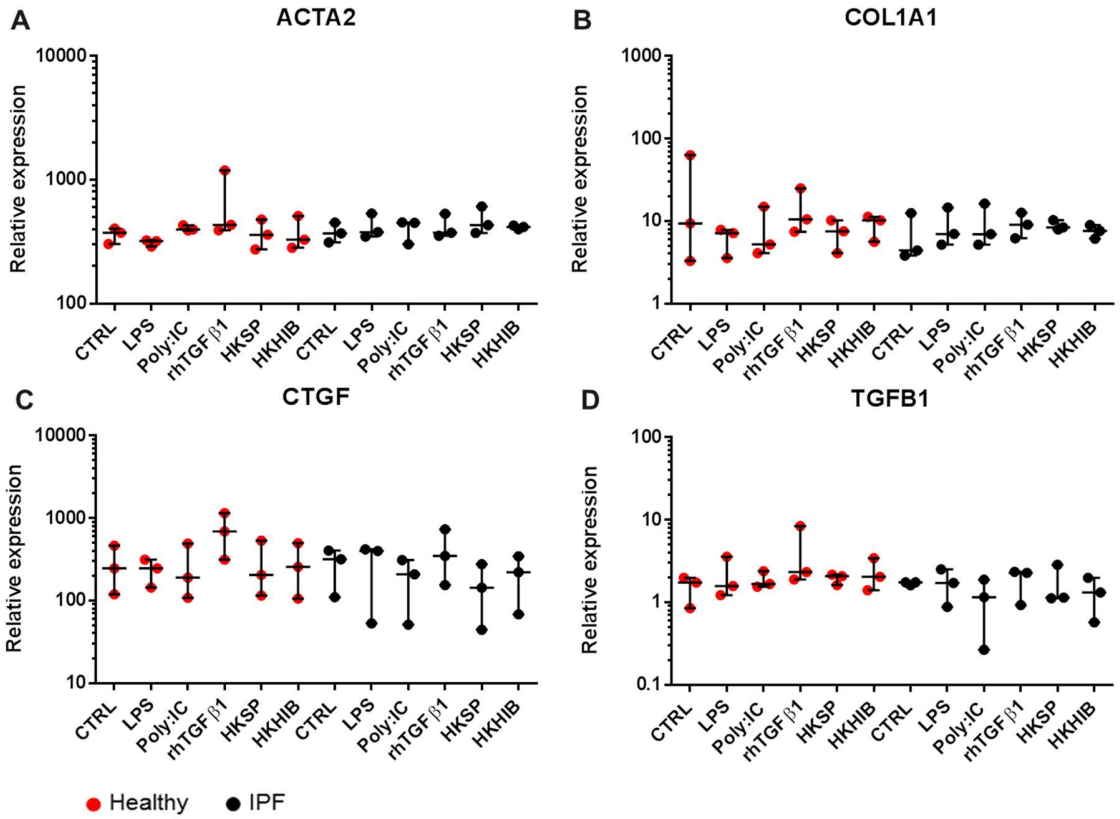


Figure 8.3.12: Relative pro-fibrotic gene expression analysis in fibroblasts stimulated with conditioned BEC media.

Relative gene expression analysis showing fold change of genes ACTA2 (A), COL1A1 (B) CTGF (C) and TGFβ1 (D). The same healthy fibroblast was stimulated with supernatant from stimulated healthy (n=3) and IPF (n=3) BEC conditioned media. Median and interquartile range for unstimulated controls compared to stimulated LPS, POLY: IC, recombinant human TGFβ1 (TGFB1), heat killed streptococcus pneumoniae (HKSP) and heat killed haemophilus influenza B (HKHIB) cells is shown. Statistical analysis using Friedman test with Dunn's multiple comparison to compare healthy or IPF cell stimulations.

8.4. List of external oral and poster presentations

8.4.1. Conference oral presentations

Lund University Respiratory Network meeting (LURN) March 16th-17th 2017
”Personalized Medicine for Respiratory diseases”
Talk: Innate Immunity in IPF: Airway Macrophages

8.4.2. Poster presentations

ATS (2016) poster presentation:

Expression of CD71 on Alveolar Macrophages Reveals Distinct Cell Populations in Human Bronchoalveolar Lavage from Patients with Interstitial Lung Disease
Sarah J. Allden, Richard J. Toshner, Adam J. Byrne, Clare M. Lloyd, Toby Maher
American Journal of Respiratory and Critical Care Medicine 2016;193:A6605
Poster Publications:

The IL-33/ST2 Axis Is Upregulated in Fibrotic Lung Disease
Richard J. Toshner, **Sarah J. Allden**, Adam J. Byrne, Clare M. Lloyd, Toby M. Maher
American Journal of Respiratory and Critical Care Medicine 2016;193:A2414

ICLAF (2016):

Expression of CD71 on Alveolar Macrophages reveals distinct cell phenotypes
Sarah J. Allden, Richard J. Toshner, Adam J. Byrne, Clare M. Lloyd, Toby Maher QJM: An International Journal of Medicine, Volume 109, Issue suppl_1, 1 September 2016, Pages S26, https://doi.org/10.1093/qjmed/hcw119.017

IRF5-expressing macrophages are protective during fibrotic lung disease.
Adam Byrne, Hasina Abdul, **Sarah Allden**, Richard Toshner, Clare Lloyd, Toby Maher
QJM: An International Journal of Medicine, Volume 109, Issue suppl_1, 1 September 2016, Pages S29–S30, https://doi.org/10.1093/qjmed/hcw119.029